Measurement of cerebral activity in response to Dopaminergic drugs: studies using Functional Magnetic Resonance Imaging in the Rat

A thesis submitted for the degree of
Doctor of Philosophy
at the University of Leicester

by

Aisling .L.Dixon
School of Psychology
University of Leicester
September 2002

ProQuest LLC
789 East Eisenhower Parkway
P.O. Box 1346
Ann Arbor, MI 48106-1346

ABSTRACT

Author: Aisling Lisa Dixon
Title: Measurement of cerebral activity in response to dopaminergic drugs: studies using functional magnetic resonace imaging in the rat

Dopamine is involved with many aspects of normal brain function, such as movement, emotion and motivation and its dysregulation is associated with diseases, such as schizophrenia and Parkinson's disease. Drug treatments for these conditions may cause side effects, hence, it is important to understand their mechanisms. Amphetamine administration is a popular model for studying reward, schizophrenia and behaviour. I modified this model to investigate changes in functional dopaminergic activity in the whole rat brain using Pharmacological magnetic resonance imaging (PhMRI). Halothane proved to be a suitable anaesthetic for these experiments because it did not affect stimulated dopamine release unlike a-chloralose.

Acute amphetamine challenge caused widespread increases in blood-oxygenation-level-dependant (BOLD) signal intensity in many subcortical dopaminergic structures, with a rim of negative BOLD observed in the cortex. Amphetamine acts by blocking reuptake of dopamine leading to activation of all dopamine receptor subtypes. To tease apart the mechanisms of the amphetamine response, I pretreated rats with specific antagonists prior to amphetamine. This had contrasting effects on the BOLD signal. D_1 antagonist blocked most of the positive BOLD response to amphetamine whereas the D_2 antagonist predominantly blocked the negative BOLD response. The acute effects of selective D_1 and D_2 agonists and antagonists on the BOLD response were observed in subcortical dopaminergic structures, largely corresponding with stimulation or blockade of the specific receptors types.

My experiments show that the recently-developed phMRI technique can be used to dissect the mechanisms of drug action in the whole brain.

Acknowledgements

I would like to thank Professor Michael Joseph and the University of Leicester for allowing me to undertake the research for this degree.

I would also like to thank my supervisor Dr Andrew Young for all his help and support throughout the years, especially with running the HPLC analysis

I would like to thank my collaborators, Prof Peter Morris, Prof Charles Marsden, Dr Malcolm Prior and of course Yasmene Shah for the opportunity to research in the Magnetic Resonance Centre in Nottingham, and also the staff in the Magnetic Resonance Centre for all the help given to me when I was there.

I would like to thank Biomedical staff in Leicester and in Nottingham Universities, especially Evelyn. Also I would like to thank computer staff and technical help in the Psychology department, Rob Hemmings and John Ashworth, who's helpful assistance made life easier.

I am also very grateful to all other friends in the Department and elsewhere who have made my working time more easy and pleasant, Diana, Lorraine and Jo.

Another very special thankyou must go to my parents Prof Padriac and Anne Dixon and my sisters Catherine and Naomi, also, without whom I would never have got this far.

I would like to say a special thank you to Nick for giving me positive encouragement supporting me during the course of my PhD

Contents

Abbreviations

CBF	cerebral blood flow
CMR_{O2}	cerebral metabolic rate for oxygen consumption
CMR_{glu}	cerebral metabolic rate for glucose consumption
CBV	cerebral blood volume
CT	computerised tomography
SPECT	single photon emission tomography
PET	positron emission tomography
MRI	magnetic resonance imaging
FMRI	functional magnetic resonance imaging
EEG	electroencephalography
MEG	magnetoencephalography
MRS	magnetic resonance spectroscopy
NMR	nuclear magnetic resonance
PhMRI	pharmacological magnetic resonance imaging
BOLD	blood oxygen level dependant
ASL	arterial spin labelling
IBT	intravenous bolus tracking
ASL	arterial spin labelling
fMRS	functional magnetic resonance spectroscopy
DA	dopamine
AMPT	α-methyl-p-tyrosine
LDOPA	L-3-4-dihydroxyphenylalanine
AADC	aromatic amino acid decarboxylase
MAO	vesicular monoamine transporter
COMT	monoamine oxidase
VTA	catechol-O-methyl transferase
MFB	medial forebrain bundle
PD	Parkinson's disease
HVA	homovanillic acid
DOPAC	dihydroxyphenylacetic acid
5HIAA	5 hydroxyindole acetic acid

MPTP	1-methyl-4-phenyl-1,2,3,6-tetrahydropyridine
TA	acquisition time
NEX	number of excitiations
SNR	signal to noise ratio
FSE	fast spin echo
RARE	rapid acquisition with relaxation enhancement
ETL	echo train legth
BMS	bulk magnetic susceptability
TEeff	effective TE
PAG	periaqueductal grey matter
2DG	2-deoxyglucose
ECF	extracellular fluid
HPLC	high performance liquid chromatograpy
PVN	paraventricular nucleus
MAC	minimal alveolar concentration
NMJ	neuromuscular blocker
PSS	peripheral sensory stimulation
SPM	statistical parametic mapping
FWHM	full width at half maximum
GLM	general linear model
PE	parameter estimates
SD	standard deviation
SE	standard error
SNR	signal to noise ratio
NMDA	N-methyl-D-aspartate
6OHDA	6 hydroxydopamine
5HT	5 hydroxytryptamine
GABA	gamma amino butyric acid
IPSP	inhibitory postsynaptic potential
EPSP	excitatory postsynaptic potential

List of Figures

List of Tables

Chapter 1

General Introduction

1.1 Brain And Behaviour:

1.1.1 Functional localisation: A Historical Perspective

In modern science, the central opinion is that all behaviour is a reflection of brain function. Thus the action of the brain underlies not only relatively simple motor behaviours such as breathing and walking, but also controls elaborative and effective behaviours such as feeling, learning and thinking. Consequently, disorders of affect and cognition are seen to characterise neurotic and psychotic illness and are thought of as disturbances of brain function. The brain is a device for processing information about the environment and this information is coded as neuronal signals. Patterns of neuronal firing generate the actions most likely to achieve the organism's goals, not only as a whole, but also as a functionally segregated model. The development of the functional segregation model throughout history has depended on many different pieces of evidence. Although these many facets of science have contributed to this unifying theory, the evidence is not equally convincing, this is described below.

In the Middle Ages there was much controversy as to where the soul was located, i.e. in the brain or in the heart. Various theories developed and it was suggested that mental processes were located in the ventricles of the brain (Descartes, 1596-1650). According to this theory, "common sense" was located in the lateral ventricles and imagination in the posterior parts of the ventricular system. The third ventricle was thought to be the seat of reasoning, judgement and thought, and the fourth ventricle held memory.

The idea of localisation of function within the brain has been accepted since mid 19^{th} century. Early in the 19^{th} century, Gall & Spurzheim (1810) were ostracised by the scientific community for their alleged science of phrenology (Fig 1.1.1a). Although the scientific community never took the phrenologist's claims very seriously, the phrenologists captured the popular imagination of the time (a published textbook on phrenology sold over 100,000 copies). Flourins (1824) vociferously contested such ideas with sound ground for criticism, one being that the skull dimensions are not correlated with brain dimensions.

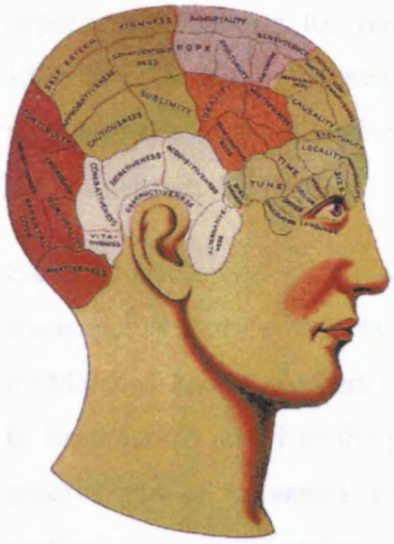

Fig 1.1.1a The phrenological map

This `science` of phrenology involved correlating the external structure of the skull with personality traits, in supporting this claim hundreds of skulls were measured representing the extensive range of `personalities` from the very gifted to the criminally insane.

From URL: www.unb.ca/psychology/likely/19th_cent/phenology_draft.htm

However, he (also incorrectly) concluded that all regions of the cerebrum participate equally in all cerebral functions. In the mid-nineteen century, Pierre Paul Broca (1861) described the first supporting evidence for specialisation of the human brain function. Broca was presented with a patient who suffered from aphasia and was unable to speak as a result of a stroke but was otherwise normal and could understand language perfectly well. After the patient died Broca autopsied the brain and concluded that a lesion in the inferior frontal gyrus of the left hemisphere caused the damage, moreover he ascertained that this area had a unique function in language.

Karl Wernicke took the next step in 1876, where he described another type of aphasia, involving impairment of speech, which was different to the aphasia described by Broca: this aphasia involved problems with expression. Also the cortical lesion was found to be in the posterior part of the temporal lobe. Inspired by Wernicke, Brodmann showed that the cortex could be mapped into 52 discrete areas on the basis of the cell structure and arrangement and hence formed the assumption that the different anatomical structures should have different functions. This was subsequently turned into a brain map (the original 1909 paper is translated by Garey, 1999). The evidence for functional segregation was initially discredited, until methods such as stimulation and recording from the cortex and the rise of cognitive neuropsychology became popular. Solid

experimental support for cerebral localisation in animals followed. For example, in 1870 Fritz & Hitzig showed that applying small electrical currents to circumscribed region of the exposed surface of the brain of a dog could elicit discrete movements (Fritz & Hitzig, 1870).

Electrophysiological techniques were first used to study the cortical representation of the somatosensory system in the late 1930s. This technique was also used in monkeys by Marshall and co-workers (1941) to map the representation of the surface of the body in Brodmann's area 1 of the post-central gyrus. Marshall et al found that by touching a specific part of the animal's body surface, he could produce an evoked potential in a particular area of the cortex.

The map was constructed by relating each point of the skin on the body surface to the point of maximal electrical activity in the cortex.

A much greater part of the somatosensory cortex was found to be associated with the hand and face, compared to regions of lesser importance with regard to tactile tasks, such as the leg. A similar organisation was found in the human cortex (Penfield & Rasmussen, 1950) (fig 1.1.1b): this neural representation of the body is known as the homunculus, meaning "little man".

Fig 1.1.1b The sensory homunculus

Electrophysiological techniques were used to study the cortical representation of the somatosensory system. A much greater part of the somatosensory cortex is associated with areas requiring great tactile innervation such as the hand and face, compared to regions of lesser importance with regard to tactile tasks, such as the leg.

From:www.furman.edu_homunc.epub.org.br/cm/n01

Different animals have different somatotopic representations and thus each have a quite different homunculus. An analogous map also exists for the motor cortex (Penfield & Rasmussen, 1950), in this latter map, the hand is given more cortical surface than in the somatosensory cortex, thus representing the highly sophisticated tasks the hands perform. These regions are described as primary cortices, as they are most closely involved with the brains input and output, secondary areas perform more abstract tasks, consequently the areas involved with higher function (interpretation and memory) are known as tertiary. These cortical maps of the body's surface and the parallel motor maps are important for understanding neurology as outlines in the following section.

1.1.2 Relationship of Brain Pathology to Function

Disturbances in the somatosensory cortex can be clinically localised because there is a direct relationship between the anatomical organisation of the brain and specific perceptual and motor functions. An example was described by Jackson (1931): while performing studies on focal epilepsy he found that convulsions moving over different parts of the body corresponded to particular parts of the cerebral cortex, the arrangement of the somatosensory cortex explained the seizure progression.

Penfield & Rasmussen (1950) gleaned much new information from studies of people who had sustained major head wounds, i.e. assigning function by virtue of dysfunction after damage. Patients with severe neurological disorders were sometimes treated by removing regions of their brain: an extreme example of this was the treatment of severe epilepsy by cutting the corpus callosum (the bundle of fibres connecting the left and right cerebral hemisphere, Sperry, 1968). However it is desirable to assess brain activity in normal function, section 1.2 describes techniques employed to image brain function.

1.2 Introduction to Functional Imaging of the Brain

In order to achieve a more complete description and understanding of brain function and anatomy, the neuroimaging techniques are required which provide both high temporal

resolution and high spatial resolution The development of new imaging techniques has had considerable impact on medical imaging on the field of neuroscience. This novel ability to observe brain function directly opens an array of new opportunities to advance our understanding of brain organization, as well as establishing potential new standard for assessing neurological status.

1.2.1 Single Photon Emission Computed Tomography (SPECT)

The earliest experiments to measure global cerebral blood flow were performed by Kety & Schmidt (1948). Using NO_2 as an indicator in the blood, they measured the differences between arterial input and venous outflow, from which the cellular uptake could be determined. Such work was built on by Ingvar and Lassen (1961) and subsequently radioisotope Xe-133, which emits gamma rays, was used to measure the regional cerebral blood flow (CBF) (Glass & Harper, 1963). The development of computed tomography (CT) and radioisotope mapping led to single emission computerised tomography (SPECT, Kuhl & Edwards, 1963). Examples of recent usage of SPECT, include measurement of rCBF (Di Piero et al, 2001; Eker et al, 2001) because Xe-133 can be introduced into the blood by inhalation and can then be detected as it flows throughout the vascular system.

Another use is receptor imaging: for example by utilising a radioisotope labelled ligand of the dopamine D_2 receptor (^{123}IS-(-)-iodobenzamide), dopamine D_2 receptors were imaged and quantified in the human brain (Brucke et al, 1991). SPECT radioisotopes have a relatively long half life (hours to days) thus they are relatively easy and cheap to produce. The gamma camera (which detects the gamma rays emitted) is rotated around the head and by filtered back projection, a three dimensional image is obtained. The spatial resolution is not particularly good, and the development of positron emission tomography (PET) and functional magnetic resonance imaging (fMRI) methods have largely superseded SPECT.

1.2.2 Positron Emission Tomography (PET)

In the 1970s imaging techniques developed, including the advent of x-ray CT that allowed clinicians to image features inside the cranium of patients without the need for surgery. The x–ray source is rotated 180° round the skull and the detector rotated on the opposite side and by back projection images of skull, the brain tissue and CSF are obtained. By making the small step of placing the source of radiation within the patient, intra-cerebral blood flow and metabolism could be examined in a relatively non-invasive way. Positron Emission Tomography (PET) uses a positron emitter (nuclei which emit a positron when they decay) as the radioisotope was another step forward. The emitted positron almost immediately collides with an electron, leading to a mutual annihilation, emitting two photons at 180° to each other. These photons are detected in a ring of scintillators and photomultiplier tubes surrounding the head. Reconstruction is performed by filtered back projection, producing a three dimensional image of the source of the annihilation. The distance travelled by the positron through the tissue before meeting an electron limits the resolution, fundamentally this restricts the resolution to 2-3mm at most (Digby et al, 1990).

Using radiolabelled water, PET became the first useful technique to allow researchers to produce maps of brain function, by measuring blood flow during execution of simple cognitive tasks (Fox et al, 1984). Since local blood flow is intimately related to cortical activity, areas of high regional blood flow indicate the areas in the cortex responsible for the task performed. The advent of the functional imaging modalities of SPECT and PET led to a new era in the study of brain function. PET has two major advantages over SPECT, i.e. better spatial resolution and sensitivity. Normally two cognitive states are imaged, one active and one resting, by subtracting the signal measured in each of these two states, a map of the regions of the brain responsible for that task is made. PET is used widely as a tool for cognitive function. In addition to its use for measuring brain activation, PET can also be used for studies on receptor localisation, and neurotransmitter function, by using appropriate positron emitting compounds (^{11}C-labelled raclopride, a dopamine D2 receptor antagonist) for looking at dopamine receptors (Drevets et al, 1999) or ^{18}F- labelled DOPA, enable dopamine function to be followed in patients with Parkinson's disease.

The main limiting factor with PET is the high costs of producing radioisotopes (Conti et al, 1994). The positron emitters have short half-lives (2-100 minutes), which requires costly on-site production of the radioisotopes using a cyclotron.

1.2.3 Electroencephalography (EEG) and Magnetoencephalography (MEG)

The measurement on the scalp of electrical signals, arising from the synchronous firing of the neurons in response to a stimulus is known as electroencephalography (EEG). This technique opened up new possibilities in studying brain function in normal subjects. Measurement of the electrical signals from the brain has been carried out for several decades (Berger, 1929). It is normally performed with silver-silver chloride electrodes attached to the scalp. One or more active sites are measured relative to a reference electrode placed in an area of low response, for example the earlobe (Hefferman, 1996). EEG analysis involves the interpretation of waveforms largely by their frequency and to a lesser extent by the morphology of the wave or complex of several waves.

Electroencephalograms provide good temporal resolution, however the signals are summations of electrical events in many individual cells, i.e. they are weighted averages, so it hard to define an anatomical structure or the spatial extent of an activated "area". Furthermore, EEGs are affected by interference from external sources, for example eye movement and other muscle activity, as the magnitude of electrical signals measured is usually about 50μV. Nevertheless, EEG methods have been used to look at functional brain activity in many situations such as studies "relaxed to alert" (LaBerge, 2001), non REM versus REM sleep (Bodiz et al, 2001), visual tracking (Makeig et al 2002) and cognitive tasks (Krause et al, 2001) and for investigating functional differences in brain pathology, such as epilepsy (Brezny et al, 2001) and schizophrenia (Chung et al, 2002). The signal is an average over several trials and the response is characterised by the latency of the signal peak. So, when a signal peak of interest is found, it can then be mapped across the scalp giving an indication of its source. This scalp source however is not necessarily representative of the underlying cortex.

The measurement of the magnetic equivalent of the EEG was first performed by Cohen (1968), who showed that the alpha rhythm, a spontaneous brain activity, could also be detected magnetically. Such magnetic measurements are called magnetoencephalographs (MEG). Brenner at al (1975), were the first to present magnetic measurements of visually evoked responses. Since then, these types of measurements have been widely used for fundamental and clinical brain research. MEG experiments are carried out in much the same way as their EEG counterpart. Having identified the peak of interest, the signals from all the detectors are analysed to obtain a field map. MEG has the advantage over EEG in that signal localisation is possible (to an extent) and advantages over PET and fMRI in that it has excellent temporal resolution of neuronal events. However MEG is costly and its ability to detect events in deeper brain structures is limited. The principles and applications of MEG have been extensively reviewed by Sato et al (1991).

1.2.4 Functional Magnetic Resonance Imaging (fMRI)

Functional magnetic resonance imaging (fMRI) uses the principles of nuclear magnetic resonance (NMR) to acquire images of brain function without having to introduce exogenous substances into the body. NMR can also take the form of magnetic resonance imaging (MRI), which is used for structural imaging and magnetic resonance spectroscopy (MRS), which involves measurement of chemical constituents of the tissue metabolites. Both techniques can distinguish between different body tissues depending on their chemical composition. fMRI is one of the more recent developments and applications of nuclear magnetic resonance (NMR), and can be used to visualise brain loci, functionally activated by visual, motor, sensory and pharmacological stimuli. This discovery extends the traditional anatomical imaging to include maps of human and animal brain function. Since functional magnetic resonance imaging (fMRI) is the topic of this thesis, the principals governing this technique are described in detail in Chapter 2 (NMR Theory). The purpose of this section is to compare fMRI to other techniques, and the following sections describe applications of fMRI that are relevant to pharmacological (phMRI) studies.

During an fMRI experiment, the brain of a subject is scanned repeatedly. The subject carries out a task or is subject to a stimulation paradigm, such that there is at least one period of rest/baseline ("off" state) in addition to the stimulated or "on" state. During this stimulation, the MR signal from activated regions will change, often due to the increased flow of oxygenated blood into that region. Signal processing reveals these activated regions. Early fMRI studies required exogenous contrast agents to be administered and their passage through the brain during stimulation was examined (Belliveau et al, 1991). It was then discovered that brain activation caused changes in the magnetic properties of blood and surrounding tissue. Consequently, methods for imaging regions of the brain that have altered activity by examining nuclear spins of tissue water, were introduced in 1992 (Bandettini et al, 1992; Ogawa et al, 1992) and these developments made fMRI even more appealing.

fMRI with blood oxygenation level dependant (BOLD) contrast is the most commonly used fMRI technique, and it has the advantage over PET in that it requires no contrast agent, and so is noninvasive. Another benefit of using fMRI is that high quality anatomical images can be obtained during the same imaging session as the functional studies using structural MRI, giving greater confidence as to the source of the activation. Consequently, the anatomical localisation of functional changes can be defined precisely and quickly. However, the functional information is derived from blood flow and not from receptor events (as with PET imaging) and it is expensive (comparable with PET). The literature documents corresponding findings between fMRI and conventional electrophysiological techniques to localize specific functions of the human brain (Puce, et al, 1995; Burgess, 1995). Consequently, the number of medical and research centres with fMRI capabilities and investigation programmes continues to escalate.

By imaging a subject at rest and whilst carrying out a specific task, it became possible to image brain function in a completely non-invasive way. It is often referred to as "brain mapping" and usually involves quantifying changes from the basal or non-stimulated state to the stimulated state. fMRI relies on detection of changes in local brain haemodynamics and metabolism after stimulation: cerebral rate of glucose consumption (CMR_{glu}); cerebral rate of oxygen consumption (CMR_{O2}); cerebral blood flow (CBF); cerebral blood volume (CBV).

fMRI is limited to activation studies which it performs with good spatial resolution. If the resolution is reduced somewhat, then it is often possible to carry out functional magnetic resonance spectroscopy (fMRS), which is chemically specific and can assess many metabolic processes. Since fMRS can assess the rate of glucose utilisation, it provides useful complementary information in the study of brain metabolism to the blood flow and oxygenation measurements from fMRI, (Sappey-Marinier et al, 1992; Frahm et al, 1996). One consideration with fMRS is that due to the low concentrations of many of the imaged substances, larger areas must be imaged to obtain detectable signals. Larger volume units imaged over longer periods are thus used with this technique, limiting both temporal and spatial resolution as compared to conventional MRI, (and BOLD-fMRI see section 1.3.1). However, the use of stronger magnetic fields in the future may improve this resolution. The use of stronger magnetic fields may also allow detection of compounds that are currently considered to be in too low a concentration to be seen with current MRS equipment. These aspects are discussed more fully in Chapter 2.

The brain imaging techniques described above all measure slightly different properties of the brain as it carried out various tasks. Thus, the techniques should be seen as complementary rather than competitive. All of these techniques can potentially reveal much about the brain function and will develop in clinical usefulness as more is understood about the underlying mechanisms of each technique. Multimodal imaging which combine haemodynamic information (i.e. fMRI/PET), electrophysiological information (EEG/MEG), holds promise for imaging patterns of the human brain activity in space and time. However, there is still much work required to improve the accuracy and the spatio-temporal resolution of multimodal imaging to elucidate the neural mechanisms of human cognition.

1.3 fMRI Studies of Brain Function

Unique among brain imaging techniques, fMRI allows non-invasive three-dimensional mapping of the entire brain function with potential spatial resolution of 1-2 millimetres and temporal resolution on the scale of 100 milliseconds (Gatley & Volkow, 1998) which is much greater than that of PET and SPECT scanning (Posse et al, 1996). fMRI

studies of brain activation have confirmed the sites of previously known anatomically distinct processing areas in the visual cortex (Blamire, et al, 1992; Schneider, et al, 1993) the motor cortex (Kim, et al, 1993), and Broca's area of speech and language-related activities (Hinke, et al, 1993). Recently Wu et al (1999) characterised a CNS pathway for acupuncture stimulation using fMRI thus allowing the process of natural nociceptive modulation to be visualised: such studies may be of use in investigating treatment of chronic pain syndromes. Unlike PET and SPECT, most fMRI techniques are non-invasive, i.e. do not involve the injection of radioactive materials. This property may allow longitudinal studies, imaging of a patient repeatedly through different disease states, for example in treatment of depression (Nahas et al, 1998). Using fMRI, one can easily compare different mental states in a single session whereas PET and SPECT scans usually rely on group differences between mental states. Thus, fMRI may be important in understanding how a given individual's brain functions and perhaps, in the future, in helping to make psychiatric diagnoses and treatment recommendations.

Currently there are two approaches to fMRI, one involves measuring changes in CBF after stimulation (perfusion imaging) and the other is based on changes in deoxyhemoglobin that occur because of increased regional blood flow in excess of oxidative metabolism, known as BOLD signal. Both perfusion and BOLD imaging rely on the linkage between increases in regional brain activity and increases in blood flow (or oxygenation levels). These aspects are discussed in more detail in Chapter 2.

1.3.1 Contrast in fMRI

In order to view an altered brain state that is induced by a researcher, a MRI machine must be able to detect some physical difference in the brain. Two methods have been developed for measuring CBF in perfusion imaging: it can be performed using either intravenous bolus tracking (IBT) where an exogenous contrast agent is administered, or arterial spin labelling (ASL) where endogenous water is labelled magnetically to be used as a tracer to directly quantify changes in regional cerebral blood flow.

Intravenous Bolus Tracking

In early fMRI studies, researchers used exogenous gadolinium-based contrast agents to follow changes in cerebral blood flow. Most biological samples are considered to be diamagnetic, meaning they have no unpaired electrons and therefore they are basically nonmagnetic (see also Chapter 2). Gadolinium, a member of the lanthanide group is the element in the periodic table with the greatest number of unpaired electrons (7), and therefore is a strongly paramagnetic substance. Gadolinium, becomes magnetised when placed into a magnetic field. This and other such agents are detectable by MRI because their paramagnetic properties form relatively large magnetic fields, which stand apart from the usual diamagnetic properties of most biological samples.

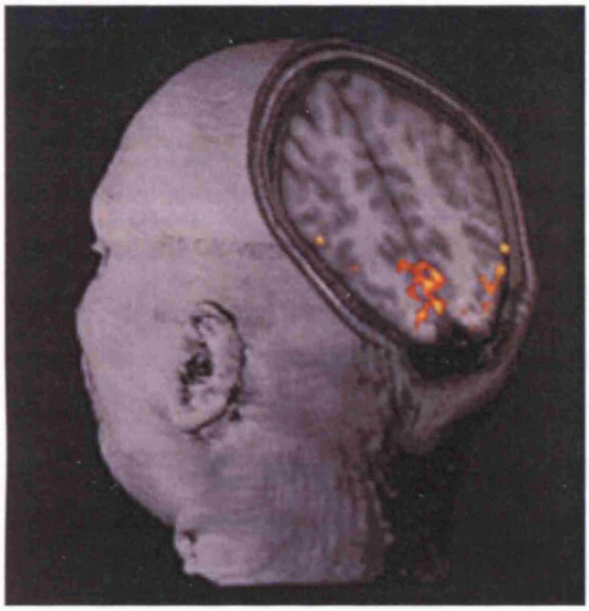

Fig 1.3.1
IBT detection of changes in MR signal

Coloured blobs indicate areas of increased CBF relating to visual stimulus

From URL:
http://www.musc.edu/psychiatry/fnrd/primer_fmri.htm

Intravenous bolus tracking relies on the intravenous (iv) injection of a paramagnetic compound such as a gadolinium-containing contrast agent which enhances the signal attributed to increased blood volume, the regional signal is then detected as it perfuses through the brain (Rosen et al (1991). Belliveau et al. (1991) used the technique to create the first functional magnetic resonance maps of human task activation using a visual stimulation paradigm. Areas perfused with the paramagnetic compound show a reduction in signal intensity, as the compound creates a magnetic inhomogeneity that decreases the signal. Relative activity patterns can be obtained over the course of a single task and by also comparing activity during rest and activation periods. The paramagnetic compound may be injected once during the control and once during the

activation task and relative differences in blood flow between the two states may be determined to develop a perfusion image (Belliveau et al 1991). Alternatively, one can measure changes in blood flow over time after a single injection to generate a perfusion map (Harris et al, 1996). Although gadolinium-based contrast agents are not radioactive, the number of boluses that can be given to an individual is limited by the potential for kidney toxicity with repeated tracer administration. This technique also only generates a map not of absolute flow, but of relative cerebral blood flow.

Arterial Spin Labelling

Arterial spin labelling is a noninvasive technique where intrinsic hydrogen nuclei in arterial water outside the slice of interest are magnetically tagged ("flipped") as they course through the blood and are then imaged as they enter the slice of interest (Williams et al, 1992; Roberts et al, 1994). Arterial spin labelling is noninvasive, does not involve an intravenous bolus injection, and (unlike IBT and PET) can be repeatedly performed in subjects, and furthermore, it measures absolute regional blood flow, unlike techniques such as SPECT or BOLD-fMRI. To perform this task using PET requires an arterial line in the subject. As absolute information is obtained, cerebral blood flow can be serially measured over separate imaging sessions such as measuring blood flow in subjects suffering from bipolar disorder as they course through different disease states (Speer et al, 1997). While there is currently no clinical indication for this technique, it may soon be used clinically to help characterize the different stages of acute ischaemic stroke (Hoggard et al, 2001).

Blood Oxygen Level Dependent Contrast

Haemoglobin has magnetic properties (Ogawa et al, 1990) and can act as a natural endogenous contrast. An important part of that haemoglobin molecule is an iron atom, bound in organic structure, and it is this iron atom, which gives blood its colour. When oxygen binds to haemoglobin, it is oxyhaemoglobin (Hb) and when no oxygen is bound it is deoxyhaemoglobin. (dHb). The haemoglobin in the blood has different magnetic properties depending on whether it is oxygenated or not, dHb is paramagnetic and Hb is diamagnetic. This area is discussed in greater detail in section 2.6.1.

Paramagnetic substances, for example dHb, cause a loss in fMRI signal whereas diamagnetic substances do not affect the signal. Upon neuronal activity, the cerebral rate of oxygen consumption (CMR_{O2}) increases, thus it would be expected that the level of dHb in the blood would increase, causing a decrease in MR signal. However, with increased neuronal activity, there is a proportionally greater increase in CBF as compared to CMR_{O2} (Fox and Raichle, 1986) bringing in more oxyhaemoglobin (Hb). This results in an increase in MR signal, and the decoupling between CMR_{O2} and CBF serves to temporarily increase the BOLD signal.

The fact that BOLD is dependant on the uncoupling of CMR_{O2} and CBF causes problems in imaging with this technique, due to the variable degrees of uncoupling in different brain regions and with different tasks (Kim et al, 1993). Consequently, quantification of neuronal activity using BOLD must be performed cautiously. There have been apparent conflicts in the degrees of CBF uncoupling under different experimental conditions (Roland et al, 1987; Seitz et al, 1992) and indeed the question is whether this process actually occurs is raised, for example by Buxton & Frank (1997) who believe that the large increase in CBF is actually due to tightly coupled CMR_{O2} and CBF. Malonek and Grinvald (1996) suggest that during cerebral functional activity only the decrease in blood oxygenation level (and BOLD signal) in the first 2-3 seconds after stimulation is localised to the region of increased oxygen metabolism. The negative response can only be demonstrated using high temporal resolution fMRI, whilst most fMRI experiments observe the larger positive signal and this is much more widespread.

However, as with all newly emerging techniques, fMRI using BOLD contrast has its own shortcomings. BOLD signal does not directly reflect neuronal activity but is a consequence thereof: this is in contrast to direct measures of neural activity such as electrical activity (Lnenicka & Hong, 1997), intracellular calcium levels (Mattson, 1992) or neurotransmitter release (Benveniste, 1989). Hence additional factors contributing to the BOLD response are possible confounding factors.

Because BOLD effects are an amalgam of the physiological changes in CMR_{O2}, CBF and CBV, one frequently overlooked and potentially confounding factor may be the haemodynamic changes via receptors on blood vessels themselves. One study has indicated that dopamine, a neurotransmitter normally associated with neuromodulatory

actions, may directly affect local CBF, and showed that dopaminergic axons innervate the intraparenchymal microvessels and that dopamine produces vasomotor responses in the cortical vasculature (Krimer et al, 1998). Functional variations in cerebral cortical activity are accompanied by local changes in blood flow, but the mechanisms underlying this physiological coupling are not well understood. Thus such studies should proceed and be interpreted with the necessary caution.

1.3.2 Pharmacological MRI: A novel fMRI application

To date, fMRI has been used as a non-invasive method of measuring regional brain activity by means of BOLD imaging. Useful as this technique is for pinpointing activity to particular area of the brain it does not reveal anything concrete about neurotransmission. Therefore it is important to understand the issues relating neurotransmitter activity to the haemodynamic response. One method of manipulating neuronal activity is by pharmacological stimulation, thus in addition to neuronal activity induced by task activation, the stimulation of neurons using pharmacological ligands is also possible. This is an area of great interest and forthcoming work may be of use in studying neurological disorders such as Parkinson's disease, and schizophrenia, and also drug dependence.

Ethyl alcohol is the most ubiquitous of psychoactive drugs and its excessive use can be associated with significant medical and neurological disease. The behavioural effects of alcohol are very well characterised but its effect on the brain remains elusive (Matthew & Wilson, 1991). BOLD patterns have been studied after alcohol ingestion to understand its effect on brain function. These observations suggest that alcohol suppresses activation below baseline and that there is also a hemispheric dominance effect (Volkow et al, 1988). Some studies implicate the dopamine system, especially the observation (using *in vivo* microdialysis) that alcohol increases extracellular dopamine in the nucleus accumbens over various concentrations (Di Chiara & Imperato, 1988). Despite other microdialysis studies (Yoshimoto et al, 1992), the primary pathways that ethanol uses to induce dependency are in doubt, as it has been suggested that the effect of a moderate amount of alcohol does not affect the function of the dopamine system in the nucleus accumbens (Yim et al, 1997), and that the effect seen with increasingly high

doses is most likely to be due to interactions from many sites. Thus the spatial resolution allowed by fMRI may help elucidate this question.

Cocaine is of particular interest in pharmacological studies of drug abuse and addiction. It is one of the most reinforcing drugs known in humans and animals (Parsons et al, 1998) and with repetitive use, cocaine may produce a state of addiction in humans which is characterised by compulsive drug use and inability to control use despite significant adverse consequences (Gawin, 1991). In a human study following cocaine infusion, cocaine-dependant individuals showed focal increases in BOLD signals at the time of onset of euphoria or craving in the putative brain circuitry involved with reward (Breiter et al, 1997). Using PET and fMRI (Gollub et al 1998; London et al, 1990) and SPECT (Pearlson et al, 1993), various human studies suggest cocaine causes widespread decreases in glucose metabolism and cerebral blood flow.

When pursuing a study of this nature in humans, many factors need to be taken into account, for example, age, sex, I.Q, bodyweight, time from last drug exposure. The potential for polydrug abuse is great including the use of "soft" drugs such as coffee, alcohol and nicotine. Other lifestyle choices may greatly affect results, for example dietary routines therefore it is appropriate to use animal models for such work. In carrying out studies, in particular drug trials, cocktails of drugs act as large confounding factors, thus studies such as these are also very well suited to animal models.

Animal models of drug action and addiction are useful tools to characterise the neurobiological determinants of mechanisms underlying drug action. Such models allow invasive technology that cannot be permitted on humans, they facilitate manipulation of specific neurotransmitter systems and receptor subtypes and enable comparisons of drug effects. Regional cerebral changes in functional activity following administration of psychotropic agents have been assessed in animals using a number of *ex vivo* techniques. Autoradiographic techniques have been used extensively to study changes in cerebral function in neuropharmacological investigations (Wechsler et al, 1979; McCabe et al 1987; Nehls et al, 1990). Receptor agonists and antagonists can be used to map receptor binding, to map out the receptor density of these sites in the brain. Such methods combine a comprehensive anatomic coverage of localised functional change with a high spatial resolution. Lindvall et al (1981) utilised [^{14}C]iodoantipyrine

and [^{14}C] deoxyglucose in conscious animals to quantify blood flow and regional glucose uptake responses following administration of pharmacologically active substances, such as methamphetamine. Such techniques only provide limited information, as each group provides data at a single timepoint. It follows that temporal changes in cerebral function induced by a compound under investigation require many experimental animals. An *in vivo* method, which allows the timecourse of drug action to be studied, is obviously preferable. The neuropharmacological profile of abused drugs display specificity, and this provides a means of studying of brain reward systems. Three major neurotransmitter systems involved in drug reward are dopamine, glutamate and GABA systems. The former is well localised but the latter two are more diffuse (Koob, 1992).

PET studies have also examined metabolic changes (CBF and CMR_{glu}) following neurotransmitter stimulation using amphetamine (Drevets et al, 1999) and other pharmacological ligands (Okubo et al, 1997). fMRI also is well suited to study these metabolic changes, consequently a number of studies have been performed using this new area of animal pharmacological MRI (phMRI) : Forman et al, 1998; Hagino et al, 1998; Marota et al, 2000; Houston et al, 2001. The pattern of activity can be visualised and has been directly correlated with other techniques to verify its validity; with PET to indicate ligand binding, and with microdialysis and behavioural data as indices of the time-course of the BOLD pattern (Chen et al, 1997). The ability to acquire multiple timepoints from a single animal is a major advantage of fMRI over autoradiography. Experimental studies capable of following the effects of a psychoactive compound's timecourse will provide greater insight into their mode of action. Such studies should be able to identify the anatomic loci of drug action, as well as the relative timing of the onset and dynamics of drug effects. Different loci may be associated with therapeutically desirable actions as well as unwanted side effects.

fMRI in humans has helped improve our understanding of the neuroanatomical organisation of behaviour and function, unfortunately fMRI in animals has not kept pace with human work. There are several reasons for this, one of them being the relative size of the human brain versus the laboratory animal brain: the BOLD signal obtained from the human brain may have sufficient resolution but when scaled down to the size of the rat or the mouse, the resolution is reduced and the signal is consequently less

regionally specific. fMRI animal work to date has been mainly concerned with the rat somatosensory cortex after stimulation. A correlation has been made with BOLD signal and electrical activity in the whisker barrel (Yang et al, 1997) and also during forepaw (Hyder et al, 1997), hindpaw (Palmer et al, 1999), and olfactory stimulation (Yang et al, 1998). A further consideration is the finding that the stimulus rates required to give a good response are also restrictive: in humans CBF increased linearly with frequencies up to 7.8Hz, whereas in the rat it was found that above 3Hz the CBF progressively decreased (Gyngell et al, 1996). It must be noted that this is probably due to (α-chloralose) anaesthetic facilitating post-excitatory inhibition and therefore occluding evoked potentials at lower stimulation rates than would occur without anaesthesia.

In the rat, it was found that low doses of ketamine, a clinical anaesthetic agent, produced increases in CMR_{glu} in the hippocampus, cerebral cortex and olfactory bulb and these were accompanied by changes in CBF (Burdett et al, 1995). These changes are thought to be mediated by NMDA receptors since MK801 causes similar effects. This would be of obvious concern as NMDA receptors are distributed widely in the brain (Khan et al, 2000) and thus the effects of anaesthetics agents in experimental animals may confound experimental results. In Chapter 3 the use of anaesthesia in small animal fMRI is reviewed and investigated in order to select the most appropriate anaesthetic for the following phMRI experiments. Nevertheless the use of fMRI as a pharmacological tool is tempting, as it is noninvasive and repeatable. However, large doses of drugs are required to obtain a response compared to PET/autoradiography because the metabolic response to neurotransmitter binding is being assessed rather than the binding itself (as is measured in PET).

The central transmitter system that has been most extensively studied to date using phMRI is the dopaminergic system. This area is of particular interest in neurological and psychiatric research because dysfunctions in this system have long been associated with Parkinson's disease (1.5.1), schizophrenia (1.5.2) and also is known to be involved with the rewarding properties of many abused substances (1.5.3). An example of such an investigation is that of Hagino et al (1998) which examines the effect of chronic and acute antipsychotic treatment, observing different patterns of activity, which is a particularly interesting and useful finding. This study would almost certainly be impossible in humans. For example, by ablating dopaminergic cells on one side of the

animal's brain, it is possible to measure the fMRI response in the ipsilateral versus contralateral side of the brain (Chen et al, 1997). The time course response shown by Chen et al appears more akin to a metabolic response to receptor binding than changes in hypercapnia or blood pressure, moreover the timecourse was similar to microdialysis measurements.

The dopaminergic system is ideal for phMRI studies because of its regional specificity, and because reproducible animal models exist for DA receptor binding (Boyson et al, 1986; Trugman & James, 1993). Since it is known that dopamine receptors exist in several different distinct forms (1.4.5), it is of interest to investigate the contribution of specific receptor subtypes to a drugs overall effect, i.e. the effect of one general dopaminergic ligand can be modulated by either blocking or further stimulating specific receptor subtypes.

In the following section, the dopaminergic system is described including synthesis, storage, release and reuptake mechanisms. This is a well researched area, the reason being that many dopaminergic agents do not act simple as "agonists" or "antagonists", instead they may affect any of the stages leading up to dopamine release and indeed following release (as amphetamine and cocaine do). Thus it is imperative to understand the possible manipulations that pharmacological agents may have on the dopamine system before interpreting results simply as receptor-mediated events.

1.4 Dopamine pharmacology

Dopamine is a member of the catecholamine family. The basic catechol structure and that of dopamine are illustrated (Fig 1.4). Dopamine transmission is of physiological importance in both the central nervous system and peripheral nervous systems. The pathway for catecholamine synthesis was first predicted by Blashko (1939), who proposed that dopamine was a precursor for noradrenaline and adrenaline. Although correct, Arvid Carlsson and co-workers (1959) found dopamine also to be a transmitter in the brain and not simply a prècursor.

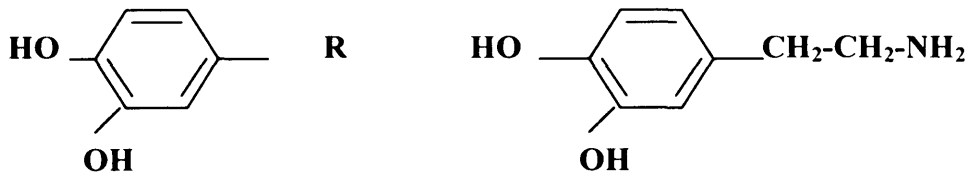

Catechol nucleus

Dopamine (3,4-Dihydroxyphenylethylamine)

Fig 1.4 Catechol nucleus and dopamine structure

Both molecules contain a nucleus of catechol (benzine ring with two hydroxyl groups) and a side chain of ethylene (or one if its derivatatives). R represents the ethylene side chain or its derivatives and thus characterises the catecholamine.

Furthermore they found the distribution of dopamine in the brain to be very non-uniform and more restricted than that of noradrenaline, suggesting a specific functional role for this transmitter (Carlsson et al, 1959). Histochemical fluorescence methods provided basic information on the localisation of catecholamine cell bodies and terminals in the brain, and based on these methods, Dahlstrom & Fuxe (1964) were the first to map out catecholamine pathways. They identified several clusters of catecholamine containing cell bodies and traced the primary axonal projections of these cell groups to various regions. In their classic mapping studies, they designated various noradrenergic and dopaminergic groups with the letter "A", the noradrenergic groups were A1-A7 and the dopaminergic groups A8-A15. Subsequent work (Ungerstedt, 1971b; Lindvall & Bjorkland, 1974) provided more precise anatomical localisation of central dopamine-containing cells, recognising specific subsections of nuclei and their projections.

These described dopaminergic systems have been implicated in a wide variety of behavioural actions including locomotor activity and stereotypy (Ungerstedt, 1971a) feeding (Siegfried et al, 1979; Hernandez et al, 1988), drinking (Gordon et al, 1985; Young et al, 1992), drug reinforcement and brain stimulation (German & Bowden, 1974; Bozarth & Wise, 1984). The pathways are described in more detail in section 1.4.3. The current understanding of the dopaminergic system in the brain is based on two fundamental discoveries: that dopamine-replacement therapy can alleviate Parkinson's disease (Hornykiewicz, 1966) and secondly, that many antipsychotic drugs

are dopamine receptor antagonists (Carlsson & Lindqvist, 1963). Deficits in dopamine systems are implicated in humans with diseases such as Parkinson's disease (P.D) (Ehringer & Hornkiewicz, 1960) and schizophenria (Seeman et al, 1976). This new interest in the localization of dopaminergic systems in the dopamine system rapidly paved the way for other experiments demonstrating the synthesis, uptake and storage, release, degradation and of course, functional effects of this neurotransmitter.

1.4.1 Dopamine Synthesis & Turnover

The precursor for the synthesis of dopamine is the aromatic amino acid tyrosine and its synthesis for dopamine occurs in several steps. Two reactions transform tyrosine into dopamine: the first is hydroxylation by the enzyme tyrosine 3-monooxygenase (or tyrosine hydroxylase, TH), which converts tyrosine into L–3,4-dihydroxyphenlalanine (L-DOPA), Fig 1.4.1a. Tyrosine hydroxylase is an Fe^{2+} containing enzyme and it requires a reduced pteridine cofactor. Consequently, the activity of TH governs the overall rate of formation of all of the catecholamines, and its inhibition is the most effective way of inhibiting catecholamine synthesis. TH inhibitors can work by chelating the Fe^{2+} ions, competing at the pteridine binding site or competing at the tyrosine binding site: an example of the latter is α-methyl-p-tyrosine (AMPT).

When administered systemically, AMPT blocks both central and peripheral TH and not only in the synthesis pathway for dopamine, but for noradrenaline and adrenaline also. Consequently AMPT is nonselective and unfortunately results in unwanted sedation due to depletion of central catecholamines.

The second stage in dopamine synthesis is the decarboxylation of DOPA (Fig 1.4.1b), catalysed by the enzyme aromatic –amino acid decarboxylase (AADC), which removes the carboxyl group from the α-carbon on the side chain. AADC does not work only on DOPA, for example tyramine can be also decarboxylised by AADC and can be taken up into catecholaminergic nerves to be released as a "false transmitter" (Carlsson, 1987). AADC is found in many tissues beside the brain, including the liver, stomach and kidneys and can be inhibited by several drugs, α-methyl-dopa-hydrazine (carbidopa) and 3-hydrobenzyl-hydrazine (NSD1015) which causes an accumulation of DOPA in

the brain. This is the basis of a valuable method for estimating the TH activity in vivo i.e. the rate at which DOPA accumulates is proportional to the rate of TH activity.

(a)

TH is considered to be the rate - limiting step in the pathway and is acutely regulated by end-product inhibition, its maximum velocity is slower than any of the other enzymes in the synthetic pathway.

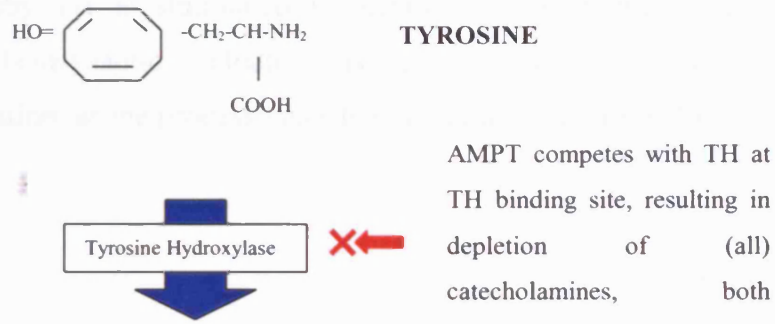

(b)

AADC decarboxylates DOPA to form dopamine. AADC acts on a variety of aromatic amino acids besides DOPA. With other catecholamines norepinephrine and epinephrine, the dopamine is then catalysed by dopamine β-hydroxylase into norepinephrine, dopamine neurons are lacking in this enzyme

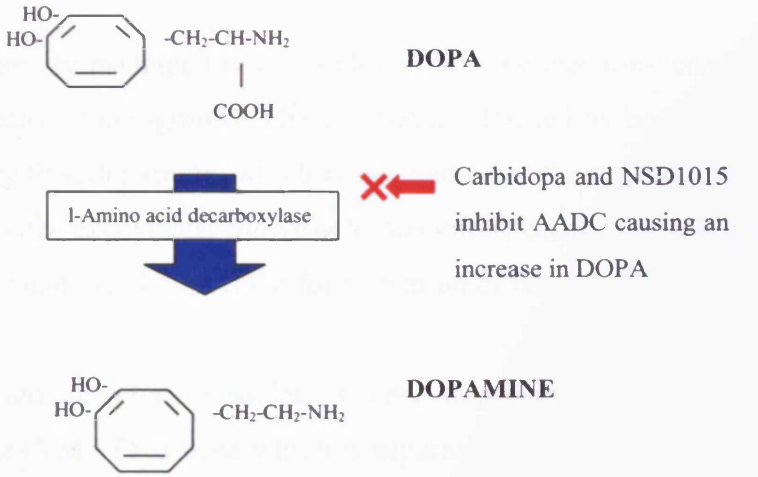

Fig 1.4.1 Dopamine synthesis pathway

Dopamine synthesis is a two-stage process and can be modulated by intervention at tyrosine hydroxylase (a) and AACD decarboxylase (b) stages of synthesis.

Various processes, many exerting their actions via TH, regulate dopamine synthesis. One acute way of regulating TH is by end-product inhibition (Maserano, 1989). This occurs when TH enzyme activity is inhibited by the accumulation of the catechoalamine (the end-product of the synthetic pathway), i.e. coordinating synthesis with ongoing neuronal and secretory behaviour. Another acute modulation of TH is by activation by phosphorylation, initial studies have shown that various protein kinases phosphorylate TH, leading to rapid activation of the enzyme (Edelman et al, 1978; Zigmond et al, 1989). The rate of tyrosine hydroxylation and subsequent catecholamine synthesis is

partly dependant on tyrosine availability, and tyrosine levels in the brain can be decreased by treatment with some amino acids such as phenylalanine, valine or tryptophan, (Wurtman et al, 1974). A more long-term regulation of TH is performed by transynaptic induction, whereby TH is stimulated by neural activity in the fibres innervating these tissues. Transynaptic induction is quite different to rapid phosphorylation induced activation, as the process takes hours (Guidotti & Costa, 1977) as opposed to minutes.

1.4.2 Dopamine Release and Storage

Once synthesized, catecholamines are packaged into vesicles, which are electron-dense and thus appear very dark in electron micrographs. The vesicles are formed by budding off the golgi apparatus, following this, dopamine, which is synthesised in the cytoplasm, is transported into the vesicle. After exocytosis, the vesicle membrane constituents are retrieved from the cell membrane and may be recycled for formation of new vesicles.

Transport of catecholamines into secretory vesicles is very important. A special vesicular monoamine transporter (VMAT) is used which is separate and different from the dopamine transporter (described below). The VMAT contains an ATPase, which translocates protons (H^+ ions) out of the vesicle interior, thereby acidifying the environment (from pH 7.0 to pH 5.5) and creating an electrical potential of around 50mV. The transporter uses the resulting electrochemical gradient across the membrane to concentrate catecholamines within the vesicle. This transporter functions as an antiporter, in that a proton is carried out of the vesicle for each molecule of catecholamine, which is carried in (Johnson et al, 1987).

Reserpine, an alkaloid drug obtained from the plant species Rauwolfia inhibits vesicular catecholamine transport by binding to sites on the transporter and preventing accumulation of catecholamines within the vesicle. By preventing storage in this way, the catecholamine synthesis is initially increased, however a profound depletion soon follows which can last for several days. Reserpine readily enters the brain, and depletion of cerebral amine stores causes sedation, nightmares, mental depression, and

Parkinsonism symptoms. Carlsson et al (1957) demonstrated the DOPA antagonism of reserpine-induced behavioural depression.

It is thought that dopamine can exist in several distinct compartmental pools within the nerve terminal. (Fig 1.4.2).

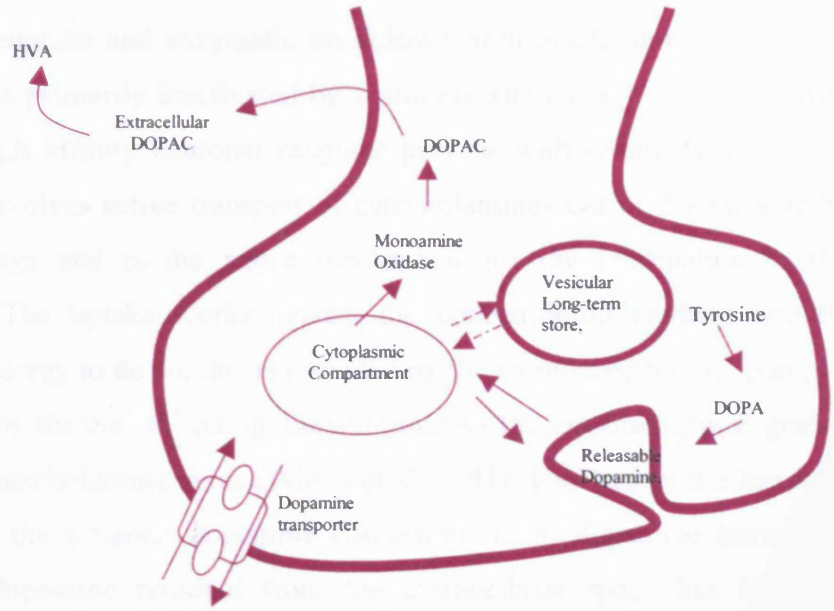

Fig 1.4.2 Model of dopamine pools within the dopamine nerve terminal

Adapted from "Principles of Neuropsychopharmacology" (Feldman et al, 1997)

In general it is thought that newly synthesised dopamine (releasable dopamine) is released preferentially and then replenished by a pool of stored transmitter (cytoplasmic and vesicular dopamine). Dopamine synthesis feeds directly back into a readily releasable vesicular pool and is in equilibrium with the other pools.

Although stimulus induced dopamine release is mainly via Ca^{2+} dependant exocytosis, dopamine release can also be Ca^{2+} independent: dopamine release can be blocked by drugs which inhibit dopamine transporter protein for instance 2β-carbomethoxy-3β-(4-flourophenyl)tropane (CFT) (Raiteri et al, 1979). The dopamine transporter protein takes up the catecholamines from the synaptic cleft after release, this is explained in more detail below (1.4.3), but the transporters can operate in reverse, releasing transmitters from the cytoplasm. In fact drugs releasing catecholamines commonly

operate through reversal of the membrane carrier, for example amphetamine, cocaine and methylphenidate (Pifl et al, 1996).

1.4.3 Dopamine inactivation: reuptake and enzymatic breakdown

Following release at nerve terminals, DA is subject to many routes of inactivation including reuptake and enzymatic breakdown both inside and outside the nerve cells. Dopamine is primarily inactivated by a process known as "Uptake 1" (Iverson, 1974), this is a high affinity neuronal reuptake process with relatively a low maximal rate. Uptake 1 involves active transport of catecholamines out of the synapse back into the nerve endings and is the major mechanism for the termination of the action of dopamine. The uptake works against the concentration gradient and thus requires metabolic energy to do so, this is provided by the membrane Na^+-K^+ pump. By blocking the uptake by the Na^+-K^+ pump, oubain destroys the electrochemical gradient, potently inhibiting catecholamine uptake (Giros et al, 1993). This transporter has a critical role in modulating the synaptic dopamine concentration, in dopamine transporter knockout mice the dopamine removal from the extracellular space has been shown using voltammetry to be 100 fold slower than in control mice. In addition, these mice also showed reduced dopamine synthesis (presumably mediated by end product inhibition), reduced dopamine (D_1 and D_2) receptor gene expression and increased locomotion (Giros et al 1996). The dopamine transporter is in the same family of transporters as 5HT, glutamate and GABA, and although each cell type expresses a particular gene for its own transporter (Amara et al, 1993) the transporter itself may not be so specific for the transmitter it is taking up: for example high concentrations of dopamine transporter have been found in some noradrenaline neurons (Di Chiara et al, 1992). Studies of transporter distribution have shown it is restricted to cells that synthesize the corresponding transmitter, thus providing anatomical segregation that contributes to the specifics of the transport process.

There are a number of drugs which act upon the transporter, for example cocaine, amphetamine (Wise & Bozarth, 1985), methylphenidate (Volkow et al, 1998), mazindol (Dersch et al, 1995) and nomifensine (Garris & Wightman, 1994). All of these have effects on both dopamine and noradrenaline transporters and some, for example

mazindol and nomifensine, are more potent at inhibiting noradrenaline than dopamine transporters (Tatsumi et al, 1997). Tricyclic antidepressants (e.g. desimipramine) are all noradrenaline reuptake inhibitors, although some also possess affinity at 5HT transporters as well (e.g. imipramine and amtriptyline: Pugsley & Lippmann, 1976) but have little or no effect on dopamine transporters. Dopamine reuptake inhibitors include benztropine and piperazine compounds and these are useful for studying binding characteristics and localisation of the dopamine transporter. Such drugs result in increased extracellular catecholamine levels and they enhance neurotransmitter function and have profound psychological and physiological effects.

Reuptake is an extremely effective way of ending synaptic effects of neurotransmitters, however in order to prevent accumulation they must be enzymatically broken down (see Fig 1.4.3). Dopamine catabolism can proceed starting with either O-methylation or oxidative deamination. Dopamine is metabolised extracellularly by catechol-O-methyl transferase (COMT), a Mg^{2+}-dependant enzyme which catalyses transfer of methyl group from S-adenosyl-methionine (SAM) to the 3-position of many catecholic compounds (Zhu, 2002). This enzyme is found in the liver, kidney and heart as well as the brain. Some catechol compounds inhibit COMT. Although useful as a method of modulation of dopamine stores, –O-methylation is a minor factor in normal catecholamine dynamics. Degradation of levodopa in the peripheral nervous system is known to be associated with motor fluctuations and dyskinesia in Parkinson's disease patients. COMT is responsible for much of this degradation, therefore inhibiting COMT activity is one of the methods of extending the action of levadopa (explained fully in section 1.5.1).

Another method of dopamine catabolism utilises monoamine oxidase (MAO) to regulate internal stores of dopamine (se Fig 1.4.3). MAO, catalises the oxidative deamination of several monoamines using flavin adenine dinucleotide (FAD) as a cofactor to produce an aldehyde formed from the primary amine and ammonia and hydrogen peroxide (Kopin 1985). MOA exists in two forms MAO(A) and MAO(B). Knockout mice studies have shown that mice lacking either the MAO (A) and (B) genes display different neurotransmitter metabolism and behaviour (Shih et al, 1999). The distinction between these forms is based on inhibitory sensitivity and substrate

specificity and these in fact are two separate enzymes encoded by separate genes (Bach et al, 1988).

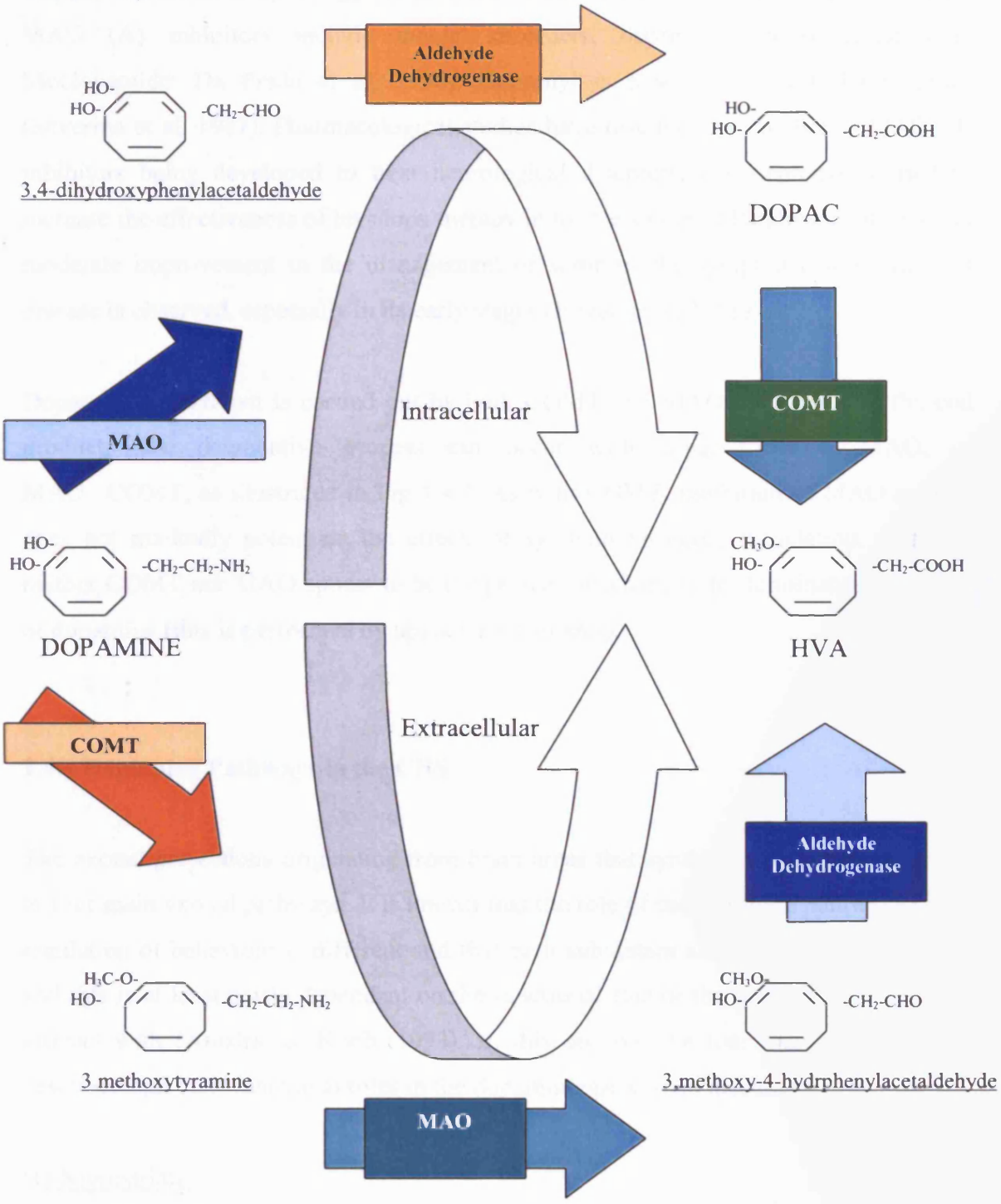

Fig 1.4.3 Dopamine catabolism

Dopamine catabolism can start by oxidative deamination with either MAO or O-methylation by COMT. The concentrations of metabolites are often used as an index of DA turnover and metabolism. These enzymes play an important role in terminating neurotransmitter activity and regulation of catecholamine synthesis in the CNS.

Adapted from "Principles of Neuropsychopharmacology" (Feldman et al, 1997)

The deamination of dopamine and noradrenaline is carried out primarily by MAO(A) and this is inhibited by clorgyline (Branco et al, 1992). Therapeutic implications for MAO (A) inhibitors include mental disorders, depression in particular (e.g. Moclobemide: Da Prada et al, 1998). Deprenyl is a specific MAO (B) inhibitor (Severina et al, 1981). Pharmacological studies have resulted in a number of MAO (B) inhibitors being developed to treat neurological disorders, e.g. deprenyl is used to increase the effectiveness of levadopa therapy in the treatment of Parkinson's disease. A moderate improvement in the management of some of the symptoms of Parkinson's disease is observed, especially in its early stages (Elizan et al, 1991).

Dopamine breakdown is carried out by both COMT and MAO with HVA as the end product. The degradative process can occur with either COMT MAO, or MAO COMT, as illustrated in Fig 1.4.3. As with COMT, inhibition of MAO activity does not markedly potentiate the effects of sympathetic nerve stimulation, therefore neither COMT nor MAO appear to be the primary mechanism for termination of action of dopamine (this is performed by uptake mechanisms).

1.4.4 Dopamine Pathways in the CNS

The axonal projections originating from brain areas that synthesize dopamine give rise to four main axonal pathways. It is known that the role of each of these pathways in the regulation of behaviour is different and that each subsystem also has several functions, and this is at least partly dependant on the functional role of the neuronal systems they interact with (Amalric & Koob, 1993). In this section, the four main pathways are described and their functional roles in the dopaminergic system discussed.

(1) Nigrostriatal

This is the main system, accounting for about 75% of dopamine present in the human brain. The cell bodies of the neurons forming this major ascending dopaminergic pathway are located in the midbrain nucleus of the substantia nigra pars compacta (SNc, A9) and ventral tegmental area (VTA, A10) and the A8 group located caudal to A9 and partly in the retrorubal nucleus (Lindvall & Björklund, 1974). The A9 dorsal component

runs along the medial forebrain bundle (MFB) and internal capsule along with noradrenaline and 5HT fibres, projecting mainly to the caudate-putamen and globus pallidus (Fuxe et al, 1985) forming the nigrostriatal dopamine system (Lindvall & Björklund, 1974). A minor component of the nigrostriatal system projects from the A8 area to the ventral putamen.

The nigrostriatal pathway is involved in the control of movement and its degeneration causes Parkinson's disease, characterised by tremors, rigidity and akinesia underscoring its role in the control of movement (Mendez & Finn, 1975, see section 1.5.1). In addition to its role in the control of motor behaviour, the nigrostriatal system is also known to be involved in certain memory and learning processes (Almaric & Koob, 1987). The nigrostriatal pathway is illustrated in Fig 1.4.4, this central projection is the A9 neurons (substantia nigra) to the caudate nucleus.

(2) Mesolimbic:

The mesolimbic pathway also originates in the midbrain ventral tegmental area (VTA), but these fibres arise mainly from the A10 cell group. The fibres also run in the MFB and project to the nucleus accumbens (ventral striatum), olfactory tubercle and parts of the limbic regions such as amygdala, hippocampus and septum. The mesolimbic dopamine pathway has been implicated in reward systems (see section 1.5.3) emotions and memory. The similarity between hyperactive dopaminergic system and schizophrenia led Arvid Carlsson to propose that the positive symptoms of schizophrenia result from the overactivity of the mesolimbic components of the dopaminergic system, as reviewed by Carlsson (1988), see section 1.5.2.

3) Mesocortical:

The A10 area also sends axons to the cortical areas, e.g. to the medial, prefrontal, entorhinal and cingulate cortices. This is called the mesocortical dopaminergic pathway (Lindvall & Björklund, 1974), and may be involved in some aspects of learning and memory (Simon et al, 1980). This pathway is also known to be involved in the mediation of complex behavioural responses (Kolb, 1984), motivational and reward processes (Bannon & Roth, 1983). However, their exact role is not known, and it is likely that ascending dopaminergic pathways have multiple roles in these functions. For

a comprehensive review of the pharmacology and behavioural pharmacology of the mesocortical pathway see Tzschentke, 2000. The mesocortical pathway is illustrated in Fig 1.4.4.

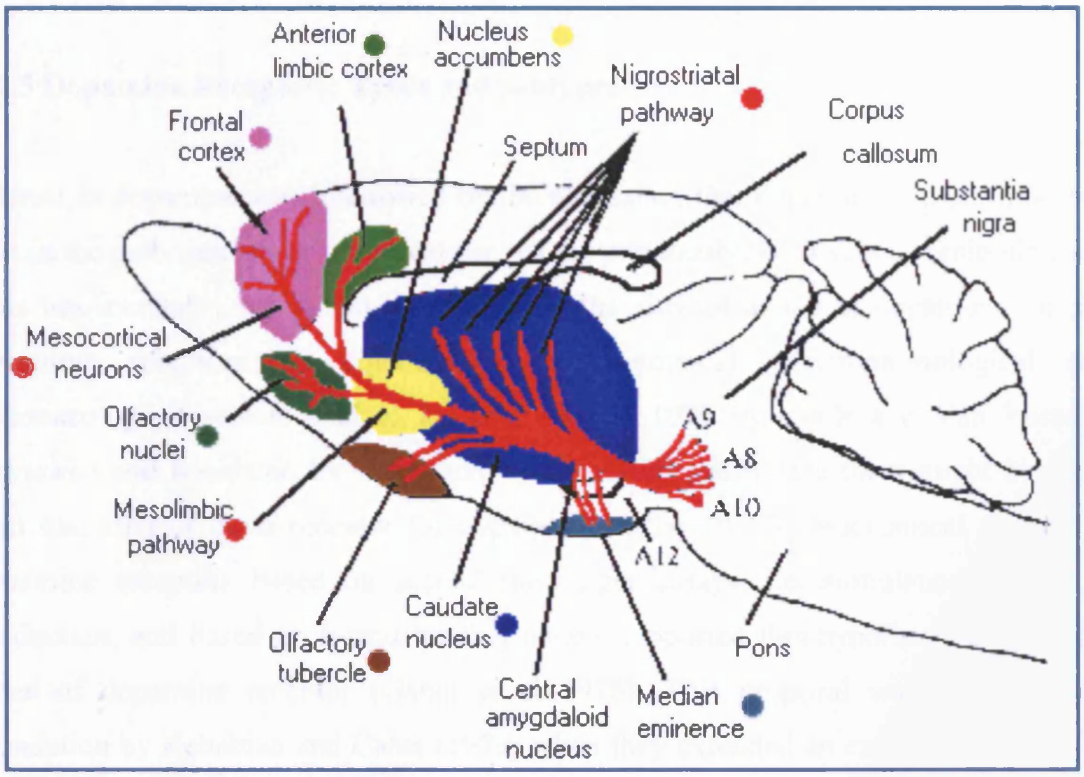

Fig 1.4.4 Dopaminergic Pathways in the rat brain

Nigrostriatal: this central projection is from the A9 neurons (substantia nigra) to the caudate nucleus.

Mesolimbic: fibres run in the MFB projecting to the nucleus accumbens, olfactory tubercle and nucleus, limbic regions, amygdala, hippocampus and septum.

Mesocortical: fibres run in the MFB projecting to the frontal cortex.

Tuberoinfidibular: small projections from the midbrain to the median eminance.

From URL: salmon.psy.plym.ac.uk/year1/DEPRESsion.HTM

(4) Tuberoinfundibular system:

This dopaminergic system consists of a group of short neurons running from the periventular and arcuate nucleus of the thalamus to the median eminance of the hypothalamus. Here they release DA into the perivascular spaces of the capillary plexus of the hypothalamic-hypophyseal portal system. DA is then transported to the anterior

pituitary where it acts on the lactotrophs to inhibit the release of prolactin (Moore et al, 1978), and thus influences lactation and fertility (Davis et al, 1985), and is illustrated in Fig 1.4.4 as small projections from the midbrain to the median eminance.

1.4.5 Dopamine Receptors: Types and subtypes

Interest in dopamine was intensified by the realisation that dopamine had an important role in the pathogenesis or drug treatment of the previously noted serious brain diseases. This has inevitably led to much research on the sites of action of dopamine, i.e. the dopamine receptors. A combination of anatomical, electrophysiological and pharmacological studies lead to the proposal, in 1976 by Cools and Van Rossum, (reviewed and translated by Cools and Van Rossum 1980), that there might be more than one kind of brain receptor for dopamine. In the 1970's, biochemical studies on dopamine receptors based on second messenger assays, i.e. stimulation of cAMP production, and based on ligand binding assays supported this hypothesis of multiple types of dopamine receptor (Garau et al 1978). This proposal was given a firm foundation by Kebabian and Calne (1979) when they extended an earlier suggestion by Spano et al (1978) and proposed that there were two classes of dopamine receptor, D_1 and D_2, with different biochemical and pharmacological properties and mediating different physiological functions. Kebabian & Calne, (1979) described subtypes of dopamine receptor according to whether or not they were linked to activation of adenylate cyclase (the enzyme responsible for converting ATP to cAMP). Thus, stimulation of D_1 receptors activates adenylate cyclase and stimulation of D_2 receptors either inhibits, or does not stimulate adenylate cyclase at all. The anatomical distributions of these two receptor types overlap in the CNS, yet their quantitative ratios differ significantly in particular anatomical areas. It is noteworthy with respect to mental disorders, that both D_1 and D_2 receptors are present in the nigrostriatal and mesocortical pathways.

For ten years, the two-subtype classification could accommodate most of the activities attributed to the dopaminergic system, although the existence of dopamine receptors different from the canonical D_1 and D_2 receptor had been proposed: this proposal had

been refuted when receptors were recognised to exist in two affinity states, inhibition and excitation of adenylyl cyclase activity (Anderson et al, 1990). However it was not until the late 1980's to early 1990s that the true extent of this heterogeneity was revealed by the application of gene cloning techniques to the dopamine receptors (Grandy & Civelli, 1992). The three unexpected dopamine receptors D_3, D_4 and D_5, were discovered using homology screening.

These five distinct dopamine receptors were isolated, characterized and subdivided into two subfamilies: D_1-like and D_2-like based on their biochemical and pharmacological properties (Civelli et al; 1993; Jarvie & Caron, 1993), the D_1-type family comprises D_1 and D_5 receptors and the D_2-type the D_2, D_3 and D_4 receptors. The two different receptor types are linked, respectively to activation and inhibition of adenylate cyclase. In subsequent useage in this work, receptor subtypes defined from cloned genes will be referred to as D_1, D_2, D_3, D_4, D_5 and where only the subfamily of receptor has been defined pharmacologically, the D_1-type and D_2-type nomenclature will be used.

One advantage to the organisms of a heterogenous population of dopamine receptors is that it permits selective tissue-specific expression. This would imply that distinct receptor types are expressed in different tissues, possibly representing functional specialisation of the tissue by receptor distribution. In the central nervous system, the five dopamine receptors each overlap but also exhibit some striking differences in location. In the periphery, the different receptors are mostly expressed in a tissue-specific fashion. Selective agonists and antagonists exist to define the two subtypes in functional assays.

The D_1 and D_2 receptor mRNAs are present in cells in dopaminoceptive regions in the rat brain (Meador-Woodruff et al, 1991). High levels of both receptor mRNAs are present in the caudate-putamen, nucleus accumbens and olfactory tubercle, lower levels in the septum, hypothalamus and cortex (Mansour et al, 1990). Regions where D_2 but not D_1 receptor mRNAs are detected are in the substantia nigra and ventral tegmental area and the hippocampus. Conversely the amygdala contains D_1 receptor mRNA but

little if any D_2 receptor mRNA (Meador-Woodruff et al, 1992). Table 1.4.4 shows the distribution of the two receptor types as detected using in situ hybridisation. The tissue distribution of the D_1 and D_2 receptor mRNAs in the CNS supports their participation in the different areas of dopaminergic neurotransmission that have been described by ligand binding and receptor autoradiography experiments.

Since the distribution of different dopamine receptors overlap in the CNS, some selectivity may be attained quantitatively rather than qualitatively. Firstly, D_3, D_4 and D_5 receptor mRNAs are of one to two orders of magnitude lower than than D_1 and D_2 receptor mRNAs (Sokoloff et al, 1990).

Receptor	Distribution	Ligands
Dopamine D1-type Receptor	Caudate-putamen, nucleus accumbens, olfactory tubercle, substantia nigra, ventral pallidum, entopeduncular nucleus, some amygdaloid nuclei, neocortex, thalamus, hypothalamus, hippocampus, and septum.	Agonists: **SKF38393**; dihydrexidine; Fenoldapam; SKF81297 Antagonists: **SCH23390**; SKF83566 NCC-112; SCH 39166
Dopamine D2-type Receptor	Caudate-putamen, nucleus accumbens, olfactory tubercle, substantia nigra, (pars compacta), lateral septum, superior colliculus, hippocampus and entorhinal cortex.	Agonists: **Quinpirole**; Apomorphine; Bromocriptine; Pergolide Antagonists: **Sulpiride**; Haloperidol Racolopride; Pimozide

Table 1.4.5 Summary of dopamine receptor distribution

The D_1 receptor is the most ubiquitous dopamine receptor. Several research groups have described dopamine receptor binding patterns as detected using in situ hybridisation. Some of the ligands used to stimulate and block D_1-type and D_2-type receptors are shown, (Meador-Woodruff et al, 1991; Jaber et al. 1996).

Relative to the D_1 and D_2 receptors, the D_3 and D_4 receptors are more selectively associated with the limbic region of the brain, a region receiving dopaminergic input from the VTA, which is associated with cognitive, emotional and endocrine functions.

The location of the D_5 receptor mRNA is said to overlap with D_1 receptor mRNA, although this is not universally agreed (Sunahara et al, 1991). However its distribution is agreed to be rather restricted to areas including the hippocampus, hypothalamus, parafacicular thalamic nucleus and thus is thought to be involved in affective, neuroendocrine or pain-related aspects of dopaminergic function. Whilst dopaminergic ligands may easily discriminate between D_1-like and D_2-like receptors, they may not be able to discriminate between members of the same subfamily. D_1 agonist, SKF38393 and D_1 antagonist, SCH23390 have similar affinities for D_1 and D_5 receptors. Table 1.4.4 summarises the relative distributions of D_1-type and D_2-type receptors and the specific ligands for these receptors.

The dopamine receptors harbouring a D_2-like pharmacology have been subdivided into pre- and post-synaptic receptors. The postsynaptic receptors convey second messenger messages in the postsynaptic cells, by affecting a second messenger system, e.g. by decreasing intracellular cAMP levels. The presynaptic or autoreceptors are present on the cells that secrete dopamine. Their stimulation by dopamine is thought to lead to an inhibition of transmitter release, dopamine synthesis and release, thereby regulating dopamine production via a feed-back mechanism. D_2 antagonists acting on such presynaptic inhibitory autoreceptors will increase dopamine release and synthesis by blocking this inhibition and consequently increase the concentration of dopamine metabolites in the brain.

Dopamine D_3 agonists are classified as being selective for presynaptic receptors. In addition, dopamine was found to bind to the D_3 receptor with a 20-fold higher affinity than for the D_2 receptor (Sotnikova et al, 2001). D_2 receptor mRNA is the predominant receptor mRNA in the substantia nigra (Meador-Woodruff et al, 1991) and the presence of the D_3 receptor mRNA in the substantia nigra (a centre of dopamine production), supports the hypothesis that the D_3 receptor also may be a presynaptic receptor.

In general, the D_4 receptor has a lower affinity for neuroleptics than does the D_2 receptor, the exception being clozapine (Van Tol et al, 1991). Clozapine is an atypical antisychotic, i.e. an antipsychotic in which actions are not accompanied by adverse motor control side effects. A corollary is that antagonism of dopamine binding to the D_4

receptor could be an important step in the prevention of psychoses: recognition and characterisation of this clozapine binding site may prove useful in the design of new drug types (Brunello et al, 1995). Data on the tissue distribution of the D_4 mRNA shows that it is most abundant in the frontal cortex, midbrain, amygdala, and medulla (all areas associated with psychotic disorders), and at very low level in the striatum, the site of motor control (Ariano et al, 1997). Thus, the lack of extrapyramidal side effects observed with clozapine treatment may be a reflection of D_4 receptor localisation in the CNS.

Under basal conditions, dopamine could provide an inhibitory influence on striatal transmission (Di Chiara, 1995) by way of D_2 receptors inhibiting neurotransmitter release. Conversely a facilitatory influence on transmission in striatal output areas such as the pallidum and substantia nigra via the D_1 receptors may facilitate neurotransmitter release (Spano et al 1977). Thus, the dopamine system although discrete in pathways, is a complex neurotransmitter system, which can be pharmacologically manipulated at many levels, from intracellular dopamine synthesis and storage stages up to extracellular receptor events.

1.5 Dopamine system dysregulation

The discovery of disorders related to organic dopamine dysregulation has greatly advanced the understanding of the functioning of dopamine systems in the brain. Additionally intervention at the level of dopaminergic transmission has allowed some of these problems to be treated. In the following three sections, dopamine dysregulation in the areas of motor control and affective disorders and the role it plays in reinforcement are discussed, in addition the pharmacological strategies, which may be employed to treat these disorders, are described.

1.5.1 Dopamine in motor disorders- Parkinson's disease

Parkinson's disease (PD) has been known for many years to be a disease of the basal ganglia, and according to Kolb and Whishaw (1990) many of the individual symptoms

of P.D were observed as far back as in the second century by Galen. In 1817 James Parkinson described the "shaking palsy" which now bears his name (Parkinson, 1817). The collective symptoms of PD include muscular rigidity, resting tremor, involuntary movements as well as postural disturbances, increased difficulty in initiating voluntary movement, as well as the less well publicised cognitive deficits (e.g. many PD patients suffer from dementia, depression and other psychological deficits: Dujardin et al, 2001; Slawek et al, 2001). However this may be a reflection of a similar degeneration occurring in other parts of the brain rather than to the damaged basal ganglia. Parkinsonism can occur under a wide variety of conditions (Gybels, 1994), it can be disease related (post encephalitic), and drug induced, for instance from schizophrenia medication.

The first histopathological studies of the brains of PD patients were carried out in the early 1900s. In 1919 Tretiakoff discovered a striking loss of pigmented cells from the substantia nigra of PD patients at autopsy (see Kopin, 1993). These cells were dopaminergic and mainly in the substantia nigra, i.e. cell group A9. Although loss of these cells is a normal process in aging, in PD the progression is far quicker. Another major histopathological finding in PD is the presence of abnormal cytoplasmic inclusions, discovered by Frederic Lewy in 1912, now termed "Lewy Bodies" (Kopin, 1993). These spherical, eosinophilic inclusions are not indicative of PD because they are present in a number of other neurodegenerative disorders such as Alzheimer's disease (Jellinger, 1987), diffuse Lewy body disease (Dickson et al, 1996) and dementia with Lewy bodies (Gomez-Tortoza et al, 1998). Furthermore, Lewy bodies are not found in all PD patients (Brooks, 1995).

The neurochemical origin of PD was discovered in the 1960s by Hornykiewicz, who reported reduced content of both dopamine (Ehringer & Hornykiewicz, 1960; Hornykiewicz, 1966) and HVA (Bernheimer & Hornykiewicz, 1965), in the striatum and substantia nigra of brains of PD patients at post-mortem (typically less than 10% of normal). Further studies have shown that the symptoms of PD only appear when the dopamine content is reduced to 20-40% of normal (Schultz et al, 1982). This loss of dopamine content in the brain can be correlated with the loss of dopaminergic cell bodies in the substantia nigra and degeneration in the striatum.

Animal models have proved invaluable in studying the dopaminergic system and especially with motor disorders: nigrostriatal lesioning or chemically induced depletion of the nigrostiatal tract produce Parkinsonian symptoms in experimental animals (Tolwani et al, 1999). In such animals, damage to the nigrostriatal tract produces a state of denervation hypersensitivity (hyperactivity of the remaining dopamine neurons and upregulation in numbers of dopamine receptors). The PD model favoured by most researchers is the syndrome produced by the dopamine neurotoxin 1-methyl-4-phenyl-tetrahydropyridine (MPTP), a selective nigrostriatal toxin. The evidence for the toxicity of MPTP was clear when Parkinson-like symptoms were produced in a rhesus monkey after MPTP treatment; 1-2 months post treatment nigral degeneration was revealed, in addition to dopamine loss in the striatum (Burns et al, 1983). Human and primates are vulnerable to MPTP-induced toxicity, whereas rats only exhibit transient behavioural deficits after acute MPTP. Mice take an intermediary position between primates and rats, but a definite PD pathology can be produced in some mice strains (Heikkila et al, 1989). Research on the mechanisms by which MPTP produces its effects revealed that the toxin needs to be converted to MPP^+ (1-methyl-4-phenylpyridinium) by MOA (B) (Di Monte et al, 1992). Consequently MAO-B inhibitor prevents MPTP induced toxicity (Stern, 1986).

The most widespread treatment for Parkinson's disease is administration of the dopamine-precursor drug L-Dopa to replete forebrain dopamine content. L-Dopa crosses the blood brain barrier and is converted to dopamine by the enzyme L-aromatic decarboxylase. In the periphery, L-Dopa can be broken down in the bloodstream prior to crossing the blood brain barrier and this degradation is mainly performed by the decarboxylase enzyme. By administering a decarboxylase inhibitor peripherally which is unable to cross the blood brain barrier (carbidopa or bensazide), the amount of L-Dopa available to the CNS increases and L-Dopa can be metabolised to active dopamine. This means the L-Dopa dosage required for a clinical effect can be reduced, thus reducing the severity of the peripheral sympathetic side effects.

L-Dopa therapy has been associated with undesirable side effects and it loses its effectiveness after several years (Sax & Tarsy, 1971; Feldman et al, 1986). Most

patients develop fluctuations in clinical state, about 30% of patients who are treated for 3 years or more, are expected to develop "wearing off effects" (Marsden & Parkes, 1977; Hardie et al, 1984). Subsequently, the motor fluctuations become more complex and unpredictable (Fabbrini et al, 1987; Pahwa et al, 1997). In response to the above controlled release L-Dopa preparations were developed, namely L-Dopa /carbidopa, (Simenet CR^{TM}) and L-Dopa /benserazide (Madopar HBS^{TM}), where the active ingredients are released over about four hours. To minimize the occurrence of PD motor fluctuations, multiple classes of antiparkinsonian drugs can be used, so that low doses of L-Dopa can be used (Mizuno et al, 1994). Dopamine receptor agonists for example, pergolide (Bonucelli, 2002) bromocriptine (Lees et al 2001), apomorphine (Dewy, 2002); anticholinergics (e.g. amantadine) may also be beneficial at an early stage; COMT inhibitors (e.g. entacapone) improved the bioavailiability of plasma L-Dopa (Piccini et al 2000); MAO (B) inhibitors (e.g. deprenyl) is sometimes used in less advanced stages of PD in conjunction with L-Dopa therapy.

L-Dopa remains the most reliably effective and best-tolerated antiparkinsonian medication. It will continue to have a central role in the medical management of PD for the foreseeable future. The most crucial unanswered question in Parkinson's disease is its fundamental cause. Since Carlsson's original suggestion that dopamine may involved in the control of motor function and in the Parkinsonian syndrome (Carlsson, 1959), and the now-classic paper by Ehringer and Hornykiewicz (1960) which showed the significant reduction of striatal dopamine concentration in patients PD and postencephalitic parkinsonism, a vast amount of work has focused on the biochemical and pharmacological correlates of this dopaminergic system failure, particularly involving the nigrostriatal pathways. However, with few exceptions, there has been less focused and concerted research effort on looking at direct causal factors or primary initiating events in this disease process. As in Alzheimer's disease, another of the degenerative diseases of the brain of unknown origin with a specific biochemical substrate, there is no single etiologic hypothesis for Parkinson's disease- such as a virus infection, an age-related immune system dysfunction, a genetic disorder, a "trophic" substance, or a toxin. The selective involvement of specific transmitter-defined neuronal pathways, the non-specificity of the brain lesions that define the disease, and

the clinical involvement of a sizeable segment of the aging population remains to be explained.

1.5.2 Dopamine in Psychotic disorders: Schizophrenia

The notion of "dementia praecox" was introduced by Kraeplin to describe a new mental illness, Eugen Bleuler renamed the group of mental disorders with poor prognosis "group of schizophrenias", because for him the splitting of personality was the main symptom (Kraeplin, 1913; Bleuler, 1950). The discovery by dopamine pharmacologists, Carlsson & Linqvist, (1963) that many antipsychotic drugs are dopamine receptor antagonists was to fundamentally change our understanding of brain disorders. The investigation of the mechanisms of action of antipsychotic agents (Creese et al, 1976) has in turn resulted in the formulation of the dopamine hypothesis of schizophrenia (Carlsson, 1988) and the generation of a large number of new antipsychotic compounds. Dopamine overactivity has been the predominant pathophysiological hypothesis of schizophrenia for the past two decades.

Schizophrenia is a thought disorder in both form and content, with age onset in late teens to early twenties. Patients suffer abstract unfounded delusions, abnormal perception. They may also experience hallucinations (mainly auditory) and may also perceive tactile stimulation. The emotional stability of schizophrenics tends to be altered and emotions may be blunted. It is common for patients to be precoccupied with thoughts and delusions, both physically and emotionally. There are a great number of symptoms, but these are not seen in all patients and there can also be great variation in the severity of this disorder. Thus schizophrenic states were further categorized into catatonic, paranoid and disorganised (Kraeplin, 1913). This historical classification system is frequently disputed, as discrete symptoms do not conveniently cluster in such a way as to validate these categories (Boyle, 1990). A more simplistic way of describing distinct schizophrenic syndromes Type I (displaying positive symptomology) and Type II (displaying negative symptomology) as proposed by Crow (1980). The positive symptomology consisting of the more elaborate symptoms like delusions, hallucinations, disordered speech and behaviour. Groups with such symptoms respond

well to dopamine antagonists and their symptoms are exacerbated with drugs that increase dopamine release, e.g. amphetamine (Kessler et al, 1996). The negative-type schizophrenia involves reductions in normal functioning, including in speech and emotion and reduced energy and drive. Antipsychotic therapy does not work well on this group.

Alzheimer (1897) was the first to investigate the neuropathology of schizophrenia. The results of subsequent neuropathological studies were disappointing because of confliciting findings. Research interest thus waned and did not flourish again until 1976, following the pivotal CT finding of ventricular enlargement (Johnstone et al, 1976). Subsequently, progress in brain imaging in this disorder has been made, with the first MRI study in schizophrenia reported by Smith et al (1984). These advances have lead to the discovery of a number of brain abnormalities in schizophrenia: i.e. the presence of ventricular enlargement in 80% of studies; third ventricle enlargement in 73% of studies; involvment of medial temporal lobe structures in 74% of studies and the superior temporal gyrus in 100% of studies and many other anatomical lesions (see review by Shenton et al, 2001), however there is no signature abnormality.

In 1952, Delay and co-workers (Delay et al, 1952) reported the use of chlorpromazine (Thorazine) to treat psychosis. They initiated an important advance in the treatment of schizophrenia without a clear understanding of the mechanisms underlying the drug's therapeutic effect. In 1963, Carlsson (Carlsson & Linqvist, 1963) first postulated that the effects of antipsychotics were secondary to dopamine receptor blockade. The thiothanxines, phenothiazines derivatives like chlorprothixine, and the butyrophenones derivative, haloperidol are amongst the traditional drugs used to treat schizophrenia.
Typical antipsychotics like haloperidol, chlorpromazine and thioridazine work by blocking dopamine D_2 receptors in the brain, which helps to limit some effects from the disorder. However the major problem with antipsychotics is their side effect profile, which included acute extrapyramidal effects (Conley, et al, 1998) due to effects on D_2 receptors in the basal ganglia (tremor, slowing down of the movements, stiffening of the muscles, a Parkinson-like syndrome) as well as tardive dyskinesia, a similar involuntary disorder (Rasmussen 1997). Haloperidol is not as effective for long-term therapy as newer drugs: thioridazine has a much lower probability of causing extrapyramidal side effects than haloperidol or chlorpromazine, (Rabinowitz & Davidson, 2001; Dufresne,

et al 1993). There are other positive aspects of typical antipsychotic drugs when compared to the atypical drugs including that typical antipsychotics have generally been found to effect memory or executive functioning to a lesser degree than "atypical" drugs (Earnst, et al, 1999).

Clozapine and the other atypical antipsychotic agents (for example sulpiride, olanzepine and risperidone) produce the lowest incidence of extrapyramidal side effects, and are effective in drug-refractory patients and more likely to exhibit improvement in the positive symptoms of schizophrenia. Some compounds have the affinity for multiple receptor, for example clozapine, which has the ability to bind to serotonergic, α-adrenergic, muscarinic and histaminergic (Roth et al, 1998). Furthermore, it appears as though the more that $5HT_2$ receptor occupancy exceeds D_2 receptor occupancy, the more atypical an antipsychotic agent is (Meltzer et al, 1996).

Determining the correct antipsychotic dosage is difficult as therapeutic effectiveness takes 3-6 weeks. It is well established that some of the beneficial/adverse clinical effects are delayed in onset, even though dopamine receptor blockade occurs immediately (Freed, 1988). The biphasic response to antipsychotics is effective in reducing symptoms of schizophrenia because it acutely blocks both and presynaptic and postsynaptic dopamine D_2 receptors. The blocking of the presynaptic auto-inhibitory receptors increases the amount of dopamine released, however the postsynaptic receptors that are also blocked, acutely attenuate dopaminergic transmission. Thus, initially dopamine D_2 receptors are upregulated and a mechanism known as depolarisation blockade occurs. Evidence that depolarisation block in the mesolimbic and nigrostriatal neurons caused antipsychotic and extrapyramidal effects, whereas those which caused depolarisation block only in the mesolimbic neurons (for example clozapine), did not show extrapyramidal effects were shown by Bunney (1992). Clinical effectiveness can be graded on the ability to create depolarisation block in the mesolimbic neurons. Additionally, the timescale for the depolarisation block to appear is similar to the clinical effectiveness of the antipsychotic.

If an animal model for schizophrenia with predictive validity could be developed, the potential for developing drugs to help combat this disease would be great. The understanding of both the long-term effect of antipsychotic treatment, neurochemically

and metabolically, would improve, as well as the investigation of the actual neurochemistry of schizophrenia *in vivo*. This is indeed a difficult task as schizophrenia is largely a disease of thought, and the complex personality changes demonstrated in humans are not possible in animals. Traditional animal models were based on direct dopaminergic manipualtions in order to simulate putative overactivity of the dopamine system, for example induced by LSD (Braff & Geyer, 1980) or amphetamine (Robinson & Becker, 1986). Consequently, it is not surprising that the resulting drugs, which emerged, exert antidopaminergic activity, whereas the actual disease process is know to also involve the transmitters 5HT and glutamate. New animal models address the possibility that altered dopaminergic activity may in fact be secondary to a developmental neurodegenerative malfunction in the cerebral cortex. Animal models as described, which aspire to possess construct validity, are gestational malnutrition, early life exposure to severe stress, social isolation, perinatal infection (Pearce, 2001), cortical neuronal dysgenesis amongst others (McKinney & Moran, 1981).

In the absence of convincing evidence that any single transmitter system is disregulated in schizophrenia, pharmaceutical research into this disorder is faced with considerable problems in developing more effective therapies. Future studies will likely benefit from studying a more homogenous population of patients so that the relationship between pathological findings and clinical symptoms becomes more meaningful, and indeed studying at-risk population such as family members diagnosed with schizophrenia would be highly advantageous. Furthermore, methods using functional brain analysis such as fMRI simulaneously with structure measurements will help move towards an understanding of this complex disease.

Having described the dysregulation of the dopaminergic system in movement (PD) and psychosis (schizophrenia), there remains another area of dopamine involvement, which also commands much research, and in the following section the involvement of dopamine systems in reward and reinforcement is discussed.

1.5.3 Dopamine involvement in brain reward systems

In humans it is known that reward controls goal-directed behaviour and involves learning because it acts as a positive reinforcer. The neural basis of reward and reinforcement has been investigated using numerous experimental approaches including creating brain lesions, psychopharmacology, electrical self-stimulation (see reviews, Di Chiara, 1995; Robbins & Everitt, 1998), single neuron recording (Apicella et al, 1991) and neuroimaging (Koepp et al, 1998; Martin-Soelch et al, 2001). These studies largely indicate that dopamine neurons are involved in reward processing and reinforcement.

Olds & Milner (1954) discovered while testing various electrode placements in the rat brain, that some areas (notably the septal areas and tegmentum) were reinforcing such that the animal would self-stimulate by means of pressing a lever at frequent and lengthy intervals. Although, several independent systems can support brain stimulation reward (Phillips, 1984), the rewarding effects from electrode placements along the medial forebrain bundle (MFB) probably represents activation of a common reward substrate. German and Bowden (1974) compared the distribution of electrode placements effective in supporting brain stimulation reinforcment behaviour with the distribution of catecholamines. They showed a close correspondence between sites supporting brain stimulation reward and brain regions containing catecholamine fibres, cell bodies, and terminal fields. Furthermore, the anatomical mapping studies seemed to provide strong support for the notion that rewarding stimulation directly activated dopamine neurons (see Wise, 1980).

Empirical evidence indicates that the reinforcing properties of psychoactive drugs are mediated by the mesocorticolimbic dopamine system. Studies show that most psychoactive drugs (including cocaine, amphetamine, nicotine, opiates and ethanol) increase extracellular dopamine concentration in this system, especially in the nucleus accumbens (Koob & Le Moal, 1997), furthermore that these drugs facilitate intracranial self-stimulation and place preference and are self-administered in both animals and humans (Wise, 1996). These observations suggest that drug addiction is a dopamine-dependant disorder in which the positive reinforcing value of the drug is mediated through the activation of the mesolimbic dopamine system (Di Chiara, 1999). It has been suggested (Di Chiara et al, 1998) that drugs of abuse are biochemically

homologous to naturally rewarding stimuli. Many drugs of abuse mimic the incentive properties of natural stimuli and their ability to stimulate mesolimbic dopamine pathways. Of course dopamine neurons did not evolve to mediate cocaine reward, but presumably evolved to mediate the reinforcing effects of natural rewards, since investigation revealed that other rewarding stimuli such as food and sex may also involve stimulation of the mesoaccumbens dopamine projection (Lupien & McEwan, 1997).

Disruption of dopamine synthesis (Cooper, et al, 1971; Stinus & Thierry, 1973) or blockade of dopamine receptors (Lippa, et al, 1973) attenuates the rewarding effects of MFB stimulation. Microinjections of the dopamine-receptor antagonists apomorphine & haloperidol (Broekkamp & van Rossum, 1975; Phillips & Fibiger, 1979), spiroperidol (Mogenson et al, 1979) or antipsychotic, cis-flupenthixol (Stellar & Corbett, 1989) directly into the nucleus accumbens attenuate brain stimulation reward. This suggests that this dopamine terminal field is critically involved in the rewarding effects of MFB stimulation. Several studies (Koob et al, 1978) suggest that severe dopamine depletions disrupt the rewarding effects of MFB stimulation. Further evidence of the involvement of these dopamine projections in reward-mediated behaviour is that 6OHDA lesions in the nucleus accumbens but not in the dorsal striatum, affect conditioned place preference of opiods (Shippenberg et al, 1993).

Drugs of abuse, belonging to widely different pharmacological classes, increase extracellular dopamine in various terminal dopamine areas as estimated using brain microdialysis in freely moving rats (Di Chiara & Imperato, 1998). This property applies to amphetamine-like and cocaine-like psychostimulants (Kuczenski & Segal, 1992; Hurd & Ungerstedt, 1989a) narcotic analgesics (Rossetti et al, 1992), nicotine (Brazell et al, 1990), ethanol (Wozniak et al, 1991), phencyclidine (Di Chiara et al 1988), and delta(9)-Tetrahydrocannabinol (^{9}THC, Ng Choung Tong et al, 1988). The mechanisms by which drugs of abuse stimulate dopamine transmission differs depending on the pharmacological class to which each belongs. For example, narcotic analgesics disinhibit dopamine receptors at the VTA by GABA (Leite-Morris et al, 2002). Nicotine, in contrast, stimulates acetylcholine receptors located presynaptically on

dopaminergic projections from the ventral tegmental area (VTA) to the NAc (Fisher et al, 1998) and phencyclidine by NMDA receptors also at the VTA.

To the extent that biological factors contribute to drug abuse vulnerability, it is important to understand the mechanisms that control the rewarding effect produced by various drugs of abuse. The observed involvement of dopamine in the reinforcing effects of cocaine and amphetamine has stimulated interest in the use of drugs that modify dopamine transmission as possible candidates for the treatment of psychostimulant abuse. However, only limited efficacy has been reported in clinical trials using a number of dopamine agonists and antagonists (Withers et al, 1995; Izzo et al, 2001). Understanding these mechanisms may provide insight into novel pharmacotherapies targeted at treating and preventing drug abuse.

1.6 Scope of this thesis

The scope of this thesis is two-fold, firstly it is intended to create a robust animal model for phMRI of the dopaminergic system, using well-documented experimental drugs within the magnet, during image acquisition. This will involve optimising of image sequencing, resolution and development of a basic technique for the experiments, in addition to development of image processing protocols. It must be noted that the software used to perform these tasks was designed for human imaging analysis and is often used clinically. Many of the groups who perform small animal fMRI use in-house software specifically designed for that purpose (Chen et al, 1997; Hyder et al 1997; Burdett et al, 1995). Therefore a further aim of this thesis is to validate the software (SPM '99) for use in small animal fMRI and phMRI and hopefully develop a useful protocol for other investigators. The second aim is to extract both spatial and temporal information from this two-dimensional data, and interpret these events throughout the whole brain, and during the entire experiment. This may permit subtle temporal and spatial characteristics of specific drugs to be observed, such that complete pathways of pharmacologically stimulated brain tissue can be visualised. Furthermore, by using ligands for particular receptor types to stimulate and block receptors, one may be able to investigate the specific functions of different receptor types.

It is hoped that this new area of phMRI shall allow more information on pharmacological events to be gleaned from single experiments than was possible with the previously noted techniques, which often focus on simply one brain area or one single time-point. Furthermore, manipulations of the well-researched dopamine system may lead us closer to the true meaning of the BOLD signal and it's relationship to neuronal and synaptic events. As described later (section 2.7) the BOLD signal is derived from a metabolic event and not directly related to synaptic events, this leads to the question of the specificity of BOLD MRI itself. Importantly, will the fMRI signal show any discrimination between excitation and inhibition? This is a particulary relevant question when approaching experiments involving systemic administration of dopaminergic psychostimulants, as other transmitters, excitatory (glutamate) and inhibitory (GABA) will be also stimulated indirectly.

Previous fMRI studies have mainly found significant increases in BOLD signal and subsequently interpreted this, as due to an increase in neurotransmitter release, this perhaps is a rather simplistic approach. All of the facets of brain activity are not individually represented by metabolic responses, i.e. synaptic activation, synaptic inhibition, action potentials, subthreshold depolarisation are all translated into just one dimension of the metabolism or blood flow according to just one energy need, (Jueptner & Weiller, 1995). This change is not induced by neuronal activity, such as synaptic activity or action potentials, but rather by their consequent energy requirement inducing a metabolic response. Uptake of glucose is found to be associated with critical, event-coupling energy consumption and neuronal activity (Mata et al, 1980). If inhibitory and excitatory events show the same type of changes, the metabolic maps and blood flow maps are ambigious with regards to the underlying neurophysiological event. Thus "increased brain activation" *really* means a state of certain volume of brain tissue which, through the summation of neuronal (and non-neuronal) events, is associated with increased energy need and blood flow, thus the physiological event could be, excitation, inhibition or any other energy consuming process.

Chapter 2

Nuclear Magnetic Resonance Theory

2.1 Introduction

Nuclear magnetic resonance, a chemical analytical tool that has been used for over 50 years, is based on the absorption of radio-frequency (RF) energy by the magnetic moments of atomic nuclei in samples placed in a strong magnetic field. The spatial resolution obtained in *in vivo* MRI is comparable to that of *in vitro* fixed and sectioned tissue, thus MRI is highly suitable for morphometric structural analysis. NMR can also take the form of MRS, which involves noninvasive measurement of chemical composition of tissue metabolites. The recent discovery that MRI can be used to map changes in brain haemodynamics that correspond to neuronal operations extends the traditional anatomical brain imaging to include maps of brain function. In having this ability to observe the structures which participate in specific functions, fMRI (often referred to as "brain mapping") provides a high resolution, non-invasive assessment of neural activity that is detected by a blood oxygen level dependent signal (Ogawa, et al, 1990, 1992, 1993; Belliveau, et al, 1991). fMRI involves relative quantification of changes in brain activation compared to the basal or non-stimulated state. Furthermore, fMRI gives superior spatial resolution compared to that of PET, thus the anatomical localisation of fMRI tissue changes can be defined precisely and quickly.

This ability to observe brain function directly opens an array of new opportunities to advance our understanding of brain organization, as well as setting a potential new standard for assessing neurological status. A rapidly emerging body of literature also documents corresponding findings between fMRI and conventional electrophysiological techniques to localize specific functions of the human brain (Ives, et al, 1993; Puce, et al, 1995; Burgess, 1995; Detre, et al, 1995; George, et al, 1995). Consequently, the number of medical and research centres with fMRI capabilities and investigational programs continues to escalate.

fMRI relies on detection of changes in local brain haemodynamics and metabolism: such as regional CMR_{glu}, CMR_{O2}, CBF and CBV that accompany neural activity in the brain. Preliminary fMRI studies required exogenous contrast agents to be administered and their passage through the brain during stimulation was subsequently examined. Subsequently, it was discovered that deoxyhaemoglobin (dHb) has magnetic properties

which oxyhaemogloblin (Hb) does not have, and as such can act as a natural endogenous contrast medium.

When there is an increase in neuronal activity, the increase in blood flow occurs without an increase of similar magnitude in oxygen extraction (Fox and Raichle, 1986), this results in a corresponding local reduction in dHb:Hb ratio. BOLD contrast is a method of detecting neural activation, based on the proportion of Hb and dHb in the brain vasculature and is the most widely used fMRI technique. As 70% of the human brain's volume consists of capillaries and venules, it is not surprising that changes in local haemodynamics result in measurable signal changes. The interplay between CMR_{glu}, CMR_{O2}, CBF and CBV leading to fMRI signal are discussed and illustrated in section 2.7. The following section introduces the fundamental principles of fMRI, current applications and some potential future directions for its potential use.

2.2 Basic principles

NMR relies on the principles of electromagnetisation and particular properties of electromagnetic waves. Electromagnetic waves travel at $3x10^8$ ms^{-1} and consist of two components, an electric field and a magnetic field, which are perpendicular to each other. Both waveforms travel at the same speed, both waveform components are sinusoidal and are 90^o out of phase with each other. The change in the magnetic field generates the electric field, the change in the electric field generates the magnetic field and consequently electromagnetic waves are self-propagating, and have the same angular frequency (ω). NMR utilises the magnetic field component, as use of the electric field component would generate potentially harmful heat: in MRI much lower energies are generated and thus lower frequencies are generated.

In MRI, substances are broadly categorised into three different magnetic susceptibilities which pertain to their ability to become magnetised when placed in a magnetic field: (i) diamagnetic substances are basically non magnetic (they contain no unpaired orbital electrons); most bodily tissues including Hb have this property; (ii) paramagnetic substances are magnetised when placed in a magnetic field and demagnetised when it is switched off, they contain unpaired electrons, examples include hydrogen with one

unpaired electron and dHb with 4 unpaired electrons; (iii) ferromagnetic substances are permanently magnetised after being placed in a magnetic field. The majority of tissues in the body are diamagnetic, including bulk water. Bulk magnetism depends on electrons, whereas NMR depends on nuclei (protons and neutrons). This is described in more detail in section 2.5.1.

NMR relies on the fact that most elements have at least one reasonably abundant isotope whose nucleus is magnetic. When there are an odd number of protons, there will always exist one proton that is unpaired and is pointing north or south giving its own net magnetic field or a magnetic dipole moment (MDM) to the nucleus, which is denoted by the symbol μ. The nuclei of elements like hydrogen (^{1}H), and Fluorine (^{19}F) have these properties, and in fact any element that has an odd atomic number can be used in MRI. NMR can only be performed on isotopes whose natural abundance is high enough to be detected. However, hydrogen being extremely abundant (in body water and fat) is most commonly assessed with this technique.

2.2.1 B_0 field

The external magnetic field is denoted B_0, in MRI, B_0 is in the order of Tesla, with one tesla being equal to 10000 Gauss. In reality, B_0 is not completely uniform, instead standard uniformity is in the order of 6-7 parts per million (ppm) and can be achieved using shim coils (these help by minimizing magnetic field inhomogeneities to create more uniform external field B_0).

In the absence of an external magnetic field (B_0) the axes of the MDMs are arranged such they cancel each other out and the net magnetisation in zero (Fig 2.2.1a). When an external magnetic field B_0 is applied, the MDMs will align (Fig 2.1.1b), approximately half pointing North and half pointing South. Hydrogen protons have 2 energy states, one parallel with B_0 and one antiparallel with B_0. The nuclei requires less energy when aligned with B_0 than when aligned against B_0, thus as time passes more protons join the net alignment of B_0. Eventually enough extra spins will point north to make the net magnetisation point in the direction of B_0 and this new equilibrium magnetisation is

known as M_0. In this configuration, B_0 is applied along the Z axis and the Z component of magnetisation M_Z equals M_0.

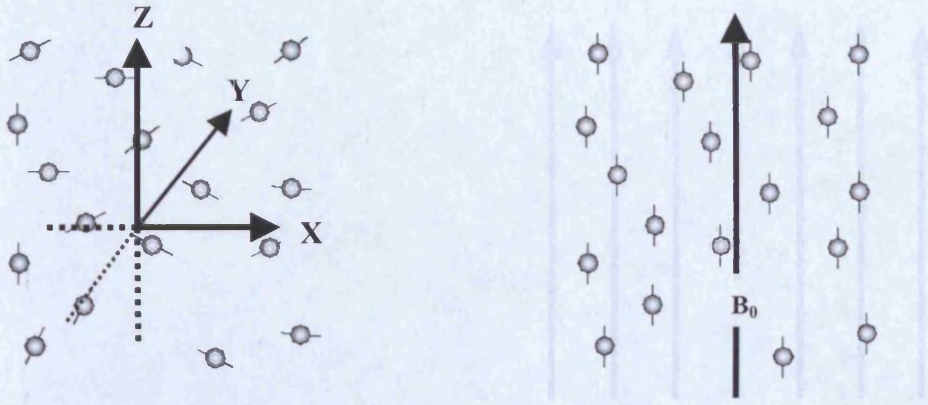

(a) (b)

Fig 2.2.1 Application of external magnetic field B_0

If spinning unpaired protons (a) are exposed to a strong magnetic field B_0, this causes their nuclei to form a net unidirectional alignment along the direction of the applied field (b) in the Z plane.
From http://www.cs.sfu.ca/people/Faculty/stella/ 2.2Basic Priniciples of MRI

2.2.2 RF Pulse

The electromagnetic pulse used to achieve a signal in MR is a weak but rapidly alternating magnetic field. It is termed an RF pulse, because its frequency corresponds to that window of the electromagnetic spectrum. If an RF pulse is placed near to B_0, the orientation of the nuclei will change relative to the direction of the strong magnetic field. Energy is absorbed and when the RF pulse is turned off, it is then is released in radiowaves (Fig 2.2.2b), allowing the nuclei return to their original equilibrium state positions.

For each atomic species investigated, a wave of a particular frequency is transmitted. Thus resonating nuclei of different elements and isotopes behave like miniature radiowave transmitters with characteristic frequencies and can be identified by the signal frequencies they release. For example, in a static magnetic field of 1T, the

resonance frequency for hydrogen is 40 MHz but for potassium it is 1.7 Mhz and so these frequencies are used to identify the chemical species.

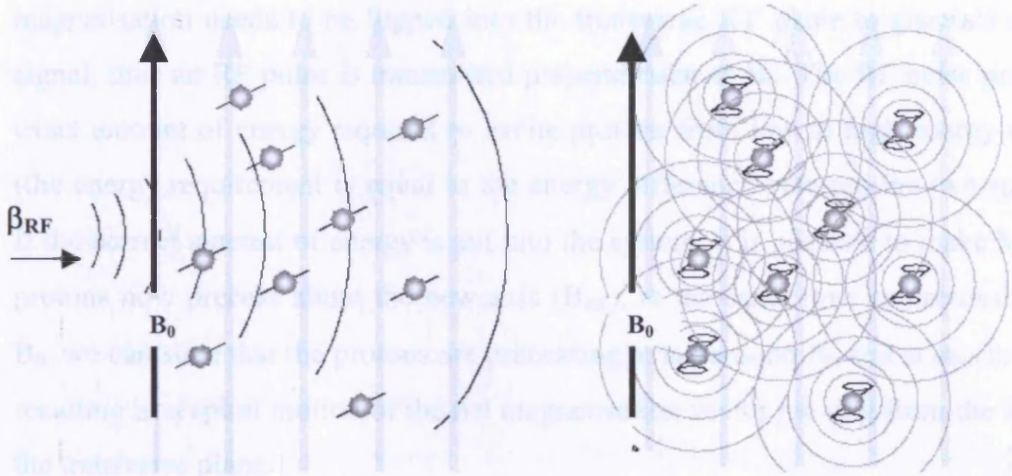

(a) (b)

Fig 2.2.2 Application of radio frequency pulse

The RF pulse knocks spins out of alignment with B_0 (a.) and provides energy for subsequent gyroscope-like motions. (b). Energy is absorbed and then is released as the nucleus returns to the equilibrium state. From http://www.cs.sfu.ca/people/Faculty/stella/ 2.2Basic Priniciples of MRI

Thus the strength of the signal is an indicator of the density of the nuclei (e.g. hydrogen) in the plane of the magnetic field, which can vary in different molecular environments. The transmitted signals are converted into images or spectra. The proton is now not only rotating about its own axis, but also the axis of B_0, and precesses much faster about its own axis than that of B_0. The rate at which the proton precesses around B_0 is given by the (Larmor) equation (Table 2.2.2).

$$\omega = \gamma B_0$$

ω=precessional frequency (The angular frequency can be described in MHz or radians/s.)

γ = gyromagnetic ratio (a fixed proportionality constant depending on the nucleus your dealing with).

B_0= external MF strength, in Tesla

Table 2.2.2 The Larmor equation

The reason an RF pulse is required to tip the oscillating nuclei out of the B_0 plane is that it is only possible to transmit and receive signals that oscillate in particular axes. The longitudinal magnetisation is not oscillating and cannot be read by the receiver, the magnetisation needs to be flipped into the transverse XY plane to generate a readable signal, thus an RF pulse is transmitted perpendicular to B_0. The RF pulse provides the exact amount of energy required to excite protons from low to high energy spin states (the energy requirement is equal to the energy difference between the two spin states). If the correct amount of energy is put into the system, it is possible to make $M_Z=0$. The protons now precess about the new axis (B_{RF}), at the same time as precessing around B_0, we can state that the protons are precessing at ωo around B_0 and at ω_{RF} around B_{RF}, resulting in a spiral motion of the net magnetisation vector moving from the Z axis into the transverse plane.

2.2.3 Signal Generation

Because of interactions between spinning protons (dephasing) and the presence of magnetic field inhomogeneities, the signal received as the protons realign with B_0 over time will decay to zero. The freely precessing spins induce a current in the receiver coil and decay over time, hence this is known as a free induction decay (FID, Fig 2.2.3a).

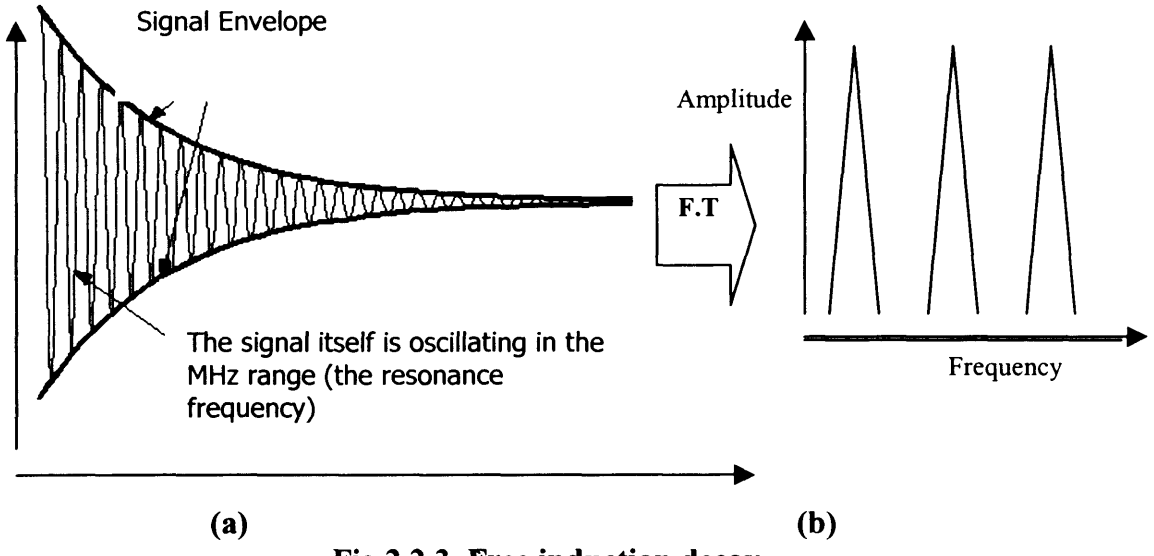

Fig 2.2.3 Free induction decay

The decaying sinusoidal waveform of the received signal. showing the decease in current amplitude after the RF pulse is switched off over time. Fourier transformation converts the FID into a range of frequencies (spikes).

To detect this NMR signal it is necessary to have an RF coil in the transverse plane, i.e. perpendicular to the B_0 field. The signal measured is an electromotive force (e.m.f), which is induced in the coil and is proportional to transverse magnetisation. A mathematical equation, i.e. Fourier transformation of the FID converts the signal from the time domain to the frequency domain to give the value of the change (Fig 2.3.3b).

2.2.4 Longitudinal (T1 relaxation)

M_Z is referred to as longitudinal magnetization, as there is no transverse (Mx or My) magnetisation in this plane. After application of a resonant RF pulse, which disturbs the spin system, there is a subsequent process of returning to equilibrium and an exchange of energy occurs between the spin system and its surroundings. Such a process is termed spin-lattice relaxation. The changing direction of magnetisation back to the direction of B_0 along Mz follows an exponential curve, which is known as T1 (Fig 2.2.4) and the equation for T1 is presented in Table 2.2.4. The constant of the curve is dependant on both the magnetic field strength and the tissue being examined, e.g. biological tissues have a shorter T1 at 0.5T than at 1.5T.

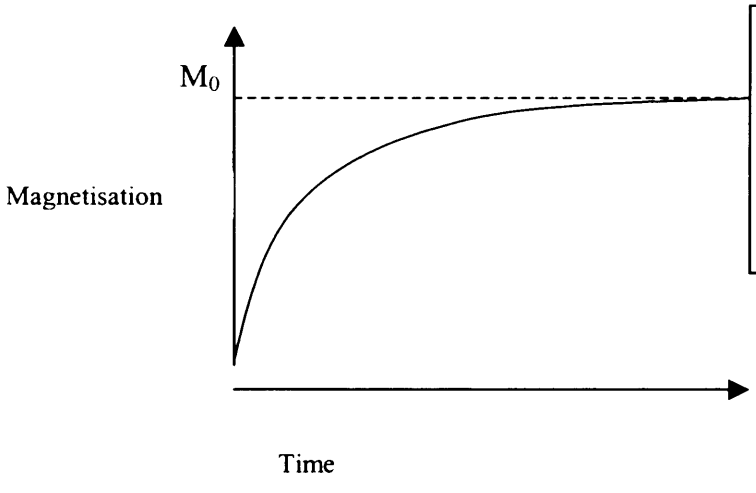

Table 2.2.4 Equation for T1

The function of the exponential curve is given as $M_z = M_0 (1 - e^{-t/T1})$.

Fig 2.2.4 T1 curve

The changing direction of magnetisation to the direction of B_0 follows an exponential curve. As time passes, more protons join the net alignment of B_0 to reach equilibrium magnetisation M_0. This curve, a representation of net magnetisation over time is given the constant T_1.

For a given compound, relaxation (loss of energy) times vary for atoms with respect to the environment, for example water in cerebrospinal fluid (CSF), bone and fat have different mobile proton densities resulting in variations in net magnetisation and T1.

2.2.5 Transverse (T2 relaxation)

The proton spins not only exchange energy with the surrounding lattice but also amongst themselves. The transverse component rotates about the direction of the applied magnetisation B_{RF} and after the RF pulse is turned off, the net magnetisation in the transverse (XY) plane returns to zero. Transverse relaxation is generally a faster process than spin-lattice relaxation and is known as spin-spin relaxation time. T2 is also affected by diffusion, i.e. on how rapidly the spins spread out and leave the lattice, however this component is very small as compared to spin-spin interaction. Meanwhile the longitudinal magnetisation grows until we have M_0 along Z, consequently T2 is always less than or equal to T1.

In reality two factors contribute to the decay of the transverse magnetisation: molecular interactions (a pure T2 molecular effect) and variations in B_0 (an inhomogeneous T2 effect). Decay of transverse magnetisation is the combination of both factors. The combined time constant is termed T2 star (T2*). T2* can be very much shorter than T2. The relationship between the T2 from molecular processes and that from inhomogeneities is given in Table 2.2.5.

Table 2.2.5 Relationship between the T2 and T2*

$$1/T2^* = 1/T2 + 1/T2_{inhomo}$$

$$1/T2^* = 1/T2 + \gamma B$$

2.2.6 Image Weighting

The relaxation times T1 and T2 are very important in imaging as they have the greatest effect in determining contrast. In fMRI, changes in the activation map are solely due to changes in either one of the two or both of ^{1}HNMR relaxation rate constants T1 and T2.

Although most MRIs reflect a complex combination of proton concentration and T1 and T2 contrast, these parameters can be separated into almost pure images. Relaxation times are affected by many variables: temperature, viscosity, and motions of the nuclei, magnetic effects of nearby nuclei. Emphasising one or more of the relaxation times can be used to discriminate tissues of various compositions or define pathological processes.

After perturbation with an RF pulse from its initial alignment, the proton changes its alignment with the magnetic field and its subsequent recovery back to B_0 is rather slow (0.1-1s). If another RF pulse is applied before the recovery is complete, then a smaller signal is obtained, as the system has not fully magnetised. Reducing the signal intensity in such a way is described as saturation. Spins that have recovered quickly will have greater available Z-magnetization prior to imaging than those that recover slowly, such that the signal produced depends on the rate of recovery of Mz. By varying the time between pulses (repetition time, TR) or varying the pulse angle, the contrast between tissue regions of both long and short T1 can be changed dramatically. Typically T1 weighted sequences employing 90^{o} excitation pulses have TR values of a few hundred ms.

It is possible to obtain the real value for T2 by refocusing the effect of field inhomogeneity on the transverse magnetisation using a spin-echo (2.4.1). The time between the RF pulse and the centre of the signal observation window (this is when the signal is digitally sampled) is the time-to-echo (TE) and is in the order of ms. T2 weighted sequences deliberately induce a delay to extend TE before measuring the signals, to allow transverse relaxation to occur (and conversely if the image is to have negligible T2 weighting, then TE is as short as is practical). A decrease in the amount of dHb during brain activation induces a signal increase in T2-weighted spin echo, and a somewhat larger signal increase in T2* in gradient echo weighted imaging: this is the

basis for BOLD imaging. A T2 map can be made from images with different in the same manner in which the T1 map is made form images with different TRs.

2.3 Spatial Encoding

A homogenous sample in a uniform magnetic field B_0 will emit a single signal when the FID is Fourier transformed. If the signal is acquired in the presence of a linear gradient Gz, the frequency spectrum will show different frequencies with a separation proportional to their spatial separation, and this can be transformed into images with the frequency of a given signal, as an indicator of spatial location. To allow slice selection in any orthogonal or paraxial direction, MR systems are equipped with 3 sets of gradient coils concentric with the magnet which produce orthogonal gradient fields. In each case, the direction of the field produced is parallel to Z (in a conventional super-conducting magnet) and B_0.

The three gradients are known as the slice select gradient (Z), the phase-encoding gradient (Y) and the frequency-encoding or readout gradient (X) and these gradients are used in a three-dimensional (3D) coordinate system. To produce a 3D image, the FID resonance signal must be encoded for each dimension and this is achieved by creating intentional inhomogeneities in the magnetic field.

2.3.1 Slice Selection

Slice selection is used to isolate a single plane in the object being imaged, by only exciting the spins in that plane. A magnetic field gradient along the Z direction (G_z) generates a distribution of magnetic field strengths, which are superimposed on the main magnetic field B_0, and consequently of frequencies which are linearly dependant on spatial positions. This causes the Larmor frequency of the RF pulse to correspond to the Larmor frequency of that slice. The protons not in that slice will not match Larmor frequency and thus will not be excited. If the RF pulse consists simply of one frequency, the slice obtained will be infinitely thin, therefore a range of frequencies is used in the RF pulse using the bandwidth to determine the slice thickness. Another way

to change the thickness of the slice is to change the steepness of the gradient: decreased for thicker slices and increased for thinner slices. Because the RF pulse does not have a simple rectangular shape a problem arises when imaging multiple slices, instead it follows a more bell-shaped or Gaussian shape (Fig 2.3.1). In changing the shape of the pulse to have a wider centre and a narrower frequency range (i.e. more rectangular) a narrower slice can be encoded. Another means by which one can obtain a narrower slice is by changing the gradient field strength, a steeper gradient means a narrower slice for a given pulse.

(a) (b)

Fig 2.3.1 Ideal and actual RF pulse shapes

Ideal RF pulse

Rectangular shaped Fourier transforms positioned side by side

Real RF pulse

Crosstalk : arrow shows overlap

When imaging two slices close together, "crosstalk" (an artefact due to interference between adjacent slices of a scan) can be introduced (2.3.1b). Having a minimum spacing between slices can eliminate this, i.e. a gap is left between consecutive slices. However, a possible trade-off is a partially sampled volume, and the possibility of missing a discrete lesion or other important structure. Another issue is the amount of time taken to encode many slices, as complete recovery from the RF pulse is required between excitation of different slices. Thus an interleaved approach is often chosen, for example 1,3,5,7,9,2,4,6,8,10. This way individual slices suffer minimal artefactual effects from previous slices. Once the slice has been selected, it must be further encoded so that spatial information about the two-dimensional (2D) slice structure can be obtained, as the echo is a signal from the whole slice. This can be achieved by performing projection or 2D Fourier transformation.

Back projection is the method that was used to acquire the first MRIs (Hounsfield, 1973). Following slice selection, a gradient is applied along the X-axis and the projections of the spin densities onto that axis are obtained by Fourier transformation of the FID. If the frequency is proportional to X position, this Fourier transform will directly give the spatial location of signals along X, i.e. a one-dimensional projection of the spin density. If the experiment is repeated at an angle to the X-axis, by using a combination of X and Y gradients, the projections can be obtained at a different angle. By repeating this operation up to 180^{o}, a set of projections can then be constructed using back projection distributing the measured spin densities evenly relative to the axis on which it was acquired. By reconstructing all of the angled projections, a 3D image is obtained. However it is unfortunately very dependent on external magnetic field inhomogeneities and is very sensitive to magnetic field gradients thus is prone to artefacts.

Projection reconstruction has largely been superseded by 2D Fourier transform or spin-warp imaging due to its lack of sensitivity to MR inhomogeneities and gradients (Fig 2.3.2b). The 2-D reconstruction in each axial slice is accomplished using phase and frequency encoding, as described in the following sections (2.3.2 and 2.3.3).

2.3.2 Phase Encoding

The G_y gradient is turned on after the RF pulse and before G_x. After the 90^{o} pulse all the protons in the selected slice precess at the same frequency (ω_0). However, this gradient causes the protons in the top row to start to precess faster than the middle row (but in phase with each other) due to the higher magnetic field. The middle protons do not experience a change in magnetic field and continue to oscillate at the same frequency as prior to the gradient being applied (Fig 2.3.2). Likewise, the protons in the bottom row will slow down relative to those in the middle row. After the Gy gradient is switched off they will return to their original precessional frequency. What is important to note is that permanent phase shift has occurred in the protons of each row.

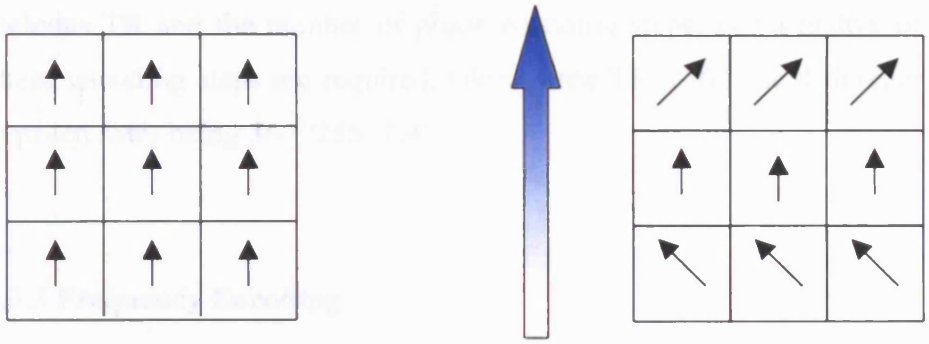

(a) **Fig 2.3.2a Phase encoding** (b)

Without phase encoding, all protons precess in phase with frequency ω_0

After Phase encoding, the phase depends on position in G_y

This gradient has caused a permanent difference in phase throughout the samples, moreover this is reflected as a difference in spatial position. The timing sequence of these gradients and the RF pulse are displayed in the spin warp diagram (Fig 2.3.2b).

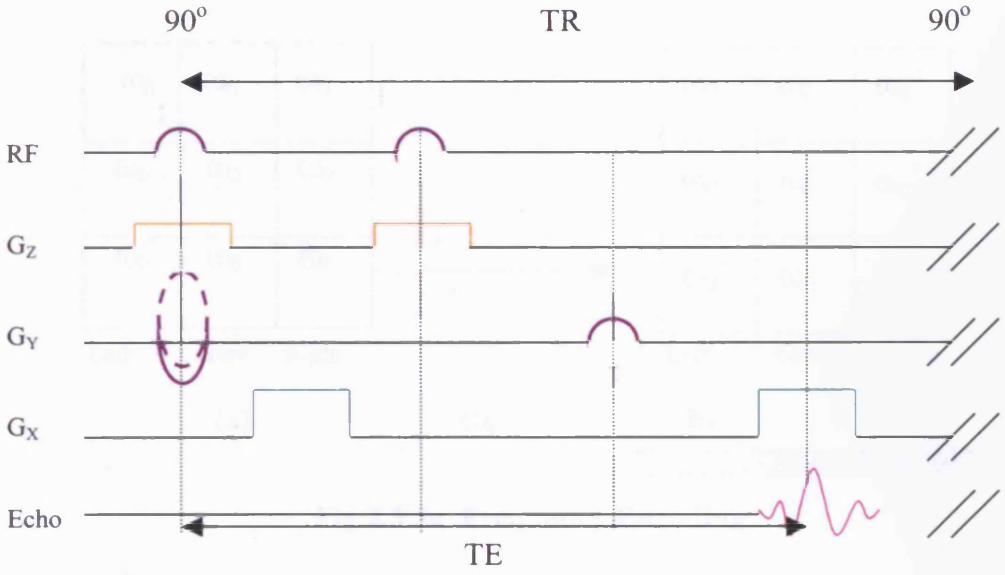

Fig 2.3.2.b Spin warp diagram

Slice selection gradient G_z is turned on during the RF pulse

The Gy gradient is usually applied between the 90° and 180° pulse or between 180° pulse and echo (as above), and the frequency encoding gradient G_x is turned on during readout.

Phase encoding is a time-consuming process. For each row of pixels, there is a phase encoding step, which is really a new spin-echo after a 90° pulse, therefore a separate TR is required for each phase encoding step. Part of the formula describing TA

includes TR and the number of phase encoding steps. For a matrix of 256x256, 256 phase encoding steps are required, taking time TRx256. The difference in phase shift between rows being $360^{o}/256=1.45^{o}$.

2.3.3 Frequency Encoding

The principle of frequency encoding is not much different from phase encoding, i.e. G_x encodes the frequency of the transverse magnetisation as a function of the position. If a gradient G_X is applied when the echo is produced and signal acquired, the frequency of the detected signal will depend on the position along X. If this gradient is applied from left to right, the centre column of the slice will experience no change in magnetic field strength, thus the frequency will not be affected. As the number of protons stays the same - the amplitude is also unaffected; the right side of the slice will experience a strengthening and on the left of the slice a reduction in magnetic field (Fig 2.3.3a).

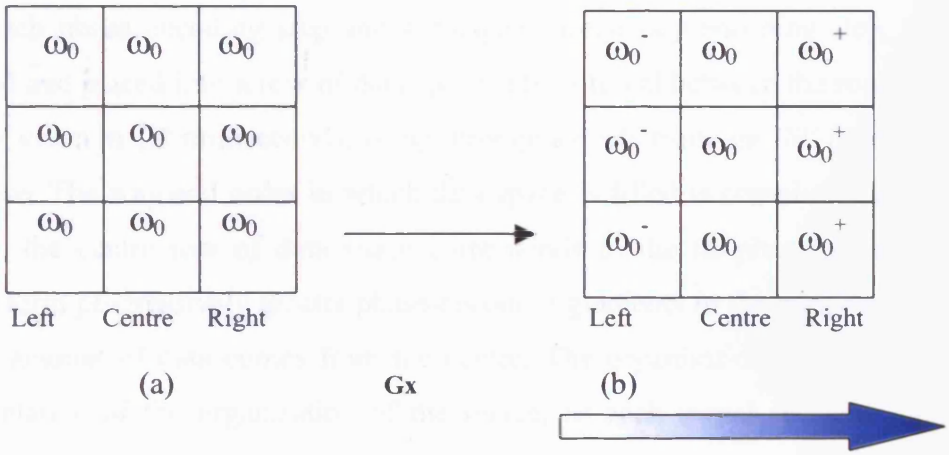

Fig 2.3.3a Frequency Encoding

Without Frequency encoding all protons precess with frequency ω_0

With Frequency encoding, the precession frequency depends on position in G_x

The sum of the signals in the column are additive. The frequency of the column represents the sum of the amplitude of the pixels in that column. The way that frequency encoding works is that frequency and position have a one-to-one relationship.

The way the 3 gradients work together to give each pixel it's own identity is illustrated in Fig 2.3.3b.

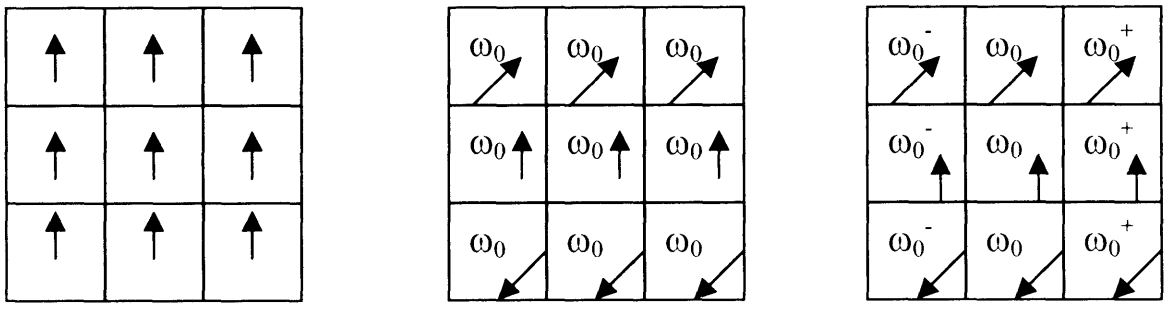

Fig 2.3.3b Spatial encoding

After phase and frequency encoding, each pixel has its own coordinate identity.

2.3.4 Data Space and k-Space

With each phase encoding step and subsequent frequency encoding step, a signal is received and placed into a row of data space. The interval between the rows in the data space is given in TR milliseconds, going through a cycle from one 90° pulse to the next 90° pulse. The way and order in which data space is filled is completely arbitrary, but usually, the centre row of data space corresponds to the no-phase gradient and the echoes form progressively greater phase-encoding gradients in the periphery so that the greater amount of data comes from the centre. The organisation of data space is not representative of the organisation of the image, as each signal contains information about the entire picture. Each signal in data space is the sum of all the signals from individual pixels in a slice and is in the time domain, therefore the data must be digitised and become k-space so that it is in the spatial frequency domain, which is accomplished via sampling. To cover the whole of k-space it is necessary to repeat the sequence with variable gradient strengths of phase encoding each time. It is desirable to have as much signal as possible for each FID, and a necessity that the amount of transverse magnetisation available immediately after the RF pulse is the same for each line. This can be achieved by keeping TR constant throughout image acquisition. Allowing the longitudinal relaxation to recover totally is costly in time and consequently it is usual to have a TR which is less than T1 and maximise the signal by

having a small flip angle (<90°): this angle is known as the Ernst angle (Ernst et al, 1966).

2.4 MR Pulse sequences

A pulse sequence is a series of RF pulses applied repeatedly during an MR study. Embedded in the pulse sequence are TE and TR parameters and related components. In the experiments described in the chapters 5, 6 and 7, spin-echo (SE) sequences were used. SE and gradient echo (GE) comprise the two most important pulse sequences, and as such are explained in this section, with examples of their usage and shortcomings. Using the principles of GE, developments have been made to improve scan time and image quality such as echo planar imaging (EPI) and 3- dimensional gradient echo however these techniques are beyond the scope of this study but are described in detail elsewhere (Hashemi & Bradley, 1997).

2.4.1 Spin Echo

The observation of NMR signal depends on the generation of phase coherence which is finite to T2* relaxation. Spin echo is one of the most important sequences in MR as it can be used to filter out components with short T2 relaxation times and allow the acquisition of an artefact-free FID. By generating spin echoes, T2 can be separated from the magnetic field inhomogeneities which is very important because, following a 90^0 pulse, phase coherence is generated and disappears exponentially with the time constant T2*, obscuring information about T2.

A simple spin echo sequence like the Hahn sequence (Hahn, 1950), firstly involves a 90^0 pulse, i.e. a transverse magnetisation along the Y axis. During the subsequent delay, magnetisation along the Y axis diminishes. Secondly, an 180^0 RF pulse is applied making the magnetisation vectors rotate about Y` by 180^0 and again the magnetisation along Y diminishes. This is very important, because the phase of each spin is mirrored in the Y axis by the 180^0 pulse and thus the spins will be aligned at the end of the second delay to form a SE. At the top of the SE, the B_0 field inhomogeneities

are refocused and the signal decrease is caused by pure T2 relaxation. Similarly, the Carr-Purcell-Meiboom-Gill method (Carr & Purcell, 1954) uses spin echo, each successive 180^0 pulse are applied forms a spin echo (fig 2.4.1a). By applying such refocusing pulses the signal is lost to magnetic field inhomogeneities but not spin-spin dephasing, thus the FIDs decay over time exponentially with T2 as given by $e^{-t/T2}$.

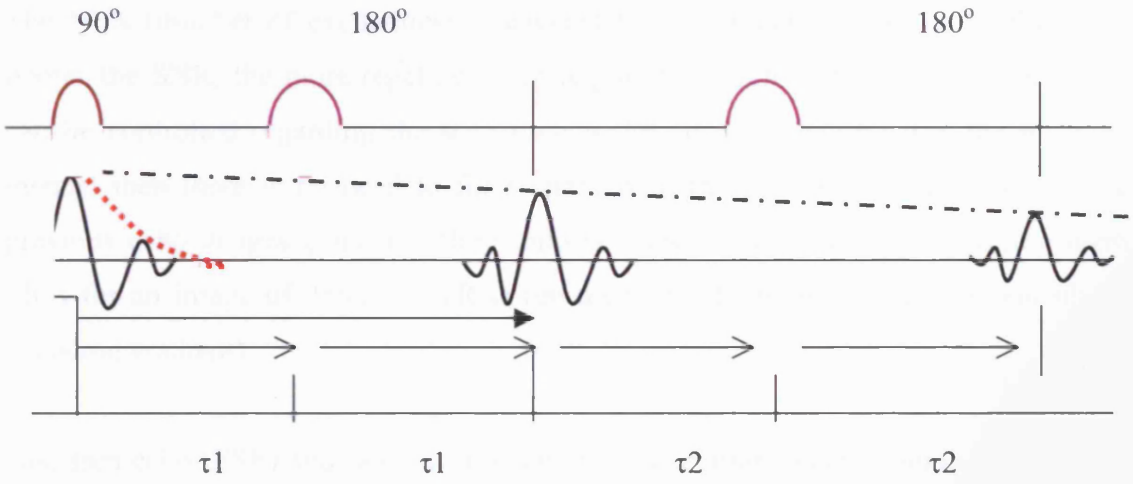

Fig 2.4.1a Spin Echo

$TE_1=2\tau1$

The decay of every individual spin echo is governed by T2* relaxation, the decrease of the amplitude of echo tops is fully controlled by T2. The refocusing pulses regains all of the signal lost to MF inhomogeneities.

($e^{-t/T2}$) Curve for exponential T2 decay

($e^{-t/T2*}$) Curve for exponential T2* decay

Adapted from Hashemi & Bradley (1997)

In conventional SE sequences two echoes are often obtained (Fig 2.4.1a), i.e. if we apply two 180^o refocusing RF pulses and obtain an echo from each one. However it is possible to have as many echoes as desired. With each TR in a conventional SE there is a single phase encoding step. Each of the echoes following each 180^o pulse is obtained after a single application of the phase encoding gradient in SE. Each echo has its own k-space and fills in one line of k-space. In SE, each k-space will generate a different image: a first echo image then a second echo image, e.g. so with eight 180^o pulses generating 8 echoes, that is 8 different k-spaces for the 8 different images. The relationship between the phase encoding steps and scan time is given in Table 2.4.1.

Table 2.4.1 Relationship between the phase encoding steps and scan time

time = (TR) x (Ny) x (NEX).

Where TR is repetition time;
Ny is the number of phase encoding steps and is dependant on the resolution required;
NEX is the number of excitations (repetitions)

The NEX (number of excitations) is selected for the signal to noise ratio (SNR), the poorer the SNR, the more repetitions are required. Therefore, the only parameter that can be controlled regarding the scan time is TR. If the last echo was the image of interest then there is no need to fill k-space with the previous echoes, however the previous echo-images come for "free" and no time is saved in not performing them. Thus for an image of 256x256, TR is repeated 256 times (each at a different phase-encoding gradient).

Fast spin echo (FSE) and rapid acquisition with relaxation enhancement (RARE) were first proposed by Hennig (1986), and have become integral aspects of routine fMRI experiments. FSE is an elegant way of manipulating the conventional SE technique in order to save time. Using the same example as above, if we start with 8 echoes but only one K space, which is to be filled 8 lines at a time, i.e. the single k-space is filled using data from all 8 echoes. Within 1 TR (one "shot") 8 lines are accumulated in the single k-space, similarly with the next echo, 8 lines will be acquired and fill the same k-space. This means that that TR need be repeated 256/8=32 times and consequently the scan time is cut by a factor of 8. Echo train length, (ETL, number of echoes) can lie anywhere between 1 and 256 and echo spacing (time interval between successive echoes) is typically 16-20 ms, the echo spacing is important as the effective TE (TE_{eff}) is an integer of multiples of the echo spacing. Therefore in a T2 weighted image, a long TR and a long TE are required. For example if a TE of 100ms is required, then with an ETL of 8 and an EPS of 17ms (100/17=5.9), the sixth echo provides the most accurate TE_{eff} at 102 ms (6x17=102, Fig 2.4.1b).

The centre of k-space carries the maximum signal, thus the 6th echo is placed into the centre slab of k-space. Unlike in conventional spin echo, in FSE a different value is placed on the phase encoding gradient before each 180° pulse.

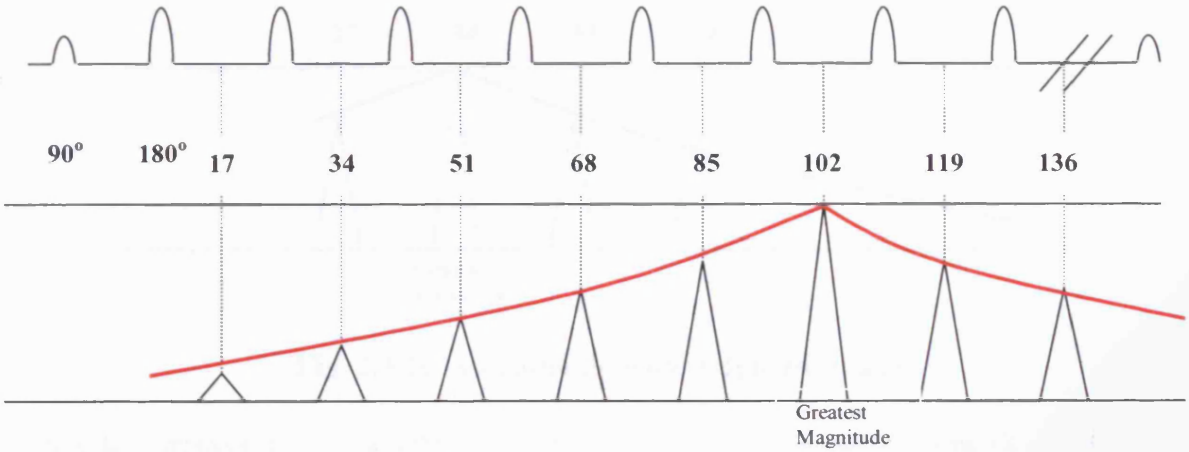

Fig 2.4.1b A T2 weighted image

In this example, a TE of 100ms is required, therefore the 6th echo with TE of 102 is the effective TE. The echo corresponding to TE_{eff}, sixth echo has the largest peak. As the TE moves from TE_{eff}, in either direction the signal amplitude gets smaller. Adapted from Hashemi & Bradley (1997)

A phase encoding step with the lowest strength is chosen for the 180° pulse before the echo chosen as the TE_{eff}. Each subsequent phase-encoding step is chosen with progressively greater amplitude of G_y. The result is that the largest signal comes from the TE_{eff} echo and progressively decreasing signals from the other echoes (Fig 2.4.1b). The signals from the 6th echo are placed in the centre of data space and the signals from the echoes experiencing greater phase encoding gradients fall into slabs further away from the centre.

By definition, the maximum signal comes from the TE_{eff} but other echoes are still obtained for the other TEs. This is because the echoes are being averaged, but it is a TE_{eff}-weighted average. By putting the echoes from the other TEs in slabs further away from the centre of k space, their influence on image contrast is reduced. Using the same echo spacing, the FSE can give a proton density weighted image (Fig 2.4.1c). Only 4 phase encoding steps are used, and k-space has only four slabs. The longest echo

contributing to the contrast of the shortest TE (17ms) is 68 ms, which is substantially smaller than TE_{eff} for T2, thereby eliminating T2 effect on a T1-weighted image.

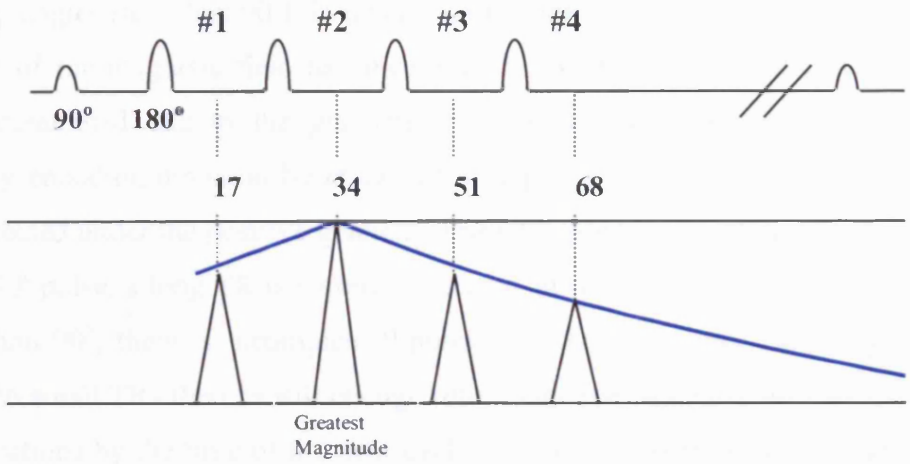

Fig 2.4.1c A proton density weighted image

The echo corresponding to TE_{eff} is the second echo. Instead of long TR and TE, a long TR and short TE are utilised. In selecting a TE of 30 ms, it is clear that the second echo (TE_{eff} of 34 ms) is the most appropriate with TE of 34 and so it has the largest peak. As the TE moves from TE_{eff} in either direction, the signal amplitude gets smaller.

Adapted from Hashemi & Bradley (1997)

Limitations of SE

If the microscopic field distortions have dimensions much smaller than 25μm, the diffusion path has lead water molecules randomly through many local field gradients, which means that the phase changes cannot be reversed by spin echo methods. Thus spin echo sequences are intrinsically sensitive to field changes with dimensions on the order of the diffusional path during the TE. The trade-off of using FSE is that the longer the ETL chosen, the fewer the number of slices can be used in a study. In one TR with an ETL of 8, a certain number of slices can be obtained, if an ETL of 16 is to be used, it will take twice as long to receive the echo thus only half of number of slices can be obtained in one TR.

2.4.2 Gradient Echo

The major purpose of GE technique is to reduce scan time. This is achieved by using small flip angles (less than 90°). In this technique, the echo is produced by reversing the direction of the magnetic field to cancel out the position-dependant phase shifts that have accumulated due to the gradient (Fig 2.4.2). GE dephases the spins in the frequency encoding direction by means of a negative gradient pulse and the signal is then collected under the positive gradient. The rationale behind GE is that when using a 90° or 180° pulse, a long TR is requires to create an echo. So if a flip angle is used that is less than 90°, there is incomplete flipping into the XY plane, still producing M_{xy}. Even with small TRs there is still enough time to recover and have enough longitudinal magnetizations by the time of the next cycle. A major proportion of the magnetisation remains in the Z plane after the RF pulse producing M_z, allowing images to be obtained in less than a second. In GE, the echo is formed by dephasing the FID, and recalling it at time TE.

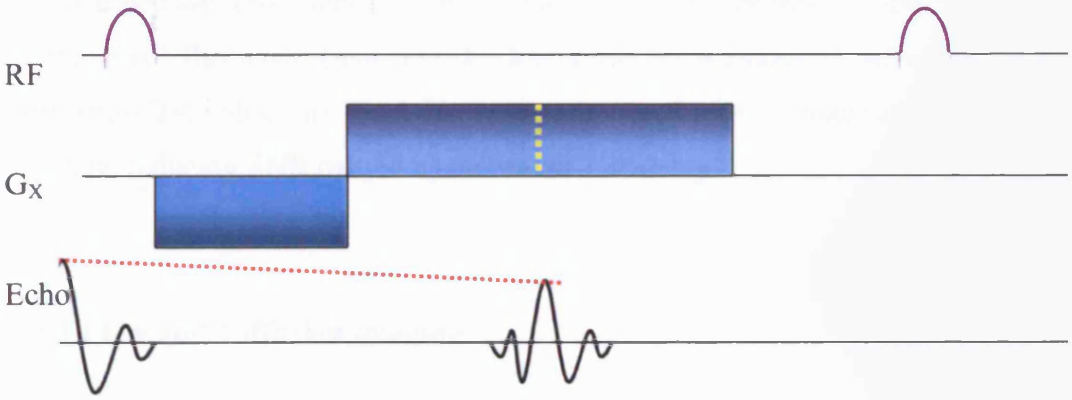

Fig 2.4.2 Gradient Echo Sequence

By applying frequency encoding gradient in G_x direction, the spins are intentionally dephased in the transverse plane thereby eliminating the FID. The area under the negative lobe is equal to half of the area under the positive lobe, and the refocusing happens at the midpoint of the positive lobe (dotted line) into a readable echo. Adapted from Hashemi & Bradley (1997)

An advantage that GE has over SE is the simplicity with which tissue contrast can be varied. In a GE sequence, contrast is proton-density weighted at small flip angles and T1 weighted at large flip angles. This occurs because with a small flip angle, there is large amount of longitudinal magnetization after the RF pulse. Consequently recovery will not take as much time, therefore there will not be much difference between the T1

of one tissue and another and thus it is not T1-weighted. This contrast is not T2-weighted either, as the transverse magnetisation is very small. However, if the TR is short (TR<3T2*) and TE is long, then T2* weighting is achieved. SNR in GE reduces per echo due to the shorter TRs used, however this can be compensated by obtaining more echoes per unit time.

Disadvantages of using GE

A particular type of chemical shift artefact can affect gradient echo imaging. Because of their individual molecular structure, hydrogen protons in water precess at slightly higher frequencies than in fat. This means that water will soon get out of phase with fat and then come back into phase again within a particular time period. This problem can be avoided by carefully selecting TE so that they are in phase, and by suppressing fat. One other disadvantageous aspect of GE sequences is the magnetic susceptibility effect of not using an 180^{o} refocusing pulse. This is caused by static field inhomogeneities and is especially prominent at bone/air interfaces. Also decreased SNR is common due to the small flip angle (reducing the transverse magnetisation), which is worsened if very short TR values are used. However compared to FID imaging, GE uses a longer TE, thus reducing SNR caused by increased T2* delay.

2.4.3 Flow and Diffusion imaging

Where a tissue slice with many blood vessels is being imaged, the spins will not be stationary throughout the imaging process. A slice is selected and all spins in that slice excited, but in the time prior to the imaging, spins in the blood have flowed out of that slice and been replaced by unexcited spins. Flow-sensitive phase encoding allows the rate of flow to be measured, by applying a magnetic field gradient along the direction in which flow is to be measured. A large gradient dephases the spins- depending on their position along the gradient, this gradient is then reversed which will completely rephase stationary spins. Spins that have moved on will not be completely rephased. If the flow is coherent within a voxel, when the spins are imaged the phase difference can

be calculated. Diffusion is measured in a similar way, but since the motion of the spins within a voxel is incoherent, the diffusion effect results in a diminished signal.

2.5 Magnetic susceptibility

The general consensus is that increases in T1 value of water ^{1}H signal from a voxel is caused by increased cerebral blood flow perfusing the tissue region represented by that voxel, and this is known as the "inflow effect". An increase in T2 value is thought to be due to an increase in bulk magnetic susceptibility effect by an increase in the small fraction of paramagnetic deoxygenated haemoglobin iron atoms, which bear 4 unpaired electrons in the blood present in the voxels. In most fMRI pulse sequences, a positive response signifies decreased T1 and increased T2 or one of the two dominating the opposite of the other. For a negative response, the opposite changes in T1 and T2 occur.

The BOLD signal is closely related to changes in CBF (Zhu et al, 1988), which has long believed to be closely coupled with functional activation (Roy & Sherrington, 1890) although not universally (Gsell et al, 2000). It is proposed that task-induced BOLD changes associated with the microvasculature are well correlated with the CBF changes, which presumably reflect alterations corresponding to variations in neuronal activity (Yarowsky & Ingvar, 1981). Studies investigating the effect of different visual stimulation paradigms on CBF and BOLD have found that both parameters change as functions of the stimulation frequency, in both group-averaged and single subject data (Kwong et al 1992). Furthermore, the results show a significant linear relationship between BOLD and CBF. Likewise, animal data has shown close relationships between CBF, BOLD and evoked potentials with regard to the stimulus frequency, indicating that BOLD may reflect neuronal events (Gyngell et al 1996).

The BOLD response is further complicated from contributions in metabolic changes in CMR_{O2} and CBV. There are many aspects of cerebral haemodynamics and metabolism that affect the relaxation parameters and ultimately the image obtained and these contributions are described in section 2.6.

All substances are magnetised when placed in a magnetic field, however the degree of magnetisation (magnetic susceptibility) varies and is quantified in χ. The physical source of χ is the sum of interactions of the nuclear spin in the sample. The bulk magnetic susceptibility (BMS) represents the magnetisation of a substance when placed in a magnetic field. Most modern MRI studies involve the detection of changes in the magnetic susceptibility of bulk blood, BMS, inside vessels during neuronal activation. The BMS value of a sample has an effect on the resonant frequency of the observed nuclear spin it contains, thus χ is also the measure of the extent to which the substance modifies the strength of the magnetic field passing through it (Schenck, 1996).

2.5.1 Classification of Magnetic Susceptibility of a substance

Diamagnetic substances include most of the substances in the body and they are essentially nonmagnetic as they have no unpaired electrons. When placed into an external magnetic field B_0, a weak magnetic field is generated in the opposite direction to B_0. The effective MF is reduced, because diamagnetic substances have a small, negative χ.

Paramagnetic substances have unpaired orbital electrons, which become magnetised when the external magnetic field is switched on, and conversely demagnetised when the magnetic field is switched off and their induced magnetic field is in the same direction as the external magnetic field (B_0). The presence of paramagnetic species causes an increase in the effective magnetic field, thus χ is small and positive and are weakly attracted by the magnetic field. An example of a paramagnetic agent is dHb which has four unpaired electrons and is thus used as an endogenous contrast agent in fMRI. Another example is gadolinium which has 7 unpaired electrons and is commonly used as an exogenously applied contrast agent. Hemosiderin on the other hand (denatured haemoglobin e.g. in an occlusion) has more than 10000 unpaired electrons and is said to be superparamagnetic.

Ferromagnetic substances are strongly attracted by a magnetic field and remain magnetised when it is turned off. They have a large positive χ, larger than superparamagnetic substances. The ferrous iron on the haem of deoxyhaemoglobin is paramagnetic, but is diamagnetic in Hb. When red cells containing dHb are placed in magnetic field, there is magnetic field distortion induced by the difference in magnetic susceptibility relative to the surrounding magnetic field. The induced field shift related to Hb is the source of BOLD contrast, the change in dHb content associated with functional activation can be detected in the MRI signal.

2.6 Bulk Magnetic Susceptibility to BOLD fMRI signal

Bulk magnetic susceptibility to fMRI signal is a complicated path. The sign (i.e. positive or negative) of the response is very instructive with respect to understanding the BMS principle (Springer 1995). The BOLD method, which is sensitive to vascular paramagnetic dHb, is dependant on regional values of cerebral metabolic rate of oxygen utilisation (CMR_{O2}), cerebral blood flow (CBF) and cerebral blood volume (CBV). Fig 2.6.1 depicts the relationship of the factors contributing to the fMRI signal. The source of the sign of the response is thus explained below

2.6.1 Bulk Magnetic Susceptibility →BOLD: negative

Changes in magnetic susceptibility ($\Delta\chi$) are caused by alterations in dHb iron (Huang 1996). Prior to the increase in activity of neurons near a blood vessel, the value of χ inside the vessel is slightly higher than that of outside the vessel. This is because of the small fraction of paramagnetic dHb iron atoms present in resting state blood. Magnetic susceptibility of blood is transiently decreased during activation as oxygenated blood flows into the area, decreasing the dHb. Any degree of deoxygenation causes $\Delta\chi$ to become positive and therefore the relationship between BMS and BOLD becomes negative (hence the red arrow).

This results in a transient decrease in $T2^{*-1}$ for the signal from the spins outside the vessel and a positive fMRI response. This is known as the extravascular mechanism and is depicted in Fig 2.6.1 by the red arrow from BOLD to BMS and the subsequent decrease in T2*.

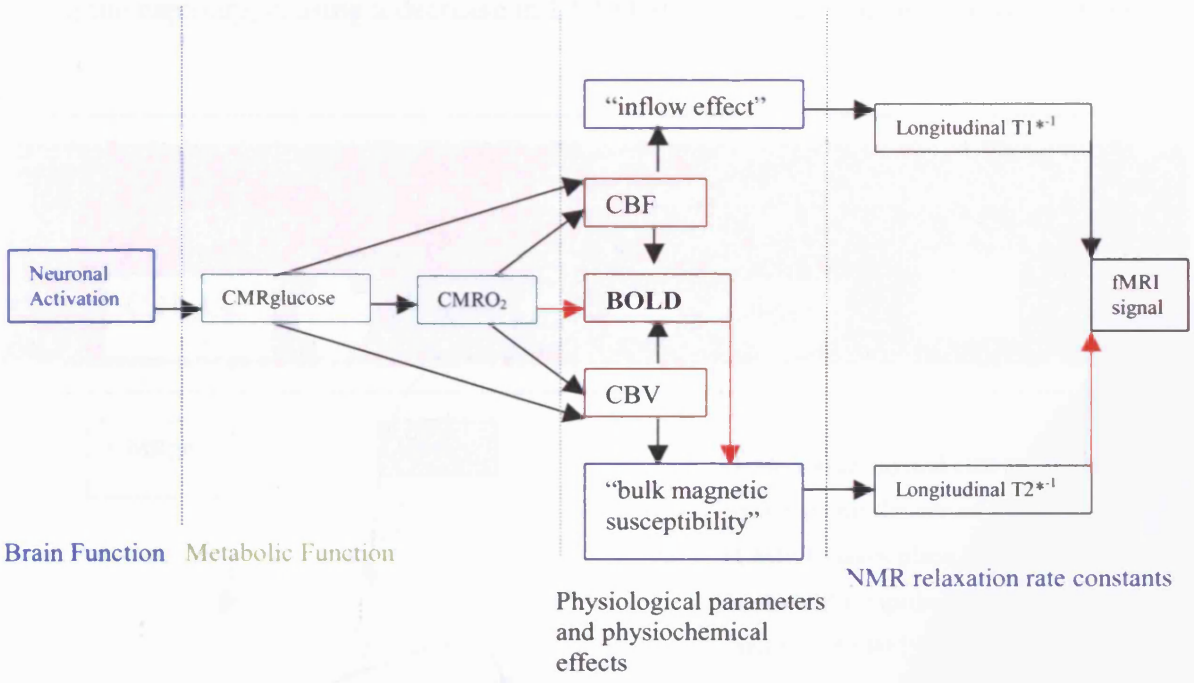

Fig 2.7.1 Mechanisms influencing the sign of the BOLD fMRI response

Black arrows indicate proportional relationship, red arrows indicate inverse proportionality, where:

CMRglu is cerebral metabolic rate for glucose consumption
CMRO2 is cerebral metabolic rate for oxygen consumption
CBF is cerebral blood flow
CBV is cerebral blood volume

Adapted from Moonen et al (2000, Chapter 9)

2.6.2 CBV →BMS: positive

CBV is increased by dilation of resistance arterioles and/or venules but probably not capillary recruitment (Huang 1996). The number of intravascular spins increases with vessel size, thus an increase in CBV increases BMS (χ_v). However, increased oxygenation level (when CBF increases) decreases the blood BMS (χ_v), this is illustrated by the bimodal action of $CMRO_2$ in Fig 2.7.1). But both can occur simultaneously.

2.6.3 $CMRO_2$→BOLD: negative

The relationship between CMR_{O2} and BOLD is inverse, so that an increase in CMR_{O2} will result in increased paramagnetic dHb and thus a decreased BOLD, it therefore follows that if CMR_{O2} increases without an increase in CBF, then dHb will increase along the capillary, causing a decrease in BOLD and increased χ inside the vessel (Fig 2.6.3).

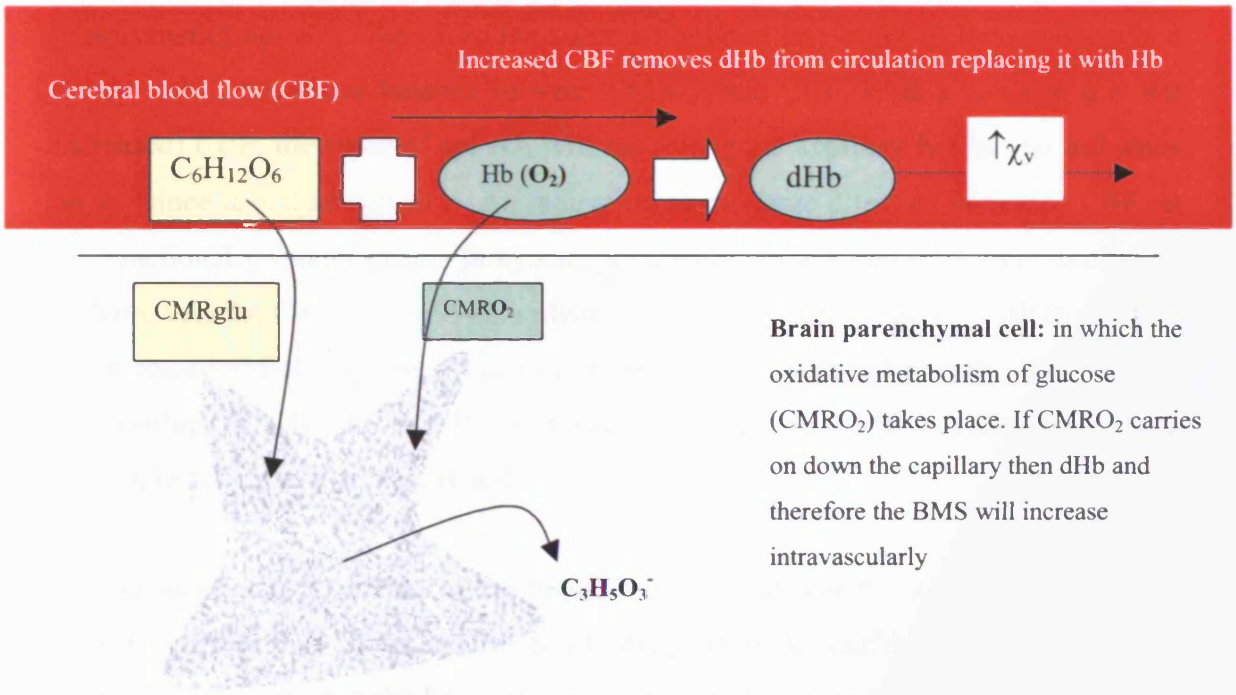

Fig 2.6.3 Brain capillary with erythrocytes flowing in direction of CBF

Haemoglobin (green) is indicated by ovals.
Blood delivers glucose (yellow) as well as erythroctytes.
With constant CBF, the dHb causes bulk magnetic susceptibility. If the CBF should increase after neuronal activity then the Hb replace the dHb reducing the BMS. This increases the T2* and therefore fMRI signal.

Adapted from Moonen et al (2000, Chapter 9)

Aerobic metabolism of glucose ($C_6H_{12}O_6$) causes apFe (the apoprotein and iron atoms conjugate in Hb) to become paramagnetic once the O_2 has been removed (Fig 2.6.3). This in turn, affects the value of blood χ_v and is the only paramagnetic species in the blood that has an effect on χ_v. It follows that with increasing apFe, (and decreasing $apFeO_2$), χ_v increases progressively down the capillary as the capillary passes an

increasing number of cells with some baseline $CMRO_2$ activity (Springer 1994). The major determinant of the dHb content in the blood is the supply and demand of oxygen at the tissue level.

2.6.4 CBF→BOLD: positive

If the CBF increases, apFe is removed from the capillary and is replaced by (diamagnetic) $apFeO_2$. Therefore the value of apFe at any point in the capillary is a steady state competitive balance between $CMRO_2$ and CBF. With a constant (i.e. not increased) CBF, the value of $apFeO_2$ will fall, along the capillary but has no influence on χ_v (since it is diamagnetic). An indication of the large effect of increased CBF on the functional response occurs in hypercapnia: there is increased CBF (due to dilation of large vessels, Chen et al 1994), without the concomital increase in $CMRO_2$ causing an increased fMRI response. When the CBF has increased sufficiently, this positive relationship of CBF to BOLD overcomes the negative $CMRO_2$ relationship with BOLD, resulting in a decease in apFe.

During functional activation of the brain, it was found that the increases in $CMRO_2$ were much less than those of CBF and CMR_{glu} (Fox & Raichle, 1986). Although it appears inefficient, it is the basis of non-oxidative glucose metabolism in response to functional activation. This apparent "decoupling" of CBF for $CMRO_2$ has been shown to be a necessary consequence of decreased efficiency of O_2 extraction from blood into tissue, with increasing velocity of CBF. Using this rationale, Springer puts forward the hypothesis that a region showing only a decrease in BOLD signal after stimulation is not caused by a simple reduction in neuronal activity (Springer et al, 1995). It actually results from arterioles, which will not or do not dilate, thus the vessels cannot increase CBF to counteract the increasing concentration of paramagnetic apFe in the blood.

It is important to distinguish between metabolic and physiological responses. CBF and CBV are relatively slow to change in response to neuronal activation, as compared to enzyme catalysed chemical reactions of aerobic metabolism, and indeed the initial dip in the fMRI signal may represent this time discrepancy. The increase in $CMRO_2$ begins immediately after stimulation, whereas the CBF starts to increase after 1s and takes 2s

to reach maximum. This is a time delay of 3s in which the $CMRO_2$ dominates, resulting in negative fMRI signal. Despite these considerations, the temporal resolution involved in the following experiments (Chapters 5, 6 and 7) is not sensitive enough to detect such transient events as the BOLD undershoot.

2.6.5 spatial resolution

Like PET and optical imaging, fMRI depends on physiological responses related to brain activation. By measuring secondary haemodynamic and metabolic changes, brain function can be mapped in response to alterations in neuronal activity. Furthermore, the spatially segmented and compartmentalised nature of brain function can be visualised due to the spatial resolution allowed by this technique. A region of interest containing only one capillary could show an fMRI response with an initial negative dip, followed by a positive signal intensity increase. However a group of neurons that are not directly activated are instead supported by a capillary bed supplied by the same arteriole. Thus this group of neurons would experience the increased CBF, and not the $CMRO_2$, thus the response would be completely due to hemodynamics rather than cerebral metabolism. The image areas displaying the negative dip are not as diffuse as those that do not. Therefore the early response is important not only because it avoids the hemodynamic time lag but also because it focuses the spatial resolution more directly on the region of brain tissue experiencing increased metabolic activity.

The spatial resolution that can be detected using fMRI (and PET) correlates not directly with neuronal activity, but with the resulting metabolic and haemodynamic changes. Several visual-stimulation tasks in humans in which it was hypothesised that the lateral geniculate nucleus, (a major target for optical input) should be activated, used 3-D fMRI to map out signal in this area and actually distinguish it from surrounding activated structures (Chen et al, 1998). For fMRI, this raises questions about macrovascular effects like inflow effects, macrovascular BOLD effects and the spatial correspondance between the site of neuronal activity and the extent of the resulting secondary effects. One efficient way is to map functionally distinct structures with a much finer spatial scale (mm) is to examine the well-defined organisation and topography in the rat brain. At an even more precise level, rat whisker-barrel activation

has been detected after electrical stimulation of the whiskers at 7T (Yang et al, 1996), thus although the spatial resolution is to an extent dictated by the vasculature of activated region- the main sites of activation detected by fMRI do represent the area of interest.

Human fMRI feasibility was demonstrated using visual stimulation task (Ogawa 1992) and motor task (Bandettini, 1992). Thus a new dimension of study was discovered regarding visualisation of functional activation using BOLD and fMRI (Ugurbil, 1994). Recently, there has been interest in clarifying the quantitative aspects of fMRI. Kida et al (2000) calibrated the BOLD signal with measured and predicted values of $CMRO_2$ using measured rates of CBF and CBV. The values were found to be in agreement with the theory of the BOLD phenomenon. This step is important for understanding the nature of the BOLD signal and also what is happening at the neuronal level. The following experiments aim to manipulate these signals pharmacologically in order to visualise metabolic events at a transmitter-receptor level.

Chapter 3

Anaesthetics and their Effects on the Dopaminergic System

3.1 Introduction

"A limitation of interpreting the results of studies of anaesthetised animals is that the effects of anaesthetic on neuronal activity are not completely characterised. The primary assumption in the analysis is that during stimulation the neuronal activity induced in the region is independent of the anaesthetic used." (Shulman et al, 1999).

In performing functional MRI on animals it is a requirement that the animal is immobilised for image acquisition, and anaesthetised where discomfort or pain may be felt prior to and during the experiment. The choice of anaesthetic in such experiments is indeed a difficult question and may depend heavily on the type of investigation being carried out. When considering fMRI in small animals, it is often the case that the animal must have one or several blood vessels cannulated for blood sampling (Gyngell et al, 1996) or administration of exogenous material, for instance drugs (Marota et al, 2000) and contrast agents (Palmer et al 1999), and also, a tracheotomy may need to be performed (Burdett et al, 1995). These techniques require general anaesthesia. Thus, if the anaesthetics are providing such a level of analgesia one can presume that they are inhibiting or blocking central pain processing pathways. Therefore it is useful to know which regions of the brain are involved in general anaesthesia as these may be affected during the experiment on the anaesthetised animal.

It has been put forward by Lhati et al (1998), that anaesthetics are not only unnecessary for animal fMRI studies, but also significantly reduce the signal change and that a period of conditioning to MRI scanner environment and training to being restrained in a stereotaxic holder should suffice. Some other groups have also developed non-anaesthetised small animal imaging protocols (Tabuchi et al, 1995; Hagino et al, 1998; Peeters et al 2001). Another method used to immobilise animals, without using stereotaxic positioning, is to use muscle relaxants, such that the animal is fully conscious but cannot move (Peeters et al, 2001), but this has ethical considerations.

Although it is a valid argument that interactions with the anaesthetic may alter the BOLD signal, it may be also noted that a non-anaesthetic approach to animal restraint may introduce its own problems affecting the signal changes measured. The environment of the MRI scanner is known to be particularly aversive to rat: i.e. loud

noises, low temperature, in addition to the head being fixed to prevent motion artifacts. Stress is known to have effects on the dopamine neurochemistry of the brain (Abercrombie et al, 1989) and immobilisation is considered to be a severe stressor and as such has been investigated with regards to brain neurochemistry and behaviour. Studies in the 1960s showed that stress increases turnover of monamines (Bliss et al, 1968). More specifically, immobilisation stress was found to increase dopamine turnover in the frontal cortex and nucleus accumbens (Anderson & Fillenz, 1984; Imperato et al, 1991). Thus, fMRI in conscious, restrained animals or immobilised animals is unacceptable either on scientific or ethical grounds.

3.1.1 Central Pain Processing Pathways and Mechanisms

It has been observed that stimulation of the periaqueductal grey matter (PAG) produced analgesia in both animals and humans (Fields, 1987) without affecting tactile sensitivity. After this discovery of stimulation-induced analgesia, two neural pathways were defined as mediating in analgesia. It was found that stimulation of the brain stem inhibited nociceptive neurons in the dorsal horn and subsequently that this was abolished by lesioning the dorsolateral funiculus (Sandkuler & Gebhart, 1984). Thus it was proposed that neurons of the periventricular grey matter (PVG) and PAG make excitatory connections to the rostroventral medulla, which contains the serotonergic nucleus raphe magnus and nucleus reticularis paragigantocellularis (Edeson & Ryall, 1983).

Administration of low doses of opioid agonists directly into areas of rat brain provides immediate and powerful analgesia (Basbaum & Fields, 1978). The opioids act in some of the same CNS areas, which can be electrically stimulated to produce analgesia (Basbaum & Fields, 1978). This is reinforced by the opioid antagonist naloxone (a structural analogue of morphine) blocking the analgesia when administered into the PAG (Fields, 1987). Two endogenous opioids of interest are enkephalins (Hughes, 1975) and dynorphins (Goldstein et al, 1979). Dopaminergic transmission is known to involve opioid co-transmission (see also Chapters 6 and 7), and dynorphin and enkephalin release are correlated with dopamine D_1 and D_2 receptor activity (Steiner & Gerfen, 1998). It follows that these endogenous opioids may modulate dopaminergic

activity in the anaesthetised rat. Therefore investigation of the effects of anaesthesia and more specifically, of particular anaesthetics, is important in the context of the following phMRI experiments.

There are 3 types of opioid receptor, mu (μ), kappa (κ), and delta (δ) (Martin & Sloan, 1977). Alkaloids like morphine have high affinities for μ receptors, endogenous enkephalins have high affinities for μ and δ receptors and dynorphins for κ receptors (Kandel et al, 1991). Their distribution throughout the CNS is such that it is thought that these endogenous opioids may be involved in other physiological functions: there is a high density of μ receptors in PAG and superior dorsal horn of spinal cord in addition to a high number of enkephalin containing neurons (Rossi et al, 1993). Opioid antagonists like naloxone are best at antagonising opioid actions at μ receptors and there is also a good correlation between analgesic properties and activity at μ receptors. In fact μ receptors were originally defined by their affinity for analgesic compounds i.e. morphine (Pasternak, 1993).

3.1.2 Anaesthetics may affect Experimental Parameters

General anaesthetics affect physiological variables, so it is of vital importance to investigate the effect of anaesthetics on the pharmacological paradigms which we desire to study. The choice of anaesthetic in fMRI is very important and any possible changes in neuronal function it may induce should be considered carefully.

General anaesthetics depress the CNS metabolic activity and reduce cerebral blood flow, hence use of anaesthetics in fMRI would be expected to reduce CBF and possibly diminish signal change, as measured using the BOLD method. The detected fMRI signal is already small and may be further confounded by some property of the anaesthetic. However significant changes in brain activity have been observed using fMRI in anaesthetised animals: Hyder in performing electrical footshock stimulation used α-chloralose and saw changes in the somatosensory cortex of up to 6-7% (Hyder et al, 1994); Yang in performing olfactory bulb stimulation under urethane anaesthesia saw change of 20-30% (Yang et al, 1998); Chen et al (1997), carried out a phMRI experiment using halothane and observed 4-5% changes in BOLD after amphetamine

administration. The signal intensity changes are of course also dependant on other factors, for instance magnet strength, the paradigm being investigated and strength of stimulation. Nevertheless, these examples show that despite the animals being surgically anaesthetised a robust change in signal is indeed measurable using several anaesthetics under different experimental conditions.

The presumption that anaesthetics "dampen" down cerebral activity resulting in reduced levels of stimulated activity (Yang et al, 1998) may be an oversimplification. Focal changes in cerebral metabolic rate for glucose utilisation (CMR_{glu}) are small during sensory activation in humans as well as in rodents and primates: in some studies of anaesthetised rats however they are much greater. The literature values show that resting anaesthetised CMR_{glu} is lower than non-anaesthetised values (Shulman et al, 1999) whereas the final stimulated values may be very similar for both the anaesthetised and non-anaesthetised state. This low resting value of CMR_{glc} for the anaesthetised rat explains why the increment from resting to stimulated, is so much greater for the anaesthetised animal.

3.2 Commonly used Anaesthetics

In animal experiments, injectable or inhalation general anaesthetics are used to provide analgesia, sedation and immobilisation. Additionally, neuromuscular junction (NMJ) blockers are used to immobilise animals but without providing sedation or analgesia. These are often given in combinations, and all three types are sometimes used in a single experiment (Gyngell et al, 1996; Hyder et al, 1997; Marota et al, 1999): before describing the aims of this study, several of the more popular anaesthetics are described.

3.2.1 Urethane

Urethane is an example of an injectable anaesthetic, which provides a long lasting anaesthesia, with moderate cardiovascular and respiratory depression and excellent depth of anaesthesia and analgesia (Field et al, 1993). It is a carcinogen, so great care must be taken when handling it. Urethane is commonly used in rodent and lagomorph

studies as it produces stable and prolonged anaesthesia (Moore et al, 1990) in some cases longer than 24 hours, thus recovery takes several hours (Field et al, 1993). It is therefore suitable for long fMRI experiments where stable anaesthesia is required (Forman et al, 1998; Yang et al, 1998), particularly if the experiment is terminal, although its use is limited due to its high mortality rate (Field et al, 1993). The mode of action of urethane anaesthesia is not completely understood although it is thought to work as an antagonist at excitatory amino acids (EAA) receptors as urethane was observed to reverse the effect of NMDA receptor agonists (Rockhold et al, 1994). Urethane was also observed to block kindling, an aspect of NMDA-induced neural plasticity, but potentiated another type i.e. long term potentiation (Cain et al, 1992), indicating a rather complex mode of action. Urethane may alter the behaviour of the electrical synapse and decrease cell membrane excitability (Moore et al, 1990) and may extert its anasthetic effects via small changes in multiple receptor systems (Hara & Harris, 2002).

Regarding dopamine release, it was observed using microdialysis that urethane anaesthesia did not affect stimulation-induced dopamine release in the striatum. Similarly, barrel cortex stimulation under urethane anaesthesia was not significantly different from that of the awake animal, although its resting state is reduced: this indicates that the magnitude of the change from resting to anaesthetised is actually greater in the anaesthetised animal (Armstrong-James & Fox, 1987). Urethane causes metabolic acidosis (Folle & Levesque, 1976) with partial respiratory compensation (Alfaro & Palacios, 1992) and moderate dose-related depression in heart rate and blood pressure (Field et al, 1993). Urethane also has an effect on endocrine control: Cheng and North (1991) found that under urethane anaesthesia, magnocellular neurons released vasopressin and oxytocin and that there was a reduction in osmotic responsiveness, perhaps through modification of cell membrane excitability. Similarly Shimokawa et al (1998) tested the effect of anaesthetics on noradrenaline release from the paraventircular nucleus (PVN): noradrenaline is known to locally affect the PVN and the hormones it controls. Urethane caused a 50% increase in PVN noradrenaline release.

3.2.2 Inhalation Anaesthetics: Halothane

Volatile anaesthetics such as halothane and isoflurane are widely used in human and veterinary clinical practice and also experimentally in animals. They are especially useful as their administration can be quickly adjusted, and the depth of anaesthesia can be controlled during the procedure, providing the anaesthesia is adequately monitored. Halothane is used in small animal fMRI experiments (Ogawa et al 1990; Silva et al 1995; Chen et al 1997; Guyen et al 2000) although it has been shown to cause metabolic decoupling (Ueki, et al, 1992). The potency of anaesthetic can be measured using the mean alveolar concentration (MAC) of anaesthetic at 1 atmosphere producing 50% immobility in subjects or animals exposed to noxious stimuli. This is equal to the reciprocal of the partial pressure of an agent required to achieve a given anaesthetic effect, 1 MAC could maintain an animal at a good level of anaesthesia without causing excessive depression.

Induction may be by means of an anaesthetic jar or using a chamber because induction using a facemask can be stressful. The use of halothane in cerebrovascular studies is criticised as halothane markedly depresses cardiovascular reflexes. Furthermore, the reactivity to hypercapnia is reduced when compared to α-chloralose (Bonvento et al, 1994) and halothane also decreases CMR_{O2} and increases CBF (Brussel et al, 1991). As these factors, and their respective dynamics are the basis of the BOLD fMRI signal, the possible influence of halothane on cerebral metabolism is an area requiring further investigation. Halothane is thought to interfere with dopaminergic transmission in the striatum, with dopamine levels increasing on induction (Stahle et al, 1990) and this effect is dose-dependant (Miyano et al, 1993). Isoflourane, enfourane and sevoflourane have also been investigated for their effects on dopamine release in the striatum. These volatile anaesthetics all cause general anaesthesia in a similar manner to halothane but have slightly different properties as clinical anaesthetics (Miyano et al, 1993). It is not clear how halothane increases dopamine release although some mechanisms have been ruled out, for example dopamine release is not amphetamine-like, as the metabolites levels do not display such patterns of change (Zetterstrom et al, 1983), there is not reuptake blockade (Hurd & Ungerstedt 1989a) and halothane does not abolish apomorphine-induced decreases of dopamine levels (Stahle et al, 1990) thus is not blocking dopamine receptors.

3.2.3 α-Chloralose

For fMRI animal experiments, the anaesthetic α-chloralose (α-monoglucochloralose or glucochloralose) tends to be the anaesthetic of choice (Bock et al, 1998; Palmer et al, 1999; Marota et al 1999). α-chloralose has minimal effects of autonomic and cardiovascular systems, and it causes minimal depression of physiological factors and reflexes (Storer et al 1997) and very importantly, surgical doses preserve functional coupling to the somatosensory cortex and enable functional activation (Ueki & Hossman, 1992) and potentiate the generation of evoked responses (Winters & Spooner 1966). α-chloralose is often used for animal research related to the cerebral circulation and especially where coupling of brain function to metabolism, e.g. fMRI (Hyder et al, 1994) and autoradiography (Fuxe et al, 1987) is important. α-chloralose is commonly used to provide light anaesthesia, and when used for fMRI procedures, it is commonly administered after the surgical procedures have been carried out. Another anaesthetic, commonly a volatile anaesthetic like halothane (Houston et al, 2001) or enflurane (Hyder et al, 1994) is initially administered for the surgical steps of the experiment. Bonvento et al (1994,) found that α-chloralose was long lasting, and suitable to maintain a rat in a painful situation. Also, in this study, tail pinches resulted in increased arterial blood pressure and motor response, but not increases in heart rate, which is associated with nociception.

Reports of intact cardiovascular reflexes and enhanced spinal reflexes under α-chloralose anaesthesia (Shimamura & Yamauchi, 1967) have lead to the popular belief that it depresses the CNS less than other anaesthetics. However observations using single cell recordings in dorsal spinal cord neurons and nucleus reticularis gigantocellularis neurons found that α-chloralose suppresses neuronal activity to the same extent as other anaesthetics and for a longer duration (Collins et al, 1983). In addition, although it works well as a sedative, it does not produce sufficient analgesia at general anaesthesia dose: Holzgrefe et al (1987) reported an absence of classical indications of anaesthesia depth and Winters & Spooner (1966) reported that surgical anaesthesia was never obtained using α–chloralose. Furthermore, Silverman and Muir (1993) recommend that it should only be used if preceded by "barbiturates, opiods, α-2

agonists or phenothiazine tranquilizers", and that it should not be used intraperitoneally (i.p) for survival surgery.

It is known that α-chloralose combines the properties of a depressant (sedation and anaesthesia) with some of those of a stimulant, and the manifestation of depressant behavioural effects explain its use an anaesthetic (Hanriot & Richet, 1893). Administered alone without the gradual removal of gaseous anaesthetic, complex behaviours are displayed, spontaneous myclonic jerks and rocking at pre-anaesthetic stages and a strong generalised clonic response is observed at the light stages of anaesthesia (Monroe et al, 1963a). These two apparently paradoxical actions are very unusual for CNS depressants, but can be explained by cortical depression and secondary disinhibition of the thalamus and mesencephalic reticular formation, at subcortical structures providing the motor hyperexcitability reaction to sensory stimuli (Balis & Munroe, 1964). Another suggestion for the hyperexcitability is the mixture of α- and β-forms of chloralose in the administered agent, and this can be somewhat reduced by filtering heated α-chloralose at 60° thereby removing its isomer β-chloralose (Kruger & Albe-Fessard, 1960). β- chloralose shares the actions of α–chloralose on the CNS but differs quantitatively (Monroe et al, 1963b) and is not as readily soluble as α–chloralose.

Massott & Longo (1978) assessed the effect of α-chloralose on dopamine content and metabolism in the rat brain to compare it to baclofen and GHBNa (GABA agonists) which both cause behaviours similar to α-chloralose and additionally increase dopamine content. Using spectrophotoflourimetry of rat brain homogenates, they found that there was no change in dopamine nor its metabolites DOPAC and HVA. Ford & Marsden (1986) also observed the lack of effect of α-chloralose on dopamine metabolism. These results have since been contested: using the push-pull cannula the effect of α-chloralose on dopamine release was measured in the caudate-putamen and substantia nigra and it was found that the level of dopamine release was reduced in both areas as compared to those obtained under the same experimental conditions using halothane and encephale isole preparation. Furthermore, the time taken to achieve steady-state dopamine release was greater, thus leading to the suggestion that α-chloralose did suppress dopaminergic neurons (Nieoullon & Dustier, 1980). These

considerations reiterate the need for further investigation into the effects of these anaesthetic agents on brain function.

3.2.4 Chloral hydrate

Chloral hydrate, an injectable agent related to chloroform is often used as a laboratory anaesthetic and as a paediatric dental sedative. It provides rapid onset of anaesthesia with analgesia sufficient for moderate to markedly severe surgical procedures and also shows a strong linear correlation between dose and duration of anaesthetic (Field et al, 1993). However recovery is rapid, easy and with little warning, furthermore severe uncompensated respiratory acidosis, severe dose-related depression of blood pressure and heart rate may occur (Field et al, 1993). Originally used as anaesthetic in humans and in veterinary practice, chloral hydrate was discontinued due to prolonged and difficult induction and recoveries (Johnson, 1949). In rats, the array of side effects after using chloral hydrate is well documented, for example respiratory depression, thermoregulatory dysfunction (Lumb et al, 1984) gastric ulcers (Ogino et al, 1990), adynamic ileus (Davis et al, 1985) and general irritation of the rat peritoneum (Valenstein, 1961), but it should be noted that these irritations can be avoided by using smaller doses (Field et al, 1993). In addition to these side effects it has been implicated in genotoxicity in mice (Crebelli & Cavere, 1989).

Experimental evidence indicates than chloral hydrate anaesthesia depresses dopaminergic activity. Hamilton et al (1992) found that striatal dialysates contained 50% less dopamine in chloral hydrate anaesthetised animals than in conscious preparations. It was also noted that chloral hydrate may slow the transport of HVA and DOPAC and give altered responses to morphine, in addition to the general depression of CNS functions. Electrophysiological data indicate that chloral hydrate mediated attenuation of burst firing occurs (Kelland et al, 1990) and that it may disrupt the electrotonic coupling phenomena observed in conscious rats (Freeman et al, 1985).

3.2.5 Neuromuscular junction Blockers

The NMJ blocking agent pancurionium has been used in fMRI models in the past (Gyngell et al, 1996; Hyder et al, 1997). NMJ blockers bind to the acteylcholine receptor and prevent the action of acetylcholine itself, they are competitive and can be reversed by anticholinesterase. They provide suitable paralysis and deep relaxation whilst allowing artificial ventilation thus removing respiration movements of the head. The use of such agents warrants serious welfare and ethical considerations as the animal is conscious and NMJ blockers do not provide any anaesthesia or analgesia. NMJ blocking agents may increase stress, but as the animal is immobilised, behavioural changes demonstrating distress would be absent, thus appropriate steps to make the animal more at ease would not be taken. Furthermore, the neurochemical changes which occur in the brain due to stress, for example, increase dopamine release (Anderson & Fillenz, 1984; Abercrombie et al, 1989; Imperato et al, 1991) and may confound the paradigm being investigated.

3.3 Aims

Studies investigating fMRI of live experimental animals are usually conducted under general anaesthesia. Significant relationships between stimulation strength and magnitude of BOLD signal have been observed in response to different paradigms in the urethane anaesthetised rat (Yang et al, 1998), the halothane anaesthetised rat (Chen et al, 1997) and probably most commonly, the α-chloralose anaesthetised rat (Hyder et al, 1993). Anaesthetic agents (as indicated in section 3.1.2) are heterogenous on their effects on transmitter release and metabolism, and as such, they are confounding variables which may compromise the interpretation of data, and limit the extrapolation of results. The comparison and characterisation of the effects of anaesthetics on baseline and stimulated dopaminergic transmission for fMRI studies is an important pre-requisite for fMRI studies. Thus we have used *in vivo* microdialysis to measure dopamine release in the nucleus accumbens to look at the effect of anaesthetics under both baseline and 3 stimulated conditions, these are described in the following sections.

Experiment 1 investigated the effect of two injections of amphetamine on the levels of dopamine and metabolites under the three different anaesthetics. It is well documented that a simple administration of amphetamine evokes an increases in dopamine release, which is largely Ca^{2+}-independent (i.e. not due to Ca^{2+}-dependant exocytosis), whereas subsequent administrations cause a sensitised release which is at least partially Ca^{2+}-dependant (Warburton et al, 1996). Thus the administration of a single dose of amphetamine is both qualitatively and quantitatively different from the administration of subsequent doses. Therefore the metabolic response to the first dose is likely to be different, to the response to subsequent doses. The amphetamine stimulation paradigm consisted of two (1mg/kg, i.p.) administrations of amphetamine, the first given after one hour of basal sampling, the second dose two hours later (see 3.3.8). The actions and mechanisms of amphetamine are discussed in more detail in Chapter 5.

Experiment 2 investigated the effects of peripheral aversive stimulation (mild footshock), and local depolarisation with potassium on the levels of dopamine and metabolites also under the effect three different anaesthetics. Aversive stimuli such as footshock lead to marked increases in extracellular levels of dopamine in the nucleus accumbens (Anderson & Fillenz, 1984; Salamone et al, 1997; Young et al, 1993) and dopamine metabolism in the prefrontal cortex (Gonenc et al, 2000), as measured by *in vivo* microdialysis. However, after similar peripheral stimulation, significant BOLD response was detected only in the corresponding somatosensory and sensorimotor cortices (Hyder et al, 1994; Marota et al, 1999), but this was not observed in the nucleus accumbens. All of these fMRI experiments were carried out using α–chloralose as the anaesthetic during the experiment, and also using neuromuscular blockers. It may be the case that the anaesthetic, or indeed combination of anaesthetics caused responses in subcortical regions to be blunted or completely blocked.

Local neuronal stimulation can be achieved by increasing the potassium in the dialysis perfusate. Under resting conditions, the intracellular concentration of K^+ ions is greater than that in the extracellular space. Normally, opening K^+ channels causes an outward repolarisation current, which contributes to rapid termination of the action potential. Increasing the extracellular concentration of K^+ ions will cause a net influx of K^+ into the cells, depolarising the cell much the same way as Na^+ ions would when the sodium

channels open. Furthermore, the repolarisation current is absent, leading to increased firing rates and enhanced transmitter release.

Potassium stimulation, although somewhat crude, provides a robust method of stimulating neuronal release of neurotransmitters, allowing comparison of basic neuronal excitability between experimental conditions. For this reason, this would be an excellent agent to use whilst performing fMRI, especially in relating BOLD signal to neuronal activity and transmitter release, complementary to studies using agonists and antagonists. The peripheral sensory stimulation (PSS) and neuronal stimulation were carried out within the same experiment.

The dialysis stages of these experiments were performed under terminal anaesthesia, the surgery having been carried out at least seven days beforehand. The advantages of separating the surgery and the main experiment are numerous: the animals have recovered thus the transmitter released are less likely to be injury-induced; surgical anaesthesia is not required for these microdialysis experiments, and importantly up to four experiments can be performed at once.

3.4 Principles of Microdialysis

In vivo microdialysis provides a method for sampling extracellular fluid (ECF), and measuring synaptic overflow of neurotransmitters and metabolites. It can be used in either anaesthetised or in conscious animals and its development has impacted greatly on *in vivo*, especially brain research, for example in addiction models (Di Chiara & Imperato, 1998), relating neurochemistry to behaviour (Young et al, 1992; Kuczenski & Segal, 1989), brain injury (Hamburger & Nystrom, 1984) and drug characterisation (Damsa et al, 1987).

The first dialysis model was introduced by Bito et al (1966), who implanted a dialysis sac into the brain of a dog. The sac was later removed and the contents analysed. Subsequently, Delgado et al (1972) described a "dialytrode" which allowed continuous dialysis perfusion, and this method was further developed by Ungerstedt & Hallstrom (1987). The principle of microdialysis is the implantation of a dialysis membrane to

permit the diffusion of solutes between the brain interstitial space and the dialysis perfusate, which lacks these substances of interest (i.e. neurotransmitters). Thus, substances can be taken from the extracellular space depending on the relative concentrations in the perfusate (in agreement with the laws of diffusion in a chemical gradient).

A dialysis probe consists of a concentric arrangement of two tubes one of which is slightly longer (the "inflow" tube) than the other (the "outflow" tube) see Fig 3.4.1. An advantage with microdialysis is that pharmacologically active compounds can be introduced into the perfusate whilst the behavioural and metabolic / biochemical effects of its action observed (Sharp et al, 1987).

There is an intervening semi-permeable dialysis membrane, which acts as a mechanical barrier to turbulence in fluid flow (Yaksh & Yamamura, 1974). A physiological solution (ACSF) is pumped through the dialysis tip, and the resultant dialysate is collected at the outflow for analysis. Solutes in the ECF diffuse across the membrane along their concentration gradient and can be measured in the resulting dialysate. The dialysate sample obtained does not need deproteinisation as the pore size of the membrane is sufficiently small (around 4000Da) to prevent high molecular weight proteins from crossing the membrane, which may otherwise cause degradation of the substances of interest. By constantly renewing the perfusate, sampling can continue over a relatively long period, from several hours to days (Westerink & Tuinte, 1986) although in long-term studies, the concentrations of transmitters and metabolites decrease substantially after 2 days. Particulars of dialysis probes used in following experiments are described below(3.5.1).

Microdialysis can be performed locally in most body organs and tissues, giving samples of extracellular fluid or other fluids, for instance, blood and sketetal muscle (Chou et al, 2001) and hepatic tissue (Klaus et al, 2001). Microdialysis is also used as a tool to monitor the brain after acute brain injury, the metabolism of the brain giving insight into the injuries sustained (Meixensberger et al, 2001). When performing brain microdialysis, the sample obtained should represent all solutes present in interstitial space, providing that the membrane pores are large enough. In studying quantitative neurogenic release of transmitters and concentrations obtained in the dialysate, the

dynamics of brain dialysis must be considered. The dialysis probe lies in the extracellular fluid (ECF) and not in the synaptic cleft and therefore the ratio in the dialysate is not representative of synaptic concentrations.

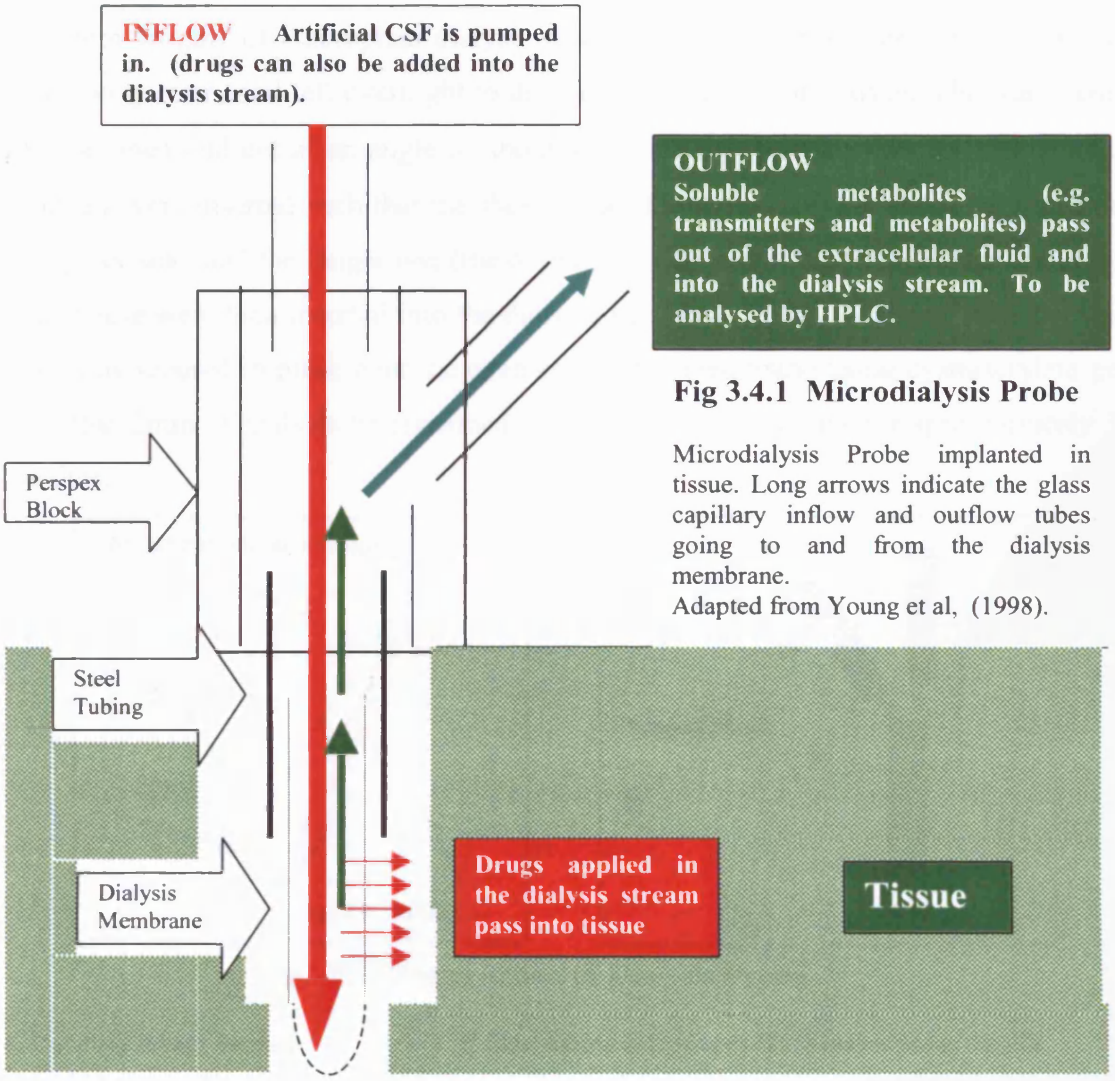

Fig 3.4.1 Microdialysis Probe

Microdialysis Probe implanted in tissue. Long arrows indicate the glass capillary inflow and outflow tubes going to and from the dialysis membrane.
Adapted from Young et al, (1998).

Dialysate analysis can be performed using immunoassays, mass spectrometry, electrophoresis and various types of clinical analysers (Robinson & Justice, 1991) although high performance liquid chromatography (HPLC) is most widely used. Appropriate analytical technique can determine the time resolution and thus the sensitivity. The analysis is described in more detail below (3.5.4).

3.5 Methods and Materials

3.5.1 Microdialysis Probes

Microdialysis probes were modified from the design described by Young et al (1988). 7-10 mm lengths of Cuprophan dialysis membrane were cut and one end was sealed with epoxy resin, and left overnight to dry. A sealed length of dialysis tube was chosen and the open end cut at an angle of about 45°. Into this opening two lengths of silica capillary were inserted such that the shorter one (the input line) lay about 0.5 mm from the epoxy seal, and the longer one (the output line) lay about 3mm back from the epoxy seal. These were then inserted into the dialysis tip (Fig 3.5.1A). A 12mm stainless steel shaft was secured in place over the open end of the membrane using cyanoacrylate gel, such that 2mm of dialysis tip remained uncovered and left to dry for approximately 30 minutes.

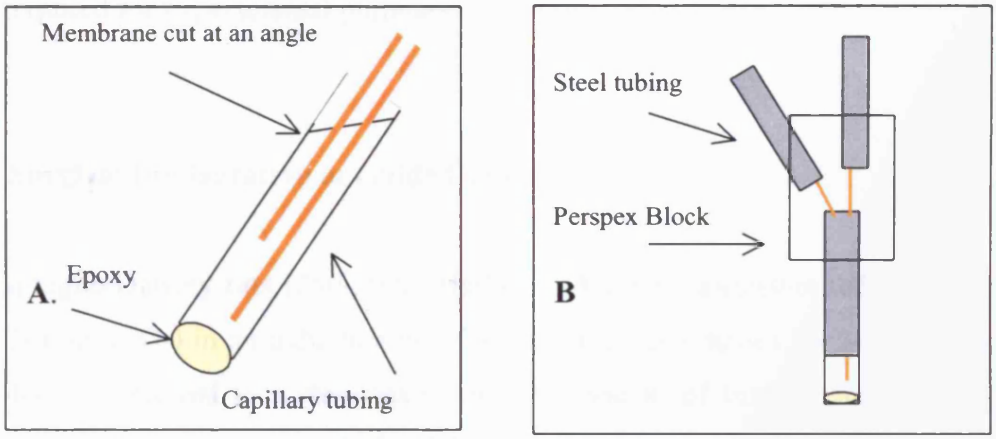

Fig 3.5.1 Construction of Dialysis Probe

A. Capillary tubing inserted **B**. Steel tubing and perspex block makes probe durable

The capillaries were then inserted into a specially made perspex block, with the shorter (input) line running down the straight arm, and glued in placed over the end of the shaft with epoxy resin. When this was dry, the remaining space in perspex block was filled with epoxy resin and a piece of 6mm stainless steel tube placed over each of the two capillary tubes, and located in the holes in the perspex block (Fig 3.5.1B). When dry, the capillaries were trimmed flush with the stainless steel, and a short length of silicone rubber tube was glued over the stainless steel tube using cyanoacrylate (being careful not to occlude the capillaries). This was left to dry thoroughly before testing.

To test, a 100µl syringe was connected to the inlet tube of the probe and water was gently pushed into the probe to check that fluid flowed through the dialysis tip and that there were no leaks. After checking that there were no leaks, the syringe was pulled back to remove the water from the probe, which was left to dry thoroughly before use.

3.5.2 Animals

All experimental procedures obtained the approval of Leicester University Ethical committee and were performed in accordance with the UK Home Office Animals (Scientific Procedures) Act 1986. Adequate procedures were taken at all times to minimize pain or discomfort to the experimental animals. Male Sprague-Dawley rats (n=8, 250-300g) were housed in cages of 3 (55cm x 37cm x 15cm) with ad libitum access to appropriate food and water under a 12:12-h light/dark cycle (lights on 08:00h) until required for experimental purposes.

3.5.3 Surgical Implantation of Guide Cannula

The Sprague-Dawley rats (250-300g: Harlan, U.K) were anaesthetised with halothane (3%, 2l/min in O_2) in an induction box (housed in a fume hood) for 3-4 minutes. They were then transferred to a stereotaxic frame (David Kopf Instruments, Tujunga, CA, USA) incorporating a facemask for delivery of gaseous anaesthetic. Anaesthesia was maintained by delivering halothane (1-2%, 1l/min in O_2) to the input line of the facemask: the output line attached to a Flouvac scavenger unit, for removal of excess halothane from the laboratory environment.

Animals were secured in place, with the incisor bar 3.3mm above the intra-aural line (Paxinos & Watson, 1998). Thus positioned, the fur on the skull was shaved, and the skin cleaned and surgically prepared above the area to be removed. A small piece of skin was removed, and the connective tissue was scraped using a scalpel to expose the skull overlying Bregma.

After marking Bregma, and with the coordinates logged, the coordinates for the nucleus accumbens were established (A:+1.5, L:+1.5, P:-6.0 from Bregma). One small hole was

drilled for implantation of the cannula and two additional holes were drilled for stainless steel anchor screws. The guide cannula (20G thin wall stainless steel tubing: 10mm length) was mounted on a 6cm length of stainless steel rod (23G) attached to the stereotaxic headpiece, and was lowered slowly into position and the cannula secured to the screws using Durelon cement (Biotech Ltd, UK). When this had dried, the implanter was raised out and a stylet (23G stainless steel rod) was placed into the cannula to prevent blockage. The area was cleaned and the wound sutured closed. The surgery complete, 0.1ml buprenorphine (Temgesic) was administered intramuscularly to provide postoperative analgesia, and 5ml (0.9% NaCl) saline was injected subcutaneously, to prevent dehydration during recovery. Following surgery animals were singly housed with food and water ad libitum and allowed to recover for at least 7 days post-operatively.

3.5.4 Experimental Procedures

Anaesthetics

A week or so after recovery from surgery, the animals were again anaesthetised with urethane, halothane or α-chloralose for the duration of the microdialysis experiments.

Full details of anaesthetics and drugs preparation techniques are given in section 3.5.6. For all three anaesthetics, appropriate depth of anaesthesia was verified by the absence of corneal, foot withdrawal and tailpinch reflexes.

Urethane was administered at a concentration of 1.75g/kg at a dose of 10ml/kg. Usually a single dose of urethane was sufficient to anaesthetise the animal for the duration of the experiment, although the depth of anaesthesia was monitored throughout (respiratory rate and periodic testing of corneal reflex) and supplementary doses given (0.5-1ml) as and when required.

α-chloralose was administered at a concentration 80 mg/kg at a dose of 5ml/kg. This level of anaesthesia was maintained by administering hourly supplemental doses of 40mg/kg.

Halothane anaesthesia was induced in an induction box, (located in a fume hood), at 3% in 2L/min O_2 for 3-4 minutes. The animals were transferred to a facemask and anaesthesia was maintained on 1-1.5% halothane in 1L/min O_2 for the duration of the experiment. At all times when using halothane anaesthesia, a scavenging system (Flouvac), attached directly to the facemask, was employed to remove excess anaesthetic and free radicals from the experimental environment.

Stimulus

After a recovery period of at least 7 days, microdialysis perfusion was performed under terminal anaesthesia. As noted above, animals were anaesthetised with urethane (1.75mg/kg, i.p.), halothane (1-1.5% at 1L/min O_2,) or α-chloralose, (80mg/kg, i.p.). The stylet was removed from the guide cannula, and the microdialysis probe inserted. The delivery tubes were connected to the probe and dialysis perfusion with ACSF commenced immediately (with a perfusion flow rate of 2.5μl/min). ACSF was made up freshly on the day of the experiment, comprising (mM) NaCl (125), KCl (3.3), $MgSO_4$ (2.4), CaCl2 (1.85), KH_2PO_4 (1.25) by diluting appropriate volumes of 1M stock solutions of each in water. For the high potassium ACSF, the KCl was increased to 1ml (with an equivalent reduction in the amount of water) creating ACSF with 100mM concentration of potassium. All the samples were collected into orthophosphoric acid(1μl is required for every 10μl of sample), which also was made up beforehand. 132 ml of phosphoric acid was added to 1L distilled water, making 2M orthophoric acid.

Following a 60 minute equilibration period, consecutive 15-minute dialysate samples were collected for HPLC analysis. Following a further 60 minutes of basal collection period (4 samples), the experimental manipulations were performed. In all cases, the dead volume of the delivery tubes was taken into account, such that samples 5 and 13 coincided with stimulus application.

In experiment 1, the effects of amphetamine (1mk/kg, i.p) were assessed. The drug was given twice, at 1hr and at 3hrs as shown in Fig 3.5.4. In experiment 2, a mild footshock (1 s train of 6ms pulses, 25Hz, 0.3mA, 5 pulse trains at 2 minute intervals) was delivered through a pair of copper wires attached to each hind paw, at the beginning at 1hr. Subsequently ACSF containing 100mM potassium was introduced into the dialysis flow, using Rheodyne (7125) injection valve with a 20μl loop, at 3hrs, as shown in Fig

3.5.4. At the end of the experiment, animals were killed by urethane anaesthetic overdose followed by cervical dislocation, and the probe positions were verified macroscopically.

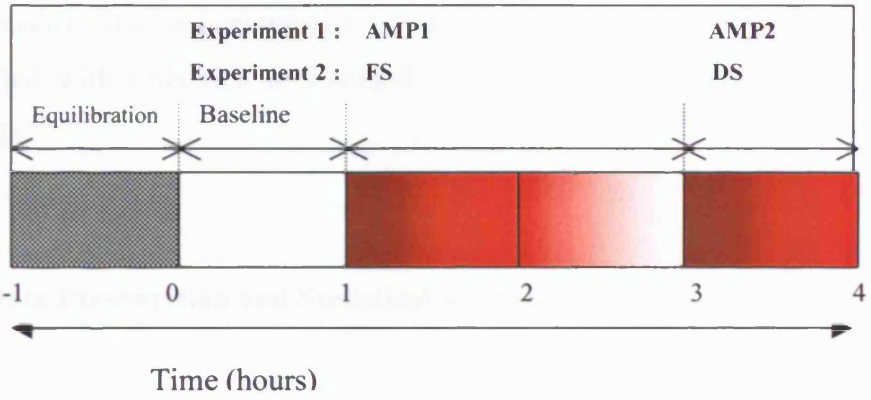

Fig 3.5.4 Timecourse of Stimulation

Animals were anaesthetised with urethane, halothane or α-chloralose (see 3.5.4). Firstly there is an equilibrium period of around 60 minutes. Steady baseline dopamine samples are collected (4 samples, 1 hr).

Experiment 1: 1mg/kg (i.p) amphetamine (**AMP1**) is administered at 1 hr. Sample collection is then continued for to 2 hours, and a second 1mg/kg, i.p dose of amphetamine (**AMP2**) is administered, and samples collected for 1 hr before the experiment is terminated.

Experiment 2: Footshock paradigm (**FS**) is applied at 1 hr and samples collected for two more hours. Depolarisation stimulation (**DS**) is then switched on (ACSF is switched to high potassium ACSF K^+, 100mM in dialysate) for the period of one sample and then returned to normal ACSF and sample collection is then continued for to 1 hr before the experiment is terminated.

3.5.5 HPLC Analysis

Samples were analysed by HPLC with elcetochemical detection. Mobile phase comprising (150mM NaH_2PO_4, 1.0mM octanesulfonic acid, 1.0mM EDTA, 20% methanol, pH 3.7, vacuum filtered and degassed) was pumped by a Rheos pump (Presearch, CMA Microdilaysis, Sweden) at a flow rate of 200µl/min. Online degassing (CMA 260) was used throughout. Samples (15µl) were injected onto the system using a Sparck Triathlon refrigerated autosampler (Presearch, U.K), and chromatographic separation was achieved on a LUNA (2) C18 column (2.0 x 150mm, 5µm)

(Phenomenex, UK). Component substances were detected electrochemically at a glassy carbon working electrode set at 750mV with respect to a Ag/AgCl reference electrode, using a VT-03 flow cell attached to an ANTEC `Intro` electrochemical detector (Presearch, U.K). Data were collected and integrated online, using Gynkosoft (Gynkotech), and concentrations of dopamine, DOPAC, HVA and 5HIAA were calculated with reference to standard solutions injected onto the column at regular intervals.

3.5.6 Data Presentation and Statistical Analysis

The concentrations of compounds measured are presented as percentages of their mean basal levels measured during the 60 minutes before the first stimulation (i.e. Samples 1-4). For analysis, the experiment was divided into four 60 min periods, designated basal 1 (samples 1 to 4), stimulus 1 (samples 5 to 8), basal 2 (samples 9 to 12) and stimulus 2 (samples 13 to 16). Statistical analysis was by repeated measures ANOVA, using a 2 x 2 x 4 design: that is experimental period (2 levels: samples 1 to 8 vs. samples 9 to 16), treatment (2 levels: basal vs. stimulated), sample number (4 levels: the 4 samples within each hour of recording). Where appropriate, increases in dopamine contributing to interactions were further investigated post-hoc, using one-tailed t-tests, with Bonferroni correction (for 5 d.f. $p<0.05$ $t_{crit} = 3.81$, $p<0.01$, $t_{crit} = 5.60$: for 6 d.f. $p<0.05$ $t_{crit} = 3.52$).

3.5.7 Materials and Suppliers

Stainless steel tubing for the guide cannulae, and stainless steel tubing for the stylettes were obtained from Coopers Needle Works (Perry Barr, Birmingham, UK). Sterile saline at 0.9% solution was obtained from Baxter Healthcare, Ltd, Thetfeld, Norfolk, UK. Halothane was obtained from Zeneca Ltd, Macclesfield, Cheshire; U.K. Fluovac obtained from International Market Supply, Congleton, Cheshire, UK. Temgesic (buprenorphine) was obtained from Schering-Plough (Welwyn Garden City, Herfordshire, U.K). D-Amphetamine, Urethane (ethyl carbamate), α-chloralose (β-Anomer <7.5%), 1,2-propanediol (propylene glycol), potassium phosphate, potassium chloride, calcium chloride, magnesium sulphate and phosphoric acid were obtained

from Sigma Chemical Company, Poole, Dorset. All needles (25 gauge, "5/8" and 21 gauge "1/2") and syringes (1ml and 2ml) used for injections were obtained from Becton Dickinson, U.K, Cowley, Oxford. 30 ml tube (Greiner Labortechnik, Stonehouse, Glos, UK).

Dialysis probes

Cuprophan dialysis membrane was obtained COBE ltd (Gloucester, U.K). Stainless steel tubing, was obtained from Coopers Needle Works (Perry Barr, Birmingham, UK). Capillary material (10VS-170OD silica tubing) was obtained from SGE (Milton Keynes Buckinghamshire, U.K). Connectors created from peristaltic pump tubing were acquired from Anachem (Luton, Beds, UK). Epoxy resin (fast drying) and cyanoacrylate gel were obtained from Loctite (Welwyn Garden City, Herfordshire, U.K).

Drug and anaesthetic preparation

D-Amphetamine sulphate was stored at room temperature. On the day of the experiments it was dissolved in 0.9% saline, at a concentration of 1mg/ml, and stored at room temperature until use. The drug was administered at 1ml/kg, i.p, giving a final dose of 1mg/kg.

α-chloralose was stored at room temperature. It was made up on the morning of the experiment and left at room temperature. 80mg of alpha chloralose was weighed out and dissolved in 16ml of propylene glycol, to be administered at the concentration 80 mg/kg at a dose of 5ml/kg.

Urethane was stored at room temperature. It was made up on the morning of the experiment and left at room temperature, and stored for up to 3 months. 17.5g of urethane was weighed out and dissolved in 100ml of (0.9% Nacl) saline, to be administered at the concentration of 1.75g/kg at a dose of 10ml/kg.

3.6 Results

The concentrations of compounds measured are presented as percentages of their mean basal levels, measured in the first 60 minutes of sample collection. Basal dialysate levels of dopamine, DOPAC, HVA and 5HIAA in conscious animals and in animals

under the three different anaesthetics are shown in table 3.6. Under both urethane and halothane, relatively stable baseline levels of all four compounds measured were achieved, but under α-chloralose, the basal levels were much more variable, both within and between animals.

Anaesthetic	Dopamine	DOPAC	HVA	5HIAA
NONE (Awake) (Young et al, 1992)	1.9+0.6 (7-8)	337+56 (7-8)	135+27 (7-8)	63+16 (7-8)
Urethane	1.45 ± 0.34 (n = 13)	102 ± 6 (n = 11)	33 ± 5 (n = 8)	29 ± 2 (n = 9)
Halothane	1.24 ± 0.15 (n = 12)	387 ± 41 (n = 11)	43 ± 6 (n = 7)	86 ± 11 (n = 8)
α-Chloralose	2.97 ± 0.33 (n = 12)	151 ± 21 (n = 11)	48 ± 5 (n = 9)	56 ± 10 (n = 11)

Table 3.6 Basal dialysate levels of dopamine, DOPAC, HVA and 5HIAA in conscious animals and in animals under the three different anaesthetics

The effects of two amphetamine (1mg/kg, ip.) administrations AMP1 and AMP2 on dopamine and metabolite levels in the nucleus accumbens are show in Fig 3.6.1A-C.
The effects of footshock (FS) and neuronal depolarisation stimulation (DS) by elevated potassium, on dopamine and metabolite levels in the nucleus accumbens are show in Fig 3.6.2A-C.

In some experiments, HPLC analysis failed to resolve peaks for 5HIAA and HVA sufficiently to enable reliable quantification of their concentrations. Consequently, n-values for these two compounds were insufficient to allow meaningful statistical analysis of effects of stimulation.

3.6.1 Amphetamine-Stimulated Dopamine Release

Fig 3.6.1a Amphetamine Stimulation under Urethane Anaesthesia

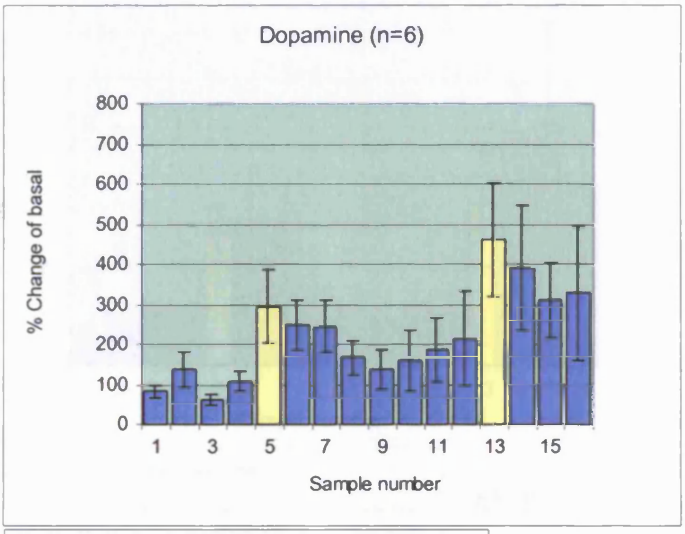

The main figure (left) shows the levels of dopamine release as normalised to baseline release (100%). (Results are ± S.E.M;. Absolute values (nM) are shown in Table 3.6.

The time points at which the amphetamine was administered are marked by the yellow columns.

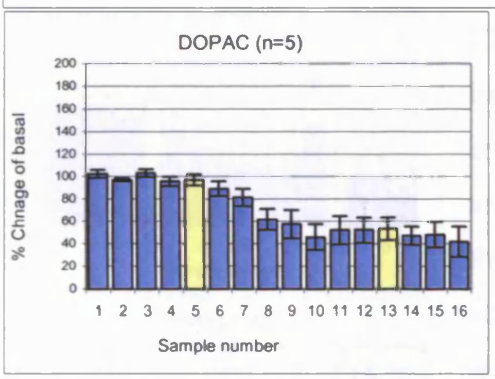

AMP1 caused dopamine release to increase to 295±90%. AMP2 causes dopamine release to increase to 460±142%. Significant main effects of stimulus were measured under urethane ($F[1,5] = 7.57$, $p = 0.04$), indicating that extracellular levels of dopamine were raised above basal following amphetamine administration.

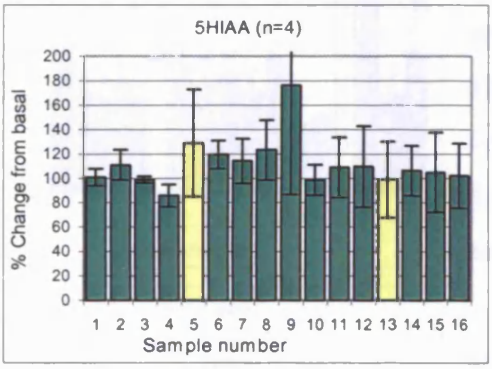

Accompanying these increases in dopamine, there was a decrease in DOPAC to around 50% of basal values. Statistical analysis showed a significant effect of experimental period ($F[1,4]=10.65$, $p=0.031$), indicating the decreases observed was statistically significant. There was some indication of a small decrease in HVA, but no change in 5HIAA. However insufficient data were collected for either compound to allow statistical analysis.

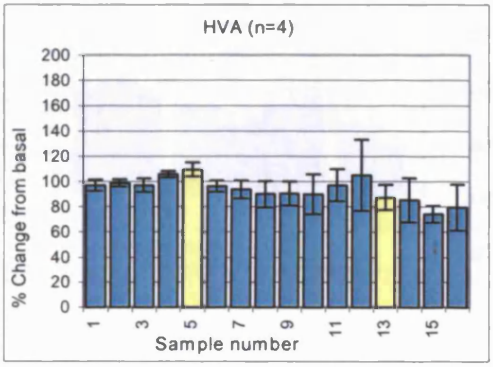

Fig 3.6.1b Amphetamine Stimulation under Halothane Anaesthesia

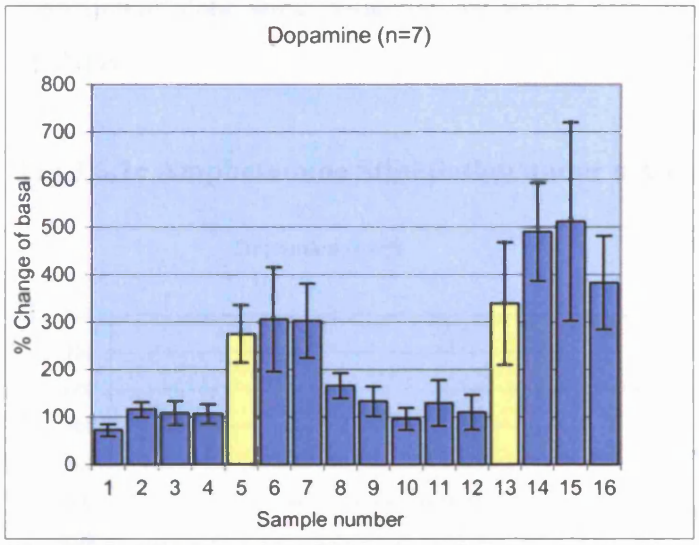

The main figure (left) shows the levels of dopamine release as normalised to baseline release (100%). (Results are ± S.E.M. Absolute values (nM) are shown in Table 3.6.

The time points at which the amphetamine was administered are marked by the yellow columns.

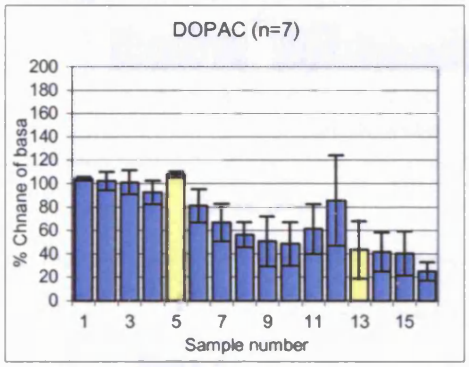

AMP1 caused dopamine release to increase to 274±61%. AMP2 causes dopamine release to increase to 339±129%. Significant main effects of stimulus were measured under halothane anaesthesia ($F[1,6] = 14.88$, $p=0.008$), indicating that extracellular levels of dopamine were raised above basal following amphetamine administration. Additionally, in halothane anaesthetised animals there were a significant stimulus x repeat interaction ($F[1,6] = 7.10$, $p = 0.037$) indicating that there was a significantly larger response to the second amphetamine treatment than to the first.

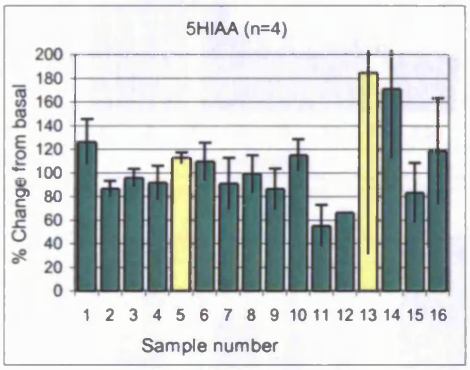

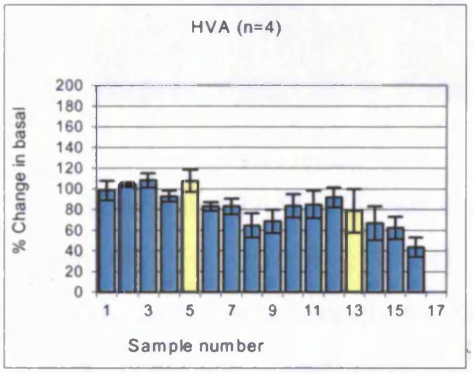

In addition, there were decreases in DOPAC, to around 50% of basal. There was some indication of return towards basal levels after AMP1, although recovery was not complete before the onset of AMP2. Statistical analysis showed a main effect of stimulus ($F[1,6]=11.81$; $p=0.014$).

Although there were some indications of a decrease in HVA (but not 5HIAA), insufficient data were collected for either metabolite to allow meaningful statistical analysis.

Fig 3.6.1c Amphetamine Stimulation under α-Chloralose Anaesthesia

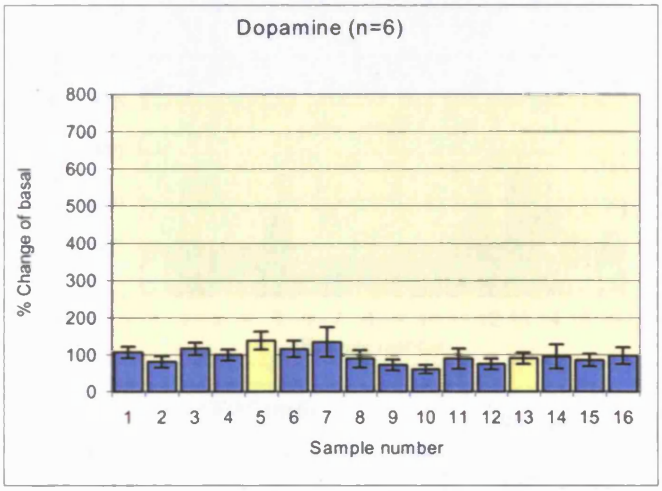

The main figure (left) shows the levels of dopamine release as normalised to baseline release (100%). Results are ± S.E.M. Absolute values (nM) are shown in Table.3.6. The time points at which the amphetamine was administered are marked by the yellow columns.

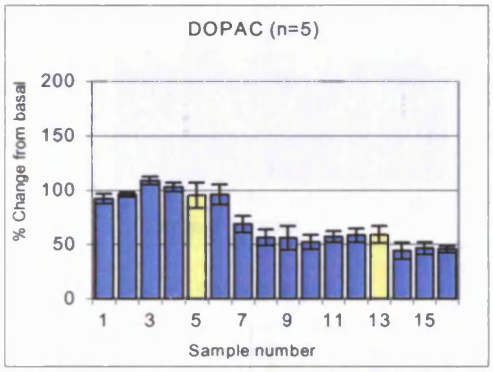

In contrast to the changes in dopamine and its metabolites under halothane and urethane, under α-chloralose anaesthesia, there was no significant effect of stimulation on dopamine levels [$F[1,5] = 2.86$, $p=0.151$. There was a significant reduction in the levels of DOPAC.

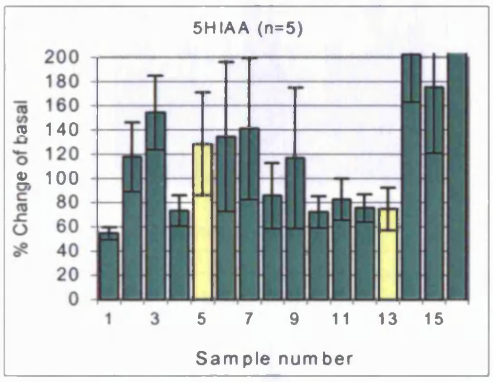

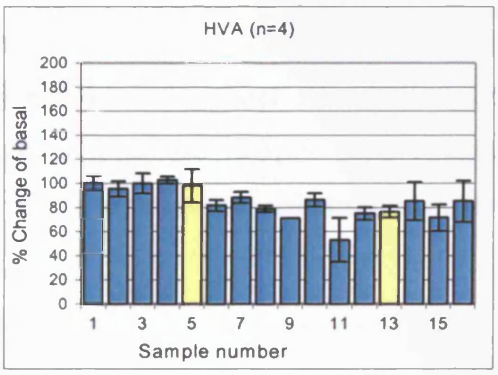

The reduction in DOPAC levels showed no sign of recovery between AMP1 and AMP2 (main effect of stimulus: $F[1,4]=53.11$, $p=0.002$). There was some indication of a decrease in HVA but results for 5HIAA were very variable and showed no consistent trends. There were insufficient data for HVA or 5HIAA to allow meaningful statistical analysis.

3.6.2 Footshock and Neuronal Depolarisation-Stimulated Dopamine Release

Fig 3.6.2a Footshock and Neuronal Depolarisation under Urethane Anaesthesia

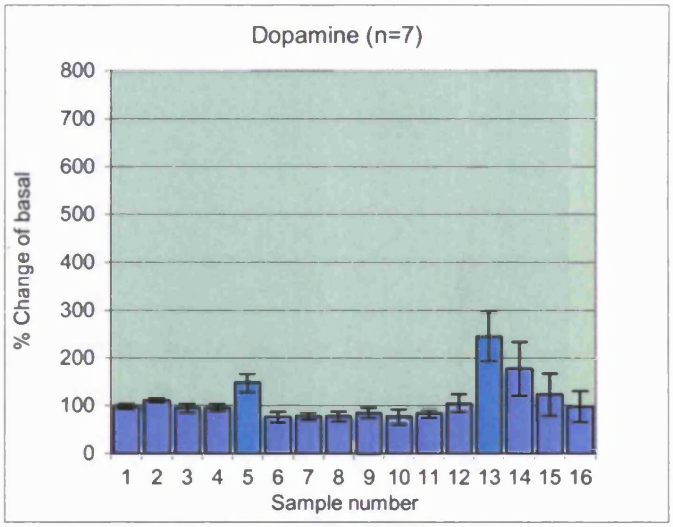

The main figure (left) shows the levels of dopamine release as normalised to baseline release (100%). Results are ± S.E.M. Absolute values (nM) are shown in Table 3.6. The time points at which the FS & DS were applied are marked by the turquoise columns.

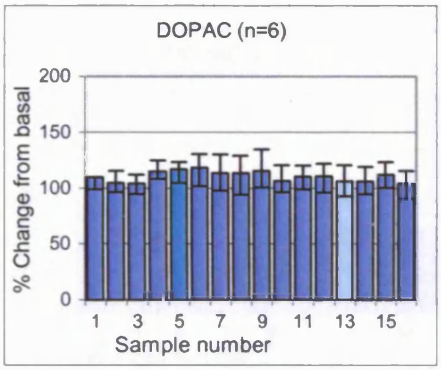

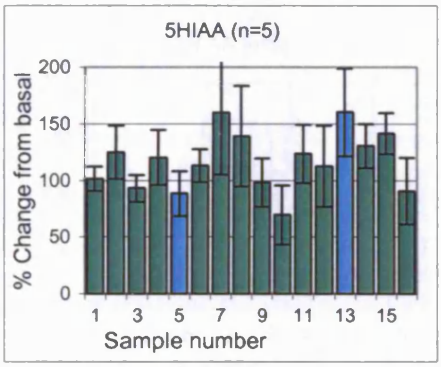

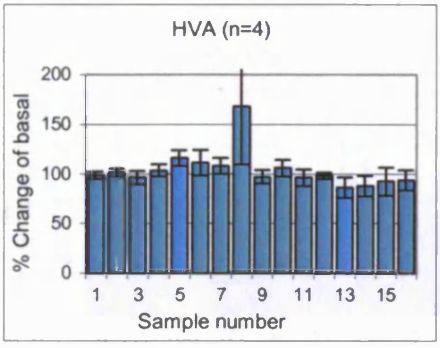

FS causes dopamine release to increase to 148 ±19%. DS causes dopamine release to increase to 245±51%. Significant main effects of stimulus were observed in the experiment measuring responses to footshock and to potassium under urethane ($F[1,6]= 6.28$, $p=0.046$). There was also a significant stimulus by sample interaction ($F[3,15] = 10.54$, $p < 0.001$). Post-hoc one-tailed t-tests with Bonferroni correction showed significant increases in dopamine during potassium ($t[6] = 3.56$, $p<0.05$) but footshock stimulation just failed to reach significance ($t[6] = 3.21$ compared to $T_{crit}=3.52$) in urethane-anaesthetised animals.

There were no indication of effects of either stimulation on levels of DOPAC, HVA or 5HIAA. No significant changes in DOPAC levels were seen: there were not sufficient data for HVA of 5HIAA to allow meaningful statistical analysis.

Fig 3.6.2b Footshock and Neuronal Depolarisation under Halothane Anaesthesia

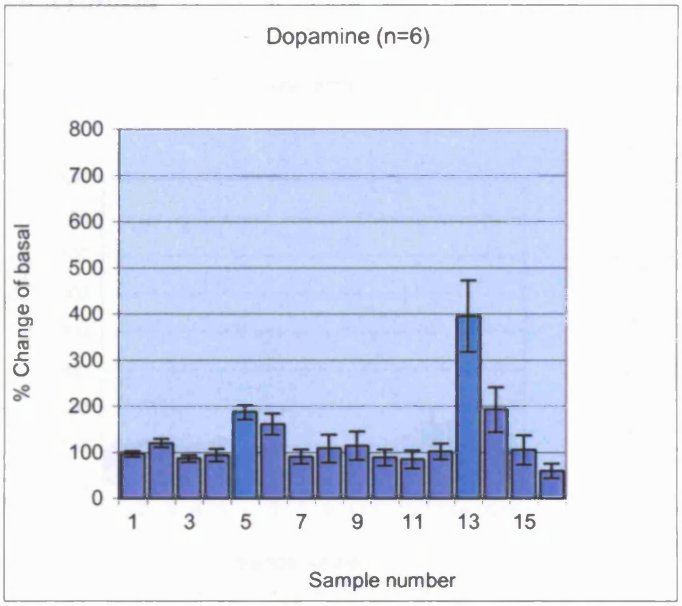

The main figure (left) shows the levels of dopamine release as normalised to baseline release (100%). Results are ± S.E.M. Absolute values (nM) are shown in Table 3.6. The time points at which the FS & DS were applied are marked by the turquoise columns.

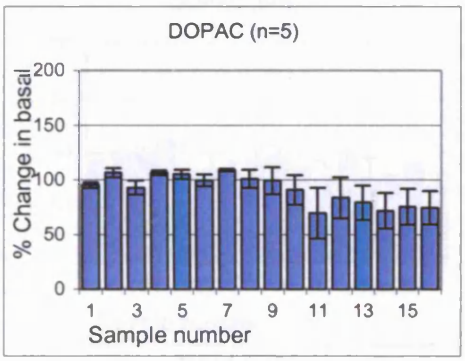

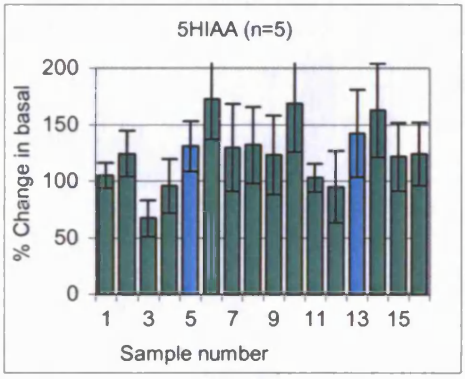

FS causes dopamine release to increase to 187±15%. DS causes dopamine release to increase to 396±78%. Significant main effects of stimulus were also observed in the experiment measuring responses to footshock and to potassium under halothane ($F[1,5] = 13.39$, $p=0.015$) and there was also a significant stimulus by sample interaction $F[3,15] = 9.36$, $p = 0.001$. Post-hoc one-tailed t-tests with Bonferroni correction showed significant increases in dopamine during footshock ($t[5] = 5.66$, $p<0.01$) and potassium ($t[5] = 3.94$, $p<0.05$) stimulation.

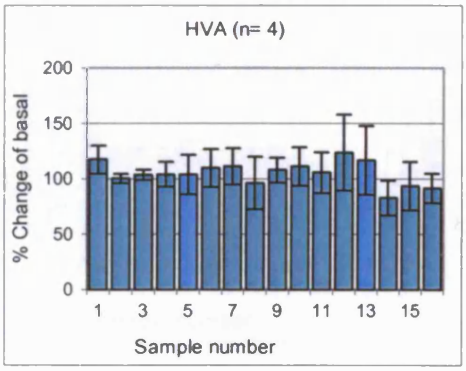

Although there was a small decrease in DOPAC this was not statistically significant. There were no indication of any effects on HVA or 5HIAA, but there were insufficient data to allow meaningful statistical analysis.

Fig 3.6.2c Footshock and Neuronal Depolarisation under α-Chloralose Anaesthesia

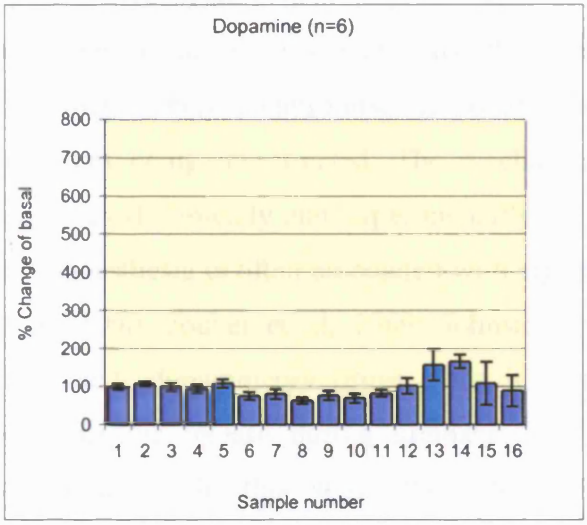

The main figure (left) shows the levels of dopamine release as normalised to baseline release (100%). Results are ± S.E.M. Absolute values (nM) are shown in Table 3.6. The time points at which the FS & DS were applied are marked by the turquoise columns.

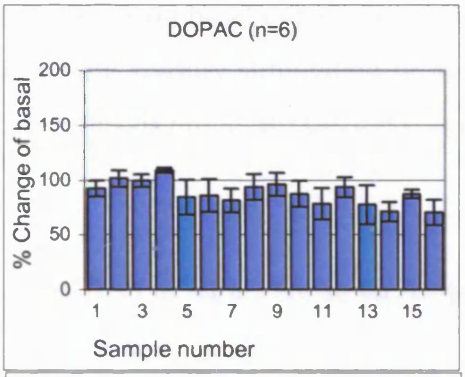

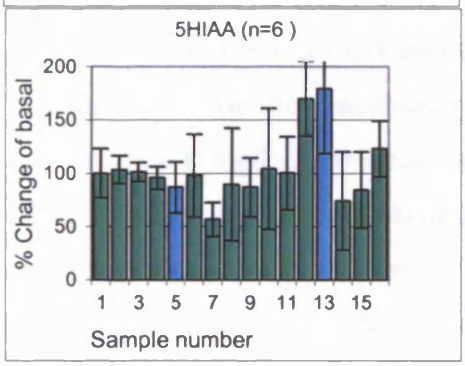

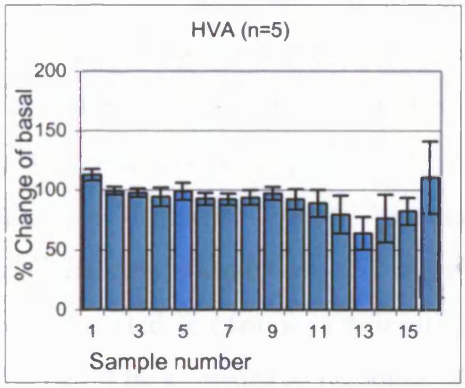

Under α-chloralose anaesthesia, dopamine levels remained unchanged during footshock stimulation, 108 ±11%) but did show a small rise during potassium stimulation (156±41%). Statistical analysis using repeated measures ANOVA showed no main effects of sample, stimulus number or stimulus. There was however a significant stimulus x sample interaction ($F[3,15] = 4.63$, $p=0.017$). Post-hoc one-tailed t-tests with Bonferroni correction showed that none of the stimulated samples were significantly above basal, although sample 14 (the sample after the potassium stimulation) did approach significance ($t[5] = 3.66$, compared with $t_{crit} = 3.81$).

There was no indication of effects on levels of the metabolites. No significant changes in DOPAC levels were seen: there were not sufficient data for HVA of 5HIAA to allow meaningful statistical analysis.

3.7 Discussion

Studies investigating neurophysiology, neurochemistry and neuroimaging have been performed in anaesthetised animals. With these preparations, concerns arise that the anaesthetics may compromise neuronal function, or that it may interact with the paradigm being investigated. The mechanisms underlying the anaesthetic action of agents used clinically and experimentally are poorly understood. It has been proposed that anaesthesia is often associated with significant changes in dopamine levels (Stahle et al, 1990; Jouvet et al, 1969; Johnston et al, 1972), and this may influence the response to dopaminergic drugs. Thus, it is of interest to investigate the characteristics of dopamine release during urethane, halothane and chloralose anaesthesia using microdialysis. In this study the effect of urethane, halothane and α-chloralose anaesthesia on basal dopamine release, and dopamine release evoked by amphetamine, peripheral sensory stimulation or depolarisation from elevated ACSF potassium in the microdialysis probe stimulation was investigated

3.7.1 Effect of Anaesthesia on Amphetamine evoked Dopamine Release

Amphetamine acts to release dopamine by blocking dopamine uptake and by reversal of the dopamine transporter (mechanisms described in detail in section 5.1). Amphetamine administration (1mg/kg, i.p) caused significant increases in synaptic dopamine levels in both halothane- and urethane-anaesthetised animals, and the percentage increases in dopamine release were similar for both agents (Fig 3.7.1a & b). In α-chloralose-anaesthetised animals no significant changes in dopamine were detected, any effects observed were small and extremely variable. In urethane and halothane anaesthetised rats there was a marked and sustained increase in dopamine release, for about an hour after amphetamine administration which then returned almost to baseline. In the same groups, the second amphetamine administration also caused an increase in dopamine release. Moreover, under halothane anaesthesia, the response to the second amphetamine stimulation was significantly higher than to the first, as has previously been reported in conscious animals (Warburton et al, 1997). The possibility arises that this could be a sensitised response, although it is not known if it could occur over a two

hour interval, since Weiner et al (1988) found that sensitisation does not occur when administrations are given one hour apart. Thus, the potentiated dopamine release could be due to residual effects of the first dose. In some urethane-anaesthetised animals, there was some indication of a larger response to the second dose of amphetamine than to the first, but over the whole group, there was no significant difference in the size of the response to the two injections.

In both the halothane- and the urethane- anaesthetised animals there was a significant decrease in DOPAC levels after amphetamine treatment. This is in agreement with results from unanaesthetised animals (Di Chiara & Imperato, 1988), and has been attributed to the known effects of amphetamine in blocking dopamine reuptake and blocking monoamine oxidase (Mann & Quastel, 1940).

Halothane has been observed to enhance dopamine release caused by dopamine reuptake blockers such as vanoxerine (GBR 12909), nomifensine and amphetamine (Fink-Jensen et al, 1994; Adachi et al 2001). The results from Experiment 1 showed halothane to potentiate the "late response" of dopamine release to this stimulation (Fig 3.6.1b), said to occur 1-3 hours after stimulation (Fink-Jensen et al, 1994). Should the late response occur, it may go undetected, as samples are collected only for two hours after the first injection (AMP1), and for one hour after the second injection (AMP2).

Despite these considerations to ascertain whether anaesthetics affect amphetamine stimulated dopamine release, the same experiment would need to be performed in non-anaesthetised rats, and the results compared to the anaesthetised cohorts. Data obtained from awake and freely moving rats show that 1 mg/kg administrations of amphetamine caused similar increases in dopamine release when administered i.p (Warburton et al, 1996). Other investigators have found dopamine release to be increased as much as 1000% (Di Chiara & Imperato, 1988 ; Kuzcenski & Segal 1989), far greater than observed in the above experiments, although the amphetamine was administered subcutaneously in these rats. Thus our data agrees with the awake and freely moving rat experiments indicating that halothane probably does not have a potentiating effect on the dopamine release caused by amphetamine administration.

Interestingly, despite the lack of reproducible effect of amphetamine on dopamine in α-chloralose-anaesthetised animals, the reason for such inhibition is not clear, but this anaesthetic is not routinely used in studying dopamine pharmacology. One fMRI investigation studying the effects of D_2 antagonist sulpiride (described in Chapter 7) in the α-chloralose anaesthetised rat, only found changes (increases) in BOLD signal in the frontal cortex. This distribution of BOLD signal is quite restricted when considering the distribution of D_2 receptors in subcortical structures (Preece et al, 2000), thus perhaps the anaesthetic was suppressing dopaminergic activity in these areas. Furthermore, 2DG autoradiography experiments indicate that α-chloralose anaesthetised rats do not show an increase in CMR_{glu} in various brain structures after amphetamine administration; but halothane anaesthetised rats demonstrate increased CMR_{glu} in the same structures (Cash, 2002 personal communication). Surprisingly, the changes in DOPAC levels observed in the α-chloralose-anaesthetised animals were very similar to those seen under the other two anaesthetics which did not suppress stimulated dopamine release, and also similar to levels previously reported in conscious animals (Di Chiara & Imperato, 1988). These results emphasise that changes in metabolite levels in response to drugs do not necessarily reflect changes in neurotransmitter levels.

3.7.2 Effect of Anaesthesia on Footshock and Depolarisation evoked Dopamine Release

Stimulation with either mild footshock or with high potassium introduced via the dialysis stream, yielded responses in halothane- and urethane-anaesthetised animals. Both urethane and halothane anaesthetised animals showed clear transient increases in dopamine release after footshock. The effect in urethane-anaesthetised animals just failed to reach significance, so this data must be treated with caution. However, it should be emphasised that the post-hoc testing used was very conservative. Further investigation is required to confirm this effect. Local perfusion for 5 minutes with 100 mM K+ significantly increased the release of dopamine, but not the metabolites. As expected, the response to potassium was around 2- to 3-fold higher than to footshock.

An interesting point about these stimuli, is that they are not specific to the dopamine system, and as such it is interesting to observe the effects of the anaesthetics on dopamine release which is evoked in a different manner. Although a stressor, footshock elicits dopamine release in the nucleus accumbens and dopamine metabolism in the prefrontal cortex (Gonenc et al, 2000) and it also involves other transmitters. Footshock was observed to enhance glutamate release (Singewald et al, 1994; Saulskaya et al, 2000). It also appears that noradrenaline (Feenstra et al, 1992) and GABA systems (Plazik et al, 1992) may contribute to the footshock-induced behavioural depression, including locomotor inhibition. Under halothane, and perhaps urethane, anaesthesia, footshock caused an increase in dopamine release and results are in agreement with those produced in conscious animals following footshock (Abercrombie et al, 1989; Hamamura & Fibiger, 1993; Young et al, 1993). α-chloralose-anaesthetised animals did not display a significant increase in dopamine release after footshock. This lack of effect of peripheral sensory stimulation on the dopaminergic system in α-chloralose-anaesthetised animals contrasts with fMRI studies in which BOLD signal in consistently increased in the somatosensory cortex after similar stimulation (Hyder et al, 1994). These data suggest that the anaesthetic, α-chloralose has regionally specific effects and differentially causes depression and facilitation of neurotransmission. This fits well with the hypothesis of Monroe et al (1963), that α-chloralose combines depressant properties with those of a stimulant, with the behavioural effects of the depressant actions are manifested as sedation (Hanriot & Richet, 1893). This, however, is observed after the spontaneous myclonic jerks and rocking, at pre-anaesthetic stages. These actions are explained by cortical depression and secondary disinhibition of the thalamus and mesencephalic reticular formation at subcortical structures thereby providing the motor hyperexcitability reaction to sensory stimuli (Balis & Munroe, 1964).

Potassium stimulation is a basic transmitter release mechanism (Dobrev et al, 1995) and acts by an exocytotic process (Drapeau & Blaustein, 1983). Depolarization-induced dopamine release by high potassium stimulation is frequently used to compare mobilization of the striatal dopamine store (for instance in comparing young and old rats, Friedemann & Gerhardt, 1992; Dobrev et al, 1995). High potassium-stimulated dopamine increase is a dynamic process involving many subcellular mechanisms, including channel opening by depolarization, influx of calcium ions, emptying of dopamine vesicles and reuptake of released dopamine (Shui et al, 1998). Thus using

such a test is good way of testing the responsivity of the brain: neither halothane nor urethane anaesthesia depress the release of dopamine, as results are in agreement with those produced in conscious animals (Cass et al, 1998). Although in α-chloralose-anaesthetised animals, there were some indication of an increase after potassium stimulation, it was small and very variable and failed to reach statistical significance.

3.7.3 Possible Mechanisms of Action

The results indicate that halothane and urethane are suitable anaestheic agents to use while studying evoked dopamine release whereas α-chloralose is not, regardless of the type of stimuli. What is not clear is how the anaesthetics act to produce the effects of the dopamine system. To understand the cellular and molecular basis of the anaesthetic state, it is important to remember that, in the intact CNS, synapses operate within elaborate nerve networks. The anaesthetic effects on different neuronal pathways may therefore depend on the nature of the receptors and of the ion channels of the cells that comprise the network. The anaesthetic state may be the result of all these actions, but the characteristics of the state may differ somewhat from agent to agent.

The effect of halothane on basal levels of dopamine release has been investigated. The modulation of dopamine release by volatile anaesthetics is controversial: *in vivo* microdialysis experiments have found increases in the basal striatal extracellular levels of dopamine during halothane anaesthesia (Stahle et al, 1990; Opacka-Juffery et al, 1991; Miyano et al, 1993) and its metabolites (Stahle et al, 1990; Adachi, et al, 2000) while no changes were reported by others (Fink-Jensen et al, 1994). It has been demonstrated that volatile anaesthetics inhibit dopamine uptake by rat brain synaptosomes (El-Maghrabi & Eckenhoff, 1993), but they also induced a significant increase in spontaneous [^{3}H]dopamine release from rat striatal synaptosomes (Mantz et al, 1994). In another investigation (Adachi et al, 2001), in which the concentration-dependent effect of halothane on striatal DA release using microdialysis techniques was

studied, changes in the basal release of dopamine, were only seen when 2% halothane was inhaled. Because hypoxia or hypoglycaemia activate the reversed operation of the transporter and [Ca^{2+}] independent release of neurotransmitters (Milusheva, et al, 1992; Milusheva et al, 1996; Uchihashi et al, 1998), this increase could be explained by hypoxia or ischaemia induced by the direct action of halothane (Adachi et al, 2001). However, Mantz (1999) claims that, volatile anaesthetics may provide a cerebroprotective effect against ischaemia.

It has been suggested that the anaesthetic state is expressed by activation and inhibition at the synapses in the inhibitory or excitatory neurotransmitter systems in the central nervous system (reviewed by Pocock & Richards, 1993). At the postsynaptic sites, the $GABA_A$ receptor is considered the most probable target of anaesthetics, supported by the electrophysiological findings that the inhibitory postsynaptic current was prolonged by various anaesthetics (halothane, ketamine and pentobarbitone, Gage & Robertson, 1985). In a behavioural study, benzodiazepines prolonged halothane-induced sleep in mice, while flumazenil, a benzodiazepine receptor antagonist, hastened emergence from halothane anaesthesia (Geller et al, 1991). Anaesthetics are also thought to act at presynaptic sites (Pocock & Richards, 1993), affecting GABA release and modulating uptake (Minchin, 1991), and also glutamate (Larsen and Langmoen, 1998) and importantly, monoamine neurotransmitters (Mantz and et al, 1994). In addition, volatile anaesthetics were found to inhibit the release of, and enhance the uptake of the excitatory neurotransmitter glutamate (Larsen and Langmoen, 1998).

Using *in vivo* microdialysis, it was observed that dopamine administration changed the anaesthetic requirement (Onozawa et al, 1999). Isoflurane, another volatile anaesthetic, has been shown to potentiate the effect of dopamine enhancer drugs, such as cocaine and GBR12909, on [^{11}C]raclopride binding in the striatum of anaesthetised as compared with awake monkeys (Tsukada et al. 1999). Instead of only examining how the anaesthetics affect dopamine release, one might question which dopaminergic drugs may affect the anaesthetic.

3.7.4 Conclusion

The results from these experiments showed that different anaesthetics commonly used in physiological and pharmacological experiments have different effects on brain dopamine systems. Basal levels of dopamine are significantly higher in α-chloralose-anaesthetised rats than in either urethane- or halothane-anaesthetised rats, neither of which differ significantly from unanaesthetised rats. The metabolite levels however, show more variation: whilst DOPAC levels in halothane-anaesthetised animals was similar to those in conscious animals, those in urethane-anaesthetised and α-chloralose-anaesthetised animals were significantly lower than in either conscious or halothane-anaesthetised animals.

Urethane is one of the most commonly used anaesthetics in animal experiments (Shimokawa et al, 1998) but the mechanisms of its action are unclear. A peculiar characteristic of urethane is represented by its ability to induce a surgical plane of anaesthesia without affecting neurotransmission in various subcortical areas or the peripheral nervous system (Maggi & Meli, 1986). This makes urethane a suitable general anaesthetic for studying neural function in both central and peripheral nervous systems and accounts for the preservation of a number of reflex responses in urethane-anaesthetised animals.

α-chloralose has been extensively used in investigating somatosensory activation as detected using fMRI (Hyder et al, 1994; Yang et al, 1998). It preserves metabolic coupling in the somatosensory cortex, as measured by CMR_{glu} coupling to evoked cortical potentials, to a similar degree to that of the awake animal (Ueki et al, 1992). However, another 2DG autoradiography study found α-chloralose to decrease basal CMR_{glu} to a greater degree than halothane and isoflurane in various brain regions, as compared to the awake animal (Cash et al, 2001). It is clear, however that under a α-chloralose anaesthesia, stimulated dopamine release is suppressed, although the basal levels are not. Furthermore it is suppressed after various types of stimuli known to increase dopamine release. Such data gives rise to the idea that α-chloralose may have a differential effect in various brain areas.

General anaesthesia with halothane is desirable as both flow-metabolism coupling and responsiveness to stimulation are preserved (Hansen et al, 1989; Ueki et al, 1992; Lindauer et al, 1993). Furthermore, comparison between fMRI and 2DG radiology studies using cocaine has found good correlations spatially and quantitatively (Jones et al, 1998; Marota et al, 2000). Despite these findings the use of halothane in cerebrovascular studies is still criticised as it markedly depresses cardiovascular reflexes (Bonvento et al, 1994), decreases CMR_{02} (Shiraishi et al, 1997) and increase CBF (Brussel et al, 1991). As these factors, and their respective dynamics are the basis of the BOLD fMRI signal, the possible influence of halothane on cerebral metabolism is an area requiring further investigation.

These results point to halothane and urethane being suited for phMRI of the dopaminergic system. Importantly, the data indicate that different anaesthetics may act very differently depending on the paradigm being investigated and highlight the importance of preliminary studies prior to carrying out investigations such as phMRI. The anaesthetic itself may turn out to be a confound in the experiment being performed. Sometimes there is an interaction between the drug and anaesthetic agent, for example, it was observed that there was an interaction between cannabinoid receptor agonist HU210 and halothane causing additional sedation and respiratory depression (Shah et al, 2001) and chloral hydrate is used instead as the anaesthetic agent, it may affect neurovascular coupling and therefore the fMRI signal being measured (Arthurs & Boniface, 2002). Anaesthetics show heterogeneity in cerebebral metabolism, thus these observations must be considered when designing fMRI protocols.

Chapter 4

Materials and Methods

4.1 Animals

All experimental procedures obtained the approval of Leicester and Nottingham Universities Ethical committees. All of the experimental procedures described in this thesis here were performed in accordance with the UK Home Office Animals (Scientific Procedures) Act 1986, and adequate care was taken at all times to minimize pain and discomfort. Male Sprague-Dawley rats (n=8, 250-300g) were housed in cages of 3 (55cm x 37cm x 15cm) with ad libitum access to appropriate food and water under a 12:12-h light/dark cycle (lights on 08:00h) until required for experimental purposes.

4.2 Materials

D-Amphetamine,R(+)-SCH23390 hydrochloride, (±)-SKF38393 hydrochloride, (-)-Sulpiride, (-)- Quinpirole, and 1,2-propanediol (propylene glycol) were obtained from Sigma Chemical Company, Poole, Dorset. Halothane was obtained from Zeneca Ltd, Macclesfield, Cheshire; U.K. Sterile saline at 0.9% solution was obtained from Baxter Healthcare, Ltd, Thetfeld, Norfolk, UK. Heparin was obtained from Holder CP Pharmaceuticals Ltd, North Wrexham, UK. All cannulations and drug administrations whilst scanning were performed using Portex tubing ®, Portex, Kent, UK. Needles (25 gauge, "5/8" and 21 gauge "1/2") and syringes (1ml and 2ml) used for injections were obtained from Becton Dickinson, U.K, Cowley, Oxford. Flouvac anaesthetic scavenger was obtained from International Market Supply, Congleton, Cheshire, UK.

4.2.1.Anaesthetics

Initially urethane being a single dose, stable anaesthetic, was thought to be the most useful anaesthetic for these experiments was made up in 0.9% saline to a concentration of 0.175g/ml to be administered at a dose of 1.75g/kg, intra peritoneally (i.p). However it proved to be difficult to dose and slow in onset. In addition to its simplicity and control of use by inhalation, halothane was then chosen as an anaesthetic agent, a further advantage was that it had minimal effects on the dopaminergic system as determined using in-vivo microdialysis (Chapter 3).

4.2.2.Dopaminergic agents

1. D-Amphetamine sulphate was stored at room temperature and reconstituted on the day it was required. It was made up to a concentration of 3mg/ml in saline (0.9% NaCl) and was stored at room temperature. The drug was administered as a single 1ml/kg injection giving a dose of 3mg/kg.
2. D_1 antagonist, SCH23390 was stored at room temperature protected from exposure to light and made up on the day when required. It was made up to a concentration of 0.25mg/ml in a 50/50 mixture of saline (0.9% Nacl) and propylene glycol and stored at room temperature. The drug was administered as a single 2ml/kg injection giving a dose of 0.5mg/kg.
3. D_1 agonist, SKF38393 was stored at room temperature protected from exposure to light and made up on the day when required. It was made up to a concentration of 10mg/ml in saline (0.9% NaCl) and was stored at room temperature. The drug was administered as a single 1ml/kg injection giving a dose of 10mg/kg
4. D_2 antagonist, sulpiride was stored at 2-8^{o} and made up on the day when required. It was made up to a concentration of 25mg/ml in ml in saline (0.9% NaCl) and was stored at room temperature. The drug was administered as a single 2ml/kg injection giving a dose of 50mg/kg.
5. D_2 agonist, quinpirole was stored at –20^{o} and made up on the day when required. It was made up to a concentration of 0.5 mg/ml in saline (0.9% NaCl) and was stored at room temperature. The drug was administered as a single 1ml/kg injection giving a dose of 0.5 mg/kg.

4.3 Surgery

On the day of the experiment, anaesthesia was induced with 1.5-2% halothane in a mixture of O_2/NO_2 (1l/min) in an induction chamber for 5-10 minutes. Once anaesthetised, the animal was removed from the induction chamber and placed on a modified adjustable heater bed (Scientific Research instruments, Ltd, Edenbridge, Kent) on which there was an attached facemask and anaesthesia maintained with 1-1.5%, 1L/min in 70%/30% mix of N_2/O_2 delivered via a facemask. The gaseous anaesthetic line was then attached to this facemask. Core body temperature was measured by means of a rectal probe (see 4.5.1). When the corneal, hind limb withdrawal and tail-pinch

reflex were absent, the level of anaesthesia was deemed suitable for surgery. The jugular vein was cannulated to allow intravenous administration of drugs (in the following experiments all drugs were administered by this route). The cannula was made by attaching a length of plastic tubing (0.2mm inner diameter, 0.3mm outer diameter, volume of 0.05ml) to a 1ml syringe and needle (25 gauge, "5/8") needle filled with saline/heparin (1part per hundred). The end of the tubing was cut at an angle to facilitate insertion into the vessel.

After locating the clavicula, the skin above this area was removed, as was the underlying subcutaneous tissue. Using two sets of small forceps, the underlying tissue was dissected until the jugular vein was located. Once detached and free of surrounding connective tissue, the distal end of the left jugular was tied off with a cotton ligature, and cotton was also loosely tied around the proximal end. Using small dissecting forceps, the jugular was raised up and a small incision made with scissors. Saline/heparin mix was immediately applied to the general area and the cannula inserted into the vessel. When blood could be drawn back into the cannula tubing by pulling back on the syringe the cannula was confirmed to be positioned in the vein. At this point the proximal end was tied to the cannula tubing and this was also attached to the cotton at the distal end. Some saline/heparin mix was slowly injected in. Great care was required to avoid the entry of air bubbles into the cannula.

Thus cannulated, the rat was transferred to the probe and placed prone at the centre of the volume resonator coil and the modified surface coil was placed on top of its skull. The gaseous anaesthetic line was also transferred and attached to the front of the probe to be delivered into a nose cone. The head was fixed in this position by means of a moulded foam insert and a nose cone made from a modified pipette. The rat and the probe (described below) were then transferred to the magnet (see 4.6.1).

4.4 Rat probe

A rat body holder was built to allow reliable positioning and immobilisation of the anaesthetised rat in the magnet. This holder was made from a 45cm length of plastic piping (6.7cm outer diameter, 3.3cm inner diameter) with most (28cm) of the upper half removed. The caudal end of the probe was left to allow attachment of the facemask,

gaseous anaesthetic lines and scavenger. This probe was made by technical staff at MR centre.

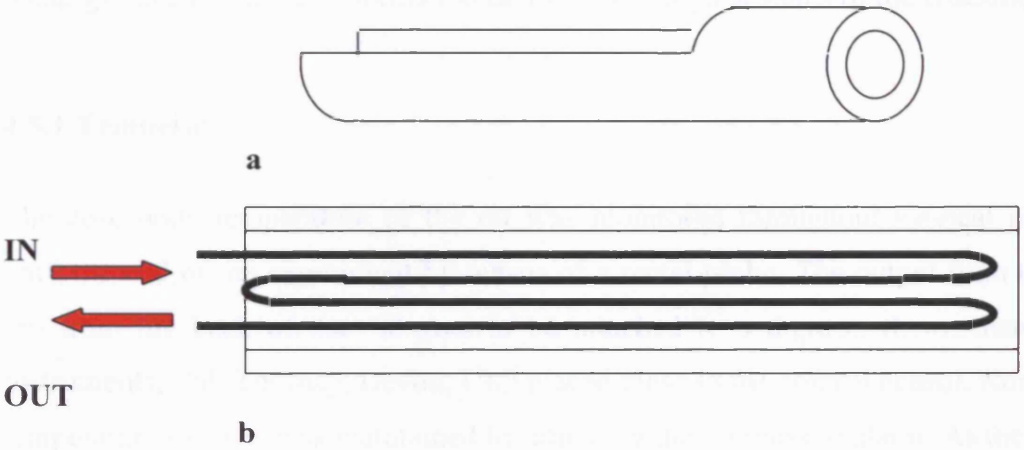

Fig 4.4 The Rat Probe

a. Rat probe made from drainpipe, caudal end intact

b. Diagram of positioning in the probe of tubing which contains warm water to maintain normal body temperature of the rat during experiments. The water is pumped to and from an adjustable thermo circulator.

It was necessary to incorporate some physiological monitoring facilities into the rat body holder (detailed in part 4.5). The combined effects of the low temperature at the core of the magnet and effects of anaesthesia result in a drop in body temperature of the rat, thus a water heater system was built and fitted into the probe. Thin, flexible tubing (1cm diameter) was wound around the base of the probe in a concentric fashion (Fig 4.4.1.b) and water continually pumped through it by an adjustable thermo circulator (Harvard apparatus, Edenbridge, Kent, UK). The water used in this heater contains manganese sulphate to eliminate the chance of signal interference from the water heater itself. This agent enhances relaxation such that after an RF pulse these protons will relax back to equilibrium rapidly and there will be no signal emitted when the image acquisition takes place.

4.5 Physiological Monitoring

In order to observe physiological parameters and more particularly, the depth of anaesthesia, physiological monitoring apparatus was included in the experimental

protocol. It was necessary to observe respiratory rate in accordance with UK Home Office animal regulations (60-90 respirations/min) and the body core temperature readings gave additional information on the physiological status of the anaesthetised rat.

4.5.1 Temperature

The core body temperature of the rat was monitored throughout surgical procedures until the end of the experiment by means of a rectal probe. The output from this probe ran from the back of the magnet to be attached to a digitron thermometer (Sifam Instruments, Ltd, Torquay, Devon, UK) placed close to the control consol. Normal body temperature of 38°C was maintained by adjusting the thermo circulator. As the RF pulse caused interference with the temperature reading, body temperature observations could only be made in between scans.

4.5.2 Respiration and Anaesthetic delivery

The apparatus used to monitor the respiratory rate as was used to deliver the gaseous anaesthetic. A pressure transducer (Druck Ltd, Groby, Leicester) was attached to the back of the facemask in the rat probe supported by a foam insert. The transducer had several taps attached to it, allowing the gaseous anaesthetic line to be connected. The output from the transducer was plugged into a Lectromed MT8P multitracer apparatus (St. Peter, Jersey, Channel Islands). A respiratory rate of 60-90 breaths per minute was deemed appropriate, and this was displayed on the trace as a peak for every expiration and a trough for every inspiration (corresponding to the detected increases and decreases in pressure, respectively). The system was equipped with a scavenger (International Market Supply, Congleton, Cheshire, UK) to remove excess anaesthetic and free radicals from the experimental environment. The cylinder was replaced when its weight approached 1440 gs. The scavenger was attached to the holder by a foam attachment by means of a large, flexible (2.5cm diameter) tube, which also attached to the caudal end.

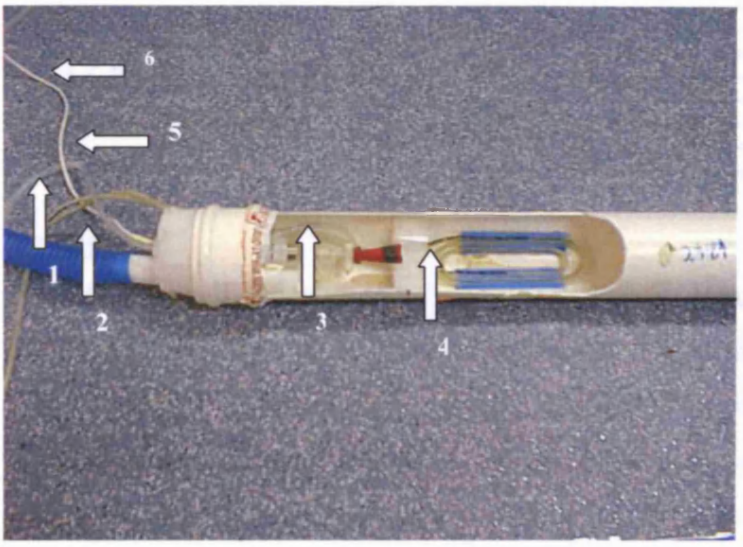

4.6 MRI Hardware

4.6.1 Magnet

MR signal acquisition was performed using a 2.3T horizontal bore superconducting magnet (40cm internal diameter), equipped with an actively shielded gradient set (200mT/m) all obtained from Bruker, Karlsruhe, Germany.

The data was acquired using a Silicon Graphics consol operating Paravision 1.4 software (1996, Bruker Medizintechnik GmbH) operating on an XWIN-NMR platform developed by Bruker for spectrometers and tomographs.

The probe containing the rat was loaded into the magnet bore and positioned using pilot scans as a guide and the magnet shimmed. Prior to commencement of each experiment, 30 contiguous coronal anatomical images providing complete coverage of the brain were acquired using a T2-weighted spin-echo RARE pulse sequence.

4.6.2 Coils

Birdcage coil

A transverse magnetic field (B_1), is generated by running a current on a cylindrical surface parallel to the cylindrical axis (Fig 4.6.2a). All RF probes supporting transverse MFs have the major part of the windings running parallel to the cylinder axis. These coils provide excellent B_1 homogeneity, provided the number of filaments is large enough to generate the appropriate sinusoidal current distribution. The actual birdcage coil used in this experiment is shown on the left hand side of Fig 4.6.2.b.

Fig 4.6.2.a Birdcage Coil

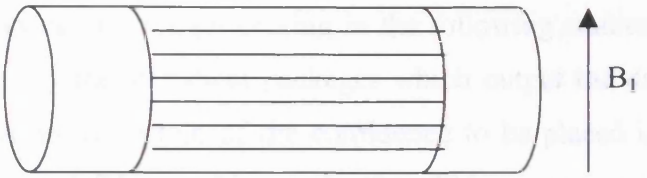

Surface coil

An electronically decoupled, receive-only coil (Bruker, Karlsuh, Germany) was employed throughout all of these experiments. With this type of coil, when the RF pulse was switched on, the receive-only (surface coil) was switched off, after the RF pulse was switched off, the receiver coil picks up the signal. When performing spin-echo sequences, a 90° pulse and several 180° pulses are required. The surface coil was placed on the dorsal surface of the rat's skull. The modified surface coil is built such that it wraps around the dorsal surface of the head and is able to pick up signals from the whole brain, thus the signal to noise ratio is very high (>200 for functional images), thus less repetitions are required and scan time is minimal (280 seconds for 30 slices).

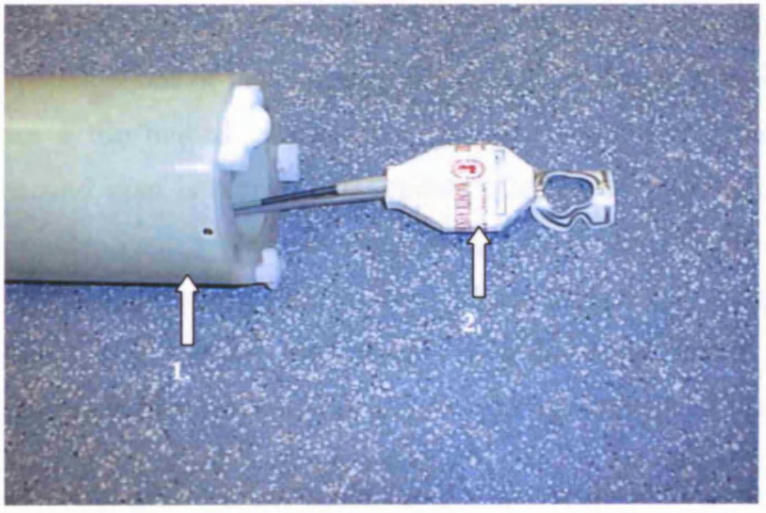

Fig 4.6.2.b

(1) Birdcage Coil and (2) Surface Coil

4.7 Data Processing

In this section, the path from raw fMRI data to useful statistical data is described. Analysis of this data allows determination of the specific brain regions where the signal has changed as a result of functional, in this case pharmacological, stimulation. There are several ways in which fMRI data can be analysed; however due to space limitation,

only the packages used for processing and pre-processing in the following studies will be described. The approach taken by the statistical packages which output the data is very important, as it is imperative to be certain of the confidence to be placed in the results and probability of random and false positive activation. This process requires basic understanding of the statistics being used.

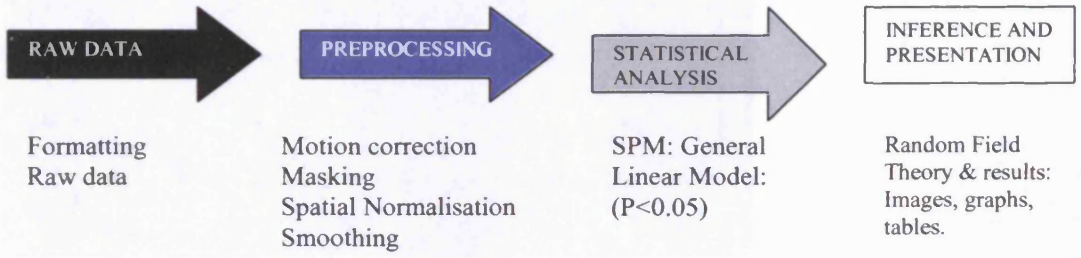

4.7.1 Formatting Raw data

The data received from the consol immediately after scanning is already Fourier transformed from time to image data. However these data cannot be opened and displayed in the programme we require, as the programme has not been given the specifications of the image. Furthermore, the data is stored in directory format, such that for a file named `Amp3mg01` the first scan is Amp3mg01/**1**/pdata/1/2dseq and the second scan is Amp3mg01/**2**/pdata/1/2dseq, and so forth. Thus in Medx (version 3.2, Sensor Systems Inc. Sterling, VA, USA)) the images are opened up one by one, specifying the image parameters (which are normally matrix dimensions of 64 x 64, 30 slices, 16-bit data). The image is then displayed; this is repeated for each scan in the dataset in chronological order. A group is created in the order of the first to the last scan. In this case the group would be saved as Amp3mg01.hdr.

4.7.2 Motion Detection and Correction

The presence of motion as a function of time (or scans) can be displayed in a `gnu` plot. This simply plots the movement over time. This process is especially useful for human MRI, where head motion can be a big problem; if the movement is more than 1mm, then the data cannot be used. As is shown below (Fig 4.7.2) the movement in this animal is minimal (less than 0.1 pixel), and thus this data can be used.

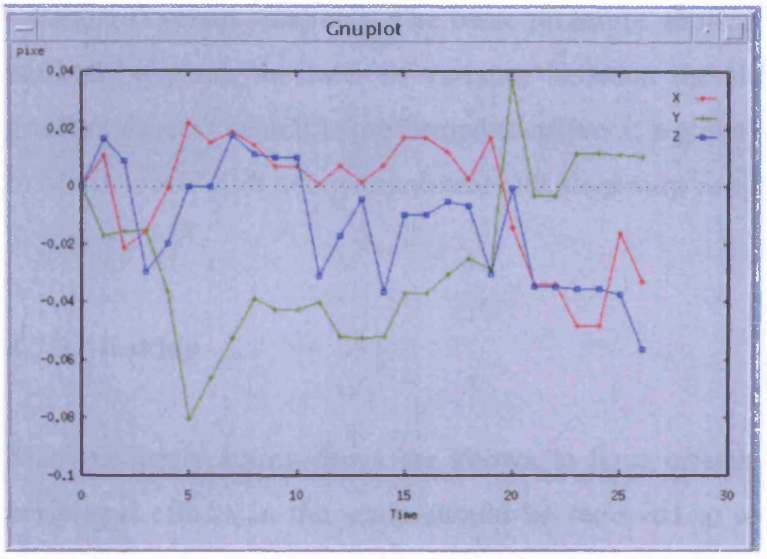

Fig 4.7.2 Gnu plot

Subject Amp3mg01 (single animal data): total movement in x,y,and z directions over the time-course of the experiment. Note the extent of movement is given in increment of pixels.

Although minimal, the movement displayed above (Fig 4.5.2) is still substantial, movement of 0.1 pixels will result in a 10% disparity between neighbouring pixels. This must be removed and this is performed in Medx. Motion correction is performed by registering all of the scans in the analysis group to the reference scan. Automatic image registration (AIR) works best on data that has easily identifiable boundaries (i.e. rigid/non-deformable). Several spatial models can be chosen for rigid or more distorted registration. The model chosen in this instance is a 6 parameter, rigid model and a threshold set so as to include the brain only. These thresholds determine the mark for the voxels that will be used for image registration. It is important to keep the threshold suitably high so as to exclude the regions outside the brain. For efficient data processing a group is created from all of the scans in the analysis (as described above) and is known as the `reslice group` and one image (the first one, by convention) is selected as the `standard image`.

The algorithms for such were developed and validated by Roger Woods (Woods, et al 1992). This method is relatively fast, no delineation boundaries are required and can be used where boundaries may have changed between acquisitions. The algorithm uses intensities of images directly, to minimise the variance if the ratio of the two images

(`standard` versus `reslice`). The basic principle applied is that if the two images were perfectly aligned, the ratio of variance between the slices would be close to one. A gradient descent search is preformed to arrive at a global minimum. The version of AIR in Medx is AIR3.08 using alignlinear and alignwarp programmes.

4.7.3 Masking

Many centrally acting drugs are known to have effects on blood circulation and thus peripheral effects in the scalp should be removed to avoid confounding the data. To minimise and simplify the data a mask was created around the brain so as to remove non-neuronal tissue. The first scan of each data set (the same one used for motion correction) was saved as a single image and given a new name, for example "Amp3mgbase". Using Analyze (version 1.0, Biomedical Imaging resource, Rochester, MN, USA) a line is drawn around the brain separating it from the surrounding bone and tissue, and the remaining undesirable tissue is omitted (Fig 4.7.3). This is done for each of the 30 volumes for the first scan.

When saving the new segmented image, the intensities are changed so that everything selected (i.e. the brain) is equal to 1 and the rest (i.e. the space surrounding the brain) is equal to 0, and the image changed from 16-bit to 8-bit.

This image is then applied to the whole motion-corrected group by using an image script. Medx allows routine image processing tasks to be automated by combining functions into a script, in this instance the script instructs that the whole motion corrected group be masked with the provided 8-bit mask. Thus the brain areas are multiplied by `1`, and so remain the same shape as the masked image. The areas outside the brain are multiplied by `0` and thus are removed in the entire group.

Neither masking nor motion correction involve changing of the voxel based data, the information contained in the image is completely preserved but are merely rotated or repositioned in space, or unnecessary data removed.

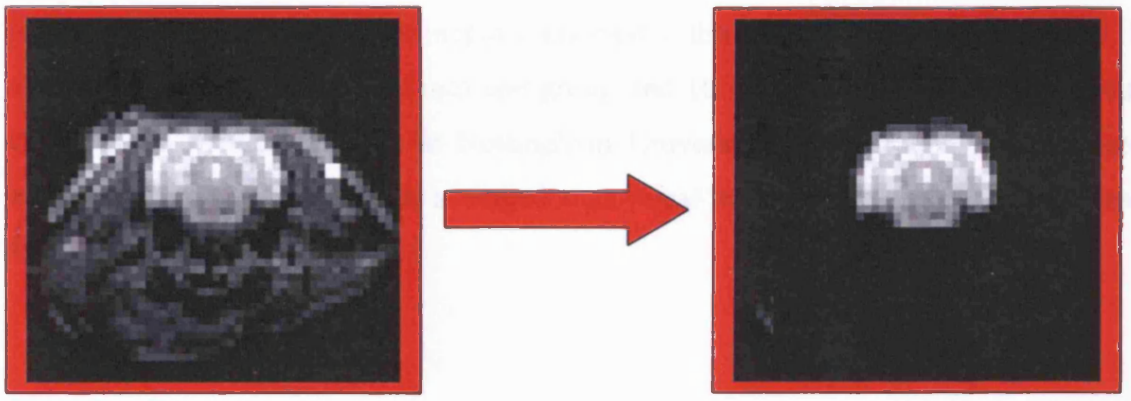

Fig 4.7.3 Single animal data before and after masking

The right hand image shows the cross section of the rats head, and this is removed in the left hand image.

4.7.4 Creating a Template Image

The fMRI images obtained in the following experiments do not have sufficient resolution or contrast to be able identify specific brain regions where changes in signal intensity occur. It was not possible to register functional images directly to an anatomical template as the image matrix dimensions were not identical (64 x 64 and 256 x 256, respectively). Thus it was necessary to overlay functional images onto high resolution anatomical images.

Instead two templates were created, one anatomical and one functional. The 16 datasets from male Sprague-Dawley rats used to create both anatomical and functional template images were not used in any of the experiments to be described and thus they did not introduce systematic bias. As was also convention in my experiments, the high resolution anatomical scan was obtained immediately prior to the first fMRI scan (the scan used to obtain a template) so approximate to the same space (movement is considered to be negligible in this short time space).

In order to create the anatomical template, one of the anatomical images was chosen as the standard and all of the group were registered to this position in space using the

shadow transform function in Medx. Similarly, the 16 fMRI images were registered to one fMRI image (corresponding to the same dataset of the standard anatomical image), resulting in all of the 16 fMRI images registered to the same space. When registered, 16 anatomical images were made into one group and 16 fMRI images into another group. Using home-written software at Nottingham University, these groups were averaged such that there was one volume averaged anatomical template and one volume averaged fMRI template.

4.7.5 Spatial Normalisation

To implement a voxel-based analysis of fMRI data, the data from individual subjects must derive homologous parts of the brain. Spatial transformations are therefore applied that move and warp the images so that they all conform to the idealised and standardised (template) brain approximately. This allows conventional result reporting using intersubject averaging if desired. In human studies, the image is transformed into standard anatomical space usually corresponding to the Talairach atlas (Talairach & Tournoux, 1988). In the following experiments the fMRI data is normalised to the data space of a template functional image on the basis of co-registering to high resolution anatomical images.

Images were converted to "Analyze" format (required by Statistical Parametric mapping software, SPM`99: Friston et al, 1995a; 1995b) using in-house scripts. Before spatial normalisation was applied, the voxel dimensions were increased in the fMRI data and template (to which they are normalised) such that they conformed to the same space as the anatomical images onto which they are to be superimposed. Another reason for this resize is that SPM recognises changes in signal intensity above a volume threshold as well as a statistical threshold such thresholds mean that discrete changes in the relatively small rat brain could go unnoticed. The reason for this theshold is that SPM is primarily a human imaging package and thus commonly sees voxel dimensions of 3x3x3 as opposed to 0.08 x 0.08 x 0.1 (as is in this case). Voxel resizing is performed using the header edit function in SPM. So the resizing parameters are 50-fold for the functional images, and 10-fold for the anatomical images. The number of pixels remained unchanged.

Spatial normalisation actually comprises three stages in SPM, resetting the origin (and possibly slice orientation), setting normalisation parameters and finally application of parameters to the whole group. Firstly when resetting the origin a brain ` landmark` is chosen so that the whole group can reliably be registered to the same place. In this case it was below the aqueduct at the level of the PAG (corresponding to -7.3mm from Bregma: Paxinos & Watson, 1998), and the header is correspondingly edited. Additionally, if the brain appears to be at an angle in X, Y or Z direction with respect to the templates then the slice can be reorientated further. Setting the normalisation parameters involves selecting the size of the template and the way the normalisation is to be performed, then (by convention) the first scan in the group is selected and normalised to the anatomical template. When complete, the directory will contain a file, in this instance **Amp3mgn3d.mat** that holds the normalisation parameters for that group. Finally the last process- write normalise, applies this mat file to the whole group. As the functional template is the same space as the anatomical, the new registered data (Fig 4.7.5) can be overlayed and displayed onto the high-resolution image after the analysis is complete.

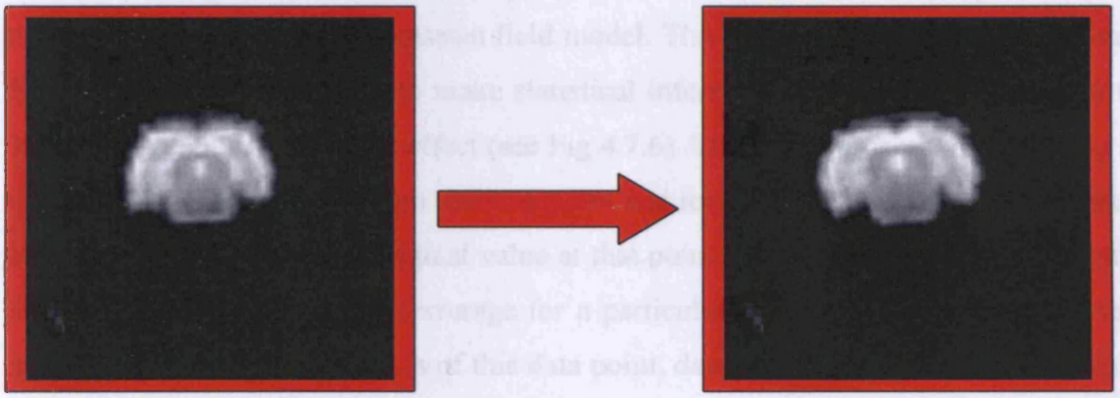

Fig 4.7.5 Single animal data before and after normalisation

The image on the left is transformed into the same data space as the template image (not shown) such that the resulting image (right) is slightly warped from its original.

4.7.6 Smoothing

Smoothing is a process in which data points are averaged with their neighbours in a series (time series, or image). This usually blurs sharp edges in the smoothed data

because of the effect of suppressing high frequency signal and enhancing low frequency signal (thus improving the signal to noise ratio). It is known that noise has higher spatial frequencies than the measured effects of neurophysiological events (hemodynamic changes expressed over spatial scales of a few millimetres). In fMRI the noise can be regarded as independent for each voxel and so has high spatial frequency components. Smoothing importantly, allows inter-subject averaging and ensures that hemodynamic changes from subject to subject are assessed on a spatial scale at which homologies in functional anatomy are typically expressed.

The kernel for smoothing defines the shape of the function that is used to take the average of the neighbouring points, the matched filter theorem states that the filter will give optimum resolution of signal from noise is a filter that is matched to the signal. A gaussian kernal is in the shape of a gaussian (normal distribution) curve. When used for smoothing the gaussian wave is described with the measure full width at half maximum (FWHM) instead of sigma (standard statistical way) as shown in Fig 4.7.6a.

Also by convolving with a Gaussian kernal, this conditions the data in the sense that it conforms more closely to a Gaussian field model. This is important if one wants to use the theory of Gaussian fields to make statistical inferences about (assign p-values) to the ensuing regionally specific effect (see Fig 4.7.6). The actual process of smoothing is simple. The data is gone through point by point and for each one generating a new value that is some function of the original value at that point and the surrounding data points. To generate a Gaussian kernel average for a particular data point, the curve is moved such that its centre on the x-axis of this data point, data point `6` as is illustrated below in Fig 4.7.6b. The values are then divided up by the whole area under the curve so that the values add up to 1 (otherwise an overall scaling of the values would occur). The Gaussian functions for 5,4,3,2,1 7,8,9,10 and 11 are also generated.

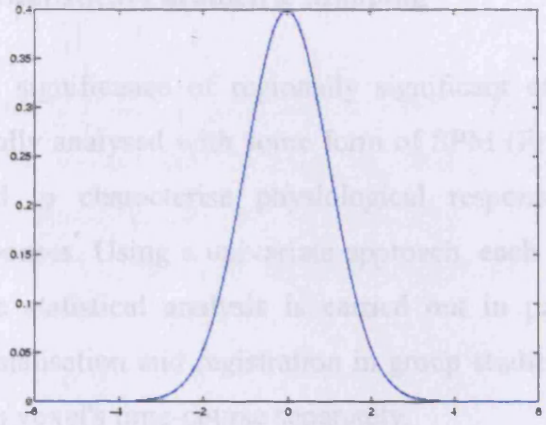

Fig 4.7.6a Gaussian wave with FWHM of 3.35

The FWHM is the width of the kernel, at half of the height of the gaussian. So for this gaussian the maximum height is about 0.4, the width of the kernal at 0.2 is the FWHM. The FWHM is 3.35.

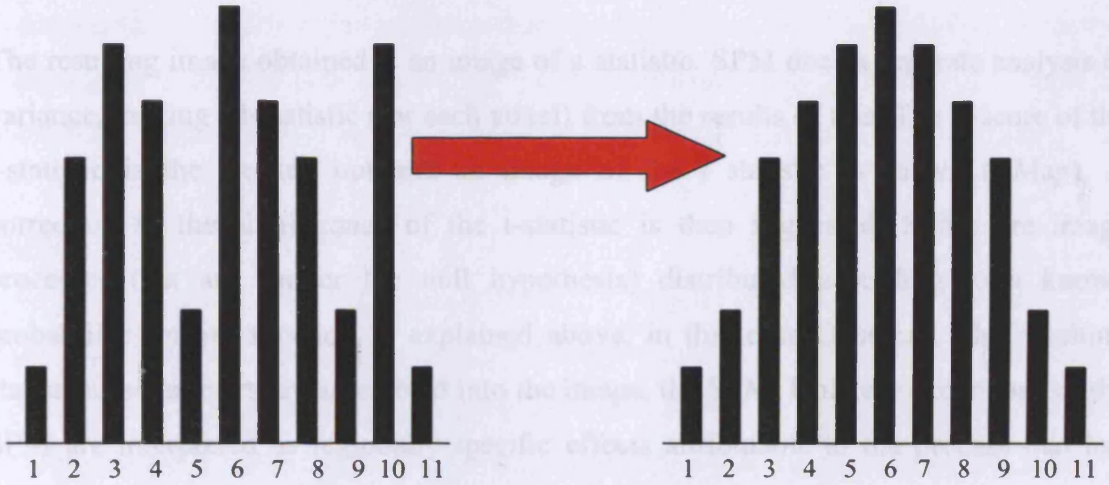

Fig 5.7.6b Effect of smoothing

Smoothing in 2D gives a cone-shape rather than a curve, giving a `normal` bell-shaped distribution. Adapted from Cambridge Imagers:An Intoduction to Smoothing (http://www.mrc-cbu.cam.ac.uk/Imaging/)

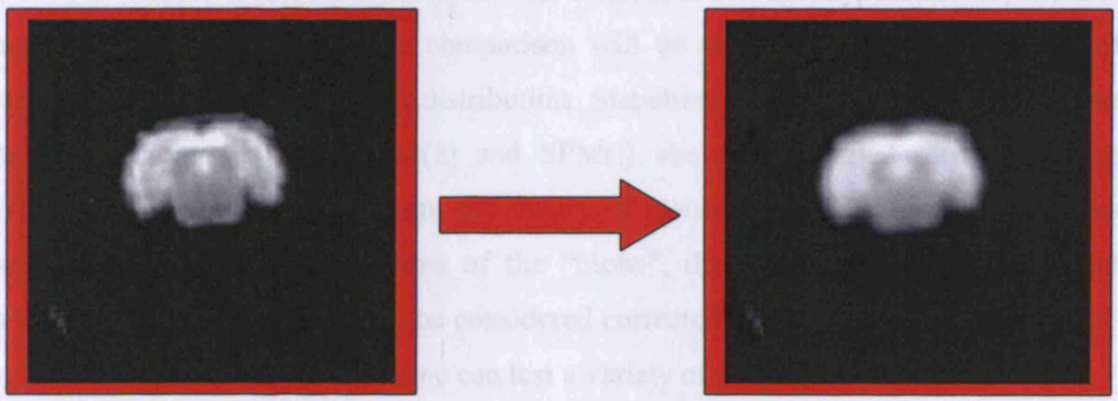

Fig 4.7.6c Single animal data before and after smoothing

Smoothing causes the original image (left) to have a more blurred appearance (right).

4.8 Statistical Parametric Mapping

The significance of regionally significant effects in functional mapping studies are usually analysed with some form of SPM (Friston et al, 1995a; 1995b). This approach used to characterise physiological responses with respect to regionally specific responses. Using a univariate approach, each voxel is treated individually and a voxel-wise statistical analysis is carried out in parallel (reiterating the need for accurate normalisation and registration in group studies). This means that the model is fitted to each voxel's time-course separately.

The resulting image obtained is an image of a statistic. SPM does a separate analysis of variance, making a t-statistic (for each voxel) from the results of this. The Z-score of the t-statistic is the worked out and an image of the t statistic is shown (t-Map). A correction to the significance of the t-statistic is then suggested. SPMs are image processes that are (under the null hypothesis) distributed according to a known probability density function as explained above, in this case Gaussian. The resulting statistical parameters are assembled into the image, the SPM. Unlikely excursions of the SPM are interpreted as regionally specific effects attributable to the process that has been manipulated experimentally.

The null hypothesis for a particular statistical comparison probably will be that there will be no change anywhere in the brain. In a comparison between activation and rest, the null hypothesis would be that there are no differences between the scans in the activation condition and the scans in the rest condition. The null hypothesis implies that the volume of t-statistic for the comparison will be similar to the equivalent set of numbers from a random normal distribution. Statistical inferences are made from the local excursions from the SPM(z) and SPM(t) above a specified threshold using distributional approximations form the theory of Gaussian fields. These distributions pertain to simple characterisations of the "blobs", their maximal value and spatial extent. The resultant p-value can be considered corrected for the volume of brain tested. By specifying different contrast, one can test a variety of effects.

4.8.1 Design Type

Effects detected usually fall into three categories; SPM is used in general activation studies by applying subtractive (categorical), parametric (dimensional) and factorial (interaction) design. In the following experiments the design is subtractive as net activation change is obtained by simple OFF- ON paradigm.

Subtractive

This is a well-established and powerful device in functional mapping. Cognitive and Sensorimotor subtraction investigates that two tasks may be formulated as separable components. The detected effects are predicted on possibly untenable assumptions about the relationship between brain dynamics and functional processes that ensue.

Parametric

This type of design avoids the shortcomings of cognitive subtraction, in testing non-linear but systematic relationships between neurophysiology and sensorimotor, psychophysical, pharmacological or cognitive parameters. It treats cognitive processes as dimensions or attributes that can be expressed on a grading scale, and also assumes that regional physiology will vary monotonically and systematically with the amount of processing, be it sensorimotor, cognitive or otherwise.

Factorial

A factorial design simply looks at changes in changes, it provides a rich way of assessing the effect of one manipulation on the effect of another and incidentally allows one to test some of the assumptions implicit in cognitive subtraction. Interactions are associated with factorial designs where two factors are combined in the same experiment. The effect of one factor on the effect of the other is assessed by an interaction term. Some psychopharmacological activation studies are examples of a factorial design. In these studies, subjects perform a series of baseline-activation pairs (on-off, on-off, see Fig 4.8.1) before and after the administration of a centrally acting drug (Uftring et al, 2001). The interaction term reflects the modulatory effect of the drug effect on the task-dependant physiological response. This type of study would give an insight into the relationship between cognitions and neurotransmitter function in man. In animals a similar study has been carried out, a centrally acting anti-epileptic

drug –lamotragine was seen to affect the response to peripheral stimulation, (Kida et al 2001).

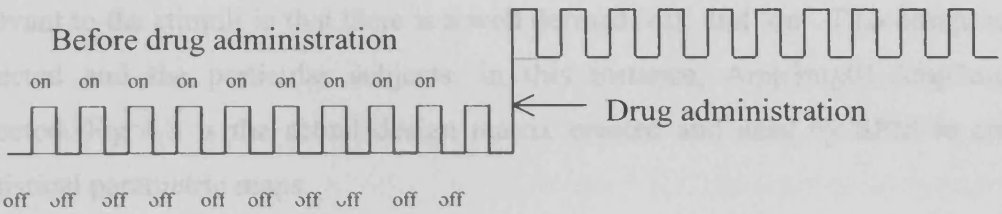

Fig 4.8.1 Factorial Design for Pharmacological Stimulation

4.8.2 Statistical Analysis: The Design Matrix

SPM requires the construction of a design matrix in which a model is specified. The design matrix embodies the experimental design and model used to test for specific neurophysiological responses. A series of prompts in SPM results in all the required data for the design matrix being used to create the SPM and the statistics along side it. For example in the following experiment (Chapter 5, Experiment 1), the parameters required to create its design matrix were 280s scan time (inter-scan interval); 8 subjects with 27 scans each (27 27 27 27 27 27 27 27); 2 conditions (basal and drug or control); 9 scans for basal and 18 scans for drug/control; a simple box-car epoch was chosen (off – on).

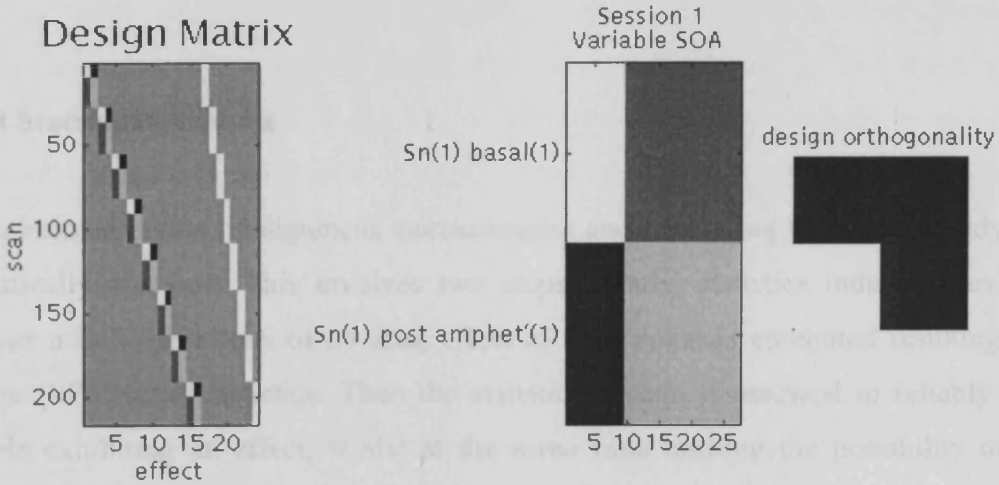

Fig 4.8.2 The design matrix: Box car design
Left: each subject and the experimental parameters are displayed from 1-8, top to bottom.
Right: each session can be enlarged for investigation.

This design is non-stochastic, having a single cycle as opposed to being event related. Although the box-car does not model the actual drug-response curves, it is certainly relevant to the stimuli in that there is a well defined `off` and `on`. This design matrix is selected and the particular subjects, in this instance, Amp3mg01-Amp3mg08 are selected. Fig 4.8 is the actual design matrix created and used by SPM to create the statistical parametric maps.

In order to compute the statistics for particular voxels, SPM has to obtain the data for that voxel for each of the scans in the analysis. Essentially it finds which of the numbers making up an image corresponds to the voxel required and extracts that number into matlab, for each scan.

4.8.3 Scaling

Although the design matrix has been created and the scans selected, there are still opportunities for processing and data manipulation before the statistics are complete. Scaling is an extremely important process. It is possible that the signal intensity for each data set may be vastly different due to variability in the imaging system. The system may also drift and thus proportional scaling is important, it scales datasets relative to one another.

4.8.4 Statistical Analysis

After reconstruction, realignment, normalisation and smoothing the data is ready to be statistically analysed. This involves two steps: Firstly, statistics indicating evidence against a null hypothesis of no drug effect at each voxel is computed resulting in an image (SPM(t)) of statistics. Then the statistical image is assessed to reliably locate voxels exhibiting an effect, whilst at the same time limiting the possibility of false positives.

4.9 The General Linear Model

The general linear model (GLM) is simply an equation that relates the observation, to what one expected to see, by expressing the observations (response variables) as a linear combination of expected components or explanatory variables (coefficients) and some residual error (Friston et al, 1995b). The GLM underlies most statistical analysis used in applied and social research and many parametric modelling techniques are special cases of this model. This framework, which was first developed for PET and was then extended for fMRI is implemented in the SPM software package (Friston et al, 1995a; 1995b). The GLM assumes that the errors are independent and identically distributed across conditions and subjects (but not from one voxel or brain structure to another).

The characterisation of changes within a SPM is in terms of multiple activation foci that ensue following thresholding. SPM is a statistical procedure that permits statistical inferences about regionally specific findings (e.g the probability of finding as activation focus by chance).

4.9.1 Parameter Estimates

The contribution of effects in the observed physiological response is estimated using the General Linear Model and Standard Least Squares. These estimated contributions are known as parameter estimates (PEs) and can be as simple as the mean activity associated with a particular condition (on and off, or drug and no drug), or as complex the interaction term in a multifactorial experiment. Regionally specific effects are framed in terms of differences among these parameter estimates

In summary, General Linear Modelling sets up a model (i.e. what you expect to see in the data) and fits it to the data, and if the model is derived from the stimulation that was applied to the subject in the MRI scanner, then a good fit between the model and the data means that the data was indeed caused by the stimulation. Thus, for each voxel, there is an estimate of the "goodness of fit" to that voxels timecourse i.e. a parameter estimate (PE). To convert PEs into statistical maps, it is necessary to divide the actual PE value by the error in the estimate of this PE value. The analysis of regionally

specific effects uses the GLM to assess the differences among the PEs (specific to a contrast), by referring to the error variance. This assessment is in terms of a t-value for every voxel (ie a SMP(t)). It follows that if the PE is low relative to its estimated error, the fit is not significant. Thus t is a good measure of whether we can believe the estimate of the PE value. All of this is done separately for each voxel. To convert a t value into a p (probability) or Z statistic requires standard statistical transformations; however, t, P and Z all contain the same information - they tell you how significantly the data is related to a particular error variance (part of the model).

4.9.2 t-Test and t-Maps

In this case the particular test used by SPM is the t-test, this allows one to determine whether the difference between the mean signal intensities of the two groups (baseline and post-drug) are statically significant. The formula of the t-test is a ratio. A t-test is a robust parametric hypothesis test, the present hypothesis being that the drug will cause increases or decreases in signal intensity, this is specified in the design matrix.
The t- test is used to compare 2 groups where the dependant variable is continuous (signal intensity) and the independent variable is dichotomous (no drug vs. drug) and measures if the average from one group is different from the other. The basic formula for the t-test is shown in Table 4.9.2a.

Table 4.9.2a

$$\frac{\text{Post drug group mean -Basal group mean}}{\text{Standard error (Basal group mean-Post drug mean)}}$$

To compute the standard error of the t-test, the variance (SD squared) for each group is divided by the number of respondents in the group, minus 1. The values for both of the groups are added together and their square root taken, the formula for the t-test is shown in Table 4.9.2b.

Table 4.9.2b

$$t = \frac{\text{Post drug group mean -Basal group mean}}{\sqrt{\frac{var_{post\ drug}}{(n_{post\ drug}-1)} + \frac{var_{basal}}{(n_{basal}-1)}}}$$

When the t-test is performed, the results in the form of a t-Map are ready to be investigated. However in order to describe the hypothesis, contrasts must be specified. These contrasts are a simplified way of expressing the hypothesis about the effects defined in the design matrix. These effects are specified in the contrast manager as "1", "-1" and "0", relating to relative increases, decreases and those contrasts not selected, respectively. Thus to investigate the hypothesis that a drug has caused increases in signal intensity the contrast for 8 subjects would be –1 1 –1 1 –1 1 –1 1 –1 1 –1 1 –1 1 –1 1, with "–1" representing a smaller mean for condition 1 (basal scans, no drug) and "1" representing a larger mean for condition 2 (post drug), pertaining to an increase in signal intensity after the drug is administered. Conversely, if the opposite hypothesis were to be investigated, i.e where the drug may have caused decreases in signal intensity, it follows that a contrast of 1 –1 1 –1 1 –1 1 –1 1 –1 1 –1 1 –1 1 –1 would be chosen instead.

In investigating the hypothesis that the drug causes increases in signal intensity (i.e. the formula above), it follows that the t-value will be positive, and if the drug is causing decreases then t would be negative Fig 4.9.2 shows the same brain slice (bregma equals –1.3mm), having put in contrast –1 1 (searching for increases in signal intensity) and 1 –1. The t-maps are positive in both cases, however the contrasts are implying opposite hypotheses.

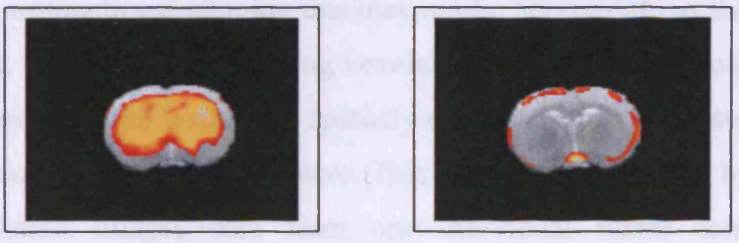

a b

Fig 4.9.2 t-Maps overlayed onto high resolution anatomical images at –1.3mm from Bregma

(a) Shows result of contrast –1 1, where increases in signal intensity are tested

(b) Shows result of contrast 1 -1, where decreases in signal intensity are tested.

4.10 Statistical Inference

In order to find out whether the t-statistic in our SPM map are more positive than in a similar volume of random numbers it is necessary to threshold. Even if the null hypothesis were true, some of the t-statistic will be significant at standard statistical thresholds. So SPM is told to show the t-statistic above a specified threshold (so that $P<0.05$ or $P<0.01$). The level of the threshold set such as to be confident of remaining peak t-statistic is known as the multiple comparison problem.

4.10.1 Bonferonni Correction

The problem of false positives can be dealt with using a Bonferroni correction,

Table 4.10.1

Alpha/number of tests

Where alpha is the false positive rate you are willing to accept often one in 20 repeats (0.05).

However in functional imaging this may not be appropriate as the t-statistics are highly correlated with their neighbouring voxels. Bonferroni correlations assume independent tests, however if the voxels are spatially correlated then the tests are not independent- thus the correction too conservative. This correlation is caused by several factors, with low-resolution images data from one individual voxel contains data from the surrounding tissue. Secondly, pre-processing such as reslicing in normalisation and smoothing to improve SNR both create strong spatial correlations. It is possible to use a Bonferroni correlation in a spatially correlated image provided that the number of independent observations is known and less conservative threshold can be obtained, this method of smoothing is known as mean-by-square-process. This is not possible when smoothing with a kernel (as has been performed here) as the averaging takes place in a continuous way across the image and it is not as simple to work out the number of independent observations.

The statistical tests so far described only account for the error variability from scan to scan thus allowing inferences to be drawn only from the subject group, this is known as fixed level analysis. The mean effects of the groups are assessed and thus it is not possible to draw inferences relating to the whole population(s), rather a case study is being described. This type of inference is criticised in that the group difference may reflect small differences between particular subjects in the study as opposed to a systematic difference between the populations from which the groups were drawn, i.e. it is unsuitable for group comparisons. The theory of fixed effects analysis is that for our example, a two condition (n=8) subject phMRI experiment, the GLM measures the responses and assesses the significance of mean activation of these subjects, only considering the error component of variance. Fixed effects represent a first level analysis.

4.10.2 Gaussian Random Field Theory

An additional analysis is therefore carried out which extends inference to the populations from which the subjects are drawn, a random effects analysis. This more stringent analysis models the variability in response from subject to subject and most designs are balanced and subject separable. In general these multi-level approaches are hard to assess, requiring special algorithms and statistics, but in functional neuroimaging it is simpler. The models are separable into individual subject models. When specifying contrasts in the group contrast, additional contrasts are specified- one for each animal so that a t-Map is created individually for each subject. This means that parameters are independent from subject to subject and thus can be separately estimated and also that individual subject models are almost identical. This second level analysis is a one-sample t-test model where the residuals are required for a population inference on the activation estimates. This extends to a population with much lower significance (Fig 4.9.7). The reason this is important is that there is usually more between-subject variability than error variance and thus there is a high chance of a fixed effects analysis producing significant results, though not representative of the population. Also random effects analysis is more dependants on the n-numbers used than the number of scans, thus may require very high n-numbers.

(a)  (b) 

Fig 4.10.2

Group 3mgAmp1-8: Fixed Effects (a) and Random effect (b) analysis of increases in signal intensity after 3mg/kg i.v amphetamine

The reason the Gaussian random field model is used is because the hypothesis is an anatomically `open` null hypothesis- there is no effect anywhere in the brain. This method provides a correction for multiple non-independent comparisons to provide a corrected p-value. This provides a number of statistical inferences, the number of activated regions (clusters above some arbitrary height and volume threshold), the number of activated voxels (volume) and a p-value for each voxel within that cluster.

This is a far more complex way of establishing t thresholds for the SPM than using a Bonferroni correction. Instead of independent observations influencing the t-statistic, resolution elements (resels) are used, these are dependant on the smoothing parameters (FWHM) and number of pixels in the image. For an image with a set number of resels, the number of "blobs" or Euler Characteristics (EC) in that image can be worked out for particular thresholds using complex mathematical functions (Worsley, 1992). When the t-statistic become high and the predicted EC drop to zero, so that the expected EC is a good approximation of the probability of observing one or more blobs at that threshold.

4.10.3 Viewing Timecourse

At this stage it is possible to obtain all the signal intensity values for each voxel (voxel values), this may be desirable to create graphs and time-response curves. Using the `VOI` command in SPM, one can either use the specified coordinates of the volume or cluster analysis (simply by highlighting a volume or cluster) or by manually inputting x,y, and z coordinates of interest. It must be noted at this point that this is only possible

with voxels of significant t-values. That is, for an area, which shows no significant changes, one cannot obtain the range of signal intensities over time, and therefore it is not possible to view a timecourse, which is not significant.

At this stage the images and timecourses deemed significant by the SPM software are obtained. The many stages in processing and analysing of fMRI data make it a lengthy and rather complicated process, often taking longer than the experiments themselves, thus development of the methods described has constituted an important part of the thesis work. Further aspects on statistical assumptions and SPM are discussed in Chapter 8. Finally the high resolution anatomical templates were annotated such that the areas showing changes in the t-Map can be compared and identified. This was performed by using the CD-rom version of the rat atlas (Paxinos & Watson, 1998) and simplifying the figure (Microsoft PowerPoint, 2000), and overlaying it onto the template image. These are displayed alongside the fixed effects and random effects analysis results in most of the images displayed (Chapters 5,6 and 7).

Chapter 5

fMRI of Amphetamine

5.1 Introduction

Functional magnetic resonance imaging (fMRI) is a powerful tool and to date has been largely used for brain mapping. One of the more recent advances in brain imaging applications, pharmacological MRI (phMRI), has provided researchers the opportunity to study regional brain activity during pharmacological stimulation (Silva et al, 1995). Typically these studies are designed to investigate the regional changes in the presence or absence of a certain drug. The results indicate that stimulant drugs may increase neuronal activity in specific regions of the brain and its potential usage in receptor localisation and drug characterisation may be of great importance. Pharmacological MRI (phMRI) may also be used as a tool in longitudinal studies to look at the chronic effects of drugs and of substance abuse, involving dosing schedules which could last from days to months and also measuring for changes in fMRI response after drug challenges by multiple scan sessions. This may be preferable to other techniques where in human studies, re-administration of radioactive substances for PET or SPECT is not possible; or in animal studies where re-use of animals is not possible, or where many groups of animals would be required for each individual time-point.

In investigating the feasibility of phMRI as a tool in pharmacology, initially a drug with a well-characterised and robust response is most suitable as the MR signal can be quite small (for example of less than 5% change after visual stimulation, Jones et al, 1998). Amphetamine works well as such an agent, creating large neuronal and haemodynamic responses. Amphetamine is an indirect dopaminergic agonist (i.e. it does not bind and activate the postsynaptic receptor, instead it facilitates through effects on other dopaminergic mechanisms, this is explained in section 5.1.2). The dopamine system has very well defined pathways and stimulation of these results in changes in signal intensity in discrete brain regions, as identified using PET and autoradiography.

Before describing the technical aspects of the experiments, the neurochemical and behavioural profile of amphetamine in humans and animals is described such that the actions of the drug and implications of the results can be more fully realised. The evaluation of neurochemical changes in multiple nuclei along with thorough characterisation of the behavioural response profile will be required to further elucidate the relative contribution of the various neurotransmitter systems and mechanisms to the

expression of amphetamine-induced behaviours. It is hoped that fMRI energy metabolism information may provide an insight into the many actions of amphetamine.

The structure of amphetamine is analogous to monoamines and exists in two forms, D-amphetamine and L-amphetamine, which are stereosiomers at the β carbon. Various doses of D- and L-amphetamine affect the temporal patterns of rat behaviour. The patterns of activity produced by D- and L-amphetamine are similar but out of phase, D-amphetamine has a shorter latency than L-amphetamine and D-amphetamine is approximately five times as potent as L-amphetamine in its effects on both locomotor activity and stereotypy duration (Segal, 1975). As D-amphetamine is so much more potent than L-amphetamine and causes more pronounced behavioural and functional effects (Weschler et al, 1979), the D-amphetamine isomer is the amphetamine form, which is discussed , and also used in the subsequent experiments.

As a powerful stimulant of catecholamine systems, amphetamine induces increased locomotor activity and stereotyped behaviour in humans (Schiorring, 1981; Greenwald et al, 1998) and animals (Kelly & Iverson, 1976). D-amphetamine increases neurotransmitter concentrations at the synapse by releasing monoamines from nerve terminals in the brain (reversal of dopamine transporter) and also by inhibiting the transporter, and therefore reuptake (Horn et al, 1990). Furthermore, dopamine transporter knockout mice do not display amphetamine-induced hyperlocomotion (Giros et al, 1996).

5.1.1 Amphetamine Action on Behaviour

In humans, amphetamine causes increased alertness and confidence, feelings of exhilaration, reduced fatigue and a general feeling of well-being (Grinspoon & Hedblom, 1975). Direct measurements of motor activity and other behaviours in animals have played an important role in evaluating the neuropharmacological mechanisms and toxicological consequences of abused drugs (Ossenkopp et al, 1987).

In experimental animals, the main behavioural effects of low to moderate doses of amphetamine are increased locomotor and exploratory activity. High doses of

amphetamine cause stereotypy (inappropriate focused sniffing, repetitive head/limb or oral movements) (Kelly et al, 1975), and anorexia, and amphetamine-like drugs have been used to treat obesity in the past (Cradock, 1976). In animals, new behaviours emerge with repeated amphetamine treatment, and these may be appropriate models for the behavioural consequences of repeated amphetamine administration in humans, which include dependence (Kuczenski & Segal, 1992; Hurd & Ungerstedt, 1989a) and psychosis (Kessler et al, 1996; Konuma, 1994; Sams-Dodd, 1998). Amphetamine psychosis is seen after a prolonged period (hours to days) of continual abuse of high doses of amphetamine (Angrist & Gershon, 1970; Gambill & Kornetsky, 1976), and can mimic the hallucinations and paranoia which are characteristic of schizophrenia positive symptomology (Sams-Dodd, 1998). Behaviours such as locomotor hyperactivity, stereotypy and disruption of the pre-impulse startle response (Geyer et al 1987) are believed to correspond to certain aspects of the positive symptoms of schizophrenia. Chronic treatment with amphetamine is also known to result in sensitisation of this locomotor behavioural response to acute amphetamine challenge, and also of the corresponding increase in extracellular dopamine in the nucleus accumbens (Robinson & Becker, 1986).

The behaviours that are observed after amphetamine administration are believed to be caused by its effects on neurotransmitter release and re-uptake at specific dopaminergic nuclei. In particular, it is thought that the nucleus accumbens may be responsible for amphetamine-induced locomotion and caudate-putamen for stereotypy (Stanton & Solomon, 1984). Evidence for involvement of these specific structures in mediating behaviour has often come from lesion experiments. Amphetamine induced stereotypy was attenuated following a 6-hydroxydopamine striatal lesion but not motor stimulation (Creese & Iverson, 1974l; Asher & Aghajanian, 1974). Furthermore, lesions in the nucleus accumbens had deleterious effects on amphetamine induced locomotion but not stereotypy (Kelly & Iverson, 1976). This is supported by the findings that injections of amphetamine, dopamine or dopamine agonists into the nucleus accumbens causes locomotion and similar injections into the striatum induce stereotypy, furthermore intrastriatal and intra-accumbens application of dopamine antagonists block, respectively stereotypy and locomotion induced by amphetamine.

Amphetamine's action as a discriminative stimulus, like locomotion and stereotyped behaviour, is thought to be mediated through the dopaminergic system, because it can be blocked by D_1 and D_2 antagonists in addition to 6OHDA lesions (Woolverton & Cervo, 1986). Using microinjections, the discriminative aspect of amphetamine stimulation was found occur when administered into the accumbens and not the caudate, furthermore this effect was blocked by the D_2 receptor antagonist, sulpiride (Nielson & Scheel-Kruger, 1986). This provides further evidence for specialisation of the dopaminergic system with respect to particular aspects of drug action.

5.1.2 Amphetamine Action on Neurochemistry

The agonist activity of amphetamine seems to stem from the fact that it is able to cause dopamine release as well as to inhibit reuptake. Amphetamine enters the nerve terminal by both passive diffusion as well as by interacting with the dopamine transporter which transports the amphetamine into nerve terminals, and by "exchange diffusion" results in a dopamine molecule being transported outside the nerve terminal (Seiden et al, 1993). Exchange diffusion is thought to happen at low concentrations. At higher concentrations, the dopamine transporter is saturated - resulting in accumulation of amphetamine by passive diffusion within the nerve ending, meanwhile the cytoplasmic catecholamine concentration rises as amphetamine inhibits uptake (Knepper et al, 1988) and also causes the catecholamines to be released from their vesicles.

Amphetamine stimulated dopamine release is largely Ca^{2+} independent and insensitive to reserpine (Butcher et al, 1988) and thus is more similar to spontaneous dopamine release which occurs mainly from a cytoplasmic pool of dopamine. Robertson and co-workers (1991) observed that amphetamine also evoked dopamine release from dendrites in addition to nerve endings and therefore does not require action potential propagation nor dopamine to be released from synaptic vesicles thus illustrating that amphetamine causes cytoplasmic dopamine to be released in an activity-independent manner.

Analysis of dopamine release and of the respective metabolites after amphetamine administration shows increased dopamine levels but reduced levels of DOPAC and

HVA. Amphetamine inhibits dopamine uptake resulting in reduced intracellular metabolism (thus explaining the decreases in DOPAC levels), amphetamine is also known to be a MAO inhibitor (Mann & Quastel, 1940) although more for MAO (A) than MAO (B) (Mantle et al, 1976), likewise explaining the decrease in HVA and DOPAC levels. Another explanation for the reduction in dopamine metabolites is the increase in dopamine levels in the synaptic cleft causing reduced spontaneous activity of the dopamine neuron due to end product inhibition and postsynaptic feedback by activation of presynaptic inhibitory autoreceptors.

One consideration when using amphetamine (and some other psychomotor stimulants) is that the induced neurochemical and behavioural responses change after repeated administration. Chronic administration of amphetamine results in sensitisation of the behavioural and neurochemical response, the latter consisting of an increased ability for psychomotor stimulants to raise extracellular levels of dopamine in the nucleus accumbens, subsensitivity of autoreceptors in the VTA and supersensitivity of D_1 receptors in the nucleus accumbens. The sensitivity effect can be seen after only a single pretreatment with amphetamine and this has also been observed in humans following methylphenidate administration (Volkow et al, 1998). Neurochemical sensitisation of dopamine release in the nucleus accumbens does not occur following a 2 hr interval between injection (Guix et al, 1992). Furthermore, the sensitised increase in synaptic dopamine concentrations was found to be calcium dependant, whereas the acute response to amphetamine was largely unaffected when calcium-free perfusate was used (Warburton et al, 1996). This is suggested to be due to a change in impulses from the VTA affecting DA release or calcium-dependant processes such as glutamate release in terminal areas indirectly potentiating dopamine release. The latter is supported by the finding that behavioural sensitisation is blocked by the NMDA receptor antagonist MK801, which also blocks the autoreceptor and D1 receptor responses, but not the increased dopamine release. This suggests that the behavioural sensitisation observed after amphetamine administration may require interaction with glutamate NMDA receptor activation (Karoum et al, 1994).

The mechanism by which amphetamine administration depletes brain dopamine content is poorly understood but it is known that axon terminal degeneration can be produced by increasing the duration of action of amphetamine in the brain (Ryan et al, 1988).

Chronic, but not acute amphetamine administration causes a long lasting decrease in dopamine uptake and content in the brain (Steranka & Sanders-Bush, 1980). During the 1980s, investigators reported that a single injection of amphetamine produced a long lasting depletion of brain dopamine concentration in iprindole-treated rats (Fuller & Hemrik-Leuke, 1980). The damage to dopamine axon terminals produced by prolonged exposure to amphetamine has been suggested to be mediated by either dopamine or glutamate excitotoxicity, this damage is prevented by treatment with haloperidol, alpha-MPT and glutamate NMDA receptor antagonist MK801 (Nash & Yamomoyo, 1993). The most popular mechanistic explanation of amphetamine and related compounds is that dopamine can be converted to endogenous neurotoxin under appropriate conditions (Seiden & Ricaurte, 1987), prolonged and excessive increases in dopamine may result in oxidation of dopamine to form quinines (Monks et al, 1992), 6OHDA (Seiden & Vosmer, 1984), hydrogen peroxide and/or associated free radicals (Cohen & Heikikila, 1974). Alone or in combination the formation of these dopamine oxidation products interact with cellular proteins, in particular those with sulfhydral groups (i.e. glutathione). Therefore a redox imbalance may exist which would result in axon degeneration in the case of amphetamine-mediated neurotoxicity.

5.1.3 Amphetamine Action on Adaptation: Dependence - Withdrawal

Amphetamine, as a psychostimulant is abused by humans and can be experimentally self-administered by primates (Bergman et al, 1989) and rats (Richardson & Roberts, 1996). Several lines of evidence indicate that a drug-induced stimulation of dopaminergic neurotransmission within limbic structures play an important role in acute drug action. There is ample evidence to suggest a role for the mesolimbic-mesocortical dopamine system in the behavioural effects of stimulants (Kelly & Iverson, 1976) and that a balance between this pathway and the nigrostriatal system may contribute to dose-related and individual differences in responsiveness to amphetamine. Furthermore, experimental data has demonstrated that the dopamine system is involved in initiating adaptations contributing to drug dependence. Two major neurobiological actions of amphetamine may represent neuroadaptions important for motivational effects of these drugs (Koob, 1996). Activation of D1 receptors stimulates a cascade of events that ultimately lead to cAMP response element-binding protein (CREB) phosphorylation

and subsequent alterations in gene expression (Hymen, 1996). These within-system adaptations could not only change the function of the dopaminergic system, but could trigger a second major neurobiological action, the increase in expression of protachykinin and prodynorphin mRNA. The subsequent activation of dynorphin systems could contribute to the dysphoric syndrome associated with dependence and also provide feedback to decrease dopamine release. Enhanced dynorphin actions could then be considered as a between system adaptation. The significance of the D_1 receptor-cAMP-CREB pathway in adaptations to drugs of abuse is supported by recent evidence of anti-amphetamine action (Trugman & James, 1993) and anti-cocaine actions (Marota et al, 2000) from dopamine D1 antagonists and effective anti- amphetamine and cocaine priming of D1 agonists (Self et al, 1996).

Following the discontinuation of amphetamine use, humans develop withdrawal symptoms similar to those associated with endogenous depression, including excessive sleep, lethargy, fatigue, and dysphoria (Gawin & Ellingwood, 1988). Rats also show an amphetamine withdrawal syndrome and the symptoms include behavioural hypoactivity (Pulvirenti & Koob, 1993) and a decrease in the efficacy of intracranial self-stimulation reward (Kokkinidis & Zacharko, 1980). There is considerable interest in the nature of neuroadaptions underlying the symptoms of drug withdrawal, and research has focused on the role of mesotelencephalic dopamine systems (Crippens et al, 1993). Indeed it is reported that withdrawal from a number of addictive drugs, including morphine, alcohol and cocaine, is associated with a decrease in the basal extracellular concentration of dopamine in the ventral striatum. Thus using phMRI as a tool to study animal models of dependence and withdrawal and possible drug interactions is of great clinical and pharmaceutical interest. For example, using phMRI, it has been shown that naxolone can precipitate morphine withdrawal (Lowe et al, 2001).

5.1.4 Amphetamine Action on other Neurotransmitter Systems

Most efforts to define the biochemical mechanisms underlying the behavioural response to amphetamine are directed at dopamine pathways (Kuczenski & Segal, 1989). However a wealth of information indicates that other neurotransmitters also modulate the amphetamine response. Biochemical (Kuczenski & Segal, 1989),

electrophysiological (Baraban et al, 1978) and cytoflourometric (Geyer et al, 1975) data all suggest that amphetamine also affects the 5HT system and some evidence indicates that manipulation of 5HT function alters amphetamine-induced locomotor activity (Mabry & Campbell, 1973) and stereotypies (Lucki & Harvey, 1979). It has been shown using *in vivo* microdialysis that glutamate also plays a role in the amphetamine response (Nash & Yamamoto, 1993) and its rising extracellular levels may be contributing factor in axonal damage following high doses of amphetamine. This is further confounded by the fact that NMDA antagonists attenuate methamphetamine-induced dopamine depletion in mice (Sonsalla et al, 1989).

5.1.5 Amphetamine Response involves D_1-type and D_2-type receptors

The concept of dopamine receptor subtypes and the development of selective dopamine receptor agonists and antagonists raises the possibility of specific subtype involvement in amphetamine stimulated functional responses, and furthermore, fMRI experimental studies provide the means to evaluate this possibility. By pretreating the animal with an antagonist for a suitable time before administering the amphetamine, specific receptors that would have normally been stimulated can be blocked, thus the residual response must be mediated by those receptors, which are not blocked. In such a manner, the effects of D_1 antagonist SCH23390 on the response to amphetamine using 2deoxyglucose autoradiography (Trugman & James, 1993) and cocaine stimulation using fMRI (Marota et al, 2000) have been investigated. In both cases the expected large increases in RCGU and fMRI signal from the stimulants was completely blocked. Interestingly, the amphetamine RCGU response was also completely blocked by a D_2 receptor antagonist, eteclopride (Trugman & James, 1993). Thus indicating that the drug response was mediated entirely through both the D_1-type and D_2-type receptors and that intact functional linkage is required for the subsequent response. It is of interest to ascertain which nuclei and receptor types are responsible for particular functions, especially as amphetamine stimulation of the dopaminergic system results in such a variety of behavioural, psychomotor and adaptive changes. With different dosing regimes and pharmacological modulation of the amphetamine-stimulated response it may be possible to find a neuronal substrate, be it pathway, nucleus or receptor type for

a drug action, for instance in such a way that amphetamine mediated stereotypy and locomotor activity were localised (partially) to the striatum and nucleus accumbens.

5.1.6 Amphetamine Action on Cerebral Metabolism and Functional Anatomy

Using 2-deoxyglucose uptake, it has been shown that D-Amphetamine stimulates brain metabolism in a region specific manner (Weschler et al, 1979). Increases in deoxyglucose uptake were observed in the cortex, cingulate, caudate-putamen, thalamus and hypothalamus indicating an increase in functional activity. Blood flow studies in rats have also found amphetamine to stimulate whole brain blood flow (Carlsson et al, 1975) and cortical blood flow (Detre et al, 1990).

The metabolic activation resulting from amphetamine stimulation can be detected using many methods, including PET (Drevets et al, 1999), microdialysis (Butcher et al, 1988) and fMRI (Chen et al, 1997). Furthermore the validity of direct dopaminergic stimulation has been established by means of 6OHDA lesioning and regional specificity (Guyen et al, 2000). As a prelude to some more complex and specific dopamine receptor stimulation, the first experiment sets out to replicate a previous phMRI experiment (Chen et al 1997).

Using fMRI, Chen et al visualised changes in activation in the rat brain after systemic administration of amphetamine and observed similar changes to those indicated by the autoradiographic studies. Thus Chen et al showed that fMRI could be used as a tool to visualise regionally specific changes in metabolic demands following pharmacological stimulation. It should therefore be possible to study the neuronal circuitry of the dopaminergic system if the BOLD signal is great in areas of high dopamine receptor density. In carrying out such experiments, one can ascertain whether the observed response is a direct consequence of activation of dopaminergic pathways or if it is a secondary action, indeed it is still not known if the so-called "activation" or increase in BOLD signal represents neuronal excitation. In a manner similar to Chen et al 1997, Guyen, et al, 2000 we administered doses of amphetamine intravenously to rats whilst immobilised in a 2.35 Tesla imaging system.

In the following experiment the nature of the functional response to amphetamine administration is investigated with regards to spatial and temporal response profiles, however the whole brain was scanned (30 x 1mm) in order to observe global changes, in contrast to the previous work where only particular regions of interest were examined (Chen et al 1997). Following on from the first single amphetamine administration, the second and third experiments investigate the effect of pretreatment with D_1 antagonist (SCH23390, 0.5mg/kg) and D_2 antagonist (sulpiride 50mg/kg, i.v) on the amphetamine-stimulated BOLD response.

Potentially important insight into the contribution of specific neuronal systems to the functional correlate of the behavioural response profile might be gained by using the animals as their own controls, through direct and continuous measurements of functional brain activity. It is possible to administer repeated doses and with the exclusion or inclusion of specific time series of scans in the processing and analysis, each animal is potentially its own control, - e.g. for comparison to baseline, comparison to single dose.

5.2 Methods

Amphetamine was intravenously administered in one cohort, and in the other two cohorts either D_1 antagonist SCH23390 or D_1 agonist SKF38393 were administered (also intravenously) prior to amphetamine to rats whilst immobilised in a 2.35 Tesla imaging system. In order to study the global spatial response profile, the whole brain was scanned (30 x 1mm). A summary of the methods for these experiments is described in this section, fuller details of these procedures and the materials used are presented in Chapter 4 as shown in parentheses.

5.2.1 Animal preparation

Male Sprague-Dawley rats (250-300g, n=8), were used for each of the three experiments); they were anaesthetised and cannulated for administration of drugs as described in sections 4.2.1 and 4.3, respectively. The physiological state of the animal

was constantly monitored using respiration rate and body temperature, as described in section 4.5. When instrumented, the animal was placed into a custom-made, heated probe which maintained the core body temperature at 37°-38°C (section 4.4). The MRI modified surface coil (section 4.6.2) was secured to the dorsal surface to the head before positioning the animal in the magnet centre of the scanner (section 4.6.1). The imaging experiments were all performed at field strength of 2.3 Tesla with a horizontal bore superconducting magnet (4.6.1).

5.2.2 Experimental prototocol

Amphetamine and sulpiride were dissolved in saline, and SCH23390 and was dissolved a propylene glycol mixture (section 4.2.2) and made up on the day of the experiment. For experiment 1, 45 minutes of baseline (no drug administration) scans were acquired before amphetamine was administered as a single intravenous bolus infusion via the jugular vein (Fig 5.2.2a, shown in green). The volumes injected (1ml/kg) took into account the saline-heparin filled dead space of 0.05ml. Data were collected for a further 90 minutes after drug administration.

Before performing the pre-treatment experiments, the effect of D_1 antagonist SCH23390 was examined as a mixture with amphetamine, and the results were virtually identical to amphetamine in images and time-course plots (the results are not presented). This presumably is due to SCH23390 competing with amphetamine at the receptor level, in Experiment 2 and 3, the 20 minute pre-treatment regime before amphetamine administration allowed for dopamine receptor occupancy and subsequent blockade or facilitation of amphetamine stimulation.

Experiments 2 and 3 involved a pretreatment regimen, in which 45 minutes of baseline (no drug administration) scans were acquired before antagonist (either SCH23390, 0.5mg/kg i.v, or sulpiride 50mg/kg, i.v) was administered as a single intravenous bolus infusion via the jugular vein (Fig 5.2.2 b, shown in red & c shown in blue, respectively). Data were collected for a further 20 minutes. Amphetamine was then administered as a single intravenous bolus infusion also via the jugular vein (Fig 5.2.2 b & c, shown in green). All volumes injected took into account the saline-heparin filled

dead space of 0.05ml. Data were collected for a further 90 minutes after drug administration.

Fig 5.2.2 Schemata of Time-course of experiments 1, 2 & 3.

Each block represents 1 scan (4 minutes 40 seconds), arrow represents exact time of drug administration.

a. Experiment 1: single bolus injection of amphetamine after 45 minutes baseline.

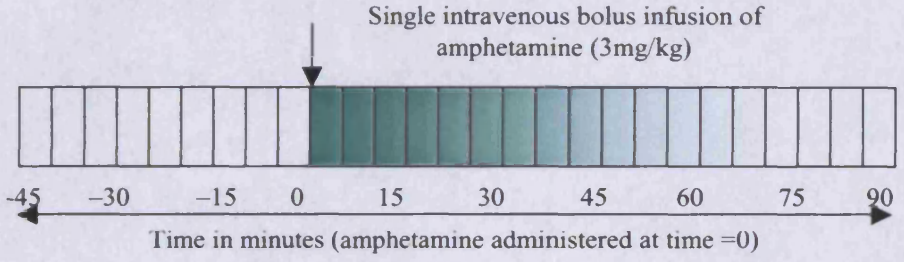

b. Experiment 2: pretreatment with D1 antagonist SCH23390 (0.5mg/kg, i.v for 20 minutes), then single bolus of amphetamine (3mg/kg).

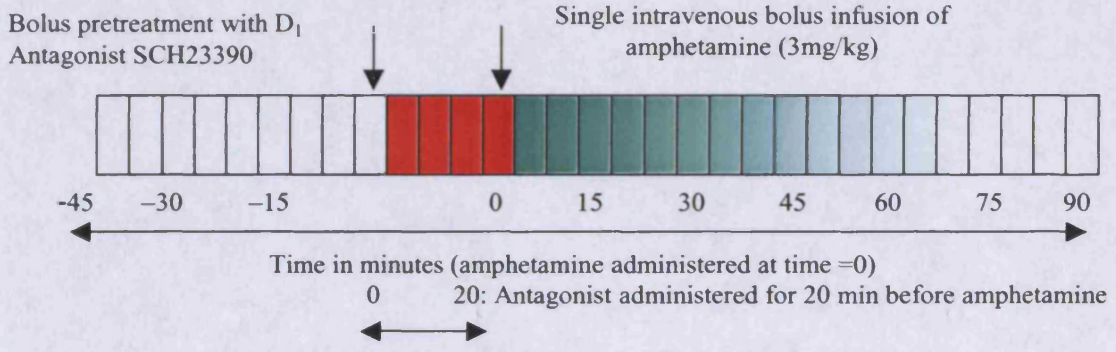

c. Experiment 3: pretreatment with D2 antagonist Sulpiride (0.5 mg/kg, i.v for 20 minutes, then single bolus bolus of amphetamine (3mg/kg).

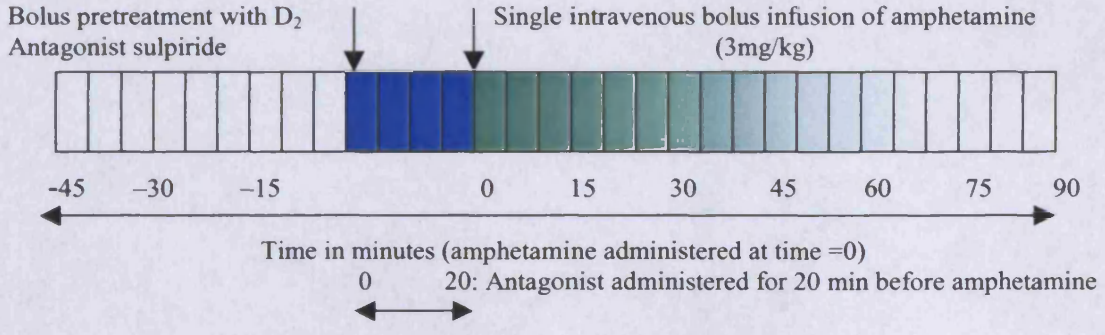

5.2.3 Statistical Processing and Analysis

The complete steps from raw data acquisition, through the pre-processing (masking, registration, normalisation and smoothing) to statistical analysis and inference are described in section 4.5. Averaging the results obtained from the 8 individual animals that received the drug challenges generates the t-Map. The colour overlay indicates the level of significance in t-values (these are converted into p-values in the tables below), assessed as a group t-test comparison between pre (baseline of 45 minutes before drug injection) and post-drug injection signal (up to 90 minutes after drug administration).

For the three experiments as described above, in order to create t-Maps in SPM, contrasts must be specified. In the case of the first experiment, the scans are separated into two groups- basal and drug. By attributing "-1" to the basal condition and "1" to the drug condition, one is effectively testing the hypothesis that the drug has caused a mean increase in signal intensity in a particular voxel. When n=8, the contrast is simply:

−1 1 −1 1 −1 1 −1 1 −1 1 −1 1 −1 1 −1 1

And the converse is true for decreases in signal intensity, choosing :

1 −1 1 −1 1 −1 1 −1 1 −1 1 −1 1 −1 1 −1

Across the whole group.

For experiments 2 and 3, it is slightly more complicated as there is another extra condition- the antagonist. Thus by assigning "0" to one of the conditions, it is possible to omit it from the test. In this situation we are not actually interested in the acute action of the antagonist itself (the 20 minute duration of sole antagonist action is too short to be able to draw conclusions from any changes that may have occurred as compared to the basal condition). Incidentally, these antagonists are administered in later experiments (see Chapters 6 & 7) and the effects of their individual activity are investigated. Thus to test the hypothesis that the amphetamine activity has caused an increase in signal intensity even after the antagonist administration the contrast now becomes:

-1 0 1 −1 0 1 −1 0 1 −1 0 1 -1 0 1 −1 0 1 −1 0 1 −1 0 1

and that amphetamine (post antagonist treatment) has caused significant decreases in signal intensity in particular voxels across the subject group the contrast is:

1 0 −1 1 0 −1 1 0 −1 1 0 −1 1 0 −1 1 0 −1 1 0 −1 1 0 −1.

This is summarised in Table 5.2.3, where the information required to create the design matrix (as described in section 4.6) and specify contrasts for the t-test is displayed. This process is described in detail in section 4.7.4.

Experiment / Condition	Start (scan no)	End (scan no)	Contrast for "increase"	Contrast for "decrease"
Experiment 1				
Basal	0	9	-1	1
Drug	10	27	1	-1
Experiment 2 & 3				
Basal	0	9	-1	1
Antagonist	10	13	0	0
Drug	14	31	1	-1

Table 5.2.3 Data summary for experiments 1, 2 and 3

The contrasts for Experiment 1 equate to a simple "Off-On" paradigm, which is true also of experiments 2 and 3 but the actual antagonist alone effect is removed in order to investigate their effect on the amphetamine response.

When these contrasts are applied to the data, images are obtained. These images are statistical maps with the colour changing on differences in levels of significance. These statistical tests generate a first and second level of statistics and two sets of images for each level, representing significant increases and significant decreases in signal intensity caused by the drug administered. Furthermore, the actual data used to generate the images is extracted on a region of interest basis, such that temporal plots of the percentage change of signal intensity at individual voxels may be generated. Thus, relatively large volumes of data may be produced from a single experiment, allowing both spatial and temporal perspectives of the drugs effect to be obtained

5.3 Results

SPM generated two sets of image data for each experiment, a fixed effect analysis and a random effects analysis. In addition to these images, graphs of timecourses from

particular voxels in regions of interest were also obtained, samples of these are displayed in the following sections, the complete results are summarised in the respective tables for each experiment.

5.3.1 Results from Experiment 1: Amphetamine Administration (3mg/Kg, i.v)

Images were collected from 30 contiguous, coronal, 1mm brain slices. The Bonferroni corrected data showed that acute intravenous infusion of amphetamine had significant ($P<0.01$) effect on the BOLD signal in many brain areas.

Increases in BOLD signal intensity

Activation of subcortical structures was striking: there were marked increases in signal intensity in olfactory areas, cingulate cortex, dorsal and ventral striatum, septum, globus pallidus, thalamus, retrosplenal cortex, hippocampus, subiculum, lateral entorhinal cortex, inferior colliculus, periaqueductal grey matter (PAG), pontine reticular nucleus, entorhinal cortex and some isolated parts of the cerebellar lobes. More discrete, yet significant increases were also observed in parts of the M1 motor cortex and primary somatosensory cortex jaw area (S1J) although from the images obtained it is obvious that this tends to be the deeper parts of these brain areas. White matter tracts such as the corpus callosum also appear to demonstrate changes on BOLD signal, this indicates some blurring of effect, possibly due to smoothing.

Six brain slices are shown below in the t-Maps to indicate the effect of the amphetamine throughout the brain. Random Effects analysis, a more stringent test showed less activation than with the fixed effect analysis (as expected). Table 5.3.1a shows which areas were also significantly affected in the random effects analysis, the areas include olfactory nucleus, M1 motor cortex, cingulate cortex, nucleus accumbens, septum, caudate-putamen, thalamus, retrosplenal cortex and PAG.

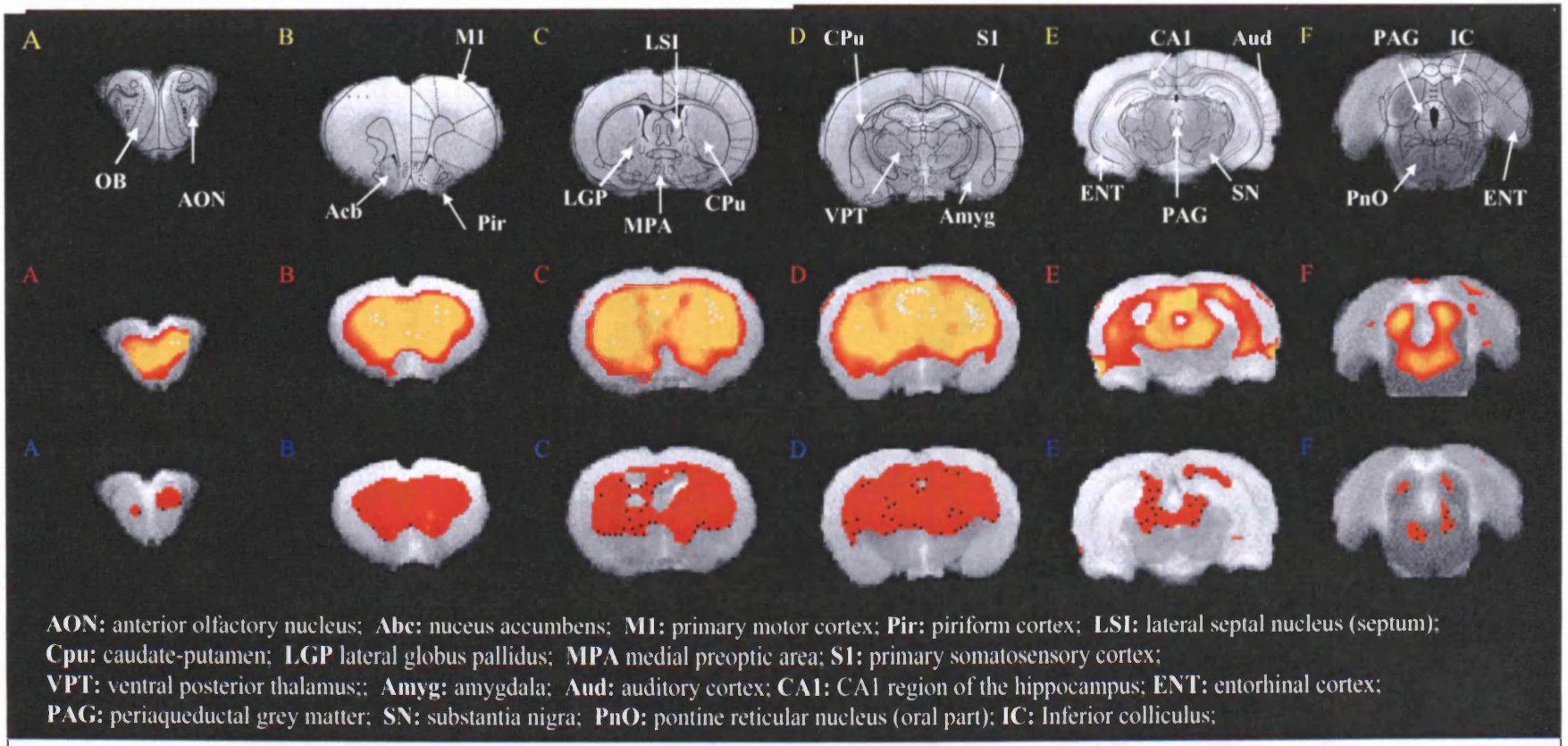

Fig 5.3.1a Increases in signal intensity following amphetamine administration (3mg/kg, i.v)

The first row shows annotated and labelled high resolution template images such that the areas displaying changes may be identified, the middle row shows the effect of amphetamine with fixed effects analysis, and the bottom-most row the effect of amphetamine with random effects analysis.

A: Bregma=+5.7mm Olfactory nucleus and cortex

B:Bregma=+2.7mm Nucleus accumbens and M1 motor cortex

C:Bregma=-0.3mm Caudate-putamen, globus pallidus and septum

D:Bregma=-2.3mm Thalamus and caudate-putamen

E:Bregma=-5.3mm PAG and hippocampus

F:Bregma=-8.3mm Inferior colliculus and Pontine reticular nucleus

Below are graphs representing the timecourse of signal intensity at specific voxels, activated as indicated by SPM t-Maps (Fig 5.3.1a). Areas of interest have been selected throughout the brain, and correspond to the brain slices of images illustrated above where possible. Arrow indicates time of administration.

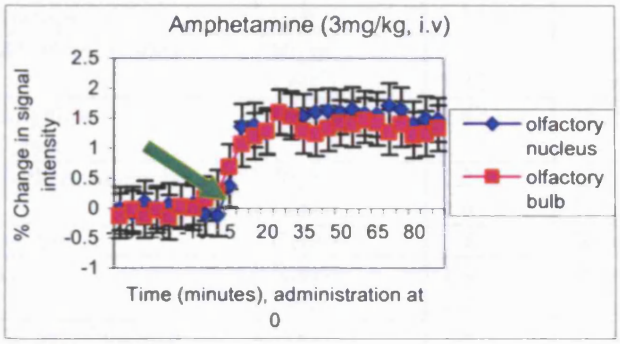

Bregma= +4.7mm

Olfactory nucleus T=15.45, P<0.001 and olfactory bulb T=15.68, P<0.001.

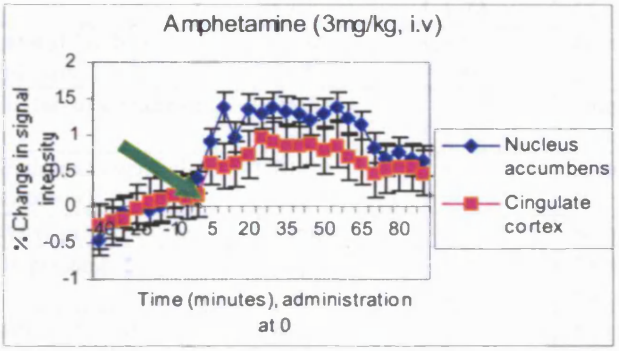

Bregma= +2.7mm

Accumbens T=13.26 P<0.001, Cingulate cortex T=8.52 P<0.001.

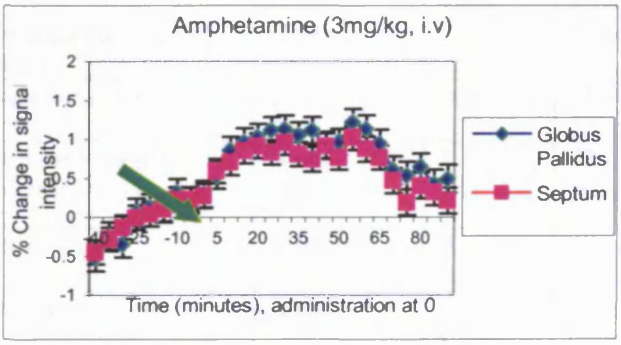

Bregma= -0.3mm

Globus pallidus T= 11.5, P<0.001, septum T= 14.63, P<0.001.

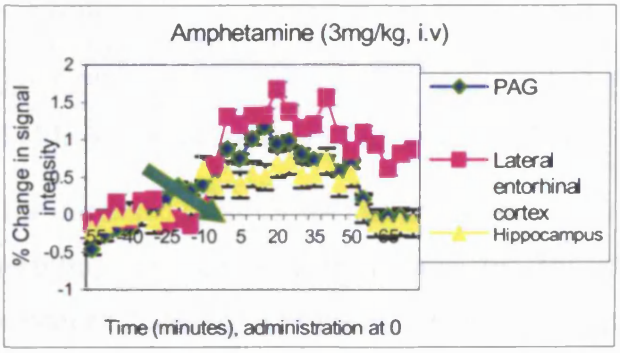

Bregma=-7.3mm

Hippocampus (CA3) regions T=14.03 , P<0.001, Periaqeductal grey matter T=10.35, P<0.001, Lateral entorhinal cortex, T=14.99, P>0.001.

Fig 5.3.1b

Graphs showing signal intensities at voxels of interest, increase in BOLD signal after administration of amphetamine 3mg/kg i.v.

Arrow indicates time of administration. Results are ± S.D of the mean

Area	Left/ Right/ Centre	% Change	Time to peak	T-Value	P-Value	Random Effect
Olfactory Bulb	Right Left	1.4 1.0	50 min 55 min	15.68 11.33	P<0.001	No
Orbital Cortex	Centre	1.3	45 min	16.30	P<0.001	No
Olfactory Nucleus	Right Left	1.7 1.65	70 min 65 min	15.45 15.83	P<0.001	Yes
M1 Motor Cortex	Right Left	1.8 1.75	30 min 40 min	15.32 15.26	P<0.001	Yes
Cingulate Cortex	Centre	1.87	75 min	8.52	P<0.001	Yes
Nucleus Accumbens	Right Left	1.2 1.6	45 min 25 min	13.26 11.99	P<0.001	Yes
Septum	Centre	1.4	50 min	14.63	P<0.001	Yes
S1J	Right Left	1.4 1.2	30 min 30 min	12.61 11.76	P<0.001 P<0.001	No
Caudate-Putamen	Right Left	1.8 1.74	30 min 55 min	15.34 14.63	P<0.001 P<0.001	Yes
Lateral Globus Pallidus	Right Left	1.6 1.6	40 min 30 min	11.50 12.56	P<0.001 P<0.001	No
Thalamus (Anterior)	Right Left	1.67 1.52	35min 30min	12.95 12.74	P<0.001 P<0.001	Yes
Thalamus (ventral-posterior)	Right Left	1.5 1.5	35min 30min	16.34 13.12	P<0.001 P<0.001	Yes
Retrosplenal Cortex	Centre	1.4	50 min	14.63	P<0.001	Yes
Hippocampus CA3	Right Left	1.5 1.6	45 min 50 min	14.03 17.09	P<0.001 P<0.001	No
Lateral Entorhinal Cortex	Right Left	3.4 2.6	45 (&75) 40 min	14.99 19.13	P<0.001 P<0.001	No
Periaqueductal grey matter	Centre	1.2	30 min	10.35	P<0.001	Yes
Superior colliculus	Right Left	0.9 1.1	25 & 35 35 min	9.45 9.30	P<0.001 P<0.001	No
Pontine Reticular nucleus (oral part)	Right Left	1.1 1.2	35 min 50 min	10.56 11.63	P<0.001 P<0.001	No
Subiculum	Right Left	0.9 0.9	45 min 50 min	5.93 8.12	P<0.001 P<0.001	No
Inferior colliculus	Right Left	1.5 1.6	35 min 90 min	8.64 12.89	P<0.001 P<0.001	No
Pontine Reticular nucleus (caudal part)	Right Left	0.85 0.9	45 min 50 min	9.58 9.18	P<0.001 P<0.001	No
Cerebellum	Centre	1.0	35 min	10.34	P<0.001	No

Table 5.3.1a Summary of increases in fMRI signal for Experiment 1

The corrected t-test shows that many areas are affected by amphetamine stimulation resulting in increases in signal intensity. The more stringent Gaussian random field model excludes some of the areas. Some examples of the time-courses are shown above (Fig 5.3.1b).

Decreases in BOLD signal intensity

In addition to increases in BOLD signal intensity, marked and statistically significant decreases in signal intensity were also observed. Decreases in signal intensity of cortical structures was striking: there were marked decreases in signal intensity in frontal cortex, M1 (primary) motor cortex, S1J (primary somatosensory cortex, jaw area), S1B (primary somatosensory cortex, barrel fields area), auditory cortex, parietal cortex, amygdalopir transition area, 6^{th} lobe of the cerebellum and simple cortex. In addition, some subcortical areas- medial preoptic area, hypothalamic areas, amygdala, substantia nigra, lateral leminiscus also showed decreases signal intensity.

Six brain slices are shown below in the t-Maps to indicate the effect of the amphetamine throughout the brain. Random effects analysis, a more stringent test showed much less obvious changes than with the fixed effect analysis (as expected). Table 5.3.1b shows that changes in these areas were not significant in the random effects analysis.

Fig 5.3.1c shows graphs representing the timecourse of signal intensity at specific voxels activated as indicated by SPM t-Maps (as above), areas are named as corresponding to particular structures in accordance with the rat atlas. Areas of interest have been selected throughout the brain, and correspond to the brain slices of images illustrated above where possible. A summary of all areas showing decreases in signal intensity are displayed below in table 5.3.1b

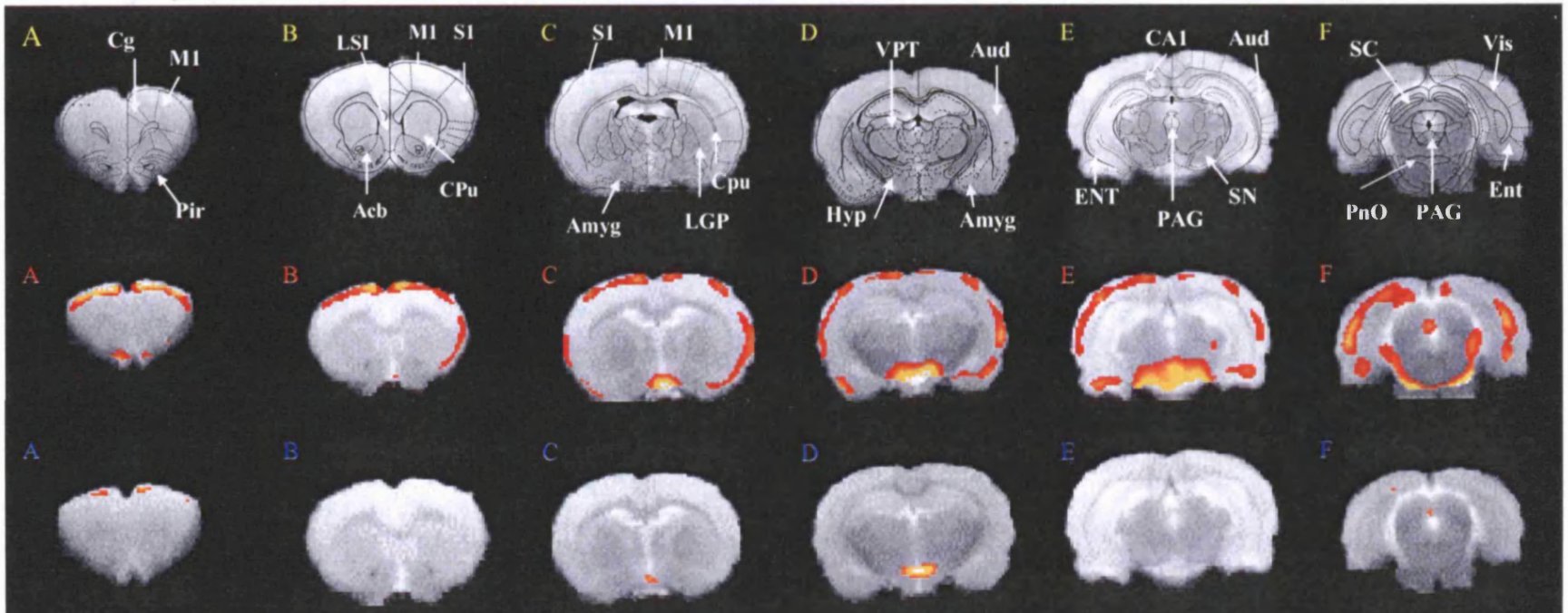

Cg: cingulate cortex; **Pir:** piriform cortex; **Abc:** nuceus accumbens; **M1:** primary motor cortex; **S1:** primary somatosensory cortex; **Cpu:** caudate-putamen; **LSI** lateral septal nucleus (septum); **LGP** lateral globus pallidus; **Amyg:** amygdala; **VPT:** ventral posterior thalamus; **Aud:** auditory cortex; **Hyp:** hypothalamus; ; **ENT:** entorhinal cortex; **PAG:** periaqueductal grey matter; **SN:** substantia nigra; **CA1:** CA1 region of the hippocampus; **SC:** superior colliculus; **Vis:** visual cortex; **PnO:** pontine reticular nucleus (oral part).

Fig 5.3.1c Decreases in signal intensity following amphetamine administration (3mg/kg, i.v)

The first row shows annotated and labelled high resolution template images such that the areas displaying changes may be identified, the middle row shows the effect of amphetamine with fixed effects analysis, and the bottom-most row the effect of amphetamine with random effects analysis.

A: Bregma=+3.7mm M1 motor cortex

B: Bregma=+1.7mm M1 motor cortex

C: Bregma=-1.3mm S1BF Somatosensory cortex

D: Bregma=-3.3mm Medial preoptic nucleus and Amygdala

E: Bregma=-5.3mm Auditory cortex and substantia nigra

F: Bregma=-7.3mm Lateral leminiscus and visual cortex

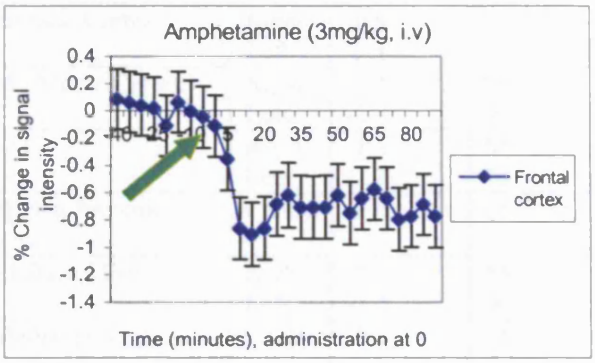

Bregma=4.7

Frontal cortex T= 21.67
P<0.001

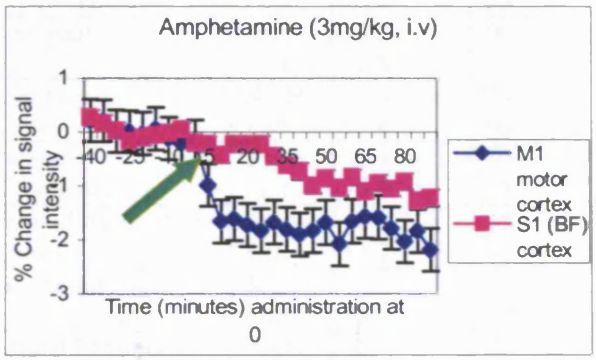

Bregma=-0.3mm

M1 motor cortex
T= 20.06 P<0.001, and
S1 (BF) somatosensory
cortex T= 10.45 P<0.001

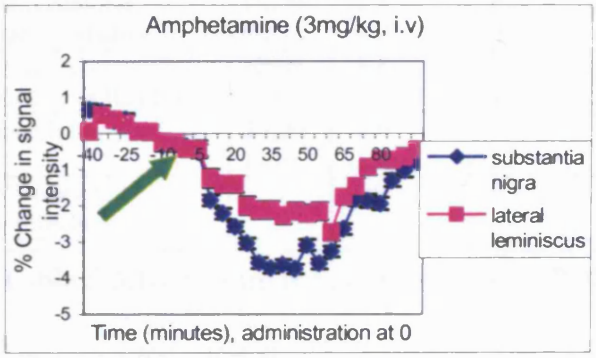

Bregma=-0.3mm

Substantia nigra
T=14.17, P<0.001 and
lateral leminiscus
T= 9.70, P<0.001.

Fig 5.3.1d

Graphs showing signal intensities at voxels of interest, decrease in BOLD signal after administration of amphetamine 3mg/kg i.v.

Arrow indicates time of administration. Results are ± S.D of the mean

Area	Right/ Left/ Centre	% Change	Time to peak	T-Value	P-Value	Random Effects?
Frontal Cortex	Right Left	-0.9 -2.1	15 25	21.67 22.10	P<0.001 P<0.001	No
M1 Motor Cortex	Right Left	-2.1 -2.3	90 90	20.06 21.16	P<0.001 P<0.001	No
S1J	Right Left	-1.3 -1.3	65 90	8.51 9.16	P<0.001 P<0.001	No
Medial Preoptic area	Centre	-2.6	35	16.62	P<0.001	No
S1 Barrel Fields	Right Left	-1.3 -1.3	85 90	10.45 9.77	P<0.001 P<0.001	No
Medial preoptic nucleus	Centre	-2.9	25	20.04	P<0.001	No
Ventromedial hypothalamus	Right Left	-3.5 -5.1	35 35	20.79 22.67	P<0.001	No
Amygdala	Right Left	-1.3 -1.8	90 85	8.90 10.54	P<0.001 P<0.001	No
Auditory Cortex	Right Left	-1.4 -1.4	80 90	8.93 8.23	P<0.001 P<0.001	No
Lateral Hypothalamus	Right Left	-5.3 -5.5	30 35	16.20 14.32	P<0.001 P<0.001	No
Parietal Association Cortex	Right Left	-1.1 -1.2	55 35	7.39 8.82	P<0.001 P<0.001	No
Substantia Nigra	Right Left	-3.7 -4.0	15 10	14.17 12.69	P<0.001 P<0.001	No
Lateral Leminiscus	Right Left	-2.7 -2.2	20 65	9.70 7.69	P<0.001 P<0.001	No
Amygdalopir transition area	Right Left	-1.7 -1.7	10 10	9.90 17.27	P<0.001 P<0.001	No
Dorsal cortex of Inferior colliculus	Right Left	-1.8 -2.2	20 65	6.79 8.49	P<0.001 P<0.001	No
Simple	Right Left	-1.6 -1.4	10 10	10.47 12.01	P<0.001 P<0.001	No
6th lobe of cerebellum		-0.9	5		P<0.001	No

Table 5.3.1b Summary of Decreases in fMRI signal for Experiment 1

The corrected t-test shows that many areas are affected by amphetamine stimulation resulting in decreases in signal intensity. The more stringent Gaussian random field model excludes most of the areas. Some examples of the time-courses are shown above (Fig 5.3.1d).

The saline control group (n=8) SPMs showed no change in fMRI signal intensity and thus no images were generated.

5.3.2 Results from Experiment 2: Pretreatment with SCH23390 (0.5mg/kg, i.v) and Amphetamine Administration (3mg/Kg, i.v).

Images were collected from 30 contiguous, coronal, 1mm brain slices. The Bonferroni corrected data showed that when pretreated with D_1 dopamine receptor antagonist SCH23390 (0.5mg/kg, i.v), acute amphetamine challenge had significant effect on the BOLD signal in many areas.

Increases in BOLD response

As compared to the results of the amphetamine administered alone group, the SCH23390 pretreated group showed a reduced BOLD response (in the positive direction). Changes in subcortical structures was still significant but they were spatially more discrete: there were increases in signal intensity in the cingulate cortex, caudate-putamen, lateral globus pallidus, hippocampus (in particular CA3), inferior colliculus, and isolated parts of the cerebellar lobes superior colliculus and lateral habenula.

Six brain slices are shown below in the t-Maps to indicate the effect of the antagonist SCH23390 on amphetamine stimulation throughout the brain. Random Effects analysis, a more stringent test showed no changes following amphetamine administration after pretreatment with SCH2339. In the following figure (Fig 5.3.2a) the results of pre-treatment on amphetamine stimulation are displayed (row 2) next to that of amphetamine alone (row 1, as shown in Fig 5.3.1a) such that a comparison can be made.

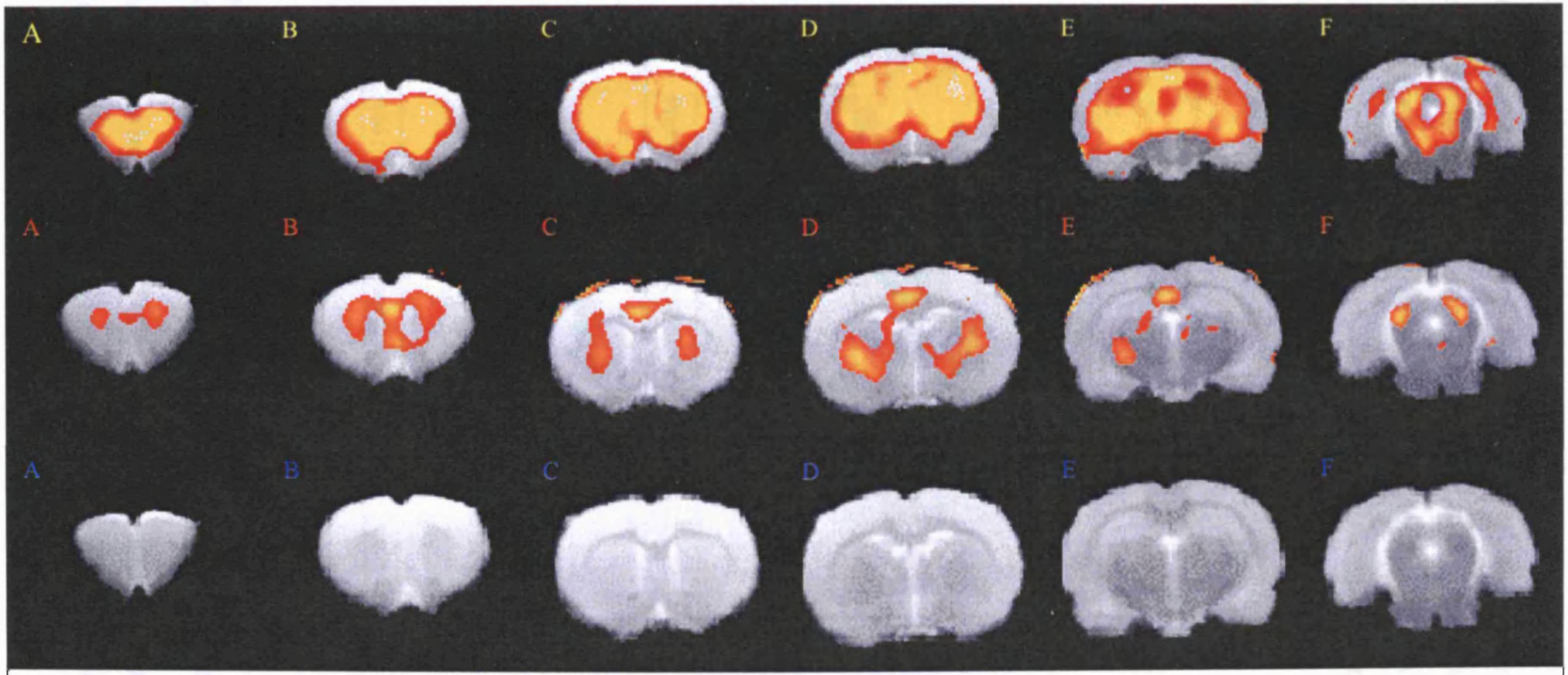

Fig 5.3.2a Increases in signal intensity following amphetamine administration(3mg/kg, i.v) after pretreatment with SCH23390 (0.5mg/kg, i.v)

The first row shows the effect of amphetamine alone, the second row shows the effect of amphetamine after SCH23390 pretreatment with fixed effects analysis, and the bottom-most row the effect of amphetamine after SCH23390 pretreatment with random effects analysis.

A: Bregma=+4.7mm Orbital cortex (assymetrical)

B:Bregma=+2.7mm Possibly corpus callossum (assymetrical)

C:Bregma=+0.7mm Cingulate cortex, caudate-putamen

D:Bregma=-1.3mm Globus pallidus, caudate-putamen

E:Bregma=-4.3mm Hippocampus (CA3 region)

F:Bregma=-7.3mm Superior colliculus

Below are graphs representing the timecourse of signal intensity at specific voxels activated as indicated by SPM t-Maps (as above). Areas are named as corresponding to particular structures in accordance with the rat atlas. Areas of interest have been selected throughout the brain, and correspond to the brain slices of images illustrated above where possible In areas which showed no change, it was not possible to obtain a timecourse for regions of interest as the image itself is statistical map, thus for areas which show no significant change there is no data available. Arrows indicates time of administration.

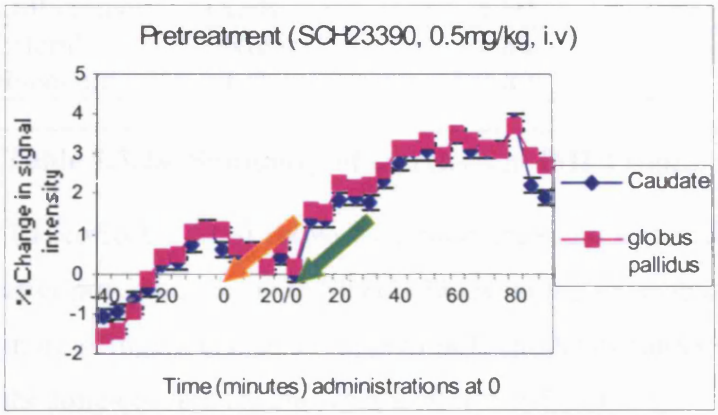

Bregma= -1.3mm
Caudate-putamen T=5.2
P<0.002, Globus pallidus
T=5.72, P<0.001.

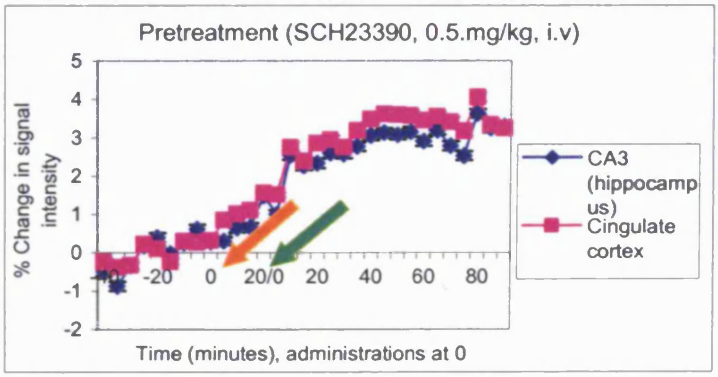

Bregma=-4.3mm
CA3 (hippocampus)
T=6.88, P<0.001.
Bregma=4.7
Cingulate cortex T=7.87
P<0.001.

Fig 5.3.2b

Graphs showing timecourse of signal intensities at voxels of interest showing increases in BOLD signal after administration of 3mg amphetamine i.v.

Orange arrow indicates time of SCH23390 administration, green arrow indicates time of amphetamine administration. Results are $\pm$ S.D of the mean.

Area	Right/ Left/ Centre	% Change	Time to Peak	T-Value	P-Value	Random Effect Significant?
Hippocampus	Right Left	3.6%	80 80	6.9 8.0	P<0.001 P<0.001	No No
Cerebellum	Centre		80	7.8	P<0.001	No
Cingulate cortex	Centre	4.1%	80	7.9	P<0.001	No
Caudate-putamen	Right Left	3.7%	80 80	5.2 5.5	P<0.002 P<0.001	No No
Inferior Colliculus	Right Left		80 80	6.8 7.1	P<0.001 P<0.001	No No
Lateral Globus Pallidus	Right Left	3.7%	80 80	5.7 5.2	P<0.001 P<0.002	No No
Superior Colliculus	Right Left		80 80	7.5 7.8	P<0.001 P<0.001	No No
Lateral Habenula	Right Left		80 80	4.8 4.5	P<0.01 P<0.01	No No

Table 5.3.2a Summary of increases in fMRI signal for Experiment 2

The corrected t-test shows that many areas are affected by amphetamine stimulation after pre-treatment with SCH23390 resulting in increases in signal intensity. The more stringent Gaussian random field model excludes these areas. Some examples of the time-courses are shown above (Fig 5.3.2b).

Decreases in BOLD signal intensity

In contrast to the lower number of areas showing increases in BOLD signal intensity, marked and statistically significant decreases were observed in many areas following amphetamine administration when pre-treated with SCH23390. Although some changes in the dorsal surface of the cortices appeared to be blocked by the antagonist SCH23390 (See the first 3 slices), the rest of the changes are not dissimilar to that found when amphetamine is administered alone. Again, similar to amphetamine alone, decreases in BOLD signal intensity in cortical structures were prominent: there were marked decreases in signal intensity in S1J (primary somatosensory cortex, jaw area), S1B (primary somatosensory cortex, barrel fields area), auditory cortex, parietal cortex, entorhinal cortex, 6^{th} lobe of the cerebellum and simple cortex. In addition some subcortical areas also displayed significant deceases in signal intensity, for example, the medial preoptic area, hypothalamic areas, amygdala, substantia nigra and lateral leminiscus.

Six brain slices are shown below (Fig 5.3.2.c) to indicate the effect of the amphetamine in the SCH23390 pretreated rat throughout the brain. Table 5.3.1b and Fig 5.3.2c (row 3) shows that these areas were non significant in random effects test. In the following figure the results of pre-treatment on amphetamine stimulation are displayed (row 2) next to that of amphetamine alone (row 1, as shown in section 5.3.1) such that a comparison can be made.

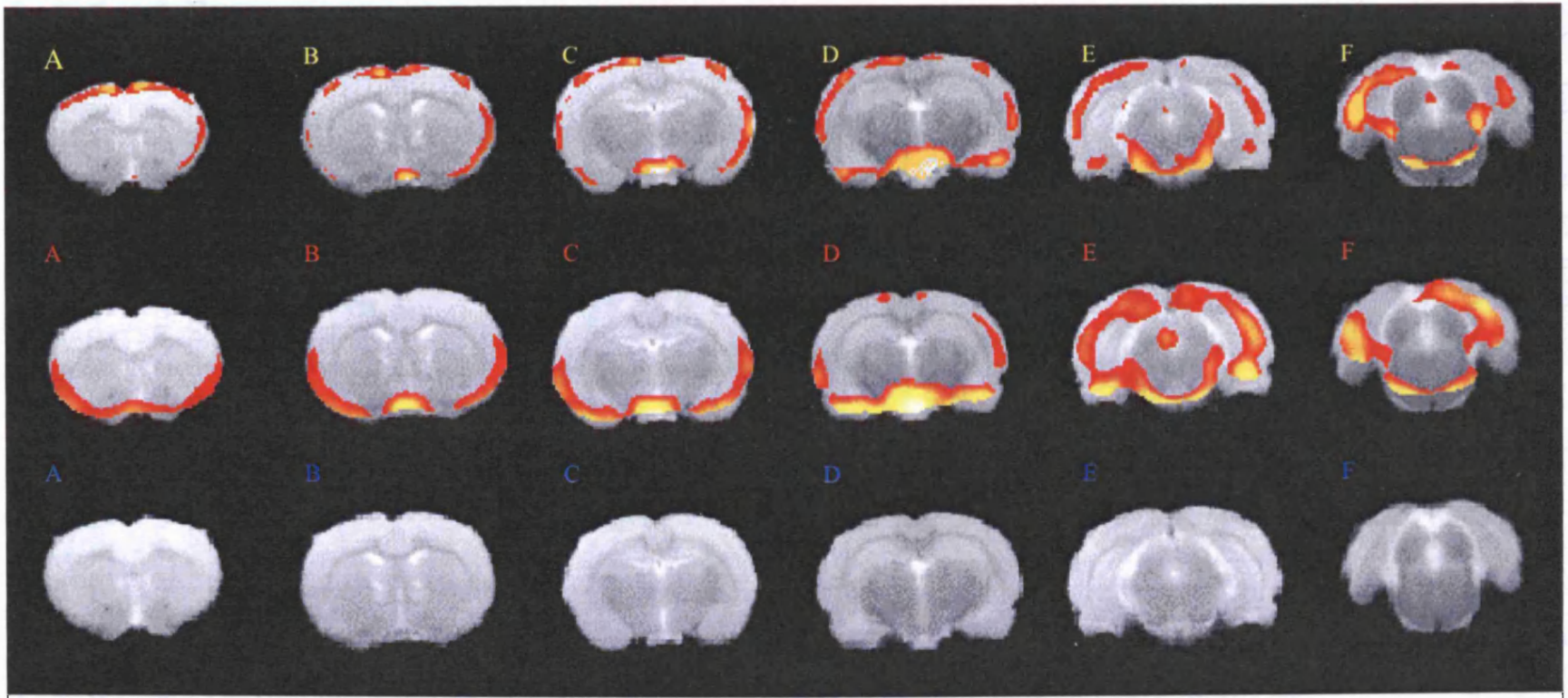

Fig 5.3.2c Decreases in signal intensity following amphetamine administration(3mg/kg, i.v) after pretreatment with SCH23390 (0.5mg/kg, i.v)

The first row shows the effect of amphetamine alone, the second row shows the effect of amphetamine after SCH23390 pretreatment with fixed effects analysis, and the bottom-most row the effect of amphetamine after SCH23390 pretreatment with random effects analysis.

A: Bregma=+1.7mm Piriform cortex

B:Bregma=-0.3mm Piriform cortex and S2 somatosensory cortex

C:Bregma=-2..3mm Hypothalamus and S2 somatosensory cortex

D:Bregma=-4.3mm Amygdala

E:Bregma=-6.3mm substantia nigra and subiculum

F:Bregma=-8.3mm Pontine nucleus and visual cortex

Shown below are graphs representing the timecourse of signal intensity at specific voxels activated, as indicated by SPM t-Maps (as above), areas are named as corresponding to particular structures in accordance with the rat atlas. Areas of interest have been selected throughout the brain, and correspond to the brain slices of images illustrated above where possible.

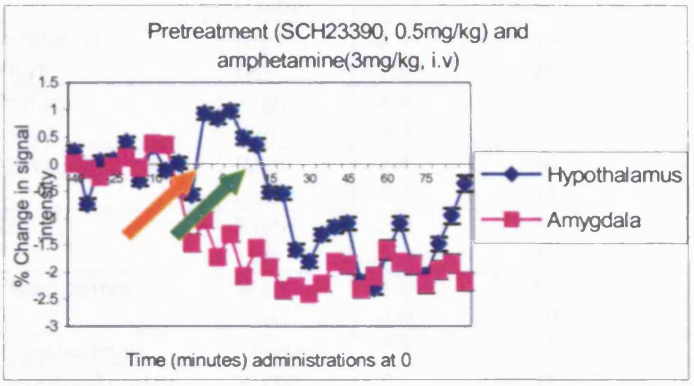

Bregma=-3.3mm

Hypothalamus, T= 8.5 P<0.001
Amygdala, T= 8.1 P<0.001

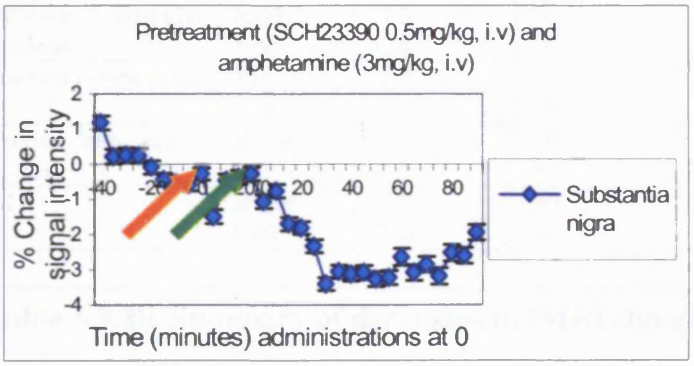

Bregma=+1.7mm

Piriform cortex, T=11.6 P<0.001

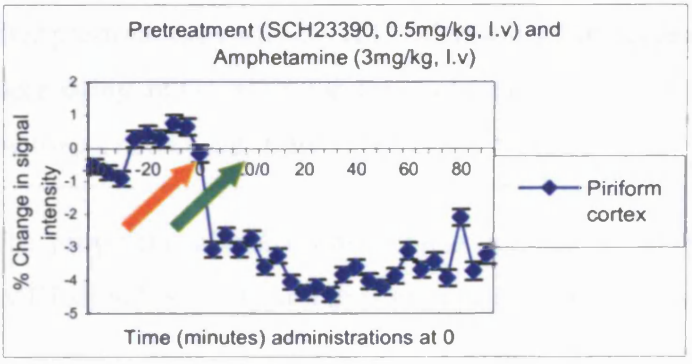

Bregma=-5.3mm

Substantia nigra, T= 7.9 P<0.001

Fig 5.3.2d

Graphs showing timecourse of signal intensities at voxels of interest showing decreases in BOLD signal after administration of 3mg amphetamine i.v.

Orange arrow indicates time of SCH23390 administration, green arrow indicates time of amphetamine administration. Results are ± S.D of the mean.

In areas which showed no change it was not possible to obtain a time-course for regions of interest as the image itself is statistical map, thus for areas which show no significant change there is no data available.

Area	Right/ Left/ Centre	% Change	Time to peak	T-Value	P-Value	Random Effect
Substantia Nigra	Right	-3.4	30	7.9	P<0.001	No
	Left	-1.8	45	9.5	P<0.001	No
Piriform cortex	Right	-4.4	45	11.6	P<0.001	No
	Left	-3.9	45	14.6	P<0.001	No
Amygdala	Right	-2.4	30	8.1	P<0.001	No
	Left	-3.3	45	11.8	P<0.001	No
S2	Right	-2.0	25	5.4	P<0.002	No
	Left	-2.4	25	6.4	P<0.001	No
Visual cortex	Right	-2.0	5	6.1	P<0.001	No
	Left	-2.0	10	7.0	P<0.001	No
Hypothalamus	Centre	-2.3	55	8.5	P<0.001	No
Entorhinal cortex	Right	-2.5	35	11.3	P<0.001	No
	Left	-2.6	30	11.1	P<0.001	No
Pontine reticular nucleus	Right	-4.5	70	10.5	P<0.001	No
	Left	-2.4	70	6.8	P<0.001	No
Auditory cortex	Right	-2.3	15	9.7	P<0.001	No
	Left	-2.6	15	8.6	P<0.001	No
Frontal association cortex	Right	-5.1	50	12.1	P<0.001	No
	Left	-2.9	50	10.1	P<0.001	No
S1J	Right	-1.7	30	8.1	P<0.001	No
	Left	-1.0	30	5.7	P<0.001	No

Table 5.3.2b Summary of decreases in fMRI signal for Experiment 2

The corrected t-test shows that many areas are affected by amphetamine stimulation after pre-treatment with SCH23390 resulting in decreases in signal intensity. The more stringent Gaussian random field model excludes these areas. Some examples of the time-courses are shown above (Fig 5.3.2d).

The propylene glycol-saline vehicle control group (n=8) SPMs showed no change in fMRI signal intensity and thus no images were generated.

5.3.3 Results from Experiment 3: Pretreatment with Sulpiride (50mg/kg, i.v) and Amphetamine Administration (3mg/Kg, i.v).

Images were collected from 30 contiguous, coronal, 1mm brain slices and the Bonferroni corrected data showed that amphetamine administration (3mg/Kg) caused both increases and decreases in BOLD contrast in multiple brain areas ($P<0.05$) when pretreated with the D_2 dopamine receptor antagonist, sulpiride (50mg/kg, i.v).

Increases in BOLD response

As compared to the results from the amphetamine administered alone group, the sulpiride pretreated group showed a similar BOLD response. Changes in subcortical structures were prominent: there were increases in signal intensity in the cingulate cortex, dorsal and ventral striatum, septum, globus pallidus, thalamus, hippocampus, subiculum, lateral entorhinal cortex, superior colliculus, inferior colliculus, PAG, pontine reticular nucleus, entorhinal cortex and some isolated parts of the cerebellar lobes. Significant increases were also observed in parts of the M1 motor cortex and S1J somatosensory cortex although it is obvious from the images that these changes are less significant than those in the deeper structures.

Six brain slices are shown below in the t-Maps to indicate the effect of the antagonist sulpiride on amphetamine stimulation throughout the brain. Random Effects analysis, a more stringent test showed similar changes on amphetamine administration after pretreatment with sulpiride as compared to the fixed effect analysis. In the following figure (Fig 5.3.3c) the results of pre-treatment on amphetamine stimulation are displayed (row 2) next to that of amphetamine alone (row 1, as shown in section 5.3.1) such that a comparison can be made.

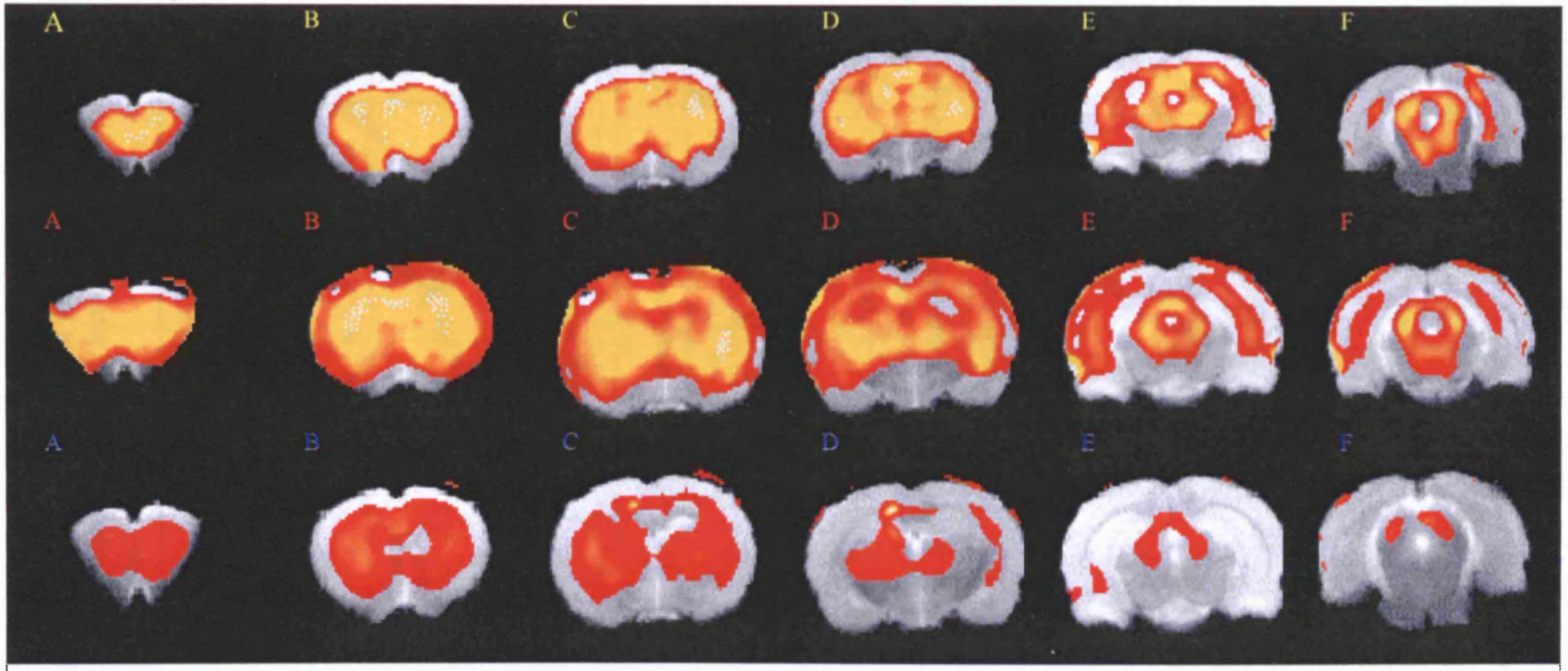

Fig 5.3.3a Increases in signal intensity following amphetamine administration (3mg/kg, i.v) after pretreatment with sulpiride (50mg/kg, i.v)

The first row shows the effect of amphetamine alone, the second row shoes the effect of amphetamine after sulpride pretreatment with fixed effects analysis, and the bottom-most row the effect of amphetamine after sulpride pretreatment with random effects analysis.

A: Bregma=+4.7mm Olfactory cortex

B:Bregma=+1.7mm Caudate-putemen and nucleus accumbens

C: Bregma=-1.3mm Globus pallidus and cingulate cortex

D:Bregma=-3.3mm Ventral posterior thalamus

E: Bregma=-5.3mm Hippocampus (CA3region)

F:Bregma=-7.3mm PAG

Shown below are graphs representing the timecourse of signal intensity at specific voxels activated as indicated by SPM t-Maps (as above). Areas are named as corresponding to particular structures in accordance with the rat atlas. Areas of interest have been selected throughout the brain, and correspond to the brain slices of images illustrated above where possible.

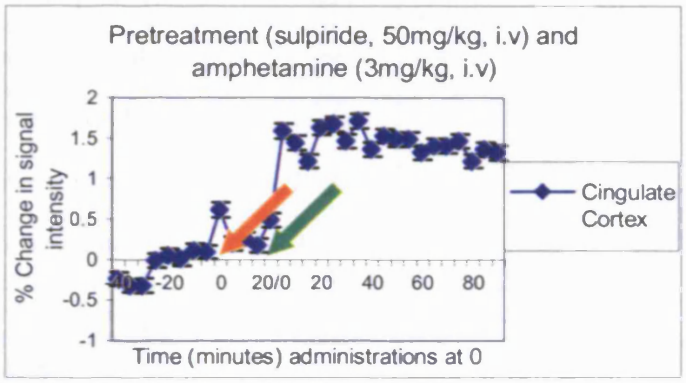

Bregma=0.7mm

Cingulate cortex, T=23.9, P<0.01

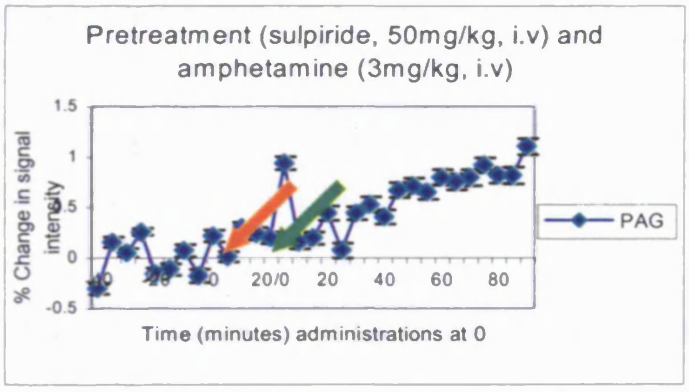

Bregma= -7.3mm

PAG, T=8.5, P<0.01

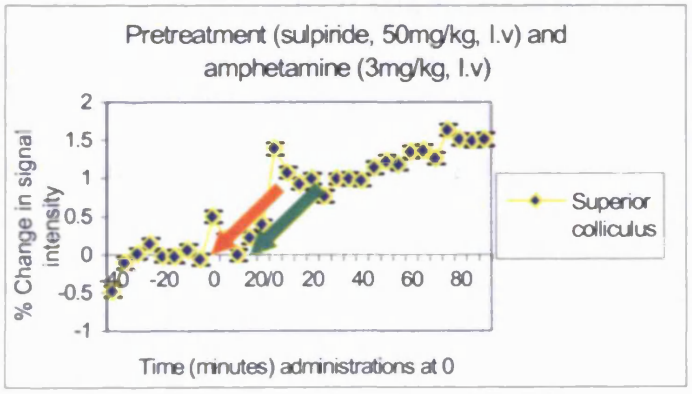

Bregma= -7.3mm

Superior colliculus, T=15.1, P<0.01

Fig 5.3.3b

Graphs showing timecourse of signal intensities at voxels of interest showing increases in BOLD signal after administration of 3mg/kg amphetamine i.v.

Orange arrow indicates time of sulpiride administration, green arrow indicates time of amphetamine administration. Results are ± S.D of the mean.

Area	Right/ Left/ Centre	% Change	Time to peak	T-Value	P-Value	Significant Random effect?
Caudate-putamen	Right Left	2.3 2.8	65min 65min	15.6 21.1	P<0.001 P<0.001	Yes Yes
Nucleus accumbens	Right Left	2.4 2.6	85min 85min	17.9 17.9	P<0.001 P<0.001	Yes Yes
Globus Pallidus	Right Left	2.9 3.3	80min 80min	22.6 23.6	P<0.001 P<0.001	Yes Yes
Ventral-posterior thalamus	Right Left	1.9 1.7	5min 5 min	9.5 18.8	P<0.001 P<0.001	Yes Yes
Periaqueductal grey matter	Centre	0.9	5min	8.5	P<0.001	No
Superior Colliculus	Right Left	1.6 1.3	75min 75min	15.1 11.3	P<0.001 P<0.001	Yes Yes
Inferior Colliculus	Right Left	1.4 1.6	70min 70min	13.2 15.6	P<0.001 P<0.001	Yes Yes
Hippocampus (CA3 region)	Right Left	1.6 1.8	85min 85min	14.1 15.7	P<0.001 P<0.001	No No
Cingulate Cortex	Centre	1.7	35min	23.9	P<0.001	Yes
Second cerebellar lobule	Centre	1.8	5min	20.9	P<0.001	No
M1 motor cortex	Right Left	1.9 1.6	40min 35min	27.0 23.4	P<0.001 P<0.001	No No
S1BF	Right Left	1.2 1.6	45min 35min	21.7 26.9	P<0.001 P<0.001	No No
S1J	Right Left	0.9 1.1	35min 35min	21.1 24.0	P<0.001 P<0.001	No No
Olfactory cortex	Right Left	0.8 1.0	50min 55min	25.11 20.1	P<0.001 P<0.001	Yes Yes
Septum	Centre	1.2	50min	22.5	P<0.001	Yes

Table 5.3.3a Summary of Increases in fMRI signal for Experiment 3

The corrected t-test shows that many areas are affected by amphetamine stimulation after pre-treatment with sulpiride resulting in increases in signal intensity. The more stringent Gaussian random field model excludes some of these areas. Some examples of the time-courses are shown above (Graph 5.3.3b).

Decreases in BOLD signal intensity

In contrast to the high number of areas showing increases in BOLD signal intensity, significant decreases were observed in a few areas following amphetamine administration when pre-treated with sulpiride. Most of the changes in the cortex appeared to be blocked by the antagonist sulpiride and the remaining changes were mainly found in very deep structures. The subcortical structures showing changes included the lateral entorhinal cortex, substantia nigra, amygdala and hypothalamic area.

Six brain slices are shown (Fig 5.3.3.c) below to indicate the effect of the amphetamine in the sulpiride pretreated rat, throughout the brain. Table 5.3.3b and Fig 5.3.3c (row 3) shows that these areas were non significant in random effects test. In the following figure (Fig 5.3.2.c) the results of pre-treatment on amphetamine stimulation are displayed (row 2) next to that of amphetamine alone (row 1, as shown in section 5.3.1) such that a comparison can be made.

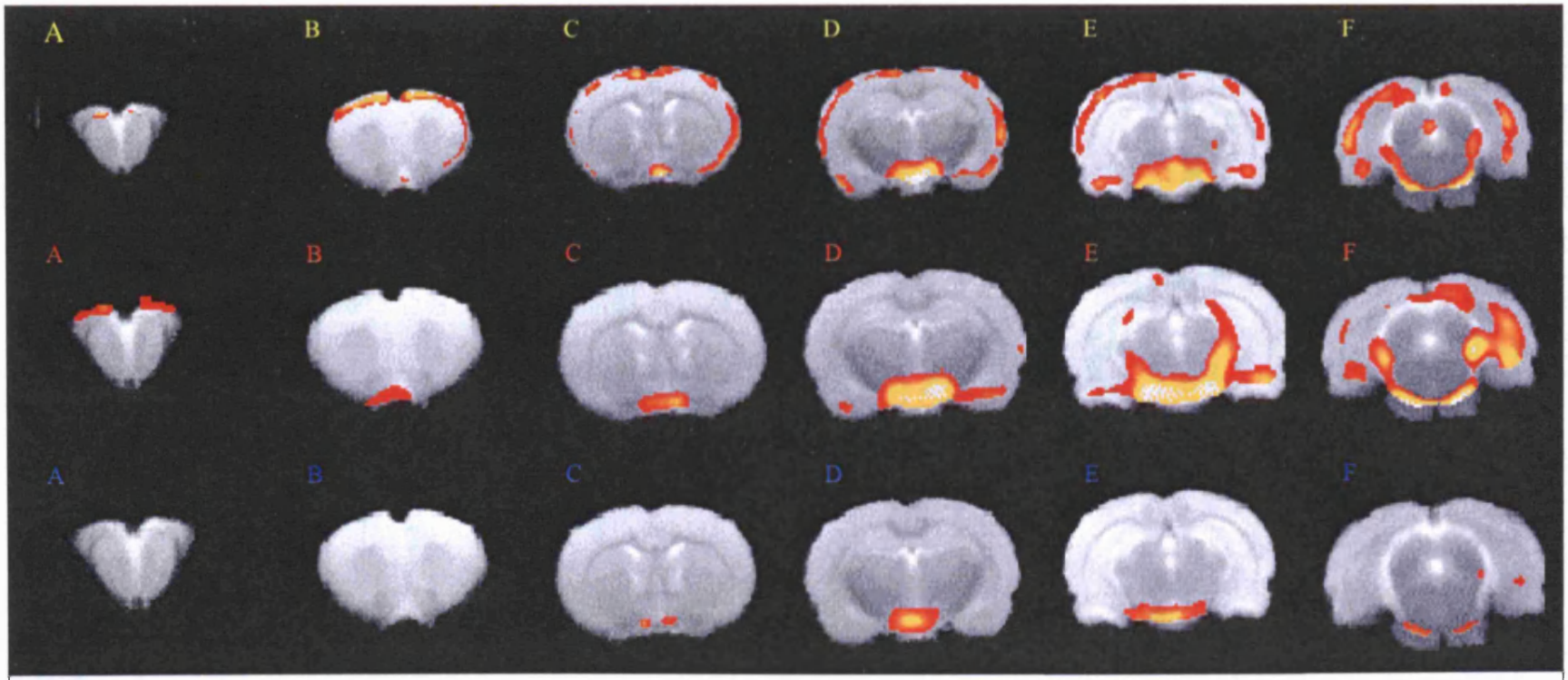

Fig 5.3.3c Decreases in signal intensity following amphetamine administration (3mg/kg, i.v) after pretreatment with sulpiride (50mg/kg, i.v)

The first row shows the effect of amphetamine alone, the second row shoes the effect of amphetamine after sulpride pretreatment with fixed effects analysis, and the bottom-most row the effect of amphetamine after sulpride pretreatment with random effects analysis.

A: Bregma=+5.7mm These changes are outside the brain.

B:Bregma=+2.7mm These changes are outside the brain.

C:Bregma=-0.3mm Medial preoptic area

D:Bregma=-3.3mm Amygdala and hypothalamus

E:Bregma=-5.3mm Substantia Nigra and amygdala

F:Bregma=-7.3mm Lateral Entorhinal cortex

Shown below are graphs representing the timecourse of signal intensity at specific voxels activated as indicated by SPM t-Maps (as above). Areas are named as corresponding to particular structures in accordance with the rat atlas. Areas of interest have been selected throughout the brain, and correspond to the brain slices of images illustrated above where possible.

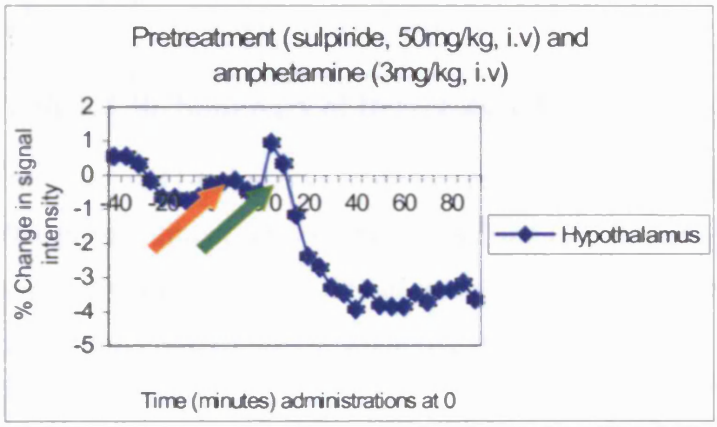

Bregma= -3.3mm

Hypothalamus

T=16.2 , P<0.001

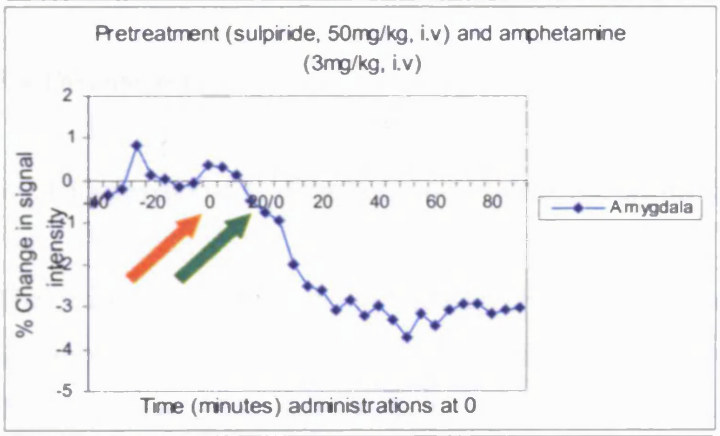

Bregma=-5.3mm

Amygdala

T=8.3 , P<0.001

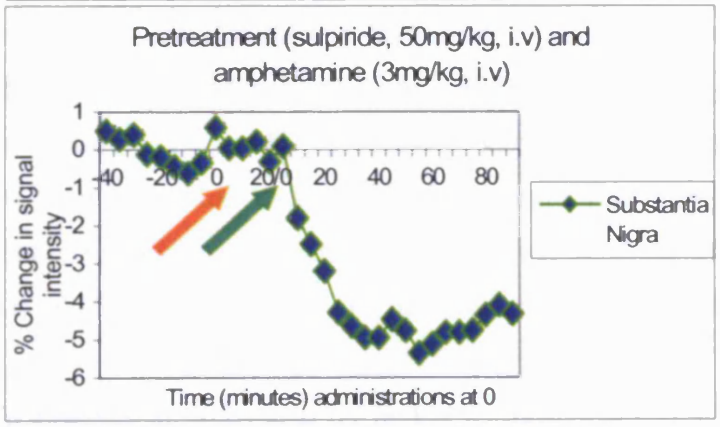

Bregma=-5.3mm

Substantia nigra

T=22.3, P<0.001

Fig 5.3.3d

Graphs showing timecourse of signal intensities at voxels of interest showing decreases in BOLD signal after administration of 3mg/kg amphetamine i.v.

Orange arrow indicates time of sulpiride administration, green arrow indicates time of amphetamine administration. Results are ± S.D of the mean.

Area	Right/ Left/ Centre	% Change	Time to Peak	T-Value	P-Value	Random Effect Significant?
Medial preoptic area	Right Left	-2.9 -1.4	40 55	18.77 7.6	P<0.001 P<0.001	No No
Substantia Nigra	Right Left	-5.4 -5.1	55 60	22.3 23.3	P<0.001 P<0.001	Yes Yes
Amygdala	Right Left	-3.7 -0.9	35 40	8.3 5.2	P<0.001 P<0.001	No No
Hypothalamic area	Right Left	-3.9 -3.0	55 60	16.2 10.94	P<0.001 P<0.001	Yes Yes

Table 5.3.3b Summary of Decreases in fMRI signal for Experiment 3

The corrected t-test shows that few areas are affected by amphetamine stimulation after pre-treatment with sulpiride resulting in decreases in signal intensity. The more stringent Gaussian random field model excludes some of these areas. Some examples of the time-courses are shown above (Graph 5.3.3d).

5.4 Discussion

5.4.1 Experiment 1: Amphetamine Administration (3mg/Kg, i.v)

The present study first applied fMRI techniques to examine the effects of amphetamine, a compound with well-characterised cerebral metabolic effects (Carlsson et al, 1975; Weschler et al, 1979; Drevets et al, 1999). Amphetamine has been widely employed for pharmacological studies in animals and glucose utilisation data is readily available in the literature (Weschler et al, 1979). By blocking and reversing the dopamine transporter, and inhibiting uptake of dopamine and noradrenaline, amphetamine exerts its primary action in the CNS by potentiating these transmitters at nerve terminals. These techniques were then applied to examine the effects of prior pre-treatment with D_1 and D_2 antagonists on amphetamine-stimulated fMRI signals.

In a demonstrative paper by Jenkin's group (Chen et al, 1997) amphetamine was used to elicit increases in BOLD response in the brain regions containing high dopamine receptor densities. One goal of the first experiment, i.e. amphetamine administration (3mg/kg i.v) was to replicate these findings and thus validate our system. Thus, we used the same dose (3mg/kg, i.v), similar timing (45 minutes baseline and 90 minutes post

amphetamine) and kept the anaesthetic regime (halothane) as similar to Chen et al's (1997) as our facilities and Home Office licensing requirements would allow in order to investigate amphetamine induced stimulation. In addition to actions on the dopamine system, amphetamine is also known to effect norepinephrine and 5HT receptors directly since these systems are not as localised as the dopaminergic system. It was of interest to us to observe the global changes. Therefore, the main difference in our protocol from that of Chen et al (1997) was the acquisition of 30 x 1mm thick slices instead of 3-5 x 1.5mm thick slices. By increasing the number of slices the temporal resolution is reduced making it lower than that of Chen et al (5 min per scan as compared to approximately 3 min per scan).

Using a simple t-test with derived p-values using (Bonferroni correction and significant threshold of $P<0.05$) resulted in conservative probability maps that would only therefore display prominent signal changes. In comparing the results obtained in Experiment 1 to those observed by Chen et al, (in approximately the same slices) we also observed signal increases in the striatum and cingulate cortex. However the changes in the frontal and parietal cortices we found to be largely in the opposite direction (decreases) to those of Chen et al (1997). These decreases in BOLD signal were also observed in the motor cortex, somatosensory cortex and deeper subcortical structures such as the substantia nigra, entorhinal cortex and hypothalamus.

The increases in BOLD signal are evident in many structures and although largely subcortical, the t-Maps seemed to extend up to the lower layers of the cortex and this is especially clear in the motor and somatosensory cortices. The images show the amphetamine response to be global, extending from the olfactory cortex through to the cerebellum. The anatomical pattern of amphetamine induced changes strongly correlate with dopamine receptors distribution and pathways (Dahlstrom & Fuxe, 1964). The olfactory cortex and nucleus accumbens have projections from the A10 cell group forming terminals for the mesolimbic pathways and also have A8 and A9 cell groups contributions from the mesocortical projections. The mesocortical pathway also has terminations at the septum and hippocampus, which showed, increased BOLD signal intensity. The caudate-putamen and globus pallidus also demonstrate increased BOLD signal intensity, these structures constitute a large proportion of the nigrostriatal system, which is responsive to amphetamine stimulation.

Acute intravenous administration of amphetamine decreased BOLD signal intensity in multiple brain regions. There were marked and significant decreases in the cortex including motor, somatosensory, parietal association and auditory cortices. Furthermore, the substantia nigra demonstrated a large and robust decrease in signal intensity as did other deep subcortical structures, such as the amygdala, hypothalamus and the amygalopiriform (transition area) and the 6th lobe of the cerebellum. The amygdala and piriform are both sites of termination of dopaminergic input (Lindvall et al, 1984). Such changes have not been documented in the literature and indeed are in contrast to previous observations where the parietal and frontal cortices show increased metabolic response to amphetamine as measured using fMRI (Chen et al, 1997), although the volume averaging used in processing the data resulted in contamination from the adjacent striatum of 10-15% which may have influenced this increase. However increases in frontal cortex activity after amphetamine administration have also been measured using PET (Vollenweider et al, 1998), glucose utilisation (Weschler et al, 1979) and dopamine release using *in vivo* microdialysis, although measurement in this region is not as reliable as in the striatum (Saunders et al, 1994; Moghaddam et al, 1993).

The temporal responses were obtained on a voxel-wise basis, using the rat atlas (Paxinos & Watson, 1998) as a guide. This atlas is overlaid onto the anatomical template such that the areas displaying changes can be clearly identified (Row 1, Figs 5.3.1a & b). The temporal responses show a general trend of increasing or deceasing 1-2 scans after administration with a maximal response at 40-45mins later and thus are quite similar to those using microdialysis (Kuczenski & Segal, 1989; Arbuthnott et al, 1990). Physiological data from Chen et al (1997)-(Fig 2) indicate that the signal change is not reflective of hypercapnia or blood pressure as it peaks after drug administration and drops immediately afterwards. This indicates that the effect is most probably due to a metabolic response to the transmitters binding.

The identification of differential responses of projections to inner and outer cortical layers may suggest a new dimension of complexity to understanding the response of the CNS to activation by amphetamine. Elucidation of the mechanisms by which activation of a subset of the cortex is negatively activated will require further studies.

In summary, region-specific changes in subcortical and cortical structures caused by amphetamine administration have been detected, and these are most notably evident in regions with significant dopaminergic innervation. These changes are mediated by D_1 and D_2 receptors, thus it is of interest to the investigate the contributions of each of these receptor types to this response, i.e. the extent to which the response can be suppressed by D_1 and D_2 receptor antagonists.

5.4.2 Experiment 2: Pretreatment with SCH23390 (0.5mg/Kg, i.v) and Amphetamine Administration (3mg/Kg, i.v)

Following pre-treatment with SCH23390, the administration of 3mg/kg amphetamine caused a reduced BOLD response as compared to when amphetamine was administered alone, indicating that the antagonist may have blocked some D_1 receptors on which the amphetamine was acting, but the response was not completely removed. The spatial extent of the BOLD pattern was however reduced and even eliminated in some areas such as olfactory areas, orbital cortex, M1 motor cortex, nucleus accumbens septum, somatosensory cortex, globus pallidus, thalamus, retrosplenal cortex, subiculum, PAG and pontine nuclei. One additional area showing increased signal intensity as compared to amphetamine alone, was the lateral habenula, to which the A10 cell group has projections. The emergence of the lateral habenula as an additional area showing BOLD increases in this cohort may simply be due to the more discrete activations allowing identification of smaller structures, which may have been obscured in Experiment 1 by activation from surrounding structures.

The same pattern was not observed when the reductions in BOLD signal intensity were investigated. Although a number of areas previously demonstrating a decrease in fMRI signal on amphetamine administration showed no change (M1, barrel field somatosensory cortex, parietal association cortex, lateral leminiscus, inferior colliculus, simple cortex and cerebellum) generally, the response profile in the form of the t-Map was very similar to that of amphetamine alone.

5.4.3 Experiment 3: Pretreatment with Sulpiride (50mg/Kg, i.v) and Amphetamine Administration (3mg/Kg, i.v)

In investigating the effect of supiride pre-treatment on increases in BOLD signal intensity after amphetamine administration, it was found that the BOLD signal was very similar, although in some of the more caudal brain slices, the changes were in fact greater in spatial magnitude, extending beyond the lower layers of cortex. Furthermore this difference was obvious in the images of the decreases in BOLD where there is very little cortical activation as compared to amphetamine alone. Although a number of areas previously demonstrating a decrease in fMRI signal on amphetamine administration showed changes (hypothalamic area, substantia nigra and amygdala and amygdalopiriform transition area) some areas which showed decreases in signal intensity were actually found to be outside the brain and most probably the result of signals from blood vessels in the scalp and loose masking (Fig 5.3.3c).

The data indicate that D_1 receptors are likely to be involved in postsynaptic facilitatory and excitatory activity. This is suggested on the basis of D_1 specific receptor antagonist having a more marked and obvious effect on the increase BOLD signal caused by amphetamine administration (as opposed to its smaller effect on the decrease component). SCH23390 is a potent inhibitor of dopamine mediated behaviours (Wolterink et al, 1993; Phillips et al, 1994) and can occupy D_1 receptors for up to 12 hours. Vanderschuren and co-workers (1999) found SCH23390 to completely reverse electrically stimulated accumbal noradrenaline release and also reverse amphetamine-mediated anorexia (Gilbert & Cooper, 1985). These findings support the idea that D_1-type receptors may be involved in amphetamine-mediated behaviours and neurochemical changes, and moreover that these can be inhibited using D_1 selective antagonists. The D_2 receptors antagonist sulpiride conversely may have primed the response to amphetamine administration by removing presynaptic inhibitory mechanisms. Such effects have been found using various different techniques. For example, Jaworski et al (2001) observed sulpiride potentiation of amphetamine stimulated striatal dopamine release and likewise, Vanderschuren et al (1999) found that sulpiride administration augmented electrically stimulated accumbal dopamine release.

5.4.4 Conclusion

The line of evidence from the current study argues that the fMRI changes described here may be the direct consequences of amphetamine induced regional increases (and decreases) in brain activity and not due to the simple systemic, global effects of amphetamine on cerebral vasculature. The relevance of the dopaminergic mechanisms is strongly confirmed by D_1 dopamine receptor antagonist mediated and D_2 receptor antagonist-mediated facilitation suppression of BOLD. These experiments reinforce the importance of ascending dopamine input to cortical and subcortical structures as critical determinants of amphetamine induced brain activation at behaviourally effective doses and the importance of signal transduction at the level of the D_1 and D_2 receptors.

Previous neuroimaging studies using the dopaminergic antagonist SCH23390 and other dopaminergic agents have not reported such results. Trugman & James (1993) found using 2-deoxoglucose autoradiography, that pretreatment with SCH23390 (0.5mg/kg, i.v) and D2 antagonist (eticlopride 2mg/kg, i.v) completely blocked the amphetamine response (5mg/kg, i.v), similarly Marota et al (1999) using SCH23390 (0.5mg/kg, i.v) blocked the cocaine stimulated fMRI response. While the antagonists clearly act to block the amphetamine response in some areas, understanding the pharmacological dynamics where there is such a response is a more difficult task. It is not possible to separate amphetamine mediated behaviours into positive and negative behaviours based on receptor types, which may be "activated", thus the effects of these antagonists are investigated separately. In the same manner in which amphetamine administration has been investigated, the effects of specific D_1 and D_2 ligands are examined in Chapters 6 and 7 respectively.

The data shown in section 5.3 indicate coupling between dopamine release and metabolic response, suggesting the metabolic response is at least in part due to dopamine release. The spatial specificity and temporal response of the detected fMRI signals correspond with brain areas with high dopamine innervation and dopamine release indicating that the effect is primarily dopaminergic.

One major difference between our experimental conditions and the previously reported studies using dopamine antagonists to block amphetamine-induced glucose utilisation

(Trugman & James, 1993) and behaviour (Wolterink et al, 1993) is the usage of general anaesthetics. Technical restrictions and United Kingdom Home Office licensing requirements necessitate the use of general anaesthesia in rodent studies. Since halothane anaesthesia has been shown to preserve cerebral blood flow metabolism and responsiveness to stimulation (Ueki et al, 1992; Hansen et al 1989), it was the anaesthetic of choice. Furthermore, studies in our own laboratory showed that halothane had the least effect on stimulated dopamine release as measured using microdialysis as compared to urethane and α-chloralose (Chapter 3).

The metabolic response resulting from stimulation of the dopaminergic system as described, is limited to the areas of the brain containing large dopaminergic innervation. The fMRI signal is a metabolic response to neurotransmitter binding as opposed to binding itself, as one would obtain with PET. The large dose of amphetamine given (3mg/kg, i.v) could lead to non-specific effects, however Silva et al (1995) used an almost lethal dose (20mg/kg, i.p.) and still observed regional CBF changes. Thus it can be assumed that the smaller although intravenous 3mg/kg dose of amphetamine required elicit a robust fMRI signal is having regionally specific effects.

In conclusion, the nature of amphetamine-induced signal is not simply due to presynaptic uptake or postsynaptic stimulation of D_1-type and D_2-type receptors, it is due to a combination of both. Therefore in the following experiments, the D_1-type and the D_2-type receptors are investigated using specific agonists and antagonists, with the intent of studying receptor localisation and response direction. It is hoped that this may explain why the D_1-type and D_2-type receptor blockade have such a different effect on amphetamine stimulation.

Chapter 6

fMRI of a Dopamine D_1 receptor antagonist and agonist

6.1 Introduction

It has been difficult to define a physiological role for the dopamine D_1-type receptor due to its complex pre synaptic (heteroreceptor) and postsynaptic localisation in brain areas like the striatum (Cameron & Williams 1993), however it seems to mediate important actions of dopamine to control movement and cognitive and cardiovascular functions (Gambarana et al, 1995; Williams & Goldman-Rakic, 1995). In discovering that the D_1-type receptor may play a role in an increased fMRI response to acute amphetamine stimulation (section 5.3.2), this inevitably leads to the question of why this specialisation should occur, i.e. what are the functional differences between the dopamine receptor types and what is the D_1-type receptor involvement in the amphetamine response?

With regards to amphetamine or any other dopaminergic psychotropic drug action, it is not possible to completely separate their effects into D_1-type receptor mediated or D_2-type receptor mediated, as the receptors are functionally linked (Goldstein et al, 1987): this is discussed in more detail in Chapter 8. However the results in Chapter 5, suggest a degree of receptor specialisation, which forms the basis for the studies described in this chapter. Many studies investigating D_1-type receptor participation in amphetamine and cocaine-mediated effects (behaviourally, histochemically and neurochemically) are not concerned with acute effects but usually involve examination of sensitised responses to chronic administration of amphetamine or cocaine. It is known that with repeated amphetamine administration, new behaviours and neurochemical profiles emerge, even following only one pre-treatment (Warburton et al, 1996). Bearing this in mind, some background work into dopamine D_1-type receptor function is described.

6.1.1 Characterisation of the dopamine D_1-type receptor

Three laboratories independently discovered the gene for the D_1-type receptor in the same year (Dearry et al, 1990; Sunaharra et al, 1990; Zhou et al, 1990); it encodes 446 amino acids and has seven membrane-spanning domains.

D1 Agonists	D1 Antagonists
SKF 38393	SCH 23390
SKF 81297	SKF 83566
Fenoldopam	NNC-112
Dihydrexidine	SCH 39166

Table 6.1.1 Commonly used D_1-type agonists and antagonists (Feldman et al, 1997)

As recently as 1982 there was said to be no known function for the D_1-type receptor (Laduron, 1982), however the availability of D_1 specific antagonists SCH23390 (Iorio et al, 1983; Christensen et al, 1984) and agonist SKF38393 (Molloy & Waddington, 1984; O'Boyle & Waddington, 1984) has made it possible to carry out functional studies to determine the role of the D_1-type receptor in the CNS. Table 1 shows some of the commonly used D_1-type agonists and antagonists. For example, the inability of SCH23390 to cause hyperprolactinemia, (considered to be a D_2-receptor effect, Iorio et al, 1983), and the ability to block dopamine-stimulated adenylate cyclase is consistent with specific D_1-receptor antagonism.

6.1.2 Dopamine D_1-type Receptor Distribution and Pathways

D_1-type receptors are the most ubiquitous of dopamine receptor and are differentially distributed throughout the brain. The D_1 mRNA is present in cells in dopaminoceptive regions in the rat brain (Meador-Woodruff et al, 1991). High levels are present in the neostriatum, substantia nigra, nucleus accumbens and olfactory tubercle; intermediate levels are found in the ventral pallidum (entopeduncular nucleus) and some amygdaloid nuclei (Boyson & et al, 1986; Wamsley et al, 1992); lower levels are found in the septum, hypothalamus and cortex (Mansour et al, 1990; Meador-Woodruff et al, 1992). As described in chapter 1, the D_1-type receptors consist of D_1 and D_5 subtypes, and the available D_1 receptor ligands cannot distinguish between them. Thus, the distribution patterns of D_1 receptors include both subtypes. The tissue distribution of the D_1-type receptor supports their participation in the different areas of dopaminergic neurotransmission that have been described on the basis of ligand binding and receptor autoradiography experiments.

In studying cortical output, the conceptual framework of the anatomical and functional organization of the basal ganglia has been developed (Gerfen, 1992): these are known as the "direct" and "indirect" pathways. The direct pathway includes projections to the substantia nigra pars reticulata and ventral pallidum and expresses substance P and dynorphin, in addition to dopamine D_1-type receptors. The indirect pathway projects to the globus pallidus and expresses enkephalin and dopamine D_2-type receptors. Activation of the direct pathway leads to disinhibition of thalamic neurons, superior colliulus and the brainstem and is associated with movement, whereas activation of the indirect pathways leads to greater inhibition of these neurons and is associated with attenuation of movement. This segregation is not maintained at other levels of the basal ganglia (Yung et al, 1996). These pathways are involved in motor output and play a role in disorders of the motor system such as Parkinson`s disease and Huntington's disease (Albin et al, 1989). Further information on the direct-indirect pathways, can be found reviewed by Gerfen (1992).

The peptide dynorphin is co-expressed with the dopamine D_1-type receptor in the nucleus accumbens (Curran & Watson, 1995), hippocampus, hypothalamus and basal ganglia (Steiner & Gerfen, 1998). Striatal dynorphin containing neurons receive dopaminergic inputs from the substantia nigra pars compacta and entopeduncular nucleus and are involved in regulating the responsiveness of striatal cells to dopaminergic input (Altar & Hauser, 1987; Steiner & Gerfen, 1995). Steiner & Gerfen (1998) proposed that dynorphin dampens excessive activation of striatal output neurons by dopamine or other transmitters.

6.1.3 Functional Implications of D_1-type Receptor Activity

The dopamine D_1-type receptor does not have a very clearly defined role. Some workers believe they may simply have a subtle function in modulating D_2-type receptors. Under moderate tone, nucleus accumbens noradrenaline release is regulated mainly by D_2-type receptors but under circumstances of increased dopamine release, recruitment of extrasynaptic stimulatory D_1-type receptors may contribute to enhancement of noradrenaline release (Vanderschuren et al, 1999). Others have suggested even more adaptive roles for the D_1-type receptor: Muly et al (1998) proposed that stimulation of

D_1-type receptors in the medial prefrontal cortex actually has a biphasic response: at sub-optimal stimulation they facilitate transmitter release but when optimally stimulated they inhibit dopamine release.

In vivo microdialysis has revealed complex roles for the dopamine D_1-type receptor including, regulation of cortical acetylcholine release, regulation of GABA and glutamate release in the ventral tegmental area (VTA). These functions have been demonstrated using specific D_1-type agonists and antagonists: the dopamine D_1 antagonist SCH23390 has been found to block both amphetamine stimulated (Day & Fibiger, 1994) and basal (Day & Fibiger, 1992) cortical acetylcholine release; dopamine D_1 receptor agonist A-77363 was found to increase acetylcholine release (Acquas et al, 1994); in the VTA and medial prefrontal cortex, D_1 agonist SKF38393 caused a dose dependant increase in glutamate and GABA, while pre-treatment with SCH23390 prevents cocaine-induced increases in glutamate release (Kalivas & Duffy, 1995; Abekawa et al, 2000).

Several investigators reported that D_1-type receptors are important for altering behavioural output, including locomotor activity (Vezina et al, 1991), cocaine self-administration (McGregor & Roberts, 1995) working memory function (Sawaguchi & Goldman-Rakic, 1991) cognition (Besheer et al, 1999) emotion (Guarraci et al, 1999) and endocrine function (Colthorpe et al, 1998). Thus the following sections describe some of the findings regarding dopamine D_1-type receptors role in various aspects of brain function.

6.1.4 D_1-type Receptor Mediated Behaviour

The selective D_1-type dopamine receptor agonist SKF38393 stereospecifically promoted episodes of prominent grooming behaviour (Molloy & Waddington, 1984; Berridge & Aldridge, 2000), and furthermore this behaviour was blocked by administration of the selective D_1 antagonist SCH 23390 (but not by D_2 antagonist metoclopramide). Another finding supporting dopamine D_1-type receptor mediated effects is that cataleptic behaviour in mice induced by administration of D_1 antagonist SCH23390, is sensitised

by repeated testing procedures as opposed to a single treatment (Chinen & Frusso-Filho, 1999).

Dopamine D_1-type receptors have been shown to be involved in the development of sensitised locomotor behaviour in response to repeated administration of amphetamine (Vezina, 1996) and cocaine (De Vries et al, 1998), and also contribute to the development of facilitated amphetamine self-administration produced by prior exposure. This response can be prevented by systemic administration of SCH23390 (Pierre et al, 1998). Similarly, pretreatment with D_1-type agonists SKF38393 and F82958 markedly enhanced the sensitising effects of both intra-accumbal and systemic cocaine (De Vries et al, 1998) and the D_1-type antagonist SCH23390 also blocks these responses. Such data suggest an important and common role in locomotor sensitisation for dopamine D_1-type receptor and imply that the nucleus accumbens may, in fact be an anatomical locus for the initiation of behavioural sensitisation. However, SCH23390 mediated attenuation of cocaine sensitisation of the locomotor response is not seen when it is administered intra-accumbally, indicating that stimulation of receptors in regions other than the accumbens is required for this behaviour (Neiswander et al, 1998). Dopamine D_1-type receptor knockout mice have deficiencies in initiating movement and fail to display increased locomotor activation following amphetamine and cocaine administration (Drago et al, 1998). While investigating amphetamine-induced anorexia, Gilbert and Cooper (1985) implicate dopamine D_1-type receptors in the control of feeding responses. SCH23390 blocked small-dose amphetamine induced anorexia and SKF38393 produced a dose-dependent reduction in food consumption.

The prefrontal cortex is involved in the cognitive process of working memory. Previous studies have revealed a role for dopamine acting on D_1-type receptors in the modulation of a prefrontal neuron's excitatory response to its preferred stimulus (Williams & Golman-Rakic, 1995). Local injections of selective D_1-type dopamine receptor antagonists into the prefrontal cortex of rhesus monkeys caused a dose-dependent deficit in performing an oculomotor task (Sawaguchi & Goldman-Rakic, 1991). Furthermore, D_1-type receptor knockout mice that show deficits in spatial learning and in responding to novel stimuli (El-Ghundi et al, 1999) and SCH23390 blocking place preference of novel object (Besheer et al, 1999).

6.1.5 Dopamine D_1-type Receptor role in Human Brain Disease

The most widely accepted hypothesis concerning the pathophysiology of schizophrenia is the dopamine hypothesis, which suggests that schizophrenia symptomology is mediated by dopamine system hyperactivity, primarily at D_2-type receptors (Farde et al, 1986). D_1-type dopamine receptors may also play a major role in this pathophysiology: a PET study showed increased variability and reduced D_1-type receptor binding in the basal ganglia and frontal cortex of drug naïve schizophrenic patients (Okubo et al, 1997). SCH 23390 resembles antipsychotics in some of its pharmacological profile; for example, its antistereotypic effects in mice, rats and dogs, its cataleptogenic effect and inhibitory effect on amphetamine circling (Christensen et al, 1984).

Rascol et al (1999) have indicated that a D_1-type agonist has antiparkinsonian efficacy without the propensity for inducing dyskenesia. ABT-431, a full selective D_1 receptor agonist showed efficacy superior to placebo and was of similar magnitude to L-Dopa and dyskinesia was as reduced in some patients on this drug. Dihydrexidine, a high affinity full D_1 agonist, was effective in L-Dopa-non-responsive primates (Watts et al, 1993). Furthermore, Blanchet et al (1998) found that dihydrexidine had a marginal therapeutic window for providing an antiparkinsonian effect. Using PET with [^{11}C]SCH23390, it was found that dopamine D_1-type receptor density declines with age and the physiological effects of aging may play a role in the expression of extrapyramidal disorders in the elderly (Wang et al, 1998). Autoradiographic (Trugman, 1995) and PET (Black et al, 1999) data indicate that D_1-type receptor stimulation importantly contributes to the effects of L-Dopa on basal ganglia circuits. Thus selective D_1 agonists may have independent antiparkinsonian activity. However Chase et al (1995) studied various dopamine agonists to examine if different dopamine receptor subtypes affect the antiparkinsonian or dyskenesia effects, as compared to L-Dopa and found that D_1 type receptor activity had little effect on either antiparkinsonian activity or the potential for dyskinesias. Although inconclusive, the hypothesis that D_1-type receptors may play role in Parkinson's disease and therefore may be useful therapeutic targets is an area worth pursuing.

6.1.6 Dopamine D_1-type Receptors in Drug Abuse

Adaptive upregulation of nucleus accumbens dopamine D_1-type receptors may underlie part of the dependency of drug-abuse. Increased D_1-type receptors (and decreased D_2-type receptors) were found in the nucleus accumbens of chronic methamphetamine treated rats (Worsley et al, 2000). Previous animal work suggested that particular aspects of methamphetamine (and possible other abused substances) use might be related to dopamine D_1-type receptor function in the limbic system. Behavioural studies carried out by Ciccocioppo et al (2001) suggest the D_1-type receptor as a substrate for motivating effects of cocaine-related stimuli. These results implicate D_1-type dependent neural mechanisms within the medial prefrontal cortex and basolateral amygdala as substrates for cocaine-seeking behaviour. Administration of D_1-type antagonist caused a dose-dependant increase in cocaine intake (McGregor and Roberts 1995; Hurd et al, 1997), suggesting that events downstream to D_1-type receptor activation may alter the firing of mPFC output neurons after a single dose.

Acute exposure to drugs (including cocaine) elicits increases in both locomotor activity and dopaminergic transmission in the nucleus accumbens (Kalivas & Duffy, 1990). Following repeated drug exposure, the behavioural and neurochemical responses augment (Parsons & Justice, 1993), a phenomenon referred to as sensitisation. D_1-type receptors are hypothesised to play a role in mediating some aspects of sensitisation behaviours. Evidence of involvement of D_1-type receptors in drug-taking behaviours came from the prevention of cocaine-mediated locomotor sensitisation by administration of D_1-type agonist SKF 81297 into the mPFC. This inhibition can be blocked by the D_1-type antagonist SCH23390 (Sorg et al, 2001). EEG studies suggest that moderate, but probably rewarding, doses of cocaine or amphetamine mainly activate D_1-type dopamine receptors (Ferger et al, 1994). This activation might be relevant for the rewarding properties of these drugs. Using *in vivo* microdialysis in the nucleus accumbens of rats, it was found that mPFC administration of SCH23390 increased accumbal dopamine levels 24 h after treatment, but not immediately (Olsen & Duvauchelle 2001).

It has been demonstrated that dynorphin plays a role in modulating responses to several psychoactive substances including cocaine (Chen et al, 2002), amphetamine (Gonzalez-

Nicolini & McGinty, 2002) and marijuana (Zimmer et al, 2001). Furthermore, cocaine-mediated changes in immediate early gene expression (*c fos* and *zif 268*) can be modulated by both kappa (κ) receptor ligands (see section 3.1.1) and D_1 dopaminergic agents (Steiner & Gerfen, 1996). Such data indicate a potentially important role for D_1-type receptors in the acute mood-altering and rewarding effects of cocaine in humans, and has given rise to the idea of D_1-type receptor antagonism as a therapy for drug addiction (Spealman et al, 1999; Self et al, 2000).

In Chapter 5, it was found that using fMRI, changes in activation in the rat brain could be visualised after systemic administration of amphetamine. Furthermore, these observed changes were similar to those indicated by the autoradiographic studies (Weschler et al, 1979). These responses, which were presumably mediated by both D_1-type and D_2-type receptors, were then investigated with respect to their individual contributions using specific antagonists. Having found a clear reduction in the amphetamine-evoked increases in BOLD signal after pre-treatment with D_1 antagonist SCH23390 (see chapter 5), it is therefore of interest to investigate the function of the D_1-type receptor. Thus the effects of acute drug challenges using either D_1 antagonist SCH23390 or D_1 agonist SKF38393 on BOLD response were determined.

6.2 Methods

D_1 antagonist SCH23390 or D_1 agonist SKF38393 were administered intravenously to rats whilst immobilised in a 2.35 Tesla imaging system. In order to study the global spatial response profile, the whole brain was scanned (30 x 1mm). A summary of the methods for these experiments is described in this section, for details of these procedures refer to Chapter 4 as shown in parenthesis.

6.2.1 Animal Preparation

Male Sprague-Dawley rats (250-300g, n=8) were used for each of two experiments. They were anaesthetised and cannulated for administration of drugs as described in sections 4.2.1 and 4.3 respectively. The physiological state of the animal was constantly

monitored using respiration rate and body temperature, as described in section 4.5. When instrumented, each animal was placed into a custom-made, heated probe, which maintained the core body temperature at 37°-38°C (section 4.4). The MRI modified surface coil (section 4.6.2) was secured to the dorsal surface to the head before positioning the animal in the magnet centre of the scanner (section 4.6.1). The imaging experiments were all performed at field strength of 2.35 Tesla with a horizontal bore superconducting magnet (4.6.1).

6.2.2 Experimental Protocol

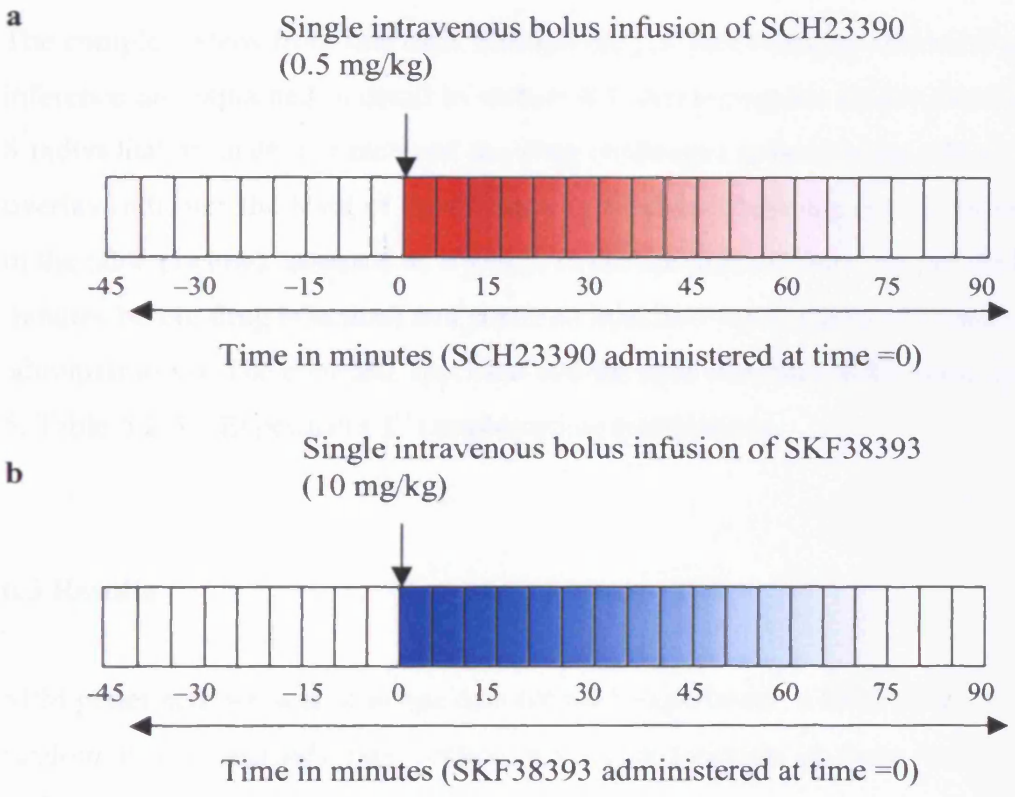

Fig 6.2.2 Schemata of time-course of experiments 1, & 2

Each block represents 1 scan with duration of 4 minutes 40 seconds; the arrow represents the time of drug administration. In experiment 1 (a), a single bolus injection of SCH23390 is administered after 45 minutes baseline. In experiment 2 (b), a single bolus injection of SKF38393 is administered after 45 minutes baseline.

For each experiment, 45 minutes of baseline (no drug administration) scans were acquired before either SCHH23390 (50mg/kg, i.v) or SKF38393 (10mg/kg, i.v) was administered as a single intravenous bolus infusion via the jugular vein (Fig 6.2.2a). The volumes injected (2ml/kg and 1ml/kg, respectively) took into account the saline-heparin filled dead space of 0.05ml. Data were collected for a further 90 minutes after drug administration. SCH23390 and SKF38393 were dissolved in saline or propylene glycol mixture, respectively (section 4.2.2) and made up on the day of the experiment.

6.2.3 Statistical Processing and Analysis

The complete steps from raw data, through the pre-processing to statistical analysis and inference are explained in detail in section 4.5. Averaging the results obtained from the 8 individual animals that received the drug challenges generates the t-Map. The colour overlay indicates the level of significance in t-values (these are converted into p-values in the tables below), assessed as a group, in the comparison between pre (baseline of 45 minutes before drug injection) and postdrug injection signal (up to 90 minutes after drug administration). The contrasts specified and the data summary is the same as in Chapter 5, Table 5.2.3: "Experiment 1" (amphetamine stimulation).

6.3 Results

SPM generated two sets of image data for each experiment, a fixed effect analysis and a random effects analysis (see section 4.8 for description of these two analyses). In addition to these images, graphs of timecourses from selected voxels in regions of interest were also obtained. Samples of these are displayed in the following sections and the complete results are summarised (Tables 6.3.1a & b, 6.3.2a & b).

6.3.1 Results of Experiment 1: SCH23390 Administration (0.5mg/Kg, i.v)

Images were collected from 30 contiguous, coronal, 1mm brain slices. The Bonferroni corrected data showed that acute intravenous infusion of SCH23390 (0.5mg/Kg) caused both increases and decreases in BOLD contrast in multiple brain areas ($P<0.01$).

Increases in BOLD signal intensity

After administration of SCH23390 activation of subcortical structures was striking: as with amphetamine there were marked increases in signal intensity in olfactory areas, cingulate cortex, dorsal and ventral striatum, septum, globus pallidus, thalamus, hippocampus, superior colliculus, inferior colliculus, PAG (periaqueductal grey matter), pontine reticular nucleus, and some isolated parts of the cerebellar lobes. More discrete, yet significant ($p<0.001$), increases were also observed in parts of the M1 motor cortex and S1J somatosensory cortex. Six brain slices are shown in Fig 6.1.3a to indicate the effect of SCH23390 throughout the brain. It is obvious that this activation tends to be the deeper parts of these brain areas although in Fig 6.3.1a, images B-C it also extends to outer layers of the cortex.

Random effects analysis showed less activation than with the fixed effect analysis. Table 6.3.1a shows which areas were also significant in the random effects analysis, including the olfactory nucleus, M1 motor cortex, cingulated cortex, nucleus accumbens, septum, caudate-putamen, thalamus, retrosplenal cortex and PAG.

Graphs of the time-course are shown in Fig 6.3.1b, these represent signal intensity at specific voxels as indicated by SPM t-Maps (Fig 6.3.1a). Areas are named as corresponding to particular structures in accordance with the rat atlas (Paxinos & Watson, 1998). A summary of all areas showing increases in signal intensity is displayed in table 6.3.1a.

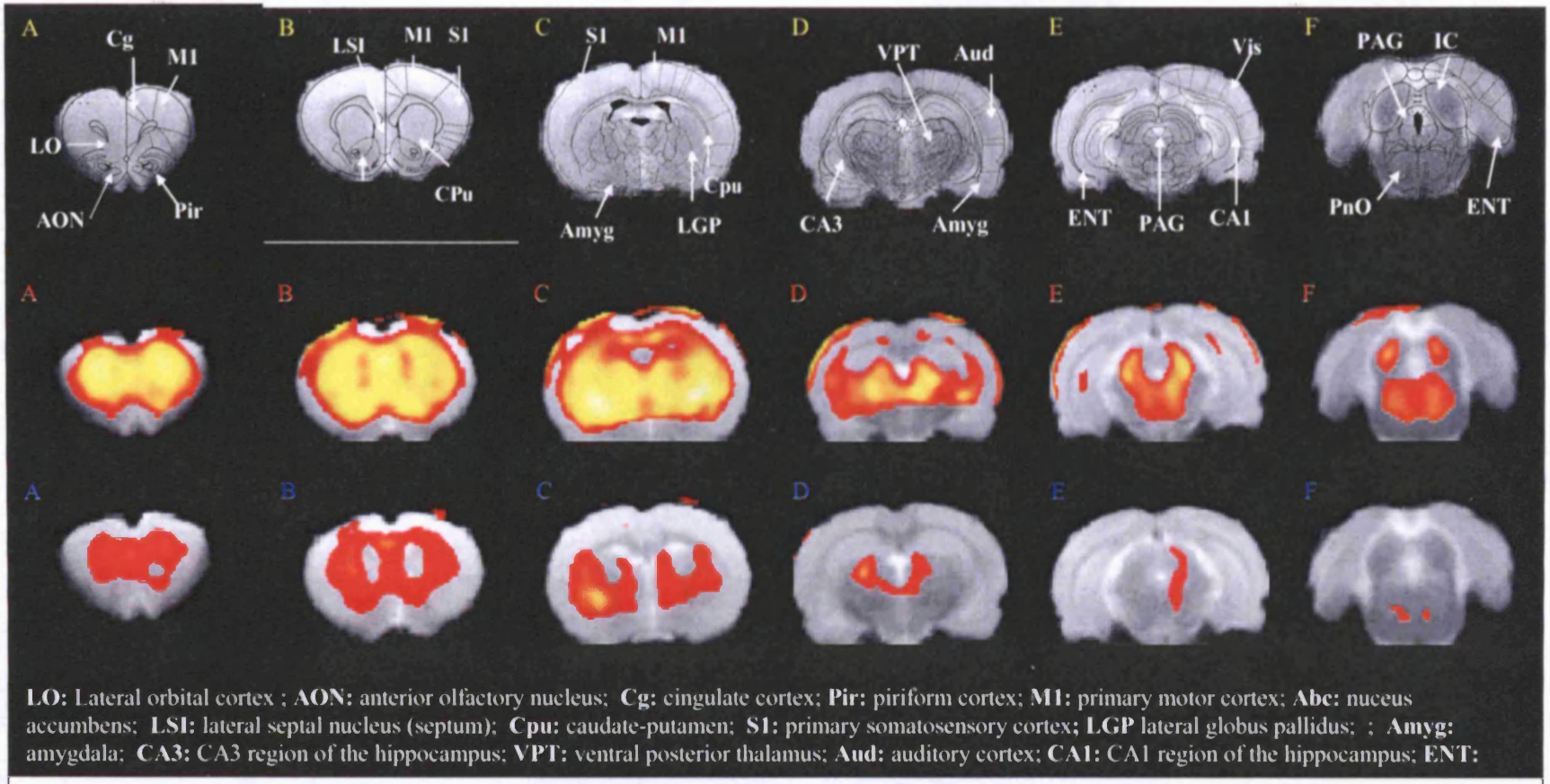

LO: Lateral orbital cortex ; **AON:** anterior olfactory nucleus; **Cg:** cingulate cortex; **Pir:** piriform cortex; **M1:** primary motor cortex; **Abc:** nuceus accumbens; **LSI:** lateral septal nucleus (septum); **Cpu:** caudate-putamen; **S1:** primary somatosensory cortex; **LGP** lateral globus pallidus; ; **Amyg:** amygdala; **CA3:** CA3 region of the hippocampus; **VPT:** ventral posterior thalamus; **Aud:** auditory cortex; **CA1:** CA1 region of the hippocampus; **ENT:**

Fig 6.3.1a: Increases in signal intensity following administration of SCH23390 (0.5 mg/kg, i.v)

The first row shows annotated and labelled high resolution template images such that the areas displaying changes may be identified according to the rat atlas (Paxinos & Watson, 1998). The middle row shows the effects of amphetamine using fixed effects analysis, the bottom row using random effects analysis.

A: Bregma= +3.7mm Orbital cortex, cingulate and olfactory tubercle. B: Bregma= +1.7mm Caudate-putamen, nucleus accumbens, M1and cingulate.

C: Bregma = -1.3mm Caudate-putamen, globus pallidus, M1and cingulate. D: Bregma= -4.3mm CA3, parafascicular and ventromedial thalamus.

E: Bregma = -6.3mm Superior colliculus, PAG and VTA. F: Bregma= -8.3mm Inferior colliculus pontine reticular nucleus.

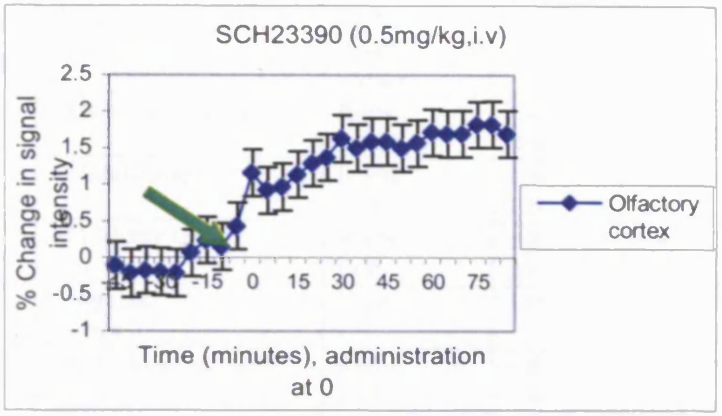

Bregma= +4.7mm

Olfactory cortex, T=14.33 P<0.001

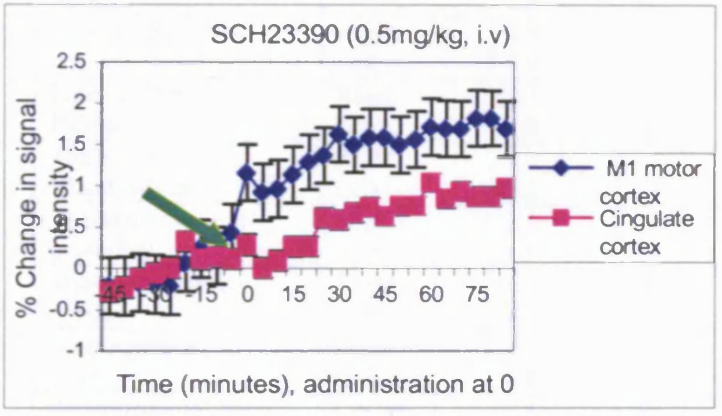

Bregma= +1.7mm

M1 motor cortex T= 17.4, P<0.001, cingulate cortex T= 11.5, P<0.001

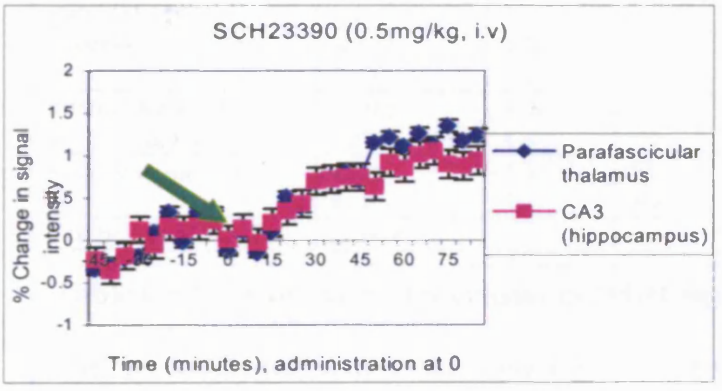

Bregma=-4.3mm

Parafasciclar nucleus T= 12.8 P<0.001, CA3 T= 8.7 P<0.001

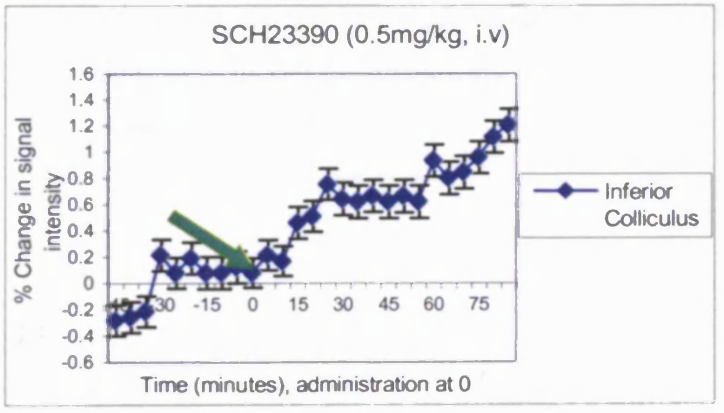

Bregma=-8.3mm

Inferior colliculus T=8.2 P<0.001

Fig 6.3.1b

Graphs showing BOLD signal intensities at voxels of interest, after administration of SCH23390 0.5mg/kg i.v.

Green arrow indicates administration of SCH23390. Results are ± S.D of the mean.

Area	Left/ Right/ Centre	% Change	Time to peak	T-Value	P-Value	Random Effect
Olfactory cortex	Right Left	1.4 0.8	70 75	14.3 14.1	P<0.001 P<0.001	Yes
Orbital cortex	Right Left	1.8 1.6	75 70	16.8 16.1	P<0.001 P<0.001	Yes
M1 Motor Cortex	Right Left	1.8 2.4	70 60	17.4 17.1	P<0.001 P<0.001	No
Cingulate Cortex	Centre	1.0	60	11.5	P<0.001	Yes
Nucleus Accumbens	Right Left	1.8 1.7	70 60	12.5 11.6	P<0.001 P<0.001	Yes
Septum		1.9	50	13.5	P<0.001	Yes
Caudate-Putamen	Right Left	1.9 1.8	65 65	15.9 15.8	P<0.001 P<0.001	Yes
Lateral Globus Pallidus	Right Left	2.5 1.8	80 70	19.9 19.9	P<0.001 P<0.001	Yes
Thalamus (Parafascicular)	Right Left	1.7 2.2	75 55	12.8 10.2	P<0.001 P<0.001	Yes
Thalamus (ventral-posterior)	Right Left	2.5 1.9	70 70	19.2 21.3	P<0.001 P<0.001	No
Thalamus (medio-dorsal)	Right Left	1.7 1.4	80 80	13.6 11.3	P<0.001 P<0.001	No
Hippocampus CA3	Right Left	1.0 0.8	65 70	8.7 8.1	P<0.001 P<0.001	No
Periaqueductal grey matter (Lateral)	Centre	1.2 1	65	8.6	P<0.001	No
Superior colliculus	Right Left	1.5 1.5	65 75	13.9 11.3	P<0.001 P<0.001	No
Pontine Reticular nucleus (oral part)	Right Left	1.4 1.4	70 60	9.9 8.1	P<0.001 P<0.001	Yes
Inferior colliculus	Right Left	1.2 1.1	85 80	8.2 10.5	P<0.001 P<0.001	No
Cerebellum (Crus 2)	Centre			8.0	P<0.001	No

Table 6.3.1a Summary of increases in fMRI signal for Experiment 1

The corrected t-test shows that many areas are affected by SCH23390 stimulation resulting in increases in BOLD signal intensity. The more stringent Gaussian random field model excludes some of the areas. Some examples of the timecourses are shown in Fig 6.3.1.b.

Decreases in BOLD signal intensity

In addition to increases in BOLD signal intensity, after SCH23390 administration statistically significant decreases in BOLD signal intensity were also detected. The decreases in signal intensity observed tended to be more caudally located, in the piriform cortex, medial preoptic area, hypothalamus, dorsal hippocampal commisure and was also evident in deep structures such as the amygdala, substantia niga and amygdalopiriform transition area, and as rostrally as the 6th lobe of the cerebellum and simple cortex.

Six brain slices are shown below (Fig 6.3.1c) to indicate the effect of the D_1 antagonist SCH23390 throughout the brain. These areas are shown below in the t-Maps. Random effects analysis, a more stringent test showed much less obvious decreases than the fixed effect analysis. Table 6.3.1b shows that many of these areas were not significant in the random effects analysis.

Graphs of the timecourse are shown in Fig 6.3.1d, these represent decreases in BOLD signal intensity at specific voxels as indicated by the SPM t-Maps (Fig 6.3.1c). Areas are named as corresponding to particular structures in accordance with the rat atlas (Paxinos & Watson, 1998). Areas of interest have been selected throughout the brain. A summary of all areas showing increases in signal intensity is displayed in table 6.3.1b.

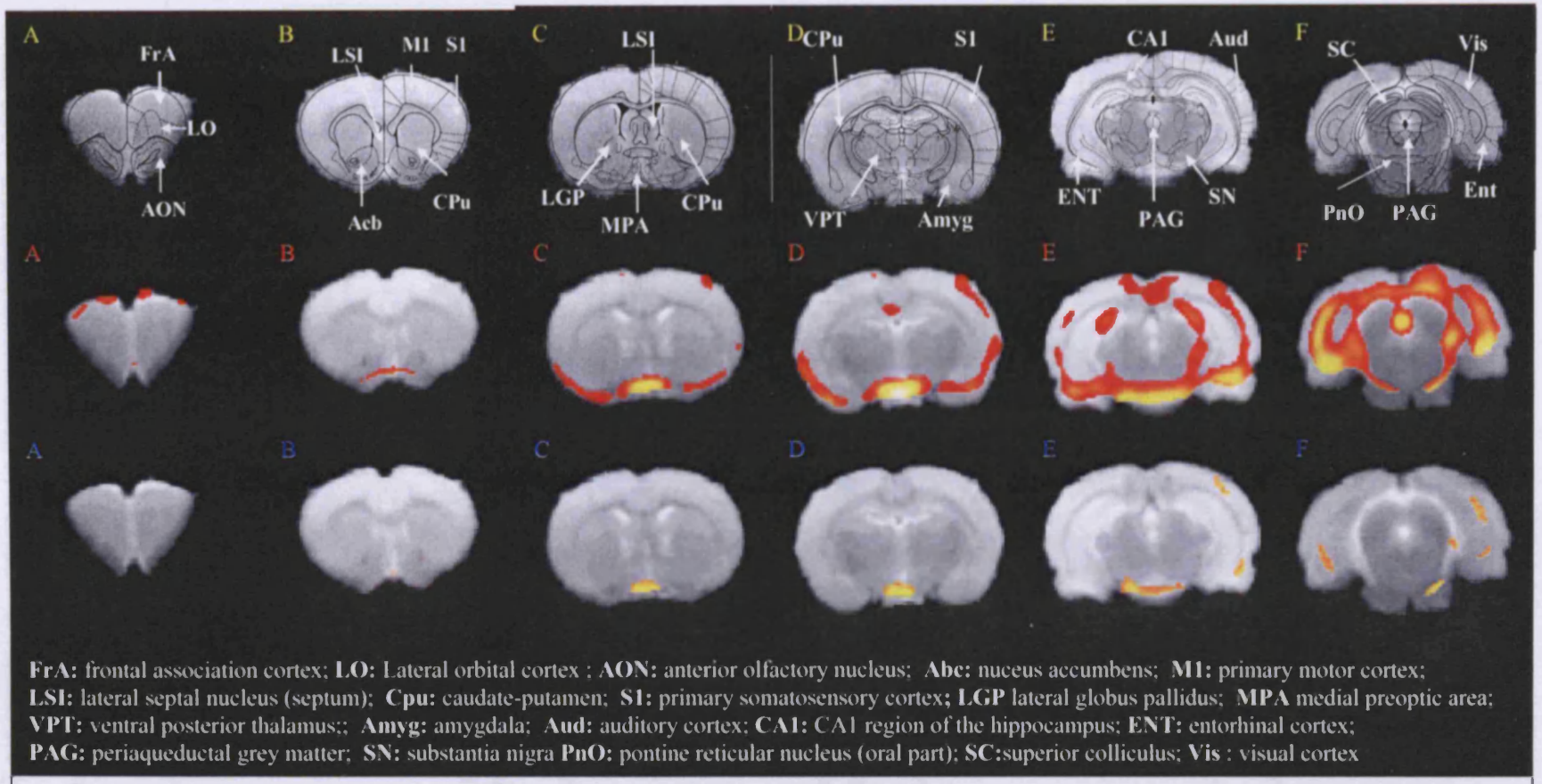

Fig 6.3.1c :Decreases in signal intensity following SCH23390 administration (0.5 mg/kg, i.v)

The first row shows annotated and labelled high resolution template images such that the areas displaying changes may be identified according to the rat atlas (Paxinos & Watson, 1998). The middle row shows the effects of amphetamine using fixed effects analysis, the bottom row using random effects analysis.

A: Bregma= +4.7mm Assymmetrical and outside the brain. B: Bregma= +1.7mm Ventral Pallidum.

C: Bregma = -0.3mm Medial preoptic area, piriform cortex. D: Bregma= -2.3mm ventromedial hypothalamus and amygdala and DHC

E: Bregma = -5.3mm Substantia nigra, amydalaopir transition area and CA1 F: Bregma= -7.3mm Retrosplenal cortex and medial entorhinal cortex.

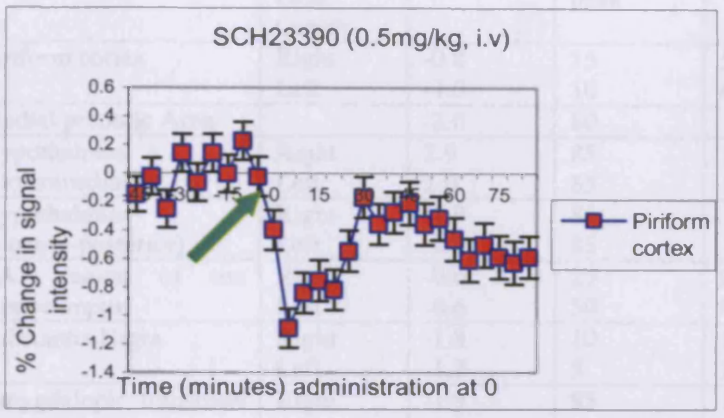

Bregma= -0.3mm

Piriform cortex, T= P<0.001

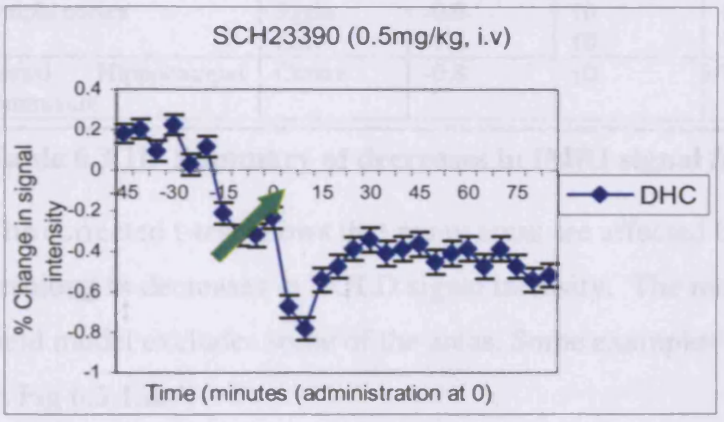

Bregma=-2.3mm

Dorsal hippocampal commisure T= 12.8 P<0.001

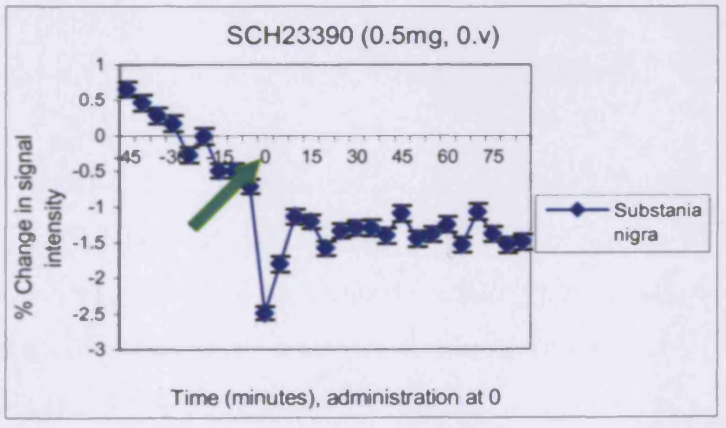

Bregma= -5.3mm

Substantia Nigra T= 13.5, P<0.001

Fig 6.3.1d

Graphs showing decreases in BOLD signal intensity at voxels of interest, after administration of SCH23390 (0.5mg/kg i.v.).
Green arrow indicates administration of SCH23390. Results are ± S.D of the mean.

Area	Right/ Left/ Centre	% Change	Time to peak	T-Value	P-Value	Random Effect
Piriform cortex	Right Left	-0.8 -1.0	15 10	5.6 6.5	P<0.001 P<0.001	No No
Medial preoptic Area		-2.0	80	16.6	P<0.001	Yes
Hypothalmus (Dorsomedial)	Right Left	2.9 2.0	85 85	18.90 12.64	P<0.001 P<0.001	No No
Hypothalmus (Ventral-posterior)	Right Left	-1.9 -2.2	85 85	14.58 16.76	P<0.001 P<0.001	Yes Yes
CA1 region of the hippocampus	Right Left	-0.6 -0.6	25 50	9.1 8.9	P<0.001 P<0.001	No No
Substantia Nigra	Right Left	-1.8 -1,7	10 5	13.5 11.8	P<0.001 P<0.001	Yes Yes
Amygdalopir transition area	Right Left	-1.9 -1.9	85 65	11.5 14.3	P<0.001 P<0.001	No No
Simple cortex	Right Left	-0.9 -1.4	10 10	13.6 11.4	P<0.001 P<0.001	No No
Dorsal Hippocampal commisure	Centre	-0.8	10	7.8	P<0.001	No No

Table 6.3.1b Summary of decreases in fMRI signal for Experiment 1

The corrected t-test shows that many areas are affected by SCH23390 stimulation resulting in decreases in BOLD signal intensity. The more stringent Gaussian random field model excludes some of the areas. Some examples of the timecourses are shown in Fig 6.3.1.d.

6.3.2 Results from experiment 2: SKF38393 Administration (10mg/Kg, i.v)

Images were collected from 30 contiguous, coronal, 1mm brain slices. The Bonferroni corrected data showed that acute intravenous infusion of SCH23390 (0.5mg/Kg) caused both increases and decreases in BOLD contrast in multiple brain areas ($P<0.01$).

Increases in BOLD signal intensity

Activation of subcortical structures was detected after administration of SKF38393. There were marked increases in signal intensity in the orbital cortex, cingulate cortex, dorsal and ventral striatum, septum, globus pallidus, thalamus, retrosplenal cortex, inferior colliculus, PAG (periaqueductal grey matter), pontine reticular nucleus, and some isolated parts of the cerebellar lobes. Additionally, significant increases were also observed in parts of the M1 motor cortex and S1J somatosensory cortex.

Six brain slices are shown below (Fig 6.3.2a) to indicate the effect of the D_1 agonist SKF38393 throughout the brain. As expected, random effects analysis, a more stringent test showed less activation than with the fixed effect analysis. Table 6.3.2a shows which areas were also significant in the random effects analysis, the areas include olfactory nucleus, M1 motor cortex, cingulated cortex, nucleus accumbens, septum, caudate-putamen, thalamus, retrosplenal cortex and PAG.

Graphs of the timecourse are shown in Fig 6.3.2b, these represent signal intensity at specific voxels as indicated by SPM t-Maps (as shown in Fig 6.3.2a). Areas are named as corresponding to particular structures in accordance with the rat atlas (Paxinos & Watson, 1998). A summary of all areas showing increases in signal intensity is displayed in table 6.3.2a

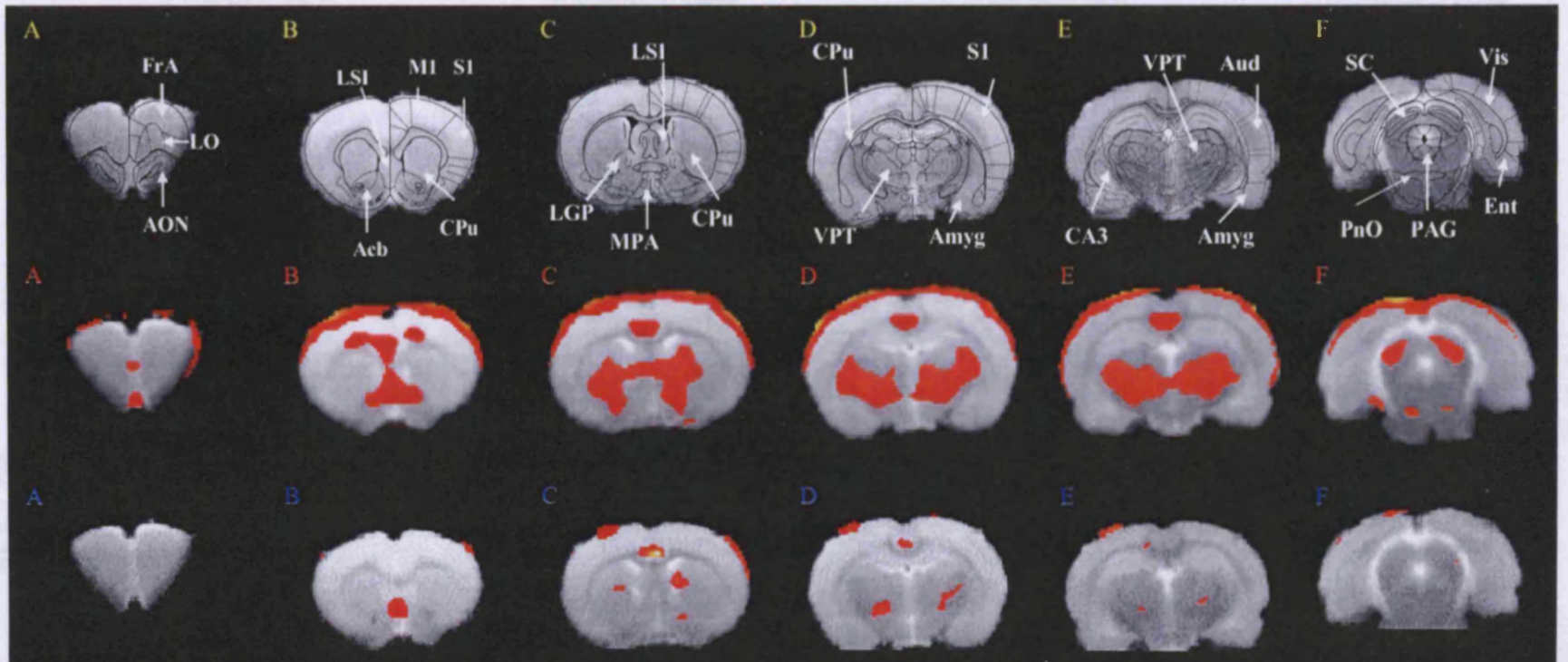

Fig 6.3.2a: Increases in signal intensity following administration of SKF388393 (10mg/kg, i.v)

The first row shows annotated and labelled high resolution template images such that the areas displaying changes may be identified according to the rat atlas (Paxinos & Watson, 1998). The middle row shows the effects of amphetamine using fixed effects analysis, the bottom row using random effects analysis.

A: Bregma= +4.7mm Orbital cortex.

B: Bregma= +1.7mm M1, S1, accumbens, septum, cingulate

C: Bregma = -0.3mm M1, S1 caudate, septum, cingulate , globus pallidus

D: Bregma= -2.3mm Ventral posterior thalamus, retrosplenal cortex

E: Bregma = -4.3mm Ventral posterior thalamus

F: Bregma= -7.3mm Superior colliculus, pontine reticular nucleus

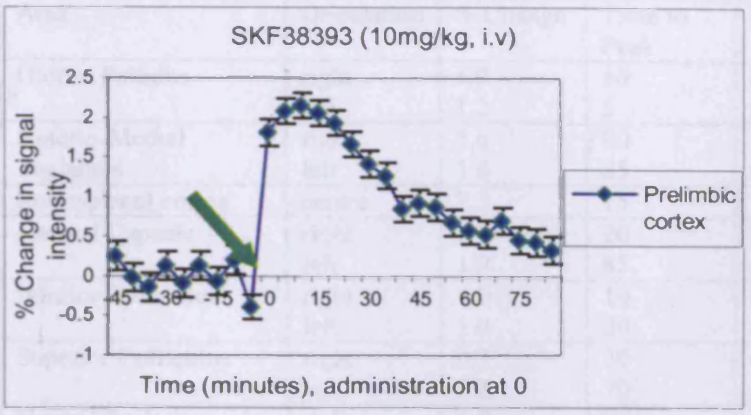

Bregma= -4.3mm

Orbital cortex, T=5.2 P<0.002

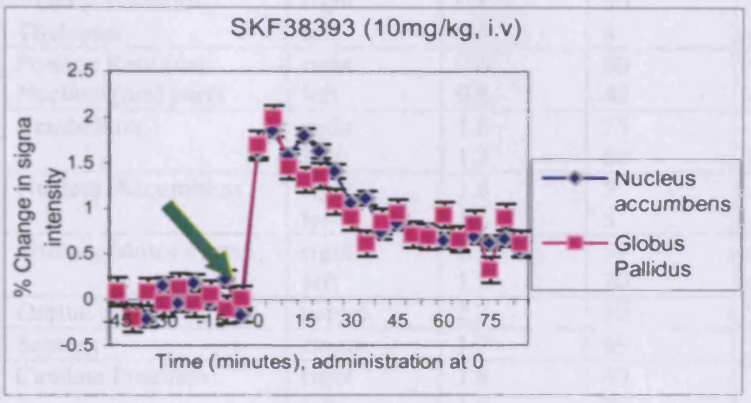

Bregma=+1.7mm; -0.3mm

Nucleus accumbens T= 5.7 P<0.001,
Globus pallidus T= 6.0 P<0.001

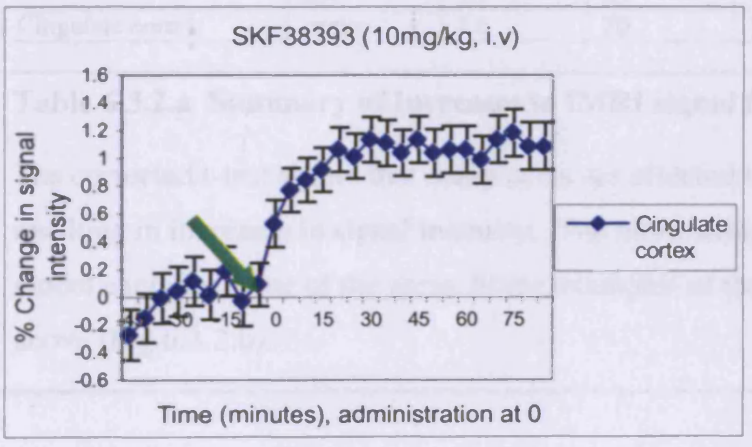

Bregma= -0.3mm

Cingulate Cortex T=7.43, P<0.001

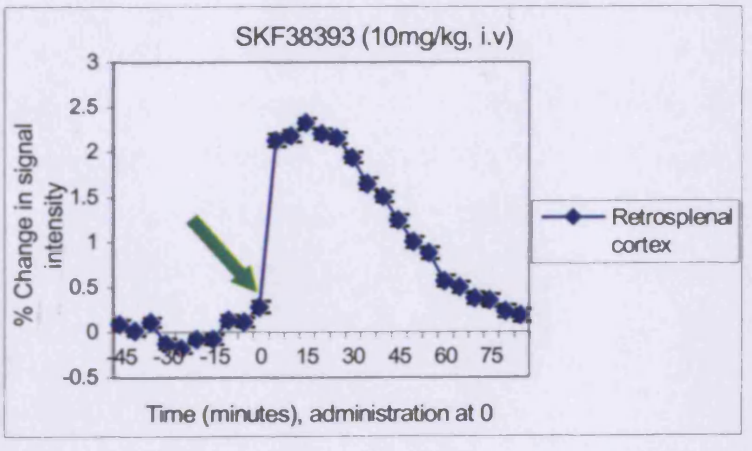

Bregma= -2.3mm

Retrosplenal Cortex T=7.41 P<0.001

Fig 6.3.2b

Graphs showing BOLD signal intensities at voxels of interest, after administration of SKF38393 (10mg/kg i.v.).
Green arrow indicates administration of SKF38393. Results are ± S.D of the mean.

Area	Orientation	% Change	Time to Peak	T-Value	P-Value	Random Effect
Globus Pallidus	right	1.9	10	6.02	P<0.001	No
	left	1.2	5	5.05	P<0.002	No
Anterio-Medial Thalamus	right	1.6	80	6.29	P<0.001	No
	left	1.6	85	6.19	P<0.001	No
Retrosplenal cortex	centre	2.3	15	7.41	P<0.001	No
Internal Capsule	right	1.1	20	9.17	P<0.001	No
	left	1.9	85	11.99	P<0.001	No
Inferior Colliculus	right	1.0	10	8.24	P<0.001	No
	left	1.0	20	8.63	P<0.001	No
Superior Colliculus	right	0.7	30	6.15	P<0.001	No
	left	0.8	70	6.03	P<0.001	No
Ventral Posterior Thalamus	right	0.8	80	6.1	P<0.001	No
	left	0.8	8	6.3	P<0.001	No
Pontine Reticular Nucleus (oral part)	right	0.6	60	5.60	P<0.001	No
	left	0.8	45	4.61	P<0.002	No
Cerebellum	right	1.6	75	10.12	P<0.001	No
	left	1.3	80	8.52	P<0.001	No
Nucleus Accumbens	right	1.8	5	5.75	P<0.001	No
	left	1.4	5	4.59	P<0.002	No
Primary Motor cortex	right	1.5	70	4.93	P<0.002	No
	left	1.5	70	4.94	P<0.002	No
Orbital cortex	centre	2.2	10	5.24	P<0.002	No
Septum	centre	1.2	85	5.46	P<0.001	Yes
Caudate Putamen	right	1.8	80	7.67	P<0.001	Yes
	left	1.7	85	7.22	P<0.001	Yes
Cingulate cortex	centre	1.4	70	7.43	P<0.001	Yes

Table 6.3.2.a Summary of Increases in fMRI signal for Experiment 2

The corrected t-test shows that many areas are affected by SKF38393 stimulation resulting in increases in signal intensity. The more stringent Gaussian random field model excludes some of the areas. Some examples of the timecourses are shown above (Fig 6.3.2.b).

Decreases in BOLD signal intensity

In addition to increases in BOLD signal intensity, statistically significant decreases in this signal were also observed. The decreases in signal intensity were observed in the frontal association cortex, amygdala, piriform cortex, amygdalopiriform transition area, CA1 region of hippocampus, substantia nigra, lateral leminiscus, subiculum and cerebellum.

Some areas, for example the PAG (Fig 6.3.3c images E&F) appears to show changes and their temporal response curves are indicative of a drug response. These "hot spots" correspond to the cerebral aqueduct (Paxinos & Watson, 1998) and therefore may represent changes in CBF or pulsation. Cardiac and pulmonary cycles in the head cause variations: with each cycle, blood pulses into the head and into the brain, because the cranium is closed and the brain, blood and CSF are essentially incompressible, there is a pulse of venous blood, CSF and even the brain stem in response to arterial output. Thus, cardiac pulsations have several effects: pulsations of arteries and large veins, pulsation of the CSF spaces, and movement of the brainstem.

Six brain slices (Fig 6.3.2c) are shown below to indicate the effect of the D_1 agonist SKF38393 throughout the brain, these areas are shown below in the t-Maps. Random Effects analysis, a more stringent test showed much less obvious decreases than with the fixed effect analysis. Table 6.3.2b shows that many of these areas were not significant in the random effects analysis.

Graphs of the timecourse are shown in Fig 6.3.2.d, these represent decreases in BOLD signal intensity at specific voxels as indicated by SPM t-Maps (as above). Areas are named as corresponding to particular structures in accordance with the rat atlas (Paxinos & Watson, 1998). Areas of interest have been selected throughout the brain. A summary of all areas showing increases in signal intensity is displayed in table 6.3.2b.

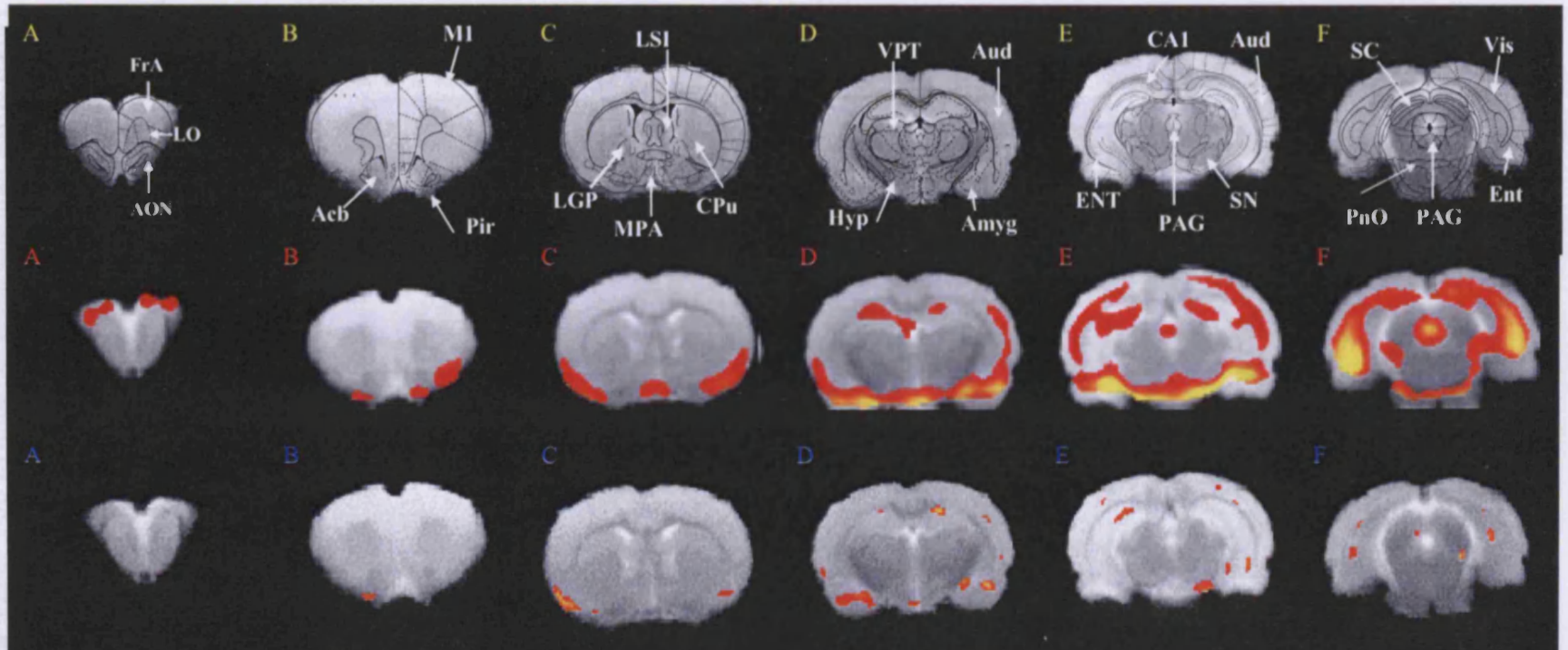

Fig 6.3.2c Decreases in signal intensity following administration of SKF38393 (10mg/kg, i.v)

The first row shows annotated and labelled high resolution template images such that the areas displaying changes may be identified according to the rat atlas (Paxinos & Watson, 1998). The middle row shows the effects of amphetamine using fixed effects analysis, the bottom row using random effects analysis.

A: Bregma= +4.7mm Frontal association cortex

B: Bregma= +2.7mm Piriform cortex, insular cortex (asymmetrical)

C: Bregma = -0.3mm Medial preoptic area, piriform cortex

D: Bregma= -3.3mm Amygdala, S1-S2 (asymmetrical), CA1

E: Bregma = -5.3mm Amygdalopir, substantia nigra, CA1, visual cortex.

F: Bregma= -7.3mm Lateral leminiscus, subiculum

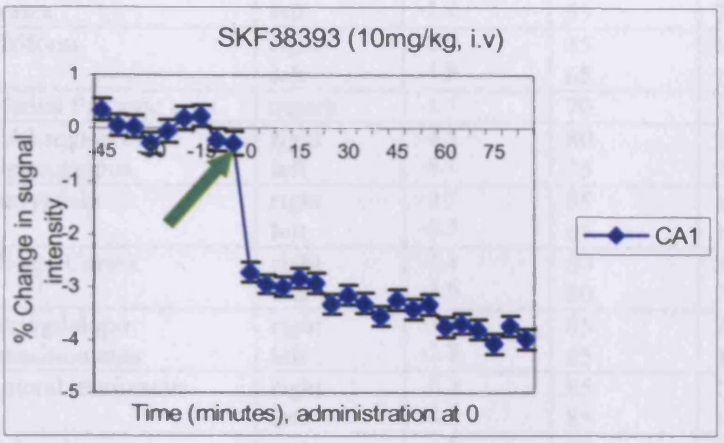

Bregma= -5.3mm

Hippocampal region CA1, T=25.5, P<0.001

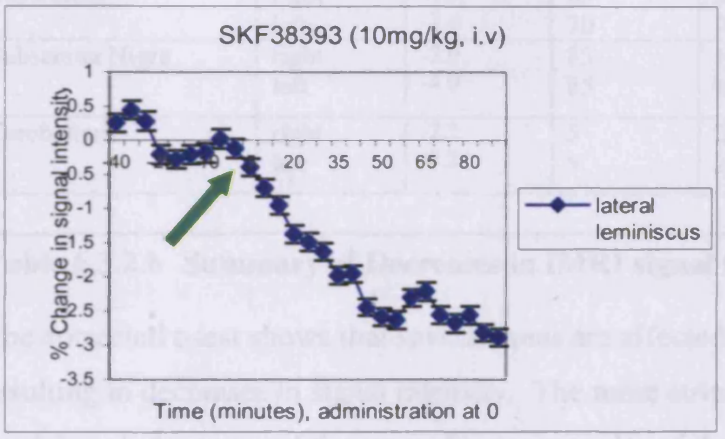

Bregma= -7.3mm

Lateral leminiscus T=11.85 P<0.001

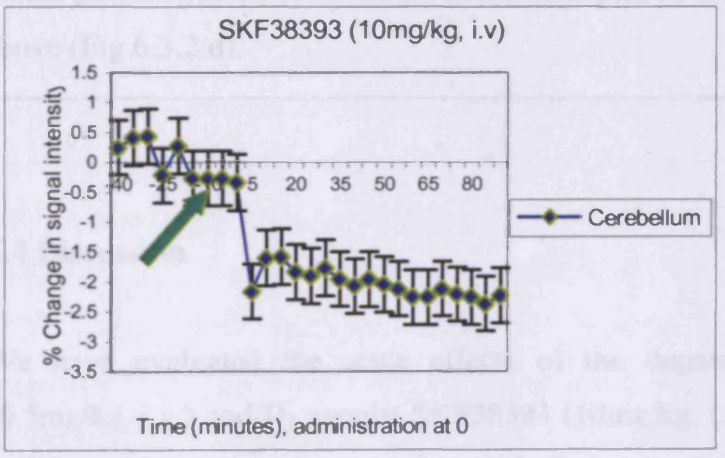

Bregma=-10.3

Cerebellum T= 20.21, P<0.001

Fig 6.3.2d

Graphs showing decreases in BOLD signal intensities at voxels of interest, after administration of SKF38393 (10mg/kg i.v.).

Green arrow indicates administration of SKF38393. Results are ± S.D of the mean.

Area	Orientation	% Change	Time to peak	T-Value	P-Value	Random Effect
Frontal Association cortex	right left	-1.2 -1.2	55 55	6.9 7.3	P<0.001	No No
Piriform	right left	-2.5 -1.9	85 65	14. 15.3	P<0.001 P<0.001	No Yes
Medial Preoptic area	centre	-1.7	70	11.1	P<0.001	No
CA1 region of hippocampus	right left	-4.5 -4.1	80 75	25.6 23.4	P<0.001 P<0.001	No No
Amygdala	right left	-2.7 -3.5	85 65	16.3 14.5	P<0.001 P<0.001	No Yes
Visual Cortex	right left	-1.4 -1.6	80 80	8.2 7.1	P<0.001 P<0.001	No No
Amygdalopir transition area	right left	-3.1 -3.8	85 85	20.1 22.2	P<0.001 P<0.001	No No
Lateral leminiscus	right left	-3.2 -2.8	85 85	11.8 11.8	P<0.001 P<0.001	No No
Subiculum	right left	-1.5 -1.4	65 70	8.5 7.8	P<0.001 P<0.001	No No
Substantia Nigra	right left	-2.9 -4.0	85 85	12.2 10.0	P<0.001 P<0.001	Yes No
Cerebellum	right left	-2.2 -2.2	5 5	20.2 20.2	P<0.001 P<0.001	No No

Table 6.3.2.b Summary of Decreases in fMRI signal for Experiment 2

The corrected t-test shows that several areas are affected by SKF38393 stimulation resulting in decreases in signal intensity. The more stringent Gaussian random field model excludes some of the areas. Some examples of the timecourses are shown above (Fig 6.3.2.d).

6.4 Discussion

We have evaluated the acute effects of the dopamine D_1 antagonist SCH23390 (0.5mg/kg, i.v,) and D_1 agonist SKF38393 (10mg/kg, i.v) in the anaesthetised rat using fMRI to determine consequences of D_1-type receptor stimulation. Quantitative autoradiographic studies, measuring receptor distribution and also measuring tissue function by means of glucose consumption, have been used to characterise both of these dopamine ligands in the past (Boyson et al, 1986; Trugman & James, 1993). Despite the findings of Palacios & Wiederhold (1985) who reported (using 2 deoxy glucose (2DG) autoradiography) that dopamine D_1 agents do not modify brain glucose metabolism,

Trugman & James (1993) found induced changes in glucose metabolism in many brain areas following administration of such agents.

Since the BOLD response is a relative change and is not quantitative, all of the increases and decreases are relative to the (non-drug) basal state. As amphetamine stimulation (Experiment 1, chapter 5) involved both D_1 and D_2 receptors, this shall be used as a standard and frequently referred to. Knowledge of the distribution of D_1 receptors may increase our understanding of the role of D_1-type receptors in central nervous system dopaminergic function.

6.4.1 Experiment 1: SCH23390 Administration (0.5mg/kg, i.v)

In this experiment a single intravenous bolus of D_1 antagonist, SCH23390 (0.5mg/kg) was administered to halothane-anaesthetised rats and the difference in fMRI signal before, and after drug administration in the whole brain was determined. Using a simple T-test with Bonferroni correction and significant threshold of $P<0.001$ resulted in conservative probability maps that display prominent signal changes.

Quantitative autoradiography has been used to visualize dopamine ligand D_1-type binding sites in rat brain (Boyson et al, 1986; Dubois et al, 1986; Dawson et al, 1986) with the highest concentration of binding was found throughout the forebrain, especially in the caudate-putamen, accumbens nucleus, olfactory tubercle, substantia nigra pars reticulata and the entopeduncular nucleus. In investigating functional effects of SCH23390 administration (0.5mg/kg, i.v) Trugman & James (1993) found it caused a reduction in RCU_{glu} in the PAG, ventral posterior thalamus and entopeduncular nucleus relative to an amphetamine treated cohort and also caused decreased RCU_{glu} in the globus pallidus, entopuncular nucleus, lateral habenula, subthalamic nucleus and substantia nigra relative to controls.

It can be clearly seen from Fig 6.3.1a that acute administration of SCH23390 has caused widespread increases in BOLD signal intensity, and the majority of rostral subcortical dopaminergic structures appear to be involved, for example, olfactory areas, nucleus accumbens, caudate-putamen, globus pallidus and thalamic nuclei in a manner similar

to amphetamine (Fig 5.3.1c). The SCH23390 cohort shows very clear changes in the parfasicular thalamus. This is an interesting finding as c-*fos* immunoreactivity studies have shown facilitatory relationship between D_1-type and NMDA glutamate receptors in this region. The increase in BOLD signal however spreads to upper layers of M1 cortex (Fig 6.3.1a images A &B) and furthermore, there is a clear omission of the lateral ventricles which is especially well illustrated in the random effects analysis (Fig 6.3.1a, bottom row). These results indicate that SCH23390 has caused widespread increases in brain activity. Further to these unexpected increases is the decrease in BOLD signal, which also is similar to amphetamine (Fig 5.3.1c) but without the rostral cortical decreases.

The pattern of BOLD in the SCH23390 treated cohort is surprising, firstly because one may have expected a reduced and differential pattern of activation as compared to that of amphetamine, as it acts on both D_1-type receptors and D_2-type receptors (Garret & Holtzman, 1994). Secondly, amphetamine serves to stimulate the D_1-type receptors by increasing the dopamine available to the receptor, whereas here, we have attempted to block the D_1-type receptors, however the changes detected are similar. These results indicate complex receptor events and the symmetricity of the images and omission of certain structures suggests spatial specificity and that these are not vague non-specific effects. While the areas affected are indeed those containing high densities of dopamine D_1-type receptor, the sign and spatial extent of the BOLD response is somewhat unexpected. Hence some potential explanations for these anomalies and ways to investigate them shall be discussed.

While the present data localise an apparent increase in neuronal activity to a specific subcortical brain regions, the nature of the responsive circuitry remains unclear. It is known that D_5 receptors (on which SCH23390 acts upon indiscriminantly) are bound to GABA-$_A$ receptors (Lui et al, 2000). This contribution would be difficult to investigate due to the lack of selectivity between D_1 receptors and D_5 receptors, one can however point out that the D_5 receptor is less numerous and has a less widespread distribution as compared to the D_1 and thus the contribution of possible D_5-$GABA_A$ coupling effects are probably minimal.

One possibility is that the attenuation of the amphetamine-evoked increase in BOLD signal observed in the D_1 antagonist pretreated group (Section 5.3.2), was not caused by blocking excitatory D_1-type receptors, but instead was caused by the action of inhibitory presynaptic D_2-type receptors. However 2DG and fMRI data indicate that this is probably not the case (Trugman & James, 1993; Marota et al, 2000). Evidence that SCH23390 may actually affect dopamine D_2-type receptors is provided by Goldstein et al (1987), in showing SCH 23390 to have D_2 antagonist-like effects on A9 and A10 dopamine neurons. It is suggested that they may be mediated via functionally linkage between D_1-type and D_2-type receptors (Goldstein et al, 1987).

The increased BOLD signal was mainly observed in striatal and basal ganglia structures, which have many projections and also involve GABA, glutamate and acetylcholine transmission, thus it is reasonable to assume that administration of a centrally acting agent will result in secondary and downstream effects. Many studies have shown dopamine to have a modulatory effect on neuronal excitability, which cannot be simply classified as excitatory or inhibitory. In vitro electrophysiological studies of dopamine on the rat caudate nucleus suggest that the postsynaptic sites of the caudate nucleus neurons have D_1-type receptors that mediate the inhibitory responses of these neurons to dopamine (Akaike et al, 1987). It is expected that the D_1 antagonist blocks postsynaptic receptors, causing disinhibition of caudate nucleus, increased neuronal activity and consequential metabolic response. Kalivas & Duffy (1997) found SCH-23390 prevented the reduction in extracellular glutamate by amphetamine, indicating that glutamate release in the nucleus accumbens is modulated by presynaptic dopamine receptors. One way to examine this possibility is by lesioning input pathways to the accumbens, to examine whether the ablation of this influence actually has an effect on the BOLD signal.

Research by several groups has indicated that the actions of SCH23390 are not completely selective to D_1-type receptors as it is also known to have agonist actions at 5-HT_{1c} and $5HT_{2c}$ receptors (Bouron & Reuter, 1999) and bound to these sites in the frontal cortex, PAG hypothalamus and cerebellum (Dawson et al, 1986), but not the striatum (McQuade et al, 1988). SCH23390 is not the only dopamine D_1-type receptor antagonist to display such properties, [^{125}I]SCH 23982 labels $5HT_2$ receptors in certain areas of the brain (Benkirane et al, 1987). Although compounds which have maximal

effects on D1 receptors may not have a significant effect on 5HT function at these doses (Towle et al 1989), the potential sites of interaction of D_1 ligands with 5HT receptors may help us understand the complex physiology and pharmacology of the primarily D_1 selective compound. This underlines the importance of finding maximally effective doses by using behavioural and neurochemical methods without causing non-specific effects. One way to ascertain the contribution of 5HT receptors to this response would be repeat this experiment, pretreating with 5HT antagonist, for example the $5HT_2$ antagonist ritanserin. Other D_1 antagonists, for example dihydrexidine could also be investigated with regards to the possible 5HT effects.

6.4.2 Experiment 2: SKF38393 Administration (10mg/kg, i.v)

The data indicate that acute intravenous administration of D_1 agonist SKF398393, at a dose of 10mg/kg, results in bilateral increases and decreases in BOLD signal intensity throughout the brain of the halothane-anaesthetised rat. The images show the BOLD response to acute SKF38393 challenge to be discrete, with the increases in BOLD localised to focal "hot spots" as compared to the antagonist SCH23390 (Section 6.4.1). This may be because a relatively small dose was used because this particular drug was relatively insoluble and could not be dissolved such that it could not be administered at the doses quoted in the literature (Trugman & James, 1993). Furthermore SKF38393 is a partial agonist, such that it produces a lower maximum effect

Nevertheless acute intravenous administration of 10mg/kg SKF38393 resulted in increases in BOLD signal evident in many structures. Although largely subcortical in site, these t-Maps also include increases in a band of the upper layers of the cortex and this extends throughout the whole of the brain. The effect was observed to develop over the time course of the experiment, such that an elevation in BOLD signal intensity was still evident at the end of the experiment, an hour and a half after drug administration.

The increases in BOLD signal were observed in the caudate-putamen, nucleus accumbens, septum, cerebellum thalamus, superior colliculus, hippocampus and cerebral cortex, and globus pallidus. Decreases were detected in the substantia nigra, amygdala hypothalamus (displayed in Tables 6.3.2a & b, respectively). These areas

have been identified using quantitative autoradiography with labelled [^{3}H]SKF38393 (Dubois et al, 1986) as being rich in dopamine D_1-type receptors. The involvement of the septum, striatum and cingulate cortex is particularly striking, as is the band of increased signal intensity in the motor cortex. The random effects analysis however, did not demonstrate a strong trend, detecting only a small cluster of significant voxels around the caudate-putamen, cingulate and thalamus, this is perhaps due to the reduced efficacy of this partial agonist.

Consistent with the present findings, neurochemical studies have also determined that administration of SKF38393 results in elevated extracellular levels of dopamine in the striatum (Walters & Howard, 1990). The septal nuclei are considered to be relay stations of sensory information that connect midbrain and brainstem structures, such as the ventral tegmental area (VTA) and hypothalamus, to forebrain limbic structures including the hippocampus and prefrontal cortex (Assaf & Miller, 1977; Lindvall & Steveni, 1978; Gaspar et al, 1985). Although not all of the septal inputs may be excitatory, the summation of events may lead to a net increase in neuronal activity and consequently display such a BOLD signal. By surgically ablating one or more of the excitatory inputs to the septum with lesions one may be able to ascertain the contribution of these signals to septal stimulation. Further evidence for the increases in metabolic activation on SKF38393 administration is provided by Bracci et al (2002), who showed that the D_1-type receptors in the striatum were responsible for excitatory action of endogenous dopamine on GABA neurons by depolarising them and that this action could be mimicked by SKF38393 (and not by a dopamine D_2 receptor agonist).

Trugman & James (1993) also examined the effect of SKF38393 (30mg/kg, i.v) on glucose metabolism in many brain areas using 2DG autoradiography. They found the only significant effect it caused was an increase in RCU_{glu} in the substantia nigra, relative to the control group. However electrophysiological studies have found SKF383 to reduce subicular activity (Behr et al, 2000) as indicated in Fig 6.3.2c image F.

6.4.3 Conclusion

Much of the literature on SCH23390 and SKF38393 involves modulation of neurochemical and behavioural changes elicited by different dopaminergic drug administrations; for example, amphetamine (Ferger et al, 1994) and cocaine (Carleo et al, 1998) and these two agents are rarely studied on their own. In many neurochemical studies with SCH23390 and SKF38393, they are administered via local intracerebral injection and their local effects elsewhere are studied, including: on dopamine in the nucleus accumbens (Olsen & Duvauchelle, 2001) other transmitter systems for example GABA in the pallidum (O'Connor, 2001), glutamate in the prefrontal cortex (Wolf & Xue, 1999) and acetylcholine in the nucleus accumbens (Arnold et al, 2000), as opposed to observing a whole brain response after systemic administration. However despite the bulk of the literature being regionally and functionally specific, the use of radiolabelled SCH23390 PET has allowed imaging of D_1 receptor distribution and also of some quantitative aspects of dopamine function in humans (Sedvall et al, 1990). This is especially useful for investigating receptor changes in illness such as psychosis (Wiesel et al, 1990) and Parkinson's disease (Rinne et al, 1990; 1991).

Most early studies have suggested that the presynaptic effects of dopamine are mediated by D_2-type receptors. Although autoreceptor activity tends to display pharmacology more similar to D_2 type receptors, D_1-type receptors also show some presynaptic (heteroreceptor) activity (Cameron & Williams, 1993; Lui et al, 2000). In the rat substantia nigra most of the ^{3}H-SCH 23390 binding sites have a presynaptic localization on the striato-nigral GABAergic afferent terminals, suggesting that dopamine released from nigral dendrites exert a tonic influence on these presynaptic D_1-type dopamine receptors (Porceddu et al 1986), and also on the terminals of afferent GABA neurons to facilitate selectively GABAB-mediated neurotransmission in the midbrain. Dopamine has also been shown to act presynaptically to influence glutamate release in pyramidal neurons by D_1 actions at a presynaptic site (Gao et al, 2001). The results indicate that dopamine depresses the excitatory input onto subicular neurons by decreasing the glutamate release, following activation of presynaptic D_1-type dopamine receptors (Behr et al, 2000.)

The temporal responses show a general trend of increasing or deceasing BOLD signal for 1-2 scans after administration of either drug._The maximal increases or decrease however, did not occur in some cases until the last scan, although a more immediate and incremental effect is apparent on examination of the time-courses in the large incremental changes, 1-2 scans after drug administration. Theoretically, the data is normalised to a very high signal intensity area (such as the globe of the eye) before each scan is acquired, meaning that all signal intensities are relative to this intensity (which should not vary with or without stimulation).

Therefore region specific changes in subcortical and cortical structures caused by dopamine D_1 ligand administration have been shown, these are most notably evident in regions with D_1-type receptors. The sign and extent of the BOLD response was somewhat unclear in Experiment 1, but the systemic effects of this drug are as yet, not fully characterised. Using BOLD responses as indices of haemodynamic events in a region containing high concentrations of a receptor of interest may be a valid way of investigating neurotransmitter pathways. However turning synaptic dopamine concentration into a haemodynamic event change needs more study to determine what neuronal events drive BOLD response, for example differentiating between excitatory and inhibitory events and understanding the consequences of downstream and upstream events. Such studies may involve using the BOLD response to spatially indicate which brain regions to focus on for more specific and localised modulations. The relevance of "positive" and "negative" BOLD responses is discussed in Chapter 8 with regard to the possible underlying mechanisms. Studies such as these current work must be interpreted carefully, especially as all the phMRI studies to date, have been performed using drugs which have a well characterised systemic response, such as amphetamine, cocaine, and are often discussed in terms "transmitter release" and "neuronal activation" (Chen et al, 1997; Marota et al, 2000). The complex presynaptic and postsynaptic localisation of dopamine D_1-type and D_2-type receptors means a variety of possible outcomes and indeed the choice of anaesthetic will invariably exert an effect. BOLD maybe a useful preliminary tool to finds out where to go next (spatially) or at which timepoint to investigate.

Chapter 7

fMRI of a Dopamine D_2 receptor antagonist and agonist

7.1 Introduction

The D_2 receptor subtype was first identified by virtue of its ability to either inhibit adenylyl-cyclase activity or by having no effect on it (Kebabian et al, 1972). The human D_2 receptor has been cloned and is found to have approximately 96% sequence homology with the rat D_2 receptor (Grandy et al, 1989). Signalling through dopamine D_2 receptors governs physiological functions related to locomotion, affect, hormone production and reward, and its dysregulation is the basis for various disorders: psychosis (Seeman et al, 1978), hyperprolactinaemia (Sarapura & Schlaff, 1993), Parkinson's disease (Leiberman & Goldstein, 1985) and drug and alcohol abuse (Wise & Bozarth, 1987). D_2 receptors are well-established as targets of antipsychotic drugs used to treat neuropsychiatric disorders such as schizophrenia. In this section, the known and possible functions of dopamine D_2 receptors are discussed along with present and future treatments of dysfunctional dopamine D_2 receptor signalling. As described in Chapter 1 (section 1.4.5) there are different subtypes of D_2 receptor (D_2, D_3 and D_4), thus where D_2 receptors are mentioned, the D_2-type receptor is being referred to.

7.1.1 Characterisation of Dopamine D_2-type Receptors

Within the D_2-type classification, this receptor was named as the somatodendritic autoreceptor on pharmacological (Morelli et al, 1988), electropysiological (Lacey et al, 1987), and molecular biological grounds (Meador-Woodruff et al, 1991). In addition to D_3 and D_4 receptors, the D_2 type receptor consists of D_{2S} (short) and D_{2L} (long) isoforms that are pharmacological similar (Picetti et al, 1997). The 2 isoforms are caused by alternative mRNA splicing, depending on the presence (or absence) of a particular stretch of 29 amino acids in the third cytoplasmic loop of the receptor (Liu et al, 1996). Both D_{2L} and D_{2S} inhibit adenylyl cyclase activity and may also increase phosphoinisitol turnover (Jackson & Westlind-Danielsson, 1994). In D_{2L} knockout mice (D_{2L}^-), the cataleptic effects of haloperidol are absent (Usiello et al, 2000), suggesting that D_{2L} receptors are actually targeted by haloperidol: this finding has implications for neuropsychiatric disorders and drug targeting. Studies using D_{2L}^- mice also reveal that D_{2S} inhibit D_1 receptor mechanisms, thus revealing a circuit of signal interference

between dopamine receptors. Another D_{2L} study using D_{2L}^- mice suggested that D_{2S} can substitute for the function of D_{2L} in the regulation of pituitary hormone secretion, and that the function of D_{2S} is not dependent on the formation of a receptor heterodimer with D_{2L} (Xu et al, 2002). The dopamine D_2 receptor is highly expressed in the central nervous system and the pituitary gland.

Many agonists and antagonists are available for the dopamine D_2-type receptors. Apomorphine is an agonist at D_2-type receptors but is not totally selective and also has some activity on D_1-type receptors (Vaccheri et al, 1986). Bromocriptine, another D_2 agonist, functions as a partial agonist (Onali et al, 1985), while quinpirole (Izzo et al, 2001) and pergolide (Wong et al, 1983) are highly selective for D_2-type, versus D_1-type receptors. However both quinpirole and pergolide have higher affinity at D_3 receptors than D_2 receptors (Gehlert et al, 1992). In addition, 7-OH-DPAT is also more selective at D_3 receptors and thus has been used in binding studies (Freedman et al, 1994). Examples of high affinity D_2 antagonists are sulpiride (Boyer, 1983) and raclopride (Farde et al, 1989). Sulpiride was used in treatment of the positive symptoms of schizophrenia (Lewis et al, 1983) and raclopride is used in its radiolabelled form in PET studies to label D_2-type receptors (Farde et al, 1986). ^{3}H-Raclopride has a high affinity for the dopamine D_2-type receptor, with much less affinity for any other receptor (also the nonspecific binding is very low both *in vitro* and *in vivo*). Raclopride enters the brain easily and has therefore also been used in *in vivo* binding, autoradiography and PET (Hall et al, 1998). Dopamine antagonists display a rather modest affinity for D_3 subtype of receptor, having 20-30 fold less selectivity than for D_2 receptors (Sokoloff et al, 1992).

7.1.2 Dopamine D_2-type Receptor Distribution and Pathways

Using quantitative autoradiography with radiolabelled [^{3}H]spiroperidol (a D_2 antagonist) widespread distribution of dopamine D_2-type receptors was found throughout the rat brain, and in most cases at a lower density than D_1-type receptors (Boyson et al, 1986). D_2-type receptors are found in the olfactory tubercle, nucleus accumbens, caudate-putamen and substantia nigra at approximately one third of the density found for D_1-type receptors (Huff & Molinoff, 1985). In vitro studies of the

human brain post-mortem, using [^{3}H]raclopride binding, found dopamine D_2-type receptors to be confined to the caudate nucleus, the putamen and the substantia nigra (Hall et al, 1988).

D_3 receptors subtype distribution is more controversial: some studies report D_3 mRNA in limbic areas (Sokoloff et al, 1990), whereas others failed to find D_3 mRNA or found it only in trace amounts (Le Moine & Bloch, 1996). The selective D_3 dopamine receptor agonist [^{3}H]PD 128907 was used to visualise D_3 dopamine receptors in the human brain (Hall et al, 1996a). [3H]PD 128907 accumulated only in the nucleus accumbens and in the ventral parts of caudate nucleus and putamen to a lesser extent, and also labelled D_3 dopamine receptors in the neocortex. Epidepride is a benzamide with high affinity for central D_2 and D_3 dopamine receptors. The human anatomical distribution of [^{125}I]epidepride binding was examined by autoradiography (Hall et al, 1996b); the density of binding sites was high in caudate nucleus and putamen, pallidum, thalamic nuclei, the neocortex, and the substantia nigra.

The other D_2-like receptor, the D_4 receptor, was cloned from rat and human tissue (Grandy & Civelli, 1992). The human D_4 receptor has received considerable attention due to its high affinity for clozapine and the unusual polymorphic nature of its gene (Catalano et al, 1993), The mRNA of this receptor subtype has been found in frontal cortex, hypothalamus, thalamus, medulla, amygdala, olfactory bulb and retina in the primate brain (De la Garza & Madras, 2000). D_4 receptors are the target of atypical antipsychotics which are given to patients who are unresponsive to typical antipsychotics (discussed in 7.1.6). Seeman et al (1994) found the density of dopamine D_4 receptors was 6-fold greater than normal levels in a cohort of schizophrenic patients. Transgenic mice lacking the D_4 receptor gene are supersensitive to ethanol, cocaine and methamphetamine (Rubinstein et al, 1997). Behavioural and neurochemical studies reveal that D_4 receptor play a role in normal, coordinated and drug-stimulated motor behaviours, as well as affecting the activity of nigro-striatal dopaminergic neurons (Rubinstein et al, 1997).

Like D_1-type receptors, D_2-type receptors are thought to be co-localised with a peptide transmitter, the opiod enkephalin (Llorens-Cortes et al, 1991). Although the relationship between D_2-type receptors and enkephalin is not fully understood, it is thought that

enkephalin modulates D_2-type receptors under conditions of increased dopamine release (Bannon et al, 1989). This hypothesis also supports the proposal that the undesirable motoric signs and symptoms observed after chronic treatment with typical antipsychotics may not be the result of increased levels of enkephalins in the basal ganglia

7.1.3 Functional Implications of Dopamine D_2-type Receptor Activity

Finding a simple definitive role for D_2-type receptors is very difficult. D_2-type receptor actions are complex; they have postsynaptic and presynaptic localisation, which mediate both facilitatory and inhibitory roles. Furthermore, drugs acting upon the receptors, differentially recruit these receptors depending on the dosage used (Kuczenski & Segal, 1989).

Within the D_2 type of dopamine receptors, the D_2 and D_3 subtypes share structure similaries, but the extent to which these subtypes may differ in functional properties is unclear (Jung et al, 1999). In generating D_2 and D_3 subtype single mutants and D_2/D_3 double mutants, it was found that double mutants developped more severe motor phenotypes and have larger increases in levels of DOPAC and HVA in the dorsal striatum, than that of D_2 subtype single mutants. These results suggest that D_3 receptors compensate for some of the lacking D_2 receptor functions and that these functional properties of D_3 receptors remain masked when the abundant D_2 subtype receptor is expressed.

Extensive studies using pharmacological, behavioural and molecular biological techniques have been carried out to define the receptor and are summarised in the following sections (7.1.4-7.1.7).

7.1.4 Dopamine D_2-type Receptor Mediated Behaviour

Dopamine D_2-type receptors are of crucial importance in the striatal processing of motor information received from the cortex. In rats moderate to high doses of D_2 agonists cause increases in locomotion (Szumlinski & Szechtman, 2002), sniffing and snout contact in a similar manner to apomorphine (Clifford et al, 2001), although the effect is not as robust.

D_2-receptor knockout mice (D_2^-) are akinetic and bradykinetic in behavioural tests, and show significantly reduced spontaneous movements (Baik et al, 1995). This phenotype presents analogies with symptoms characteristic of Parkinson's disease (Baik et al, 1995). These mice have great potential as a model for studying and correcting dysfunctions of the dopaminergic system, although the interaction of multiple genetic factors in complex behaviours must be considered (Kelly et al, 1998). D_2^- mice were also used to investigate the role of this receptor in the generation of striatal synaptic plasticity where found that in brain slices, LTP is produced, in contrasts to LTD in wild type mice. Thus it shows that D_2 receptors are involved in synaptic plasticity at the corticostriatal level (Calabresi et al, 1997).

The potential behavioural and physiological effects of activating D_3 receptors have been investigated using 7-OH-DPAT. This agent causes a bi-phasic, dose-dependant effect on spontaneous sniffing and locomotion, and these are thought to be inhibited at low doses, and stimulated at high doses. In the unilateral lesioned animal, 7-OH-DPAT causes contralateral turning behaviour, similar to apomorphine, suggesting that D_3 receptors may be selectively stimulated at low doses, while at higher doses, the D_2 receptors are then recruited (Kim et al, 2000). It was also found that 7-OH-DPAT caused hypothermia, which is blocked by D_3 antagonists (Millan et al, 1994). Thus, in summary, D_3 receptors are involved in locomotor activity and temperature regulation.

It is well known that dopamine D_2-type receptors found in the area postrema (Stafanini & Clement-Cormier, 1981) play an important role in the regulation of emetic responses in humans, ferrets, and dogs (Harding et al, 1987; Andrews et al, 1990). Apormorphine is an analogue of morphine and similarly, causes nausea and vomiting and is used accordingly in both medical and veterinary clinical practice as an emetic after ingestion

of toxic or poisonous substances (Feldman et al, 1997). D_2 receptors are also located in lactotrophs in the pituitary gland where they modulate secretion of prolactin (Piano & Pogacnik, 2001). *In vivo,* D_2 receptor blockade in animals can be gauged by measuring the changing levels of circulating prolactin. Bromocriptine is used to treat hyper-prolactinaemia, a condition brought on by particular naturally occurring diseases as well as following long-term treatment with some antipsychotics (Sarapura & Schlaff, 1993). D_2^- mice have a striking, progressive increase in lactotroph number, commonly progressing to tumours of these cells in aged animals (Saiardi et al, 1997). This points to prolactin as functioning as an autocrine proliferative factor in the pituitary gland. Further evidence for a role for D_2 receptors in prolactin secretion occurs in aged female D_2^- mice which develop uterine adenomyosis in response to prolonged prolactin exposure. This indicates a critical role of hypothalamic dopamine in controlling pituitary growth (Kelly et al, 1997).

7.1.5 Dopamine D_2-type Receptor role in Human Brain Disease

Based on the utility of various classes of drugs in the treatment of human illness, the inference has been drawn that D_2-type receptors play a more significant role in the pharmacotherapy of psychosis and movement disorders than do D_1-type receptors. D_2-type receptors appear not to be the sole receptors involved in the pathology of schizophrenia, and it is not certain whether changes in D_2-type receptor functioning are causative or as a result of the disease process.

The dopamine theory of schizophrenia is based in part, on the correlation between clinical potency of antipsychotic drugs and dopamine D_2 receptor occupancy as quantified by inhibition of ^3H haloperidol binding (Seeman et al, 1978). A PET study using spiroperidol binding found a 2-fold increase in D_2 receptor density in schizophrenic brains, but no changes in D_1 receptors (Seeman & Grigoriadis, 1985). This finding provides indirect evidence that hyperactivity of the dopaminergic system and specifically of dopamine D_2 receptors occurs in schizophrenia. Subsequently, many efforts have been made to find a more direct biochemical evidence for this role. Further implication of D_2 receptor involvement in the etiology of schizophrenia is the reduction

in adenylyl cyclase activity found when chronic low doses of antipsycotics are administered (Feldman et al, 1997).

These results prompted the development of selective D_2 receptor antagonists. Sulpiride was the first of such drugs and is effective in treatment of schizophrenia and additionally, it does not carry as a high risk of causing extra-pyramidal symptoms, as does haloperidol (Gerlach et al, 1985; Coffin et al, 1989). Chronic antipsychotic administration results in increased D_2 receptor binding and supersensitivity to dopamine, not dissimilar to denervation sensitivity (Stoff et al, 1984). A selective loss of dopamine D_3 receptors was measured in the parietal and motor cortices of chronic schizophrenics (Schmauss et al, 1993). Seeman et al (1995) revealed upregulation of D_4 receptors in schizophrenic patients. Thus the interpretation of studies on schizophrenic patients must consider the potential brain changes induced by long-term antipsychotic administration.

Most antipsychotic drugs probably owe their activity to blockade of D_2 receptors. Carlson & Lindqvist (1963) suggested that the ability of phenothiazines to block presynaptic inhibitory autoreceptors was responsible for the increases in dopamine turnover and in cell dopamine firing. Nowadays, it is accepted that initial increased levels of plasma HVA are an indicator of a immediate response to neuroleptics and the greater the reduction of HVA over time is an indication of positive responsiveness to the drug therapy (Seiver et al, 1993). Patients suffering from negative symptoms do not demonstrate the biphasic response of plasma HVA (Davila et al, 1988).

D_2-type receptor dysfunction is also involved the etiology of other diseases such as depression and Parkinson's disease. The antidepressants, fluoxetine and desipramine caused increases in D_2 mRNA in nucleus accumbens shell (and not D1) mRNA, suggesting a (more) specific role for D_2-type receptors in emotion (Ainsworth et al, 1998). Bromocriptine therapy in low doses, is commonly used as an adjunct to L-DOPA, it is effective in patients with mild to moderate Parkinson's disease, while bromocriptine in higher doses is required in patients with advanced disease (Leiberman & Goldstein, 1985).

7.1.6 Dopamine D_2-type Receptor role in Drug and Alcohol Abuse

The observation that dopamine transmission underlies the reinforcing effects of drugs of abuse, including alcohol (Wise & Bozarth, 1987; Di Chiara et al, 1992), has prompted interest in the use of drugs which modify dopamine transmission as candidates for treatment of psychostimulant abuse (see review by Withers et al, 1995). Another method of intervention is usage of partial agonists (Izzo et al, 2001); e.g with their high affinity and intrinsic activity they can act as either antagonists or agonists, depending on the conditions of the resting dopaminergic activity. In mice with a genetic disruption of their dopaminergic D_2-type receptors, the behavioural expression of morphine withdrawal was unchanged, but a total suppression of morphine-rewarding properties was observed in a place-preference test (Maldonado et al, 1997). The D_2-type receptor plays a crucial role in the motivational component of drug addiction.

An interesting effect of chronic exposure to psychostimulant drugs is the resultant transformation in the organization of activity, following quinpirole administration for instance, elicits strikingly organized behaviour, despite a marked increase in hyperactivity: sensitised rats move repeatedly along paths that are rigid and restricted to a localised portion of the environment, stopping in specific places along their route and display fixed motor acts (Szechtman et al, 2001). This quinpirole-induced transformation may represent an animal model of obsessive-compulsive disorder (Szechtman et al, 2001).

There is increased evidence that dysfunction of the dopamine system is involved in the pathogenesis of alcoholism and it has been proposed that dopamine is one of the transmitters modulating predisposition to alcohol abuse (Blum, 1996). Epidemiological studies have shown the important role of genetics in the predisposition to alcoholism (Thanos et al, 2001). Several lines of evidence indicate that the D_2 receptor underlies reinforcing effects of drugs of abuse including alcohol: projections of dopamine cells to nucleus accumbens are implicated in the reinforcing effects of alcohol (Murphy et al, 1987); D_2 receptor knockout mice show reduced reinforcing effects of alcohol (Phillips, 1998); alcohol causes dose-dependent increases in dopamine concentration (Di Chiara & Imperato, 1988); alcoholics have reduced brain D_2 receptors (Tajuddin & Druse, 1996). Some epidemiological studies have shown increased frequency of D_2 receptor A_1

taq allele (Blum et al, 1990) in severe forms of alcoholism. The D_2 receptor A_1 *taq* allele is associated with low D_2 receptor density, because the increased frequency of the A_1 *taq* allele and low D_2 receptor have been documented in other drugs of abuse (Suzuki et al, 2001).

Dopamine plays a crucial role in reinforcing effects of alcohol and other addictive substances as well as the euphoric aspect of usage, and dysregulation of the dopamine system is also associated with various neurological disorders, which are often coupled with alcoholism. The D_2 receptor is also implicated in the impulsive-compulsive-addictive behaviours (Comings et al, 1996). Furthermore it has been hypothesised that low levels of D_2 receptor predispose subjects to abuse drugs or alcohol as a means of compensating for the reduced activation of associated reward circuits (Phillips et al, 1998). Increasing the expression of dopamine D_2 receptors in the nucleus using gene transfection resulted in reduced alcohol preference and intake, suggesting that high levels of D_2 receptors protect against alcohol abuse (Thanos et al, 2001). It would be useful to investigate strategies aimed at increasing D_2 receptor A_1 levels and this may be beneficial for prevention and treatment of alcoholism. When more is known about the D_2 receptors and their regulation, it may be possible to develop interventions that can increase their expression. The A_1 allele has been associated with other drug problems including cocaine, nicotine and polysubstance abuse (Noble, 1998). The identification of the D_2-type receptor gentotypes suggests that the D_2-type receptor mutations may have functional consequences that predispose individuals to a variety of substances use disorders.

On the basis of this, in addition to results from Chapter 5, it is of interest to investigate the functionional distribution of the D_2-type receptor. Thus, the acute effects of administration of sulpiride (50mg/kg, i.v) and quinpirole (0.5mg/kg, i.v) were then investigated using fMRI.

7.2 Methods

D_2 antagonist sulpiride or D_2 agonist quinpirole were administered intravenously to rats whilst immobilised in a 2.35 Tesla imaging system. In order to study the global spatial

response profile, the whole brain was scanned (30 x 1mm). A summary of the methods for these experiments is described in this section, for details of these procedures refer to Chapter 4 as shown in parenthesis.

7.2.1 Animal Preparation

Male Sprague-Dawley rats (250-300g, n=8), were used for each of two experiments. They were anaesthetised and cannulated for administration of drugs as described in sections 4.2.1 and 4.3, respectively. The physiological state of the animal was constantly monitored using respiration rate and body temperature, as described in section 4.5. When instrumented, the animal was placed into a custom-made, heated probe, which maintained the core body temperature at 37°-38°C (section 4.4). The MRI modified surface coil (section 4.6.2) was secured to the dorsal surface to the head before positioning the animal in the magnet centre of the scanner (section 4.6.1). The imaging experiments were all performed at field strength of 2.3 Tesla with a horizontal bore superconducting magnet (4.6.1).

7.2.2 Experimental Protocol

Sulpiride and quinpirole were prepared on the day of the experiment (section 4.2.2). For each experiment, 45 minutes of baseline (no drug administration) scans were acquired before either sulpiride and quinpirole was administered as a single intravenous bolus infusion via the jugular vein (Fig 5.2.2a). The volumes injected (2ml/kg and 1ml/kg, respectively) took into account the saline-heparin filled dead space of 0.05ml. Data were collected for a further 90 minutes after drug administration.

a

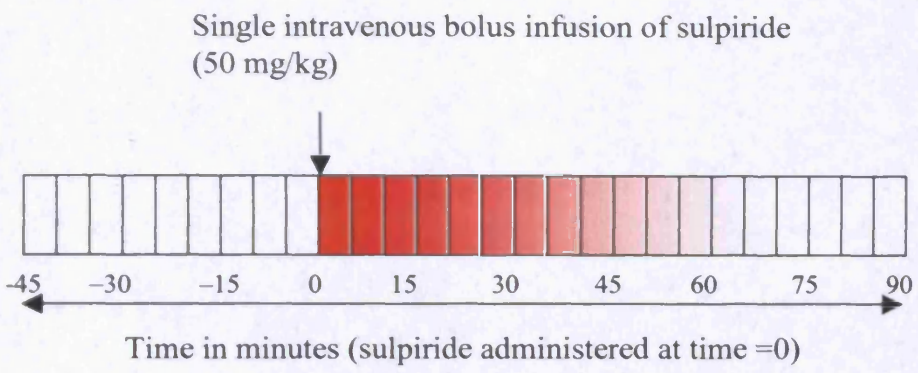

b

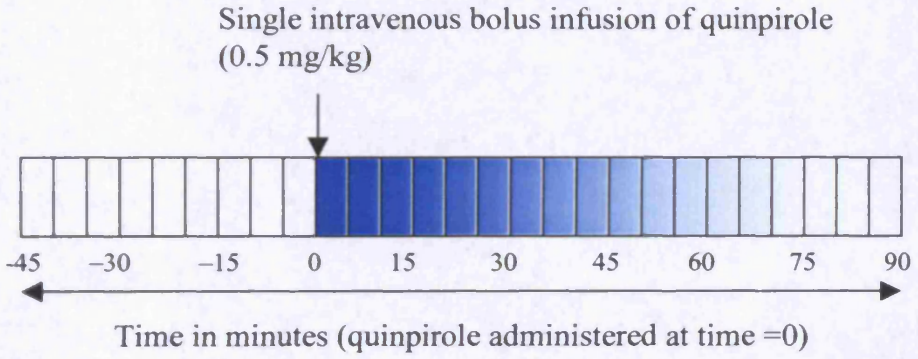

Fig 7.2.2 Schemata of Time-course of experiments 1 & 2

Each block represents 1 scan with duration of 4 minutes 40 seconds; the arrow represents exact time of drug administration.

Experiment 1 (a), single bolus injection of sulpiride after 45 minutes baseline.

Experiment 2 (b), single bolus injection of quinpirole after 45 minutes baseline.

7.2.3 Statistical Processing and Analysis

The complete steps from raw data, through the pre-processing to statistical analysis and inference are explained in detail in section 4.5. Averaging the results obtained from the 8 individual animals that received the drug challenges generates the t-Map. The colour overlay indicates the level of significance in t-values (these are converted into p-values in the tables below), assessed as a group t-test comparison between pre (baseline of 45 minutes before drug injection) and post-drug injection signal (up to 90 minutes after drug administration).The contrasts specified and the data summary is the same as in Chapter 5, Table 5.2.3: "Experiment 1" (amphetamine stimulation).

7.3 Results

SPM generated two sets of image data for each experiment, a fixed effect analysis and a random effects analysis (see section 4.8 for description of these two analyses). In addition to these images, graphs of timecourses from selected voxels in regions of interest were also obtained. Samples of these are displayed in the following sections and the complete results are summarised (Tables 6.3.1a & b, 7.3.2a & b).

7.3.1 Results from Experiment 1: Sulpiride Administration (50mg/Kg, i.v)

Images were collected from 30 contiguous, coronal, 1mm brain slices. The Bonferroni corrected data showed that acute intravenous infusion of sulpiride brain areas ($P<0.01$) had significant effect on the BOLD signal in many areas.

Increases in BOLD signal intensity

After administration of sulpiride, the observed increases in BOLD signal intensity in subcortical structures were very prominent: as with amphetamine there were marked increases in signal intensity in olfactory cortex, dorsal and ventral striatum, septum, globus pallidus, thalamus, superior colliculus, inferior colliculus, and the cerebellar lobes. Widespread increases were also observed in parts of the M1 motor cortex and S1J somatosensory cortex.

The t-Maps indicate that the cingulate cortex and hippocampus were not activated. Images of six brain slices are shown below in the t-Maps to indicate the effect of sulpiride throughout the brain. Random Effects analysis, a more stringent test showed less activation than with the fixed effect analysis as expected.

Table 7.3.1a shows which brain areas were also significantly changed in the random effects analysis; these areas include olfactory nucleus, M1 motor cortex, cingulated cortex, nucleus accumbens, septum, caudate-putamen, thalamus, retrosplenal cortex and PAG.

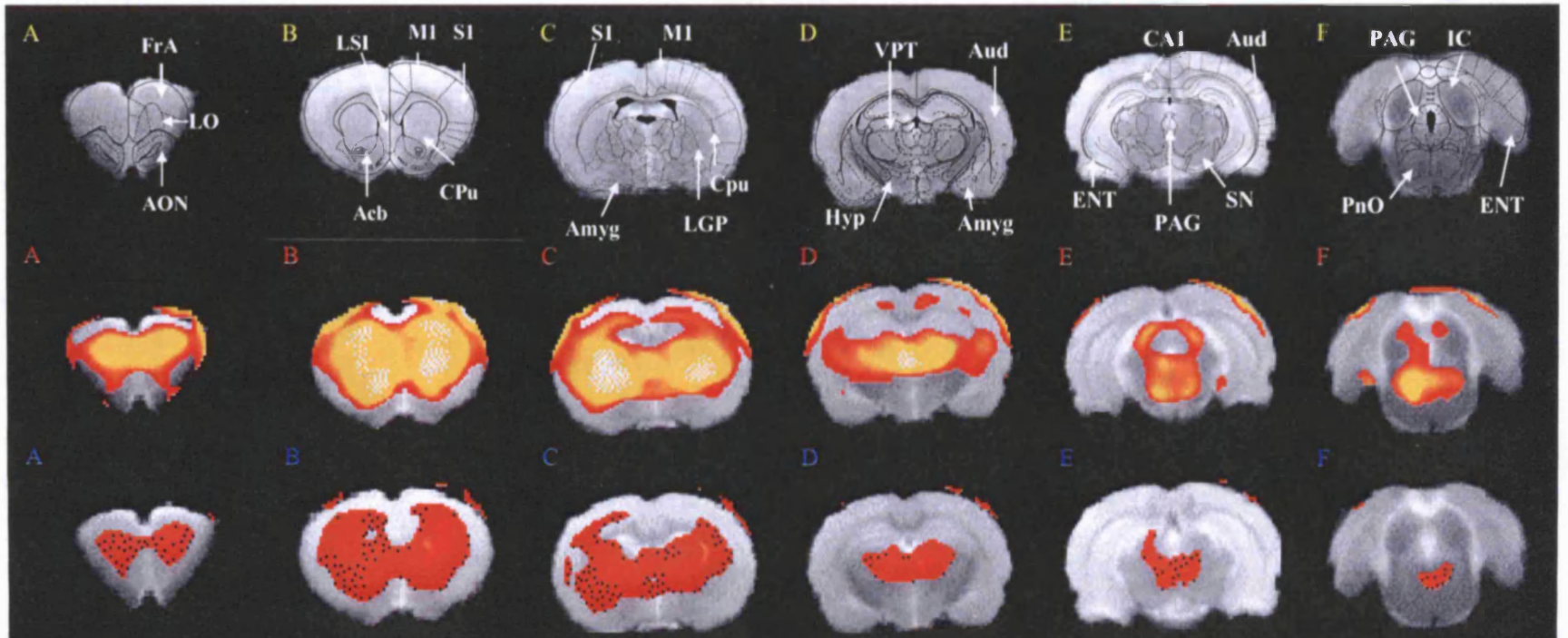

Fig 7.3.1a Increases in signal intensity following administration of Sulpiride (50mg/kg, i.v)

The first row shows annotated and labelled high resolution template images such that the areas displaying changes may be identified according to the rat atlas (Paxinos & Watson, 1993). The middle row shows the effects of amphetamine using fixed effects analysis, the bottom row using random effects analysis.

A: Bregma= +47mm Olfactory cortex

B: Bregma= +1.7mm Nucleus accumbens, caudate-putamen, septum, M1

C: Bregma = -1.3mm Caudate-putamen, globus pallidus, septum, cingulum

D: Bregma= -3.3mm Ventral-posterior and ventromedial thalamus, cingulum

E: Bregma = -6..3mm Superior colliculus, VTA

F: Bregma= -8.3mm Inferior colliculus, Pontine reticular nucleus

Fig 7.3.1b shows the graphs representing the timecourse of signal intensity at specific voxels, activated as indicated by SPM t-Maps (Fig 7.3.1a), areas are named as corresponding to particular structures in accordance with the rat atlas. Areas of interest have been selected throughout the brain, and correspond to the brain slices of images illustrated above where possible.

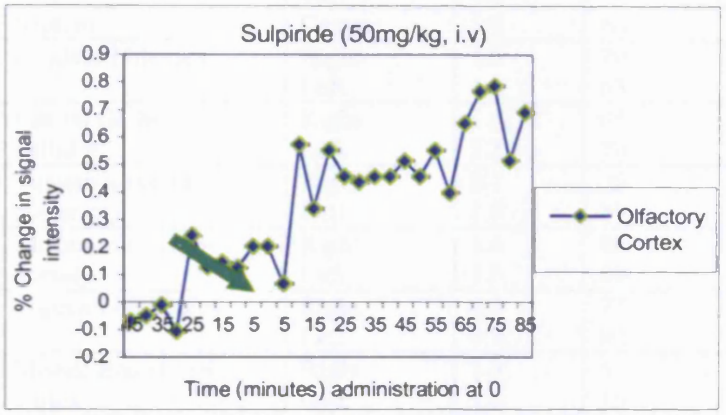

Bregma=-4.7mm

Olfactory cortex
T= 8.15 P<0.001

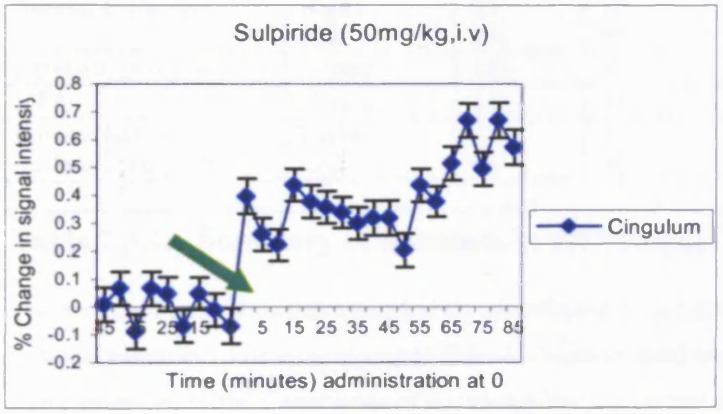

Bregma=-0.3mm

Cingulum
T= 8.05 P<0.001

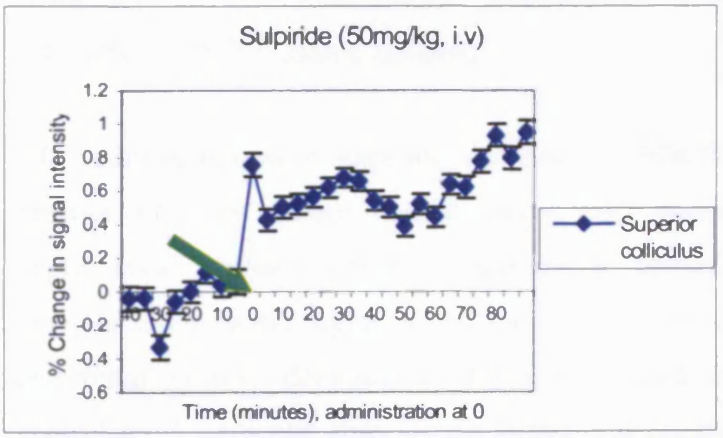

Bregma=-7.3mm
Superior colliculus
T= 10.0 P<0.001

Fig 7.3.1b

Graphs showing signal intensities at voxels of interest, increases in BOLD signal after administration of sulpiride (50mg/kg i.v.).

Green arrow indicates administration of sulpiride. Results are ± S.D of the mean.

Area	Left/ Right/ Centre	% Change	Time to peak	T-Value	P-Value	Random Effect
Olfactory cortex	Right Left	0.8 0.9	75 70	8.15 9.36	P<0.001 P<0.001	Yes Yes
M1 Motor Cortex	Right Left	1.4 1.3	70 70	17.2 15	P<0.001 P<0.001	No No
Cingulum	Centre	0.7	65	8.05	P<0.001	Yes
Nucleus Accumbens	Right Left	1.4 1.5	70 70	14.1 16.6	P<0.001 P<0.001	Yes Yes
Septum	Centre	1.8	60	13.24	P<0.001	Yes
Caudate-Putamen	Right Left	1.5 1.6	70 65	14.2 15.8	P<0.001 P<0.001	Yes Yes
Lateral Globus Pallidus	Right Left	1.9 2.3	65 70	18.6 18.9	P<0.001 P<0.001	No Yes
Thalamus (ventral-posterior)	Right Left	0.7 1.0	70 70	11.2 9.0	P<0.001 P<0.001	Yes Yes
Thalamus (medio-dorsal)	Right Left	1.6 1.6	80 80	14.7 14.6	P<0.001 P<0.001	No No
Superior colliculus	Right Left	0.9 0.9	75 80	10.0 10.6	P<0.001 P<0.001	No No
Medial Entorhinal cortex	Right Left	1.8 1.2	5 15	7.28 5.62	P<0.001 P<0.001	No No
Inferior colliculus	Right Left	0.7 0.8	80 80	6.8 7.4	P<0.001 P<0.001	No No
Cerebellum (Crus 2)	Centre	1.0	80	11.1	P<0.001	No
VTA	Centre	1.6	75	7.9	P<0.001	Yes
Pontine Reticular nucleus (oral part)	Right Left	1.1 1.3	70 70	13.21 11.67	P<0.001 P<0.001	Yes No

Table 7.3.1a Summary of increases in fMRI signal for Experiment 1

The corrected t-test shows that many areas are affected by sulpiride stimulation resulting in increases in signal intensity. The more stringent Gaussian random field model excludes some of the areas. Some examples of the timecourses of the stimulation are shown above (Fig 7.3.1.b).

Decreases in BOLD signal intensity

After administration of sulpiride, decreases in BOLD signal intensity were observed in anterior olfactory nucleus, frontal cortex, "M2" motor cortex, ventral pallidum, medial peptic area, piriform cortex, hippocampus commisure, lateral hypothalamic area, amygdala, substantia nigra, (V2)visual cortex, CA3 region of the hippocampus, lateral entorhinal cortex, dorsomedial PAG, brachium of the inferior colliculus (BIC), ventrolateral tegmental area, simple lobule and cerebellum (5^{th} /6^{th} lobules). Six brain slices are shown below to indicate the effect of sulpiride (0.5 mg/kg, i.v) throughout the brain. Table 7.3.1b shows that many of these areas were not significantly changed in the random effects analysis.

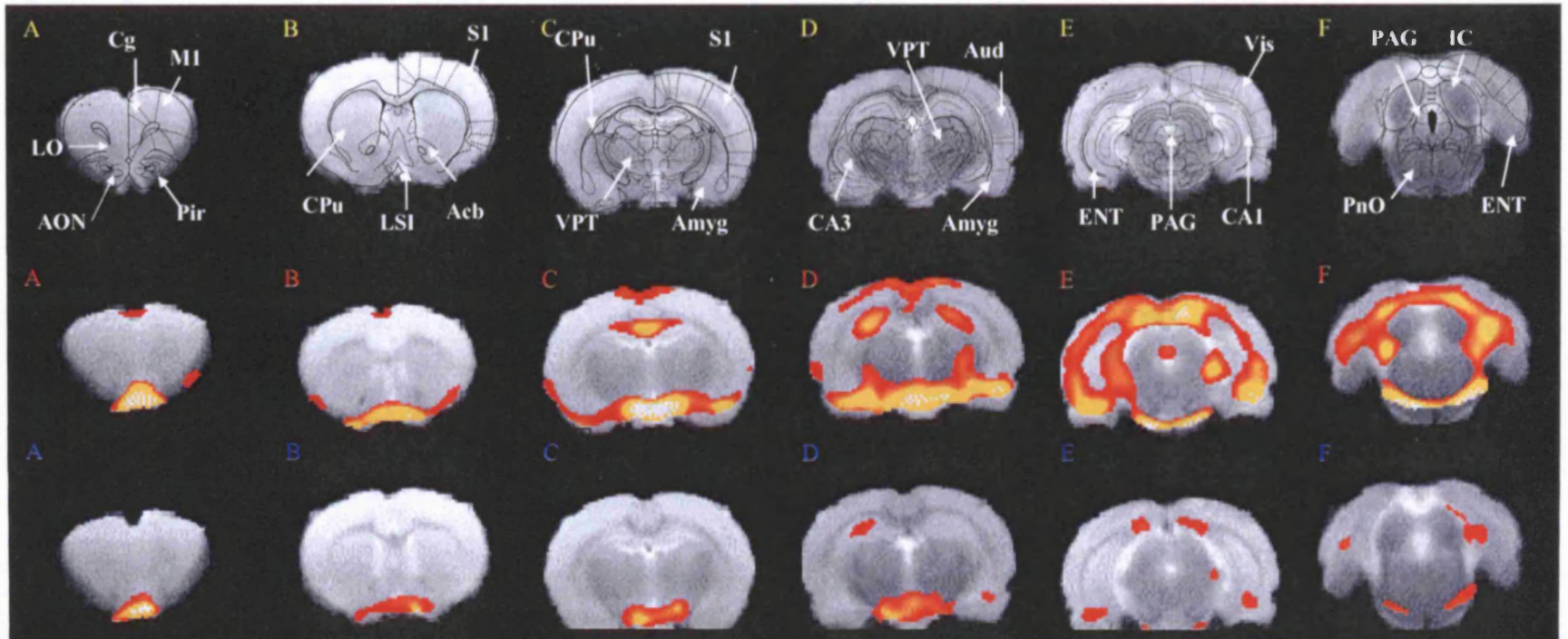

Fig 7.3.1c Decreases in signal intensity following administration of Sulpiride (50mg/kg, i.v)

The first row shows annotated and labelled high resolution template images such that the areas displaying changes may be identified according to the rat atlas (Paxinos & Watson, 1998). The middle row shows the effects of amphetamine using fixed effects analysis, the bottom row using random effects analysis.

A: Bregma= +3.7mm Anterior olfactory nucleus

B: Bregma= +0.7mm Ventral pallidum, piriform cortex

C: Bregma = -2.3mm Hypothalamus, dorsal hippocampal commisure

D: Bregma= -4.3mm Amygdala, piriform cortex, CA1

E: Bregma = -6.3mm Lateral entorhinal cortex, PAG, substantia nigra

F: Bregma= -8.3mm Visual cortex, ventrolateral tegmental area

Fig 7.3.1d shows graphs representing the timecourse of signal intensity at specific voxels, showing reduced BOLD as indicated by SPM t-Maps (as above), areas are named as corresponding to particular structures in accordance with the rat atlas. Areas of interest have been selected throughout the brain.

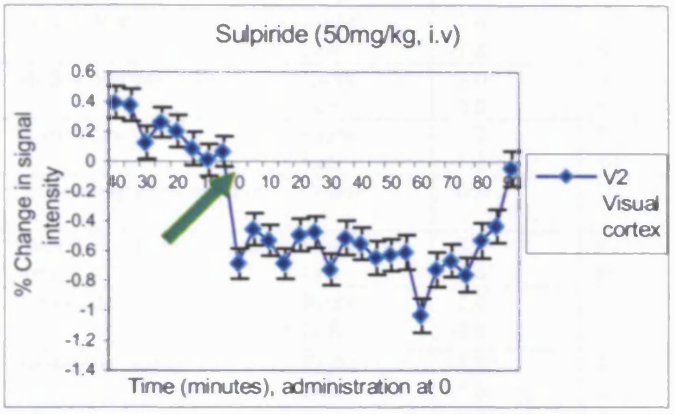

Bregma= -6.3mm

V2 Visual cortex
T= 8.4 P<0.001

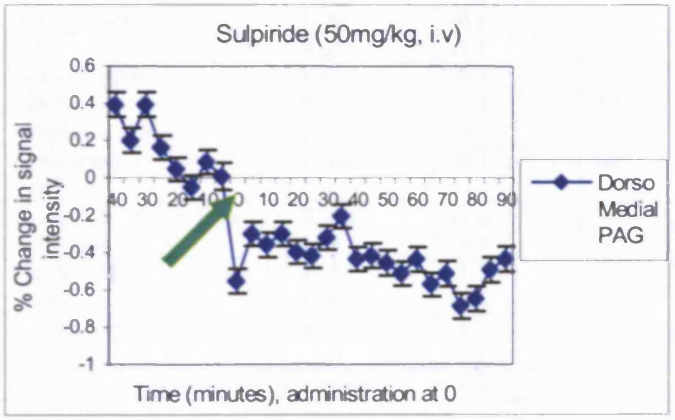

Bregma= +0.7mm

Piriform cortex
T=13.0 P<0.01

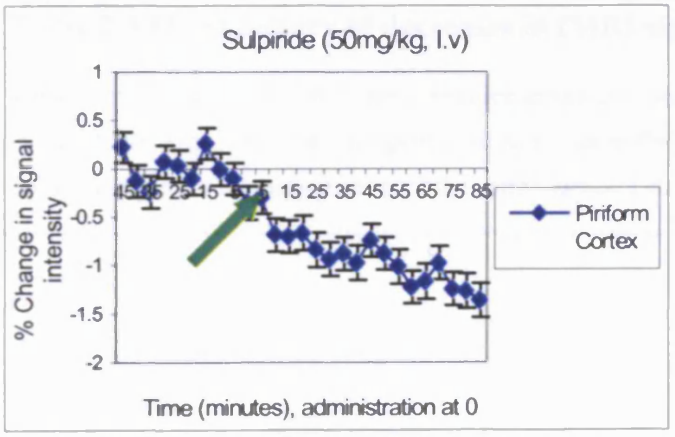

Bregma= -8.3mm

Dorsomedial PAG
T= 9.0 P<0.001

Fig 7.3.1d

Graphs showing signal intensities at voxels of interest, decreases in BOLD signal after administration of sulpiride (50mg/kg i.v.).

Green arrow indicates administration of sulpiride. Results are ± S.D of the mean

Area	Right/ Left/ Centre	% Change	Time to peak	T-Value	P-Value	Random Effect
Anterior olfactory nucleus	Right Left	-2.2 -1.3	55 45	17.94 15.92	P<0.001 P<0.001	Yes Yes
Frontal cortex	Right Left	-1.2 -0.7	80 60	8.96 8.31	P<0.001	No No
"M2" motor cortex	Right Left	-0.8	45	7.84	P<0.001	No No
Ventral Pallidum	Right Left	-2.0 -1.8	60 50	17.38 15.92	P<0.001 P<0.001	Yes Yes
Medial preoptic area	Right Left	-2.0 -2.0	60 50	17.52 19.02	P<0.001 P<0.001	Yes Yes
Piriform cortex	Right Left	-1.7 -1.2	75 70	13.0 6.9	P<0.001 P<0.001	Yes Yes
Hippocampal commisure	Centre	-0.9	70	14.1	P<0.001 P<0.001	No
Lateral Hypothalimic area	Right Left	-2.5 -2.4	85 80	19.2 21.5	P<0.001 P<0.001	Yes Yes
Amygdala	Right Left	-2.0 -1.4	75 75	10.1 10.9	P<0.001 P<0.001	Yes Yes
Substantia Nigra	Right Left	-1.9 -1.6	40 40	13.1 15.2	P<0.001 P<0.001	Yes Yes
V2 Visual cortex	Right Left	-1.0 -0.8	50 50	8.4 9.1	P<0.001 P<0.001	No No
CA3 region of the hippocampus	Right Left	-1.7 -0.9	55 40	12.4 9.0	P<0.001 P<0.001	No No
Lateral entorhinal cortex	Right Left	-3.9 -1.9	80 75	18.1 13.3	P<0.001 P<0.001	Yes Yes
Dorsomedial PAG	Centre	-0.7	65	9.0	P<0.001	No
Brachium of the inferior colliculus (BIC)	Right Left	-1.6 -0.9	70 60	13.0 10.1	P<0.001 P<0.001	No No
Ventrolateral tegmental area	Right Left	-2.7 -1.8	80 80	16 17.6	P<0.001 P<0.001	No No
Simple lobule	Right Left	-1.3 -1.7	80 60	12.0 11.1	P<0.001 P<0.001	No No
Cerebellum 5^{th}//6^{th} lobule	Centre	-1.1	15	12.0	P<0.001	No

Table 7.3.1b Summary of decreases in fMRI signal for Experiment 1

The corrected t-test shows that many areas are affected by sulpiride stimulation resulting in decreases in signal intensity. The more stringent Gaussian random field model excludes some of the areas. Some examples of the time-courses of the stimulation are shown above (Fig 7.3.1.d).

7.3.2 Results from Experiment 2: Quinpirole Administration (0.5mg/Kg, i.v)

Images were collected from 30 contiguous, coronal, 1mm brain slices. The Bonferroni corrected data showed that acute intravenous infusion of quinpirole caused significant changes in some brain areas ($P<0.01$).

After administration of quinpirole, increases in BOLD signal intensity were observed only in small clusters in discrete areas such as the prelimbic cortex, caudate-putamen, lateral septal nuclei, cingulate cortex, lateral habenula, ventral posterior thalamus, ventromedial thalamus, retrosplenal cortex, lateral PAG, superior colliculus and cerebellum.

Six brain slices are shown below to indicate the effect intravenous infusion of the D_2 agonist quinpirole throughout the brain, these areas are shown below in the t-Maps. Random Effects analysis, a more stringent test showed much less obvious decreases than with the fixed effect analysis. Table 7.3.1b shows that many of these areas were not significant in the random effects analysis.

Below (Fig 7.3.2b) the graphs representing the timecourse of signal intensity at specific voxels, showing increased BOLD as indicated by SPM t-Maps (as above), areas are named as corresponding to particular structures in accordance with the rat atlas. Areas of interest have been selected throughout the brain.

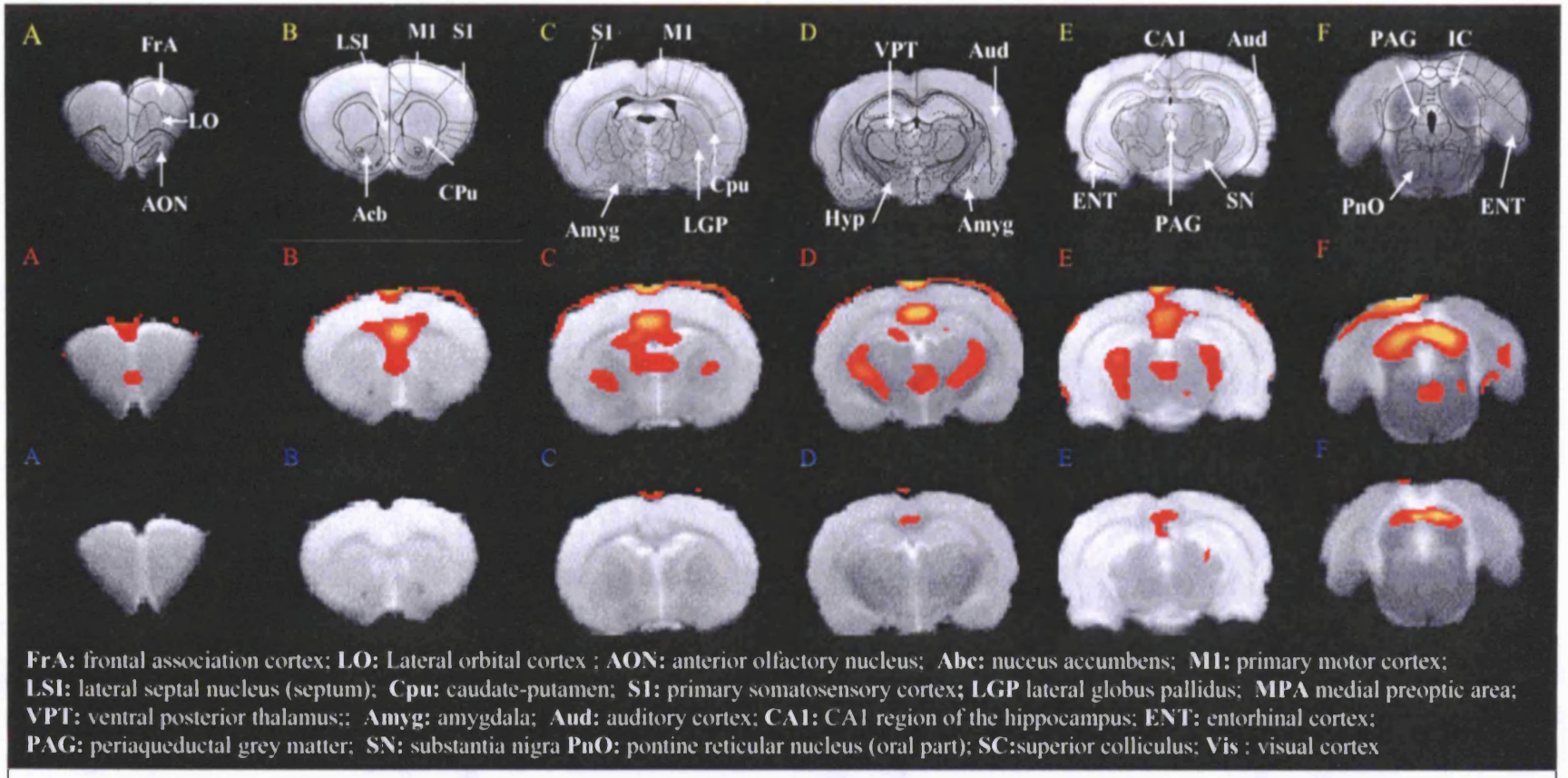

Fig 7.3.1a Increases in signal intensity following administration of Quinpirole (0.5mg/kg, i.v)

The first row shows annotated and labelled high resolution template images such that the areas displaying changes may be identified according to the rat atlas (Paxinos & Watson, 1998). The middle row shows the effects of amphetamine using fixed effects analysis, the bottom row using random effects analysis.

A: Bregma= +47mm Prelimbic cortex

B: Bregma= +1.7mm Lateral septal nuclei, cingulate cortex

C: Bregma = -1.3mm Cingulate cortex, caudate, ventromedial thalamus

D: Bregma= -3.3mm Ventral posterior thalamus, retrosplenal cortex

E: Bregma = -5.3mm Lateral PAG, medial geniculate nucleus

F: Bregma= -8.3mm Superior colliculus

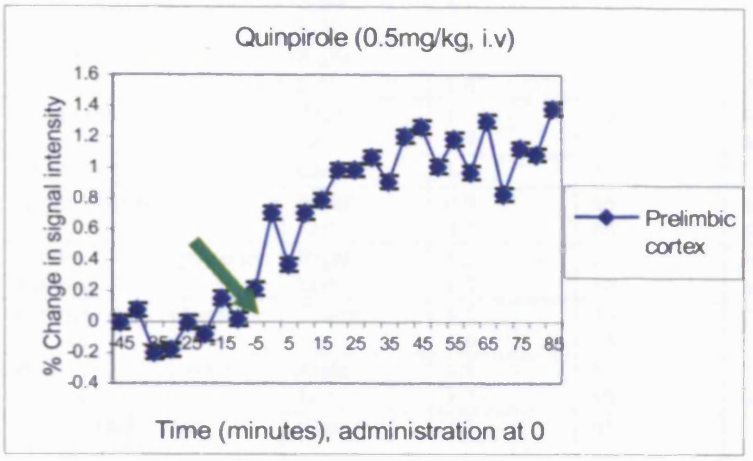

Bregma=+4.7mm

Prelimbic cortex
T=14.6, P<0.001

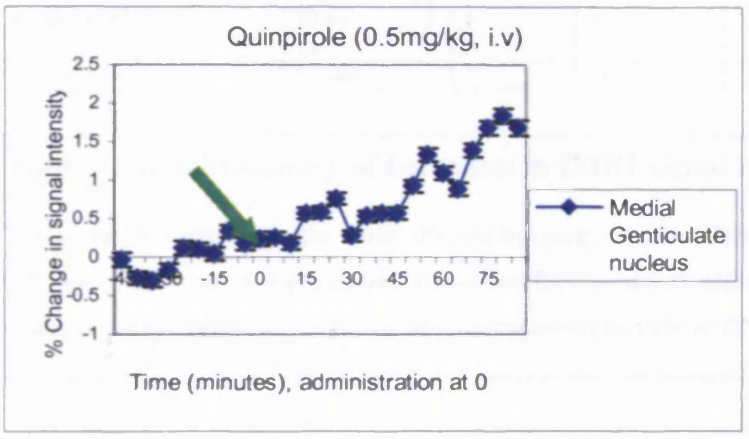

Bregma=-5.5mm

Medial geniculate nucleus
T=7.0, P<0.001

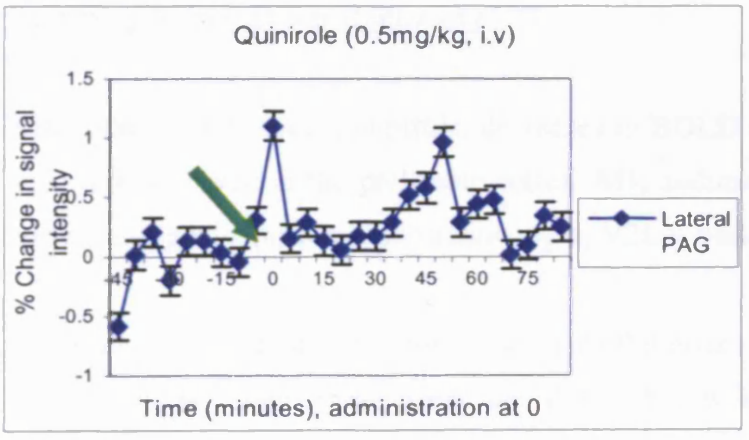

Bregma=-7.30mm

Lateral PAG
T=6.2, P<0.001

Fig 7.3.2b

Graphs showing signal intensities at voxels of interest, increases in BOLD signal after administration of quinpirole (0.5mg/kg i.v.).

Green arrow indicates administration of quinpirole. Results are ± S.D of the mean

Area	Right/ Left/ Centre	% Change	Time to peak	T-Value	P-Value	Random Effect
Prelimbic cortex	Right Left	1.1	75	14.6	P<0.001	No
Caudate-putamen	Right Left	2.1 1.6	55 35	7.0 7.2	P<0.001 P<0.001	No No
Lateral septal nuclei	Right Left	1.7 1.7	20 20	4.5 4.5	P<0.002 P<0.002	No No
Cingulate cortex	Centre	1.1	65	5.6	P<0.001	Yes
Lateral Habenula	Right Left	0.9 0.8	65 60	6.4 8.5	P<0.001 P<0.001	No No
Ventral posterior thalamus	Right Left	1.5 1.3	5 10	10.6 8.9	P<0.001 P<0.001	No No
Ventromedial thalamus	Centre	1.2 1.0	75 75	7.5 5.7	P<0.001 P<0.001	No No
Medial geniculate nucleus	Right Left	1.8 1.7	85 80	7.0 8.9	P<0.001 P<0.001	No No
Retrosplenal cortex	Centre	1.1	65	5.1	P<0.001	Yes
Lateral PAG	Centre	1.0	50	6.2	P<0.001	No
Superior colliculus	Right Left	1.4 1.3	80 80	8.3 8.0	P<0.001 P<0.001	Yes Yes
Cerebellum	Centre	1.4	60	5.81	P<0.001	Yes

Table 7.3.2.a Summary of Increases in fMRI signal for Experiment 2

The corrected t-test shows the areas affected by quinpirole stimulation resulting in increases in signal intensity. The more stringent Gaussian random field model excludes some of the areas. Some examples of the time-courses of the stimulation are shown above (Fig 7.3.2.b).

Decreases in BOLD signal intensity

After administration of quinpirole, decreases in BOLD signal intensity were prominent and were observed in the prelimbic cortex, M1, auditory cortex, S1 BF somatosensory cortex, amygdala, piriform, substantia nigra, V2L visual cortex and cerebellum.

Six brain slices are shown below to indicate the effect of the D_2 antagonist quinpirole throughout the brain, these areas are shown below in the t-Maps. Random effects analysis, a more stringent test showed much less obvious decreases than with the fixed effect analysis. Table 7.3.1b shows that many of these areas were not significantly changed in the random effects analysis.

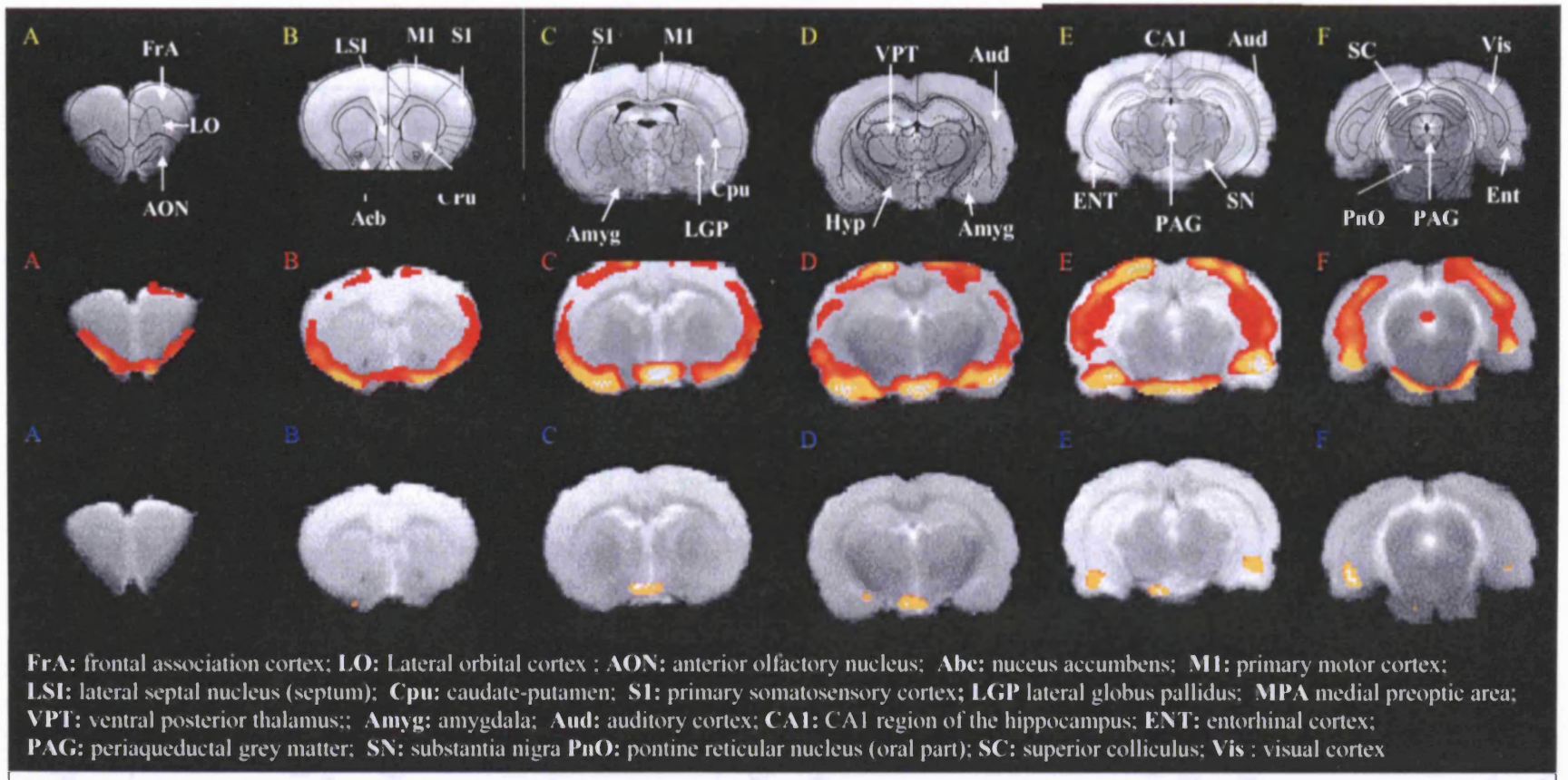

Fig 7.3.2.c Decreases in signal intensity following administration of Quinpirole (0.5mg/kg, i.v)

The first row shows annotated and labelled high resolution template images such that the areas displaying changes may be identified according to the rat atlas (Paxinos & Watson, 1998). The middle row shows the effects of amphetamine using fixed effects analysis, the bottom row using random effects analysis.

A: Bregma= +5.7mm Olfactory cortex

B: Bregma= +2.7mm Piriform cortex, M1 motor cortex

C: Bregma = -0.3mm Piriform cortex, S1 somatosensory cortex

D: Bregma= -3.3mm Piriform cortex, amygdala, hypothalamus

E: Bregma = -5.3mm Amygdalopir, visual cortex, auditory cortex

F: Bregma= -7.3mm Pontine reticular nucleus, visual cortex

Below are graphs representing the timecourse of signal intensity at specific voxels, showing decreased BOLD as indicated by SPM t-Maps (as above), areas are named as corresponding to particular structures in accordance with the rat atlas. Areas of interest have been selected throughout the brain.

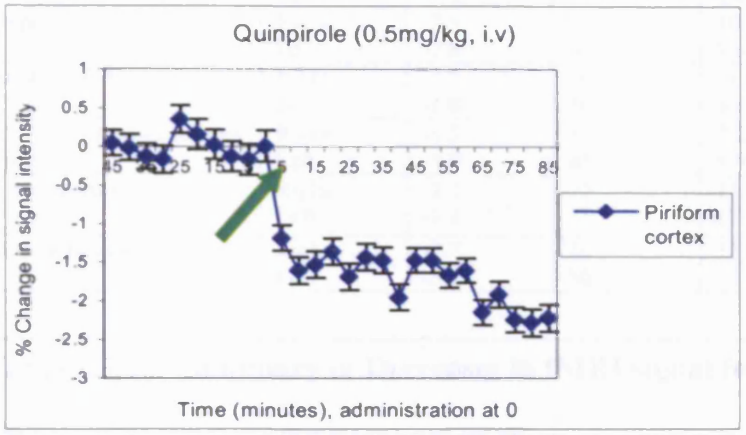

Bregma= +2.7mm

Piriform cortex
T= 16.2 P<0.001

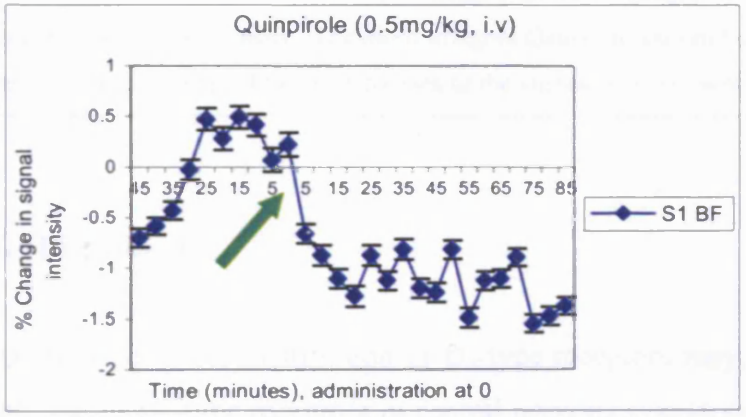

Bregma=-0.3mm

S1 Barrel Fields,
T=8.5 P<0.001

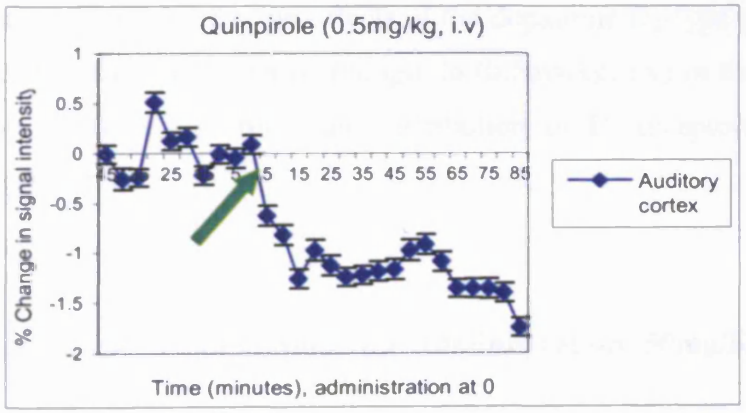

Bregma=-5.3mm

Auditory Cortex
T=11.6 P<0.001

Fig 7.3.2d

Graphs showing signal intensities at voxels of interest, decreases in BOLD signal after administration of quinpirole (0.5mg/kg i.v.).

Green arrow indicates administration of quinpirole. Results are ± S.D of the mean

Area	Right/ Left/ Centre	% Change	Time to peak	T-Value	P-Value	Random Effect
Piriform cortex	Right	-2.1	65	16.2	P<0.001	No
	Left	-1.4	70	12.2	P<0.001	No
M1 motor cortex	Right	-1.0	75	5.5	P<0.001	No
	Left	-0.7	75	6.5	P<0.001	No
Amydala	Right	-1.4	60	8.5	P<0.001	Yes
	Left	-1.6	65	9.6	P<0.001	Yes
Hypothalamus	Right	-2.5	55	10.1	P<0.001	Yes
	Left	-2.8	60	9.6	P<0.001	Yes
Auditory Cortex	Right	-1.7	80	11.6	P<0.001	No
	Left	-1.0	70	8.4	P<0.001	No
S1 somatosensensory cortex	Right	-1.5	55	7.2	P<0.001	No
	Left	-1.0	85	8.9	P<0.001	No
Visual cortex	Right	-1.1	75	11.0	P<0.001	No
	Left	-1.4	75	17.1	P<0.001	No
Substantia Nigra	Right	-2.7	50	12.0	P<0.001	Yes
	Left	-3.2	50	16.3	P<0.001	No

Table 7.3.2.b Summary of Decreases in fMRI signal for Experiment 2

The corrected t-test shows that many areas are affected by quinpirole stimulation resulting in decreases in signal intensity. The more stringent Gaussian random field model excludes some of the areas. Some examples of the time-courses of the stimulation are shown above (Fig 7.3.2.d).

7.4 Discussion

Knowledge of the distribution of D_2-type receptors may increase our understanding of the role of D_2-type receptors in central nervous system dopaminergic functionality. We have assessed the acute effects of the dopamine D_2-type antagonist Sulpiride (50mg/kg, i.v.) and D_2-type agonist quinpirole (0.5mg/kg, i.v) in the anaesthetised rat as detected by fMRI to determine the distribution of D_2 receptors and consequences of acute stimulation.

7.4.1 Experiment 1: Sulpiride Administration (50mg/Kg, i.v)

In this experiment, a single intravenous bolus of sulpiride (50mg/kg, i.v) was administered to halothane-anaesthetised rats and the difference in fMRI signal in the whole brain before, and after drug administration was determined. Using a simple T-test with derived p-values Bonferroni correction (fixed effects) and Gaussian random fields

(random effects) with a significant threshold of P>0.05 resulted in conservative probability maps that display prominent signal changes.

Numerous quantitative autoradiography studies using D_2 antagonists have been used to visualize dopamine ligand D_2-type binding sites in rat brain (Gehlert & Wamsley, 1984; Boyson et al, 1986). The highest concentration of binding to the D_2-type site is largely restricted to the "striatal complex", i.e. the caudate-putamen, nucleus accumbens septi, and olfactory tubercle (Camps et al, 1989), but significant densities are also observed in substantia nigra, globus pallidus, CA1, CA3, dentate gyrus and the amygdala. Using [^{125}I]iodosulpride labelling in receptor studies: many other areas were also found to contain D_2-type receptors, including large areas of the cerebral cortex, tectal areas and numerous brainstem areas (Bouthenet et al, 1987). [^{125}I]iodosulpride also identified sites corresponding to dopamine in the cerebellum, in the hippocampal formation, several septal, thalamic and hypothalamic nuclei. Large numbers of D_2-type receptors were also shown in areas corresponding to cells of origin and established projection fields of the mesostriatal and mesolimbocortical systems (Bouthenet et al, 1987).

It can be seen from Fig 7.3.1a that acute administration of sulpiride has clearly caused increases in signal intensity in many areas, including many of the areas observed using quantitative radiography. The majority of rostral, subcortical dopaminergic structures appear to be involved, including, olfactory areas, nucleus accumbens, caudate-putamen, globus pallidus and thalamic nuclei in a manner similar to amphetamine (Fig 5.3.1c). A number of brain regions shown here (7.3.1) are known to contain terminals from several different dopaminergic neuronal systems (Lindvall & Bjorklund, 1976; Moore & Bloom, 1979), including the nigrostriatal pathway (caudate-putamen) and the mesocortical system (nucleus accumbens and the olfactory tubercle).

The increases in BOLD are also visible throughout the rostral motor and somatosensory cortices (Fig 7.4.1a, imgs B & C). In studying images generated by the more significant random effects analysis, the subcortical activation is most obvious, as is the omission of activity of the cortical layer (compare the middle and bottom row of images B & C in Fig 7.3.1a). Using microdialysis, Moghaddam & Bunney (1990b) found that following many doses of sulpiride, the extracellular level of dopamine in the medial prefrontal cortex was significantly affected and also that dopamine uptake inhibitors and dopamine

D_2 antagonists were found to have a lesser effect in this region than in the striatum and nucleus accumbens (Hadfield & Nugent, 1983; Moghaddam & Bunney, 1990b). This may be due to the low levels of D_2 autoreceptors found in this area (Sokoloff et al, 1990). Despite the lack of positive functional evidence involving D_2 receptors in the cortex in sulpiride-mediated behaviours, [^{125}I] iodosulpiride autoradiography studies found D_2 receptors to be present in the sensorimotor cerebral cortex and cerebellum (Martres et al, 1995).

The globus pallidus showed increased BOLD response following acute sulpiride challenge, although there is a dense dopaminergic innervation in these regions, BOLD signal changes are not usually detected in this region (Chen et al, 1997: Preece et al, 2001). However many other physiological techniques have indicated action of dopamine D_2 antagonists in basal ganglia and striatal regions: using *in vivo* microdialysis, acute administration of various classes of antipsychotic drugs may differentially increase the extracellular concentration of dopamine in the mesotelencephalic systems (Moghaddam & Bunney, 1990b) and in the striatum (Jaworski et al, 2001) and this is evident over a range of concentrations (Inoue et al, 1995); local hypothalamic injection, systemic infusion and intraperitoneal administration of sulpiride all induce an increase in basal accumbal dopamine and DOPAC, and also enhance eating (Westerink et al, 1994; Parada et al, 1995). These results indicate that a behaviourally induced stimulation of dopamine release is modified by autoinhibition of D_2 receptors. Thus these data are in agreement with the current fMRI data, which detected robust BOLD increases in and around the striatum and globus pallidus.

Sulpiride induced significant BOLD decreases in the substantia nigra and several limbic structures. These specific brain areas are involved in the control of cognitive functions and motivational and emotional behaviour (Heath, 1976), and the interaction with D_2-type receptors in these areas may explain the efficacy of this compound in the treatment of the negative symptoms of schizophrenia. However, these areas have also been studied using 2-deoxyglucose autoradiography where results show increases in RCGU (Cudennec et al, 1997). It was found that dopaminergic activity in the accumbens was under the inhibitory influence of dopaminergic transmission in the amygdala (Louilot et

al, 1987). However, functional interdependence exists between the different dopaminergic pathway arising in the ventral mesencephalon, as the nucleus accumbens can be oppositely modulated by pharmacological intervention in the septum or prefrontal cortex. Thus it is useful to have some studies investigating the effects of systemic administration in the intact brain, so the overall affect of this agent on the dopamine system can be more fully understood. However, as described in chapter 2, it is a misconception to believe that a negative BOLD response always equates to reduction in neuronal activity, and more specifically to dopamine release. This area is discussed in chapter 8.

In comparing the results of sulpiride administration with quantitative autoradiographic data, the areas displaying changes show many similarities, although some 2DG autoradiography experiments, (using haloperidol as the D_2 antagonist) revealed decreased uptake in most brain areas (McCulloch et al, 1982; Pizzolato et al 1984). It is noted that many areas showing the decrease are not functionally related to the dopaminergic system and this may be due to indirect propagation of the primary effects of haloperidol, i.e the metabolic response to haloperidol depends on brain concentration and duration of exposure to the drug. One can compare the present results with a similar fMRI experiment also carried out in rats, in which changes were only observed in the frontal cortex (Preece et al, 2001). That particular study study involved comparing several doses of sulpiride (3, 10 and 30mg/kg) and unusually imaging in the transverse plane, whereas most rat phMRI studies display changes in the coronal plane to make comparisons between results easier and to also helps visualisation of the dopamine system (Chen et al, 1997; Marota et al, 2000).

The temporal responses show a general trend of incrementally increasing or deceasing, 1-2 scans after administration of either drug. The maximal increases or decrease however, did not occur in some cases until the last scan. Although a previous fMRI study, investigating various doses of sulpiride in the alpha chloralose anaesthetised rat saw elevations in BOLD signal intensity that were evident up to 3 hrs after the drug was administered (Preece et al, 2001), the initial incremental change on injection was not observed in this study. The results obtained by Preece et al (2000) are different those described in the current work (7.3.1) but this may be due to the differences in anaesthetics used in the two studies. α-chloralose is thought to suppress dopaminergic

activity in subcortical structures (see chapter 3). Furthermore, although Preece et al (2001) used asymmetrical spin echo, which provides good resolution and SNR, they used a surface coil (unlike the multisurface coil used in the experiments described), thus the signals from the subcortex would not be detected as reliably as from the cortex.

Although the negative changes are not fully understood, the action of acute administration of sulpiride in causing a widespread increase in BOLD response is indeed in agreement with its effect on neurochemistry and behaviour. One fMRI investigation examined at the effects of acute, and acute after chronic administration of haloperidol, and found both dosing schedules to cause widespread deceases in BOLD signal (Hagino et al, 1998). The D_2 autoinhibitory receptors are blocked by sulpiride and thus a disinhibition of many structures is thought to occur, thus facilitating neurotransmission. This is what happens on commencement of a course of antipsychotics (Parada et al, 1995). It would be very interesting to investigate the adaptive changes to the dopaminergic system with chronic antipsychotic treatment, and to carry out fMRI studies in parallel with microdialysis to measure concentrations of dopamine and HVA. In performing such a longitudinal study, it would be of great interest to observe how the BOLD response changes as depolarisation block occurs, and to correlate the changes with neurotransmitter release patterns. Such a study would give a true validation of BOLD and would help elucidate the contributions of the BOLD signal, especially as the dopamine system would be dynamically and temporally adapting.

Another interesting study would be to repeat the experiments carried out by Preece et al (2001), thereby investigating dose responses to sulpiride using halothane anaesthetised rats and SE imaging. Preece et al suggested that differential effects caused by different doses of sulpiride may be due to sulpiride acting at "both inhibitory and activating sites that act in opposition physiologically". Should this be the case, it would be interesting to carry out this experiment, using different dosing schedules and observe the changes in the whole brain.

7.4.2 Experiment 2: Quinpirole Administration (0.5mg/Kg, i.v)

The data in experiment 2 indicate that acute intravenous administration of quinpirole at a dose of 0.5 mg/kg, results in bilateral increases and decreases in BOLD signal intensity throughout the brain of the halothane-anaesthetised rat. The images show the response to acute quinpirole challenge to be very discrete, and the increases to be localised to small clusters. Nevertheless, acute intravenous administration of 0.5mg/kg quinpirole resulted in increases in BOLD signal in several sub-cortical structures (Fig 7.4.2a), and these t-Maps also show patterns of BOLD activation, which extend throughout the whole of the brain. The increases in BOLD were observed to develop over the time course of the experiment, such that an elevation in BOLD signal intensity was still evident at the end of the experiment, 1.5 hours after drug administration (Fig 7.3.2.b & d).

The increases in BOLD signal were observed in the prelimbic cortex, caudate-putamen (dorsally), lateral habenula, ventral-posterior and ventro-medial thalamus, medial geniculate nucleus, retrosplenal cortex, lateral PAG, superior colliculus and cerebellum (displayed in tables 7.3.2a & b, respectively). Some of these areas have been identified using quantitative autoradiography (using labelled [^{3}H]quinpirole- Gehlert, 1993) as being rich in dopamine D_2-type receptors. The highest densities of [^{3}H]quinpirole binding were found in the caudate-putamen, nucleus accumbens, islands of Calleja, and olfactory tubercle (Gehlert, 1993).

Although the increased BOLD response with quinpirole is unexpected, when it is compared to that of the amphetamine treated group as displayed in section 5.3.1 (where the D_1-type receptors are also stimulated) and the sulpiride treated group as shown in section 7.3.1 (where the D_2 inhibitory receptors are blocked), it is clear that quinpirole has caused a much lesser dopaminergic effect on the brain. In fact when once compares the results of amphetamine pretreated, with D_1 antagonist treatment as displayed in section 5.3.2 (such that the amphetamine is theoretically acting only on D_2 receptors), the results are strikingly similar, although the quinpirole treated cohort display smaller changes in striatal BOLD signal. Dopamine D_2 agonist induced increases in local brain metabolism has been documented: a 2DG study investigating the effect of acute bromocriptine administration also found metabolic increases in various brain areas, such

as the thalamic nuclei, cerebellum and brainstem nuclei (Pizzolato et al, 1985) and an fMRI study found metabolic increases in the thalamus and parietal cortex (Hagino et al, 1998).

The involvement of the medial geniculate nucleus (Fig 7.3.2a, img E) is particularly interesting. In rats and cats ionotophoretic administration of both quinpirole and dopamine can produce both facilitation and inhibition of evoked activity in the medial geniculate cells (Albrecht et al, 1996; Zhao et al 2001). Engber et al (1993), found quinpirole to reduce 2-deoxyglucose uptake in the lateral habenula, a region which receives afferent input from entopeduncular nucleus, however quinpirole was also found to induce small increases in *fos*-like immunoreactivity within the lateral habenula (Wirtshafter & Krebs, 1997). These dose-dependant, opposite behaviours may be the reason why some structures, which are classically inhibited by activation of dopamine D_2-type receptors, do in fact show small, yet measurable increases in BOLD signal. Acute application of dopamine/apomorphine to dopamine cell bodies in the substantia nigra or ventral tegmentum stimulates D_2 autoreceptor and decreases dopamine firing (Aghajanian & Bunney, 1977), quinpirole could be expected to have the same effect.

Quantitative autoradiographic analysis revealed that the density of D_2-type receptors was decreased following chronic treatment with quinpirole (Subramaniam, et al, 1992) as does the level of D_2 receptor mRNA (Chen et al, 1993). Using microdialysis, various studies in primates and rodents have shown that quinpirole decreased accumbal spontaneous dopamine release (Davis et al, 1997) and also caused a dose-dependant inhibition of dopamine and acetylcholine release in the striatum (DeBoer et al, 1996), and also in the amygdala (Bull et al, 1991). It is inhibitory to such a degree that Engberger et al (1990) observed that quinpirole did not increase glucose utilization in any brain region.

The random effects analysis did not demonstrate a strong trend in changes in BOLD signal after quinpirole administration: a number of clusters of significant voxels were observed around the cingulate and retrosplenal cortex, superior collicuclus and decreases in the amygdala and hypothalamus and right substantia nigra. Thus, the results indicate that quinpirole does not have as large an effect on BOLD as compared to sulpiride and amphetamine. This indicates that the D_2 receptors may have a tonic

inhibitory action, and therefore blocking of the presynaptic receptors results in large a increase in midbrain dopamine systems BOLD response. Furthermore, the similarity between the results of acute quinpirole challenge and challenge with amphetamine pretreated with dopamine D_1 receptor antagonist SCH23390 (5.3.2), indicates that a large proportion of amphetamine action is not due to stimulation of dopamine D_2 inhibitory preysnaptic autoreceptors.

7.4.3 Conclusion

Stimulating dopamine D_2 autoinhibitory receptors results in spatially restricted increases and decreases in BOLD effect and in areas directly and indirectly innervated by the dopaminergic system. Blocking dopamine D_2 autoinhibitory receptors with specific antagonists results in large and marked effects throughout the brain.

When the random effects of sulpiride and quinpirole administration are compared, the differences are striking. The increases in BOLD caused by sulpiride as detected using random effects analysis include most of the subcortical striatal, thalamic and basal ganglia structures, whereas quinpirole administration only causes a significant random effect in the cingulate and retrosplenal cortex. This would suggest that these receptors are normally, tonically inhibited by dopamine, thus after administering sulpiride, the tonic inhibition is removed resulting in a net increase in activity in the region where the disinhibited receptors are situated. As such, many structures show an increase in BOLD signal, indicating increases in metabolic demand and activity. Quinpirole, on the other hand, (which will have the same effect as endogenous brain dopamine) causes little change to the normal physiology. When comparing the random effect analysis results of the decreases in BOLD, the results from sulpiride and quinpirole are more similar, but again sulpiride shows a more robust response thoughout the hypothamalus, medial preoptic area, amygdala and piriform cortex. Such widespread effects have not been reported using fMRI to date, whether this is due to imaging hardware constraints (if the surface coil is unable to obtain a signal from deep structures) or if the investigators have not been sampling the whole brain remains to be seen. Although the sign of the response is not necessarily indicative to whether excitation or inhibition is happening, it is clear that the pharmacological agents are modulating the dopamine system. This may

be beneficial in characterising new drugs, dopaminergic, or otherwise for their temporal and spatial effects throughout the brain, for example in looking for an antipsychotic which does not result in extrapyramidal symptoms.

What is interesting is that in both cases the BOLD decreases are generally in these same (often limbic) structures, where the drugs are theoretically acting in opposition. One reason may be that both sulpiride and quinpirole have actions on dopamine D_2 postsynaptic receptors, which are facilitatory. If the doses allowed differential activation of D_2 pre- and postsynaptic receptors, although the major influence would be on the presynaptic receptors, perhaps some postsynaptic activity also occurs.

Most early studies have suggested that presynaptic effects of dopamine are mediated by D_2-type receptors, as autoreceptor activity tends to display a pharmacology similar to D_2-type receptor. However Filloux et al (1988), demonstrated that postsynaptic D_2-type dopamine receptors in the caudate-putamen. Furthermore, sulpiride, in addition to blocking D_2 presynaptic receptors also blocks postsynaptic D_2 dopamine receptors (Gordon et al, 1987). Quinpirole is though to have some action at postsynaptic receptors, this explains its biphasic effect on locomotion (Storey et al, 1995): high doses of quinpirole initially suppress and later activate locomotion during a single test session and the activation is presumably due to stimulation of postsynaptic receptors (Frantz & Van Hartesveldt, 1995).

Functional MRI studies using pharmacological agents, and specifically dopaminergic drugs can be difficult to interpret, especially when one drug may target different types of receptor, i.e presynaptic and postsynaptic. Further to the possibility of non-specific (or unintentional) effects, is the fact that the dopamine system is working in concert with other systems, for example GABA and glutamate. Moreover, the 5 minute scan time is supposed to be a "snapshot" of the metabolic events relating to the pharmacologically stimulated synaptic activity. Thus from the spatial and temporal data obtained we can attempt to build a picture, but finer details require either sacrificing temporal resolution for spatial resolution, or vice versa, or incorporating another technique, such as *in vivo* microdialysis in such studies.

Chapter 8

General Discussion

8.1 Pharmacological MRI to study Dopaminergic Activity

The last decade has brought a considerable progress in understanding dopamine physiology of the brain. The suggestions that dopamine systems are involved in "motor control" and "reward" represent the classic working hypotheses on the behavioural functions of these systems (as described in Chapter 1). However, the research generated by many techniques has revealed that the dopaminergic system is far more complicated than the above (Salamone, 1992). Dopamine receptors may be important in the pathogenesis of several human diseases, including movement disorders (Agid et al, 1993), drug abuse (Self et al, 1996), major depression (Gambarana et al, 1995), schizophrenia (Okubo et al, 1997), working memory function (Williams & Goldman-Rakic, 1995) and are also thought to be important in the control of normal movement and appetitive behaviour (Jackson & Westling-Danielsson, 1994).

The study of receptor function in the brain following perturbation of dopamine transmission helps our understanding of the consequences of blockade of dopamine receptors (as occurring following antipsychotic treatment); interruption of dopaminergic transmission (as occurring in Parkinson's disease), or following hyperactivation of the dopamine system (observed following abuse of psychostimulants like cocaine and amphetamine). One approach in such studies is to administer a receptor-specific agonist and evaluate its acute effects on regional CBF or metabolism as an index of a regional change in neural activity. This has been widely performed using the 2DG approach by examining regional metabolic responses to an acute dose of various dopaminergic drugs (Ingvar et al, 1983; Pizzolato et al, 1987). These studies have revealed substantial information about the rodent brain's functional response to lesions in the dopaminergic system or treatment with dopaminergic agents (Orzi et al. 1993; Trugman 1995; Wooten and Trugman 1989). Notably, this method is sensitive to functional changes that cannot be detected by measuring receptor binding alone (McCulloch and Teasedale 1979; Trugman and James 1992). Images acquired using the 2DG method still constitute some of the most precise and reliable depictions of brain activation available, due to their high spatial resolution and the apparently direct relationship between cellular activity and

glucose activation (Raichle et al, 1976; Sokoloff, 1981). The disadvantage of the 2DG technique is that only one time-point for each cohort of animals is obtained, and thus to study dynamic pharmacological changes, many groups of animals may be required. A more indirect approach includes PET and fMRI, which offer far better spatial resolution allowing precise matching of functional changes to anatomical structures. The physiological basis of these methods is the fact that brain cell activity is associated with local changes in metabolism, especially glucose and O_2 consumption via neurovascular coupling. The process of producing functional images by these devices can be thought of as a functional convolution. In this respect, fMRI is an attractive application of NMR In particular the possibility of studying pharmacological agents, therapeutic or otherwise, has made it possible to map both spatial and temporal drug effects throughout the brain.

While fMRI has been widely used in cognitive neuroscience, its applications in neuropharmacology have been scarcer. Nevertheless, the direct effects of cocaine (Breiter et al, 1997) and nicotine (Stein et al, 1998) in humans and of amphetamine and other dopaminergic drugs in rats (Chen et al, 1997) on localized brain activation have been studied by means of BOLD-fMRI. Due to the small signal changes in response to neuronal activation this approach necessitates the use of potent and rapidly acting drugs.

In this study, fMRI was applied to assess the neurostimulatory effects of D-amphetamine (3mg/kg, i.v) and other dopaminergic ligands. The first study (Chapter 5) initially applied fMRI techniques to examine the effects of amphetamine alone and these techniques were then applied to examine the effects of prior pre-treatment with D_1 and D_2 antagonists on the amphetamine stimulated fMRI signal.

Acute intravenous administration of amphetamine changed BOLD signal intensity in multiple brain regions. The increases in BOLD signal were evident mostly in subcortical structures, and decreases in BOLD signal were largely observed in the motor cortex somatosensory cortex and some deeper subcortical (limbic) structures. This

anatomical pattern of amphetamine-induced changes strongly correlated with dopamine receptor distribution and pathways. The identification of differential responses of projections to inner and outer cortical layers may suggest a new dimension of complexity to understanding the response of the CNS to activation by amphetamine.

Following pre-treatment with D_1 antagonist (SCH23390), the administration of 3mg/kg amphetamine caused a spatially reduced BOLD response, as compared to when amphetamine was administered alone, indicating that the antagonist may have blocked some D_1-type receptors on which the amphetamine was acting. In fact the response is similar to that of the D_2 agonist quinpirole (Chapter 7), indicating that the residual response could be attributed to D_2-type receptor stimulation. Investigation of the effects of D_2 antagonist (sulpiride) pre-treatment on increases in BOLD signal intensity after amphetamine administration, were found to give very similar results. However, a number of areas previously demonstrating a decrease in fMRI signal on amphetamine administration showed no such decreases.

As discussed in Chapter 5, these data highlight the importance of signal transduction at the level of the D_1-type and D_2-type receptors, and reinforce the importance of ascending dopamine input to cortical and subcortical structures as critical determinants of amphetamine induced brain activation at behaviourally effective doses. While the antagonists clearly block the amphetamine response in some areas, understanding the pharmacological dynamics where a BOLD response is still present, a more difficult task, because the nature of amphetamine-stimulated BOLD response is not simply due to presynaptic uptake or post synaptic stimulation of D_1-type and D_2-type receptors, it is due to a combination of both.

The components contributing to the fMRI signal (CMR_{O2}, CBF and CBV) have been correlated over a range of activity using MRI and MRS in pharmacological experiments, and from these data the BOLD signal has been calibrated (Kida et al, 2000). Despite the linearity of the data, the "resting" condition in this study was morphine anaesthesia. The effects of anaesthesia and systemic drug administration must not be ignored: as demonstrated in Chapter 3, anaesthetics may have heterogeneous effects in particular brain regions and on specific transmitter systems and also may affect neurovascular coupling.

8.2 Dopamine Pharmacology and Anaesthetics

As discussed in Chapter 3, when performing fMRI on animals, it is a requirement that they are immobilised and anaesthetised prior to and during the experiment. Lhati et al (1998), found that the propofol-anaesthetised rat had a significantly reduced fMRI signal change as compared to the conscious rat. The regulators of animal experimentation in the UK (Home Office Inspectors) state that procedures such as these should be under anaesthetic. Furthermore, immobilisation is considered to be a severe stressor and as such has significant effects on neurochemistry and behaviour (Bliss et al, 1968; Abercrombie et al, 1989). More specifically, immobilisation stress was found to increase dopamine turnover in the frontal cortex and nucleus accumbens (Anderson & Fillenz, 1984; Imperato et al, 1991).

It is worthwhile to consider the effects of anaesthesia on brain dopamine function before commencing an fMRI study. In Chapter 3, a review of the literature showed that different anaesthetics commonly used in physiological and pharmacological experiments have heterogeneous effects on brain dopamine systems. The results showed that amphetamine stimulation, footshock and potassium stimulation evoked increases in dopamine levels were preserved in both halothane- and urethane-anaesthetised rats and these responses were similar to levels observed in unanaesthetised rats (Abercrombie et al, 1989; Hamamura & Fibiger, 1993; Young et al, 1993; Warburton et al, 1996; Cass et al, 1998). Any stimulated dopamine effects that were seen in a-chloralose-anaesthetised rats were small and extremely variable. Thus, halothane anaesthesia was used in the current fMRI experiments. The choice of anaesthetic in such experiments is indeed a difficult question and may depend heavily on the type of investigation being carried out.

Whilst investigating the effects of anaesthesia on dopaminergic transmission, it should be noted that catecholamines have been implicated in the mechanisms of general anaesthesia, (Jouvet, 1969; Johnston et al, 1972) and by manipulating the dopamine system, possible confounds may be introduced into the experiment. The possibility that the extra neuronal concentration of catecholamines might be an important factor for anaesthetic requirement or anaesthetised state has been reported (Stoelting et al, 1975). Changes in transmitter levels do not distinguish cause from effect of anaesthesia, and experiments are needed to delineate what role, if any, the specific areas play in muscle

relaxation, analgesia, sleep or anaesthesia. Anaesthetic agents may also affect the coupling between CBF and $CMR_{O2;}$ for example pentobaribitone had more of a pronounced effect on CBF than on CMR_{O2}, resulting in a negative BOLD signal (Martin et al, 2000). Thus it is imperative that the level of anaesthesia is very stable throughout experiments, otherwise regional changes in BOLD may occur. Since it is easier to monitor and maintain stable anaesthesia with halothane than with urethane, this is the anaesthetic of choice for fMRI studies using dopaminergic drugs.

These data indicate that anaesthetic actions are far more complex than a general depression of cerebral activity, and are as yet, largely unexplored. The possibility that they may affect the magnitude and also direction of the response are discussed further in sections 8.3 & 8.4.

8.3 Dopamine D_1 and D_2 Receptor synergism

The results from studies with pre-treatment with specific dopamine D_1-type or D_2-type receptor antagonists caused quite differential effects on the amphetamine induced BOLD response. In Chapters 5, 6 and 7, specific dopamine ligands were used to selectively stimulate or block dopamine receptors.

Acute administration of SCH23390 caused both increases and decreases in BOLD signal intensity in a number of brain regions, which was strikingly similar to the effects produced by amphetamine. However this is surprising because the D_1-type receptors were blocked. These results indicate complex receptor events, and the symmetricity of the images and omission of certain structures suggests spatial specificity for the induced changes. While the areas affected are indeed those containing high densities of dopamine D_1-type receptors, the sign and spatial extent of the BOLD response was somewhat unexpected. Acute intravenous administration of D_1 agonist SKF398393, results in bilateral discrete increases and decreases in BOLD signal intensity throughout the brain of the rat and these areas have been identified using quantitative autoradiography with labelled [^{3}H]SKF38393 (Dubois et al, 1986) as being rich in dopamine D_1-type receptors. This is also in agreement with neurochemical findings (Walters & Howard, 1990; Bracci et al 2002).

Sulpiride administration caused increases in signal intensity in many areas, and these areas include many of those observed using quantitative radiography, in a manner similar to amphetamine:(Gehlert & Wamsely, 1984; Boyson et al, 1986). The action of sulpiride having a widespread increase in BOLD response is indeed in agreement with its effect on neurochemistry and also on behaviour following acute administration. The D_2 autoinhibitory receptors are blocked by sulpiride and thus a disinhibition of many structures is thought to occur, thus facilitating neurotransmission. This is exactly what happens on commencement of a course of antipsychotics (Parada et al, 1995).

Quinpirole, however did not have a large effect on BOLD as compared to sulpiride and amphetamine. This indicates that the D_2-type receptors may have a tonic inhibitory action and therefore blocking of the presynaptic receptors results in large increases in midbrain dopamine systems BOLD response. Furthermore, the similarity between the results of acute quinpirole challenge and amphetamine pretreated with dopamine D_1-type receptor antagonist SCH23390 (5.3.2), indicates that a large proportion of amphetamine action is not due to stimulation of dopamine D_2 inhibitory presynaptic autoreceptors. Stimulating dopamine D_2 autoinhibitory receptors results in spatially restricted increases and decreases in BOLD effect in dopaminergic areas. Blocking dopamine D_2 autoinhibitory receptors with specific antagonists results in large and marked effect throughout the brain. What is interesting is that in both cases, the decreases are in generally in these same (often limbic) structures where the drugs are theoretically acting in opposition. If the doses allowed differential activation of D_2 pre and postsynaptic receptors, although the bulk influence would be from the presynaptic receptors, perhaps the drugs did involve some postsynaptic activity also.

While the possible reasons for changes in BOLD response are discussed in sections 6.4.3 and 7.4.3 respectively, another aspect of dopamine pharmacology is put forward-i.e.synergism. Acute challenge with either D_1 or D_2 ligands caused some effects which were widespread and also some BOLD changes overlapped, indicating that the drugs may not be selectively targeting the receptor type in all brain areas. It may not be possible to completely identify the functions of the two receptor types as they have been shown to be functionally linked, (Goldstein et al, 1987) and in some brain areas may be acting synergistically.

Synergism involves concomitant stimulation of D_1-type and D_2-type receptors for the expression certain behaviours. There are various examples of dopamine D_1-D_2 synergism *in vivo*. The stereotypic behaviour induced by drugs such as apomorphine or amphetamine are blocked by either D_1 or D_2 antagonists (Iorio et al, 1983; Molloy & Waddington, 1984). This indicates that the behavioural effects of dopamine agonists involve both types of dopamine receptor. When D_1 and D_2 agonists are administered simultaneously, more intense stereotypy is observed than with D_2 agonists alone (Braun & Chase, 1986; Arnt & Perregaard, 1987). These behaviours illustrate that D_1-type and D_2-type receptors interact positively, or synergistically, in controlling aspects of motor function. Synergism is also illustrated in the fact that expression of immediate early gene *c-fos* in the basal ganglia of the intact dopaminergic system is elicited only by concomitant activation of both D_1-type and D_2-type receptors: specific D_1 or D_2 agonists will only elicit *c-fos* when the synergism is disrupted by means of a lesion (6OH-DA) or repeated reserpine treatment (LaHoste et al, 1993).

The co-localisation of D_1-type and D_2-type receptors within the same neuron is a topic which gives rise to controversial reports: some have found D_1-type and D_2-type receptors to be completely segregated into different populations of neurons (Gerfen et al, 1990; Curran & Watson, 1995) and others have found co-localisation (Surmeier et al, 1992; Ariano et al, 1992; Lester et al, 1993). It has been proposed that D_1/D_2 synergism may be occurring by the co-expression in the same neurons of D_1-type and D_2-type receptors (Carter-Russel et al, 1995). Interestingly, it was found that D_3 receptors were co-expressed with both D_1-type and D_2-type receptors differentially in the ventral striatum with subpopulations of substance-P and enkephalin neurons respectively, suggesting that this receptor may influence the synergistic D_1/ D_2 effects of dopamine in the nucleus accumbens (Le Moine & Bloch, 1996).

Even using the most specific of ligands, the fMRI changes detected after receptor stimulation or blockade may not be so discrete, firstly if the D_1-type and D_2-type receptors types are acting synergistically and secondly if they are co-localised. Using a selection of D_1 and D_2 agonists, Carlson and co-workers (1987) found that stimulation of D_1-type and D_2-type receptors might be necessary for full expression of postsynaptic effects of dopamine agonists. Positive interactions of D_1-type and D_2-type receptors were evident in the dependence of D_1 agonist effect on endogenous D_2 dopamine tone

(Ruskin et al. 1999). Another possible example of synergism is clozapine, which has been found to be a mixed but weak D_1/D_2 receptor antagonist (Brunello et al, 1995). This has prompted speculation that the synergism between D_1-type and D_2-type receptors might allow antipsychotic effects to be achieved below the threshold for unwanted motor side effects. It is thought that the D_1 antagonistic activity exerted by clozapine at low doses may preferentially enhance the extracellular concentration of dopamine in specific areas of the brain, such as the prefrontal cortex, where a dopaminergic hypoactivity has been suggested to be responsible in part for the negative symptoms of schizophrenia (Brunello et al, 1995). Dihydrexidine, the first high-affinity dopamine D_1-type receptor full agonist, is only 10-fold selective for D_1-type versus D_2-type receptors, having D_2 affinity similar to the prototypical agonist quinpirole (Mottola et al, 2002). Quantitative receptor competition autoradiography demonstrated that dihydrexidine bound to D_2-type receptors in striatum (predominantly postsynaptic receptor sites) with equal affinity as to D_2 sites in the substantia nigra (autoreceptor sites).

Thus, whilst investigating the fMRI signal by pharmacologically manipulating the function of a singular receptor type by using "selective" agonists and antagonists, there may be interactions from other receptor types. Granted, this is likely to be at lower affinities, but it may interact with the receptor being investigated, thus results of such studies must be interpreted carefully.

Thus the potential confounds in the experimental procedure have been described (i.e. the anaesthetics and the drugs themselves). In the following sections (8.4- 8.6), some BOLD fMRI issues relating to the experiments are considered, and subsequently (section 8.7) the topic of energetics is briefly discussed in the context of phMRI.

8.4 Source of "Negative BOLD"

All of the drugs administered in the studies described in Chapters 5, 6 and 7 show some level of negative BOLD. The decreases in BOLD signal were generally detected in limbic areas such as the amygdala, hypothalamic areas, piriform cortex, as well as some cortical areas and the substantia nigra (Fig 5.3.1b & c). This is a topic which has not

been thoroughly investigated, despite several groups observing such changes (Hagino et al, 1998; Born et al, 2002; Czisch et al, 2002; Rother et al 2002). Many fMRI studies are based on the detection of an increased BOLD response and consequently it is commonly related to task induced increases in "neuronal activity", such as visual tasks (Heeger et al, 1999), motor tasks (Karni et al, 1995) and pharmacological stimulation (Volkow et al, 1998). However, the experiments described in Chapters 5, 6 and 7 have demonstrated adjacent positive and negative BOLD response. In this section, the possible sources for negative BOLD are discussed, and the factors that may influence such changes are described.

8.4.1 Negative BOLD and Inhibition

Major contributions in the field of fMRI have been made with activation paradigms in which changes of the level of synaptic transmission and therefore in neuronal activity are detected through the measurement of cerebral blood flow (CBF) variations. Since the development of non-invasive imaging modalities have contributed to the advanced understanding of brain function, care should be taken in interpreting the data such techniques provide. In general, a negative BOLD response can be caused by an increase in the paramagnetic dHb concentration, which could result from a reduced regional CBF due to deactivation, or from altered neurovascular coupling during activation with impaired regional CBF increases in the light of elevated dHb production. Providing that neurovascular coupling is not altered during the experiment, does the negative BOLD responses reflect inhibition?

Experiments using 2DG autoradiography have shown inhibition to be a metabolically active process at the level of the synapse (Waldvogel & Van Gelderen, 2000). Using 2DG in the lateral superior olive during acoustic stimulation, Nudo & Masterton (1986) observed increased glucose metabolism in known excitatory and inhibitory afferents. Since there is a very close relationship between glucose consumption and blood flow, it may be that that both excitatory and inhibitory synaptic events produce CBF changes in the same direction. Thus, with excitation and inhibition inducing changes in the same direction, maps of metabolism and CBF may be in principal, ambiguous with respect to the underlying neurophysiological event. However, inhibitory synapses are less

numerous and strategically better located than excitatory synapses, indicating that inhibition may be more efficient (Koos & Tepper, 1999) and therefore less energy consuming, than excitation. Unlike excitation, inhibition evoked no measurable change in the blood-oxygenation-level-dependent signal in the motor cortex, indicating that inhibition is less metabolically demanding. Therefore, the "activation" seen in functional imaging studies probably results from excitation rather than inhibition (Waldvogel & Van Gelderen, 2000). However other groups have observed fMRI BOLD signals even under conditions that appear to involve inhibitory interactions (Heeger et al, 1999).

8.4.2 Mechanisms leading to Negative BOLD

So if inhibition does not cause negative BOLD, what are the decreases observed in chapters 5, 6 and 7 caused by? Negative BOLD has been observed in the vicinity of activated regions (Harel et al, 2001; Shmuel et al, 2001). This effect is generally explained by the "draining or stealing" of blood from adjacent non-neuronally active areas. Shmuel et al (2002) suggests that this may occur via a mechanism that involves a reduction in CBF to the less demanding regions in the human brain, i.e. a redirected CBF change. If this was the mechanism occurring in the described experiments, it would mean that on administration of amphetamine, the increased CBF is shunted from the cerebral cortex, limbic structures (amygdala and piriform cortex) and substantia nigra to other subcortical areas such as the striatum and basal ganglia. It need not represent reduced "activation" or inhibition of tonic dopaminergic activity: it could simply be a reflection of increased CMR_{O2} without the compensatory increase in CBF, which for some reason has been shunted to other structures. Increased CMR_{O2} with the same or reduced CBF would result in a reduction in T2*.

8.4.3 Cerebrovascular Uncoupling may cause Negative BOLD

Functional variations in cerebral cortical activity are accompanied by local changes in blood flow, but the mechanisms underlying this physiological coupling are not well understood. The sole issue of uncoupling between metabolism and CBF may remain as

a confounding factor for interpretation of neuroimaging studies. Experimental manipulations (for example, pharmacological or pathophysiological) may result in CBF or local brain metabolism becoming unreliable indices of neuronal activity. As such, activation studies or diagnosis of disease may be inaccurate since the regulatory mechanisms of CBF and metabolism coupling could be altered. Uncoupling between neuronal activity, metabolism and CBF can occur in various conditions such as pharmacological manipulations. For example, one study, which is especially relevant in the context of the experiments described (Chapters 5, 6 & 7), has indicated that dopamine causes a vasoconstriction in some blood vessels in the ferret frontal cortical slice preparation (Krimer et al, 1998). Similarly, physostigmine, a cholinergic antagonist, was also found to interfere with coupling-acteylcholine is a potent vasodilator innervating cortical interneurons, cerebral capillaries and microarterioles (Moro et al, 1995) and application of physostigmine increases basal CBF and decreases CMR_{glu} but leaves CMR_{O2} unchanged (Blin et al, 1997). Neurovascular coupling is also thought to be affected in pathophysiological states, i.e. Alzheimer's disease, where build-up of amyloid plaques may decreases CBF and energetic supplies to the cerebral parenchyma (De La Torre, 1994).

In these situations CBF may not be the most reliable index of cerebral metabolism and, putatively, of neuronal activity. Another problem is the unknown relationship between oxidative metabolism and CBF. Techniques such as fMRI actually record a very complex signal linked both to variations of CMR_{O2} and CBF, thus might fail to distinguish between the two parameters. Technological and physiological studies should be undertaken to characterise precisely the situation of coupling and or / uncoupling. Different techniques (autoradiography, PET, fMRI), species and paradigm conditions including pathophysiological models should be studied to elucidate such a pivotal concept.

The drug under investigation may also alter the coupling to result in the negative BOLD described. Dopamine, a neurotransmitter normally associated with neuromodulatory actions, may directly affect local cortical blood flow. Dopamine has been variously reported as relaxing cerebral vessels in spasm (Boullin et al, 1977) and constricting vessels in vitro (Edvinsson et al, 1977). Furthermore, dopaminergic axons were found to

innervate the intraparenchymal microvessels and in an *in vitro* slice preparation, dopamine induced vasomotor responses in the cortical vasculature (Krimer et al, 1998). These findings may be relevant to the mechanisms underlying changes in blood flow observed in circulatory and neuropsychiatric disorders.

Amphetamine administration is known to have an effect on CBF. Using SPECT, Devous et al (2001) found that amphetamine induces focal increases and decreases in regional CBF in healthy volunteers, in areas primarily innervated by dopamine pathways. Moreover, in agreement with our findings, Devous et al (2001) found CBF decreases in the motor cortex, thus if the CBF was enhanced in the subcortical structures as opposed to the cortex, although not necessarily indicative of inhibition or deactivation, a negative BOLD may be observed as the blood is shunted from the cortex. Additionally, the anaesthetic agent can also affect the neuronal activity as well as the neurovasular coupling (Arthurs & Boniface, 2001). Different anaesthetics, for example a-chloralose or halothane, may have differential effects on resting metabolism in dopaminergic structures (Chapter 3; Cash et al, 2001). Thus if an area is suppressed by the effects of an anaesthetic, it may have reduced energy requirements, consequently the CBF may be shunted to another brain region demonstrating a negative BOLD response. If anaesthetic requirement alters the dopamine monoamine transmission (as discussed in Chapter 3), this may in turn, also have an effect on cerebral vasculature.

8.4.4 Children display Negative BOLD

Another example of the negative BOLD signal change is observed in children: where a visual stimulation paradigm, which normally causes increases in BOLD in adults, causes BOLD decreases in children (Born et al, 2002). Similar results have been confirmed using near infra-red spectroscopy (Meek et al, 1995; 1998). This could be due to a greater increase in oxygen consumption than CBF increase, or to a CBF decrease. The BOLD decrease observed in children could be attributed to a greater proportional increase in CMR_{O2} and this is related to rapid synapse formation (Yamada et al, 1997) and children under the age of 8 weeks do not show this. Synapse formation is not (evidently) related to increased metabolism, but the presence of more synapses is

(Huttenlocher et al, 1982). In adults, the amount of CBF increase during functional activation seems to attenuate with age (Hock et al, 1995). Alterations in human CNS transmission occur with aging, and is also observed in rats: a reduction in stimulated dopamine release can be seen as soon as 10 months in the rat (Dobrev et al, 1995). If the changing BOLD pattern present in different developmental periods was evident in experimental animals, it may help elucidate this phenomenon and indeed provide further insight into the nature of the BOLD response.

8.4.5 Altered Cerebrovasculature can result in Negative BOLD

One other reason for a negative BOLD response is severely disturbed cerebral autoregulation (due to extracranial artery disease). This is thought to be due to oxygen consumption in the absence of a haemodynamic response (Rother et al, 2002). This rare case of a persisting uncoupling of oxygen metabolism and CBF serves as a model that supports changes of the cerebral blood oxygen saturation as the major contributor of the BOLD effect. Abnormal regional CBF responses are seen in PET studies in response to physiological stimulation of the sensorimotor cortex, despite normal brain function (Powers et al, 1988). The finding of a negative effect during somatosensory activation may be explained by oxygen utilisation and subsequent increases in dHb, in the absence of a haemodynamic response. This has implications on fMRI studies, as an absent or decreased BOLD response does not necessarily imply a lack of neuronal activation, it may be due to disturbed cerebrovascular reserve capacity in the presence of normal cortical function, i.e. we should consider if an experimental factor such as anaesthetic or drug, caused this.

8.5 Influence of Imaging Techniques: Spin Echo versus Gradient Echo

The detection of BOLD changes (positive and negative) throughout the whole brain, from the olfactory bulb to the cerebellum, were carried out in the using spin echo (SE) fMRI. In comparing our results, with those obtained by other groups performing pharmacological MRI, the changes observed here appear more widespread. Chen et al (1997) observed changes in the striatum and cortex; Preece et al (2001) detected

significant changes only in the frontal cortex; Marota et al, (2000) measured fMRI signal increases in various cortical areas, striatum and dorsal thalamus. Indeed, quantitative and functional autoradiographic data indicate that dopaminergic drugs have effects in many more brain regions (Weschler et al, 1979; Trugman & James, 1993) than the areas described in many fMRI investigations (Chen et al, 1997; Marota et al, 2000). A peripheral sensory stimulation such as footshock, was found to cause robust and significant release of dopamine in the nucleus accumbens, as detected using *in vivo* microdialysis (section 3.7.2). When this procedure is performed using fMRI, the accumbens does not display BOLD changes, instead, only the somatosensory cortex is described as showing changes (Hyder et al, 1994). This may be due to calibration of imaging coil to the cortical surface as opposed to subcortical structures. However, even simple tasks can involve extensive networks of neurons, distributed across the cerebrum and cerebellum. The use of techniques that allow a hypothesis to be adequately tested on the entire brain is essential to the identification of these networks.

Preliminary studies aimed at comparing the SE and GE techniques (ultimately in order to choose the most suitable imaging sequence) were performed prior to commencing the studies described in Chapters 5-7 (Shah, personal communication, 2002). This is briefly described below.

Studies in which the GE technique were used to investigate the effects of amphetamine administration revealed only 4 brain regions to be affected by the psychostimulant, whereas many more were detected by RARE SE (see Chapters 5, 6 & 7). The percentage change in signal intensity induced by amphetamine in GE was greater (3 - 8%) than when using SE (1-5%), proving to be more sensitive to change. However using GE, no negative BOLD response was detected after amphetamine administration. The use of gradient echo was deemed unfeasible for phMRI: in order to scan the whole brain within a 5-minute time frame, the number of excitations had to be kept to a minimum, thus the SNR was reduced (from >200 to <50). Ultimately, due to the SNR and time restraints, only 9 coronal brain slices were acquired. Thus as the experiments were aimed to investigate the effects of ligands throughout the whole of the brain, rather then specific areas highlighted in the literature, the quality of image was inferior to that which could be obtained using SE RARE. Additionally, artefacts (due to a lesser sensitivity to differences in magnetic susceptibility by tissue / air interface [Simonsen et

al, 2000]) meant that large segments of the hindbrain were unable to be imaged due to positioning of the ear canals.

As illustrated above, the type of imaging sequence may greatly influence the magnitude, spatial extent and variability of the results. In the experiments described (Chapters 5, 6 and 7), spin echo (SE) imaging was employed which measures T_2 contrast. The use of T_2 contrast in fMRI offers possible advantages in comparison with T_2* contrast: T_2 varies far less through the brain than T_2* does between cortical and subcortical structures and hence the degree of functional activation may be more readily compared between brain regions (Norris et al, 2002; Lowe et al, 2000). Subcortical regions have a lower volume of macrovessels and CSF protons than cortical regions, this indicates that T_2* changes have larger dependence on macrovessels and CSF than T_2 changes. Thus in using T_2* methods, in subcortical areas may require higher levels of imaging sensitivity to observe significant changes. The sensitivity of the experiment should hence be independent of position, in marked contrast to GE in which a large variation in T_2* values is to be expected. This point is especially important where the whole brain is being investigated, and where different pathways are affected. SE sequencing is advantageous over GE in that in that it is weighted towards the microvasculature, making it especially useful in depicting morphologic or functional changes specifically in the microvasculature (Kwong et al, 1992; Weisskoff et al, 1994; Boxerman et al, 1995).

SE methods are intrinsically more sensitive to field changes, with dimensions on the order of the diffusional path during echo time, (TE). GE times are sensitive to field changes over each volume - regardless of the scale of the distortions. The optimum sensitivity of SE methods is close to the diameter of the capillaries, this natural filter in SE BOLD fMRI can be used to ascertain predominant contribution of capillaries. However the BOLD signal change is evidently much weaker than for GE methods, due to a much reduced contribution form venules and veins.

GE imaging can reduce MR scan time dramatically. This is accomplished by using a very short TR so that total TA is reduced. However, the signal to noise ratio decreases as compared to SE, due to shorter TRs, but more echoes can be obtained per unit time, which can compensate somewhat for the former effect. One application of GE is echo

planar imaging (EPI), which allows whole brain images to be rapidly acquired. However, its main limitation is that magnetic field inhomogeneities in brain regions close to bone/air-filled sinuses result in a reduced signal to noise ratio and signal loss. The evidence indicates that SE may be more appropriate for whole-brain phMRI experiments. However in order to be certain, the experiments would need to repeated using optimised GE while keeping all experimental factors identical. The temporal resolution offered by GE is indeed tempting and may give a better insight into the shorter time-scale effect caused by the drugs. It may be of interest to look at other pulse sequences to examine CBF for "inflow effects" (section 2.7), as well as BOLD. If uncoupling occurs between CBF, CMR_{O2} and CMR_{glu}, then these features should show up as disparities in the signals

8.6 Statistical Assumptions and SPM

A critical factor determining the number of subjects to be used in a neuroimaging study is differentiating between inferences that pertain to the particular subjects studied and to those inferences that pertain to the population from which the subjects came. This is the equivalent to distinguishing between fixed and random effects analyses and points out that when making an inference at the population level, it is only possible to account for having a sample of subjects from the population. The distinction rises when one has several observations from each subject or session and this is clearly the case in fMRI.

All neuroimaging studies, and ensuing inferences, aim to make some comment about the population from which the studied subjects were sampled. There are two classes of inference. The first aims to establish the observed effect as a typical characteristic of the population while allowing for the fact that some of the subjects may not show this effect. This sort of inference may be entirely sufficient when trying to characterise generic aspects of human functional brain architectures, sufficient in the sense that a particular characteristic is typical, is more useful than not knowing this fact. Fixed-effect analyses are generally more sensitive than equivalent random-effect analyses. This is because fixed-effect analyses can harness the large degrees of freedom and small scan-to-scan variability (relative to the variability in responses from subject to subject) when assessing the significance of an estimated response. However, a disadvantage for

the apparent sensitivity of fixed-effect analyses is that the ensuing inferences pertain to, and only to, the subjects studied. The second inference, random effects analysis, aims to make an inference at the population level.

The data were analysed using a conventional, fixed effects, statistical model using subject - specific parameter estimates as described in Chapter 4 (a design matrix that is separable over subjects or sessions) and a random effects model. In order to ascertain whether a randomly selected voxel would show activation, it is necessary to find out the between-subject variability: clearly this would be large compared to the actual % signal intensity change itself. It is almost always the case in fMRI studies that use intra-subject variance is much smaller than inter-subject variance. Therefore random effects analysis is essential, otherwise situations can easily arise where apparent effect is dominated by the results from a small minority of the subjects studied, and consequently is not remotely typical of the population. Examination of the data (subject-by-subject) is always a reasonable way of developing hypotheses to be tested on a larger representative group.

An alternative to random effects is conjunction analysis (Friston et al, 1999), in which all the subjects maps are used to localise a region where *all* the subjects are activated. These commonalities can be identified by a conjunction analysis of the activation effects, which are specified separately for each subject. However, a conjunction analysis, using a fixed-effect model, allows one to infer: (i) that the particular voxel every subject studied was activated *and* (ii) that at least a certain proportion of the population would have shown this effect. This approach retains the sensitivity of fixed-effect analyses when the inference that only a substantial proportion of the population activates is sufficient.

Another statistical concern is the use of the off-on paradigm, which clearly does not model the BOLD response to pharmacological stimulation. In using this simple contrast, the resultant data must be interpreted carefully as artefacts, such as linear drift could be interpreted as a signal change. Ideally, one should use a behavioural or neurochemical correlate to plot against the fMRI signal changes in the t-test, as has been performed (Chen et al, 1997). However, as the amphetamine and the other drugs were administered intravenously, it is not possible to create a behavioural correlate as one may introduce

additional difficulties, such as a stress / pain responses from the injection. Another option, which would be of great use in validating the fMRI response, would be to use *in vivo* microdialysis as a neurochemical correlate, measuring dopamine release in various brain areas. This would require a shorter sampling time, as the 15-minute sampling which was required to collect a measurable volume (Chapter 3), may result in transient changes being missed and reducing the temporal resolution. The concept of multimodal measurements is an area of great interest and would certainly help validate the data with respect to neurotransmitter activity and behaviour in pharmacological studies, as well help to clarify other BOLD fMRI issues, such as negative BOLD and neurovascular coupling.

8.7 Molecules and BOLD: the Energetics behind the Image

Functional brain imaging is a powerful tool for examining the CNS response to pharmacological challenges. The work described in this thesis is essentially an investigation on whether BOLD fMRI can detect regionally specific changes in the rat brain, which are elicited by systemic administration of pharmacological agents, and this indeed has been demonstrated. The effects caused by dopaminergic agents, such as amphetamine in the brain have been well described, in terms of transmitter release and behaviour (Kuczenski & Segal, 1989) and brain metabolism (Weschler et al, 1979; Sokoloff et al, 1980). fMRI is widely assumed to measure neuronal activity, but no satisfactory mechanism for this linkage has been identified. It is difficult to define "neuronal activity" as it includes several complex processes in the brain. It can refer to biochemical events (release/reuptake of neurotransmitters) and electrophysiological processes (IPSPs and EPSPs). Thus, usually when describing neuronal activity, an index is used which includes field potentials (Mathieson et al, 1998; Logothetis et al, 2001); neurotransmitter release (Sibson et al, 1998) and evoked potentials (Ances et al, 2000). This implies that there are different types of neuronal activity, each accounting for one aspect of work carried by neurons and/or astrocytes. Changes in CBF caused by functional activation are used as a surrogate for neural activity in many functional neuroimaging studies. Although CBF-metabolism coupling is well characterised in the resting state (Raichle et al, 1976; Sokoloff, 1981), the parallelism between CBF and metabolism appears far from clear during cerebral activation studies. However within

the topic of coupling, it seems reasonable to assume that neuronal activity is referring to the level of synaptic transmission, which can vary either in intensity or frequency. Thus, cerebral energetics remains a frequently discussed topic for those interested in the cellular and molecular events contributing to the BOLD signal.

The energy expended on signalling is a large fraction of the total energy used by the brain; this favours the use of energy efficient neural codes and wiring patterns. Various groups have attempted to solve the brains energy budget, below are two main lines of thought, and the possible implications in the context of our paradigm.

In measuring the rates of the tricarboxylic acid cycle over a range of synaptic activity, Sibson et al (1998) determined the stoichiometry between CMR_{O2} and glutamate-neurotransmitter cycling in the cortex to be close to 1:1. Furthermore, subsequent studies, using extracellular recordings to measure changes in cerebral spiking frequency have determined that CMR_{O2} is also related to spiking frequency (Hyder et al, 2002: Smith et al, 2002). Such a relationship between BOLD and neuronal spiking activity has been suggested previously on the basis of macaque (Rees et al, 2000) and human (Heeger et al, 2000) visual stimulation (motion coherence) studies. The hypothesis is that the majority of cortical energy production supports synaptic glutamatergic neuronal activity, therefore brain activation studies that map cortical CMR_{O2} provide a quantitative measure of synaptic glutamate release (Shulman & Rothman, 1998). The glutamate-glutamine neurotransmitter cycle between neurons and astrocytes plays a major role in the generation of the functional imaging signal. Activation of voltage-dependent Na^+ channels is involved in the (BOLD) functional magnetic resonance imaging (fMRI) responses during somatosensory activation: after lamotrigine (a neuronal voltage-dependent Na^+ channel blocker and glutamate release inhibitor) treatment, the fractional increase in CBF during forepaw stimulation was an order of magnitude less than that observed before the treatment, but had no effect on baseline CBF in the absence of stimulation (Kida et al, 2001). This model relating energy metabolism to BOLD signal is based on the forepaw stimulation of the rat and relates to events occurring in the somatosensory cortex. However, one must question is it likely to yield similar results in subcortical areas, and importantly, when using a different procedure, such as pharmacological stimulation? It would be very interesting to observe

whether lamotragine would cause reductions ("fractional" or otherwise) in pharmacologically mediated responses.

Using data mainly obtained from rat studies, Attwell & Laughlin (2001) have calculated the energy budget for synaptic processing (including vesicular release, calcium entry to terminals, postsynaptic receptor ion fluxes, and post-synaptic transmitter recycling), in terms of ATP molecules. Such modelling of cerebral energetics (Attwell & Laughlin, 2001) has come up with a different energy budget in the brain to that of Sibson et al (who say that astrocytic recycling of synaptically released glutamate, is responsible for BOLD signal changes: Sibson et al, 1998), - in postulating that glutamate recycling uses only 3% of the brains energy budget. Attwell & Laughlin (2001) calculated that postsynaptic processing accounts for 86% of all cortical ATP consumed, with action potentials and postsynaptic effects of glutamate predicted to consume much of the energy, and the resting potential consuming a smaller amount. According to this hypothesis, fMRI signals are likely to be dominated by changes in energy usage associated with synaptic currents and action potential propagation.

Thus on the basis of weighting the energy budget of Attwell & Laughlin (2001) to postsynaptic processing, it can be assumed that the signal sent to the feeding arteriole to cause it to dilate for change in CBF, is probably coming from the post-synaptic side of excitatory synapses. The next step is to establish what kind of signal triggers CBF changes. It is apparently not due to lack of glucose (Powers et al, 1996), lack of oxygen (Mintun et al, 2001), or CO_2 levels (via decrease in pH) as increase in CBF would cause an alkaline pH rather than acidic. In contrast to the suggestion by Hyder et al (2002), Lauritzen (2001) believes that BOLD does not represent spiking output, by showing that increase in CBF does not correlate with spike frequency of neurons and that increased glutamatergic activity can occur with decreased spiking output. Furthermore, altered glutamate release causes changes in BOLD without changes in spiking frequency (Lauritzen 2001). It is established however, that BOLD signal is dependant on glutamate and NO: exogenously applied glutamate increases CBF in the cortex and hippocampus (Fergus & Lee, 1997); if glutamate is removed/inhibited then there is no BOLD signal (Akgoren et al, 1996); and increased CBF can be blocked by glutamate release blockers and NO blockers (Akgoren et al, 1994).

8.8 Pharmacological MRI: Future Directions

The studies described in Chapters 5-7 demonstrate that fMRI permits detection of regionally specific changes in BOLD activation following administration of centrally acting dopaminergic drugs in anaesthetised animals. Furthermore, the results showed that using this technique, one can modulate the response of one drug, and probably the neuronal activity associated with its stimulation by blocking specific receptors. Overall, the results suggest that the specific involvement of dopamine receptor types in the amphetamine response are important aspects of amphetamine stimulation, and that fMRI provides an efficient survey tool for studying pharmacological interactions.

Pharmacological MRI studies to date, have been performed using drugs which have a well-characterised systemic response, such as amphetamine, cocaine, and as such are often discussed in terms "transmitter release" and "neuronal activation" (Chen et al, 1997; Marota et al, 2000). The complex presynaptic and postsynaptic localisation of dopamine D_1 and D_2 receptors means a variety of possible outcomes is possible following drug administration, and indeed the choice of anaesthetic will also invariably exert an effect. BOLD may be a useful preliminary tool to find out where to examine (spatially) and to determine at which timepoint to investigate.

Although BOLD has been used to detect drug-stimulated changes, as illustrated in this Discussion, there are many factors which influence the signal, and these potential confounds should be assessed. Interpreting stimulated dopamine release into a haemodynamic event requires better understanding about the neuronal events drive the BOLD response, for example, differentiating between excitatory and inhibitory events and understanding the consequences of downstream and upstream events. In order to be able to effectively use fMRI as a pharmacological tool, one must be certain that it detects drug-induced changes, thus an investigation into the complete response, metabolic and haemodynamic changes to a well-characterised CNS drug must be undertaken. In carrying out a simple paradigm (such as was carried out in Chapter 5, i.e. a single acute amphetamine challenge), several different components could be measured: BOLD, CBF, CBV, CMR_{02} and CMR_{glu}. Furthermore, these could be all measured under different anaesthetic regimes to more completely characterise the drug and potential anaesthetic effects, and importantly, to assess why the BOLD signal is

positive or negative in particular brain regions in relation to local CBF and metabolism changes. In such a way, Lawrence et al (2001) measured CBF and BOLD simultaneously after drug challenge and assessed its subsequent effect on a motor task, validating the technique for measuring CBF and CMR_{O2}.

phMRI studies, such as those which were carried out in Chapter 5-7, may shed light on neurochemical systems relevant in mediating amphetamine-induced brain activation in drug addicts, to further our understanding of the induced neurochemical changes, with the ultimate goal of treating dysfunctional brain neurotransmitter systems. Human studies investigating dug abuse can be extremely difficult to assess due to polydrug use and general difficulties in finding control populations and thus animal models are attractive alternatives. Animal studies have already revealed the potential for fMRI applications in drug abuse: Luo et al (2002) detected heroin induced changes using BOLD and also detected a drug sensitisation response as compared to rats who had an abstinence period. The sensitivity manifested by phMRI may be a useful tool for pre-screening of PD in early stages, as clinical signs do not appear until about 80% of the dopamine innervation in the striatum is depleted. It would be advantageous if MR sensitivity could be increased to detect such changes, since relatively large does are required to sdetect BOLD effects in phMRI, i.e. to detect dopamine innervation at levels in the order of 80% loss or greater.

One of the beneficial aspects of NMR compared to PET in human studies is the non-invasiveness of the technique. Unfortunately, due to physiological monitoring and administration of exogenous agents, this is often not the case with animal studies. However, longitudinal animal studies using fMRI and phMRI is an area of great potential and should be a fruitful area in future investigations. Using PET, developmental studies investigated changes in cerebral metabolism at several during the primate's life (Moore et al, 2000). This work could be also exploited by fMRI, without needing to administer potentially harmful agents. Using fMRI in longitudinal studies, repeated administrations could be used up-regulate or down-regulate receptors over a long period of time to investigate how and when changes such as depolarisation block occur, and to correlate the changes with neurotransmitter release patterns. Another application of fMRI in longitudinal studies is in CNS development. By carrying out an

fMRI procedure over a period of weeks or months, it may be able to ascertain critical periods of functional development.

As demonstrated in Chapters 5-7, fMRI detected the BOLD response resulting from stimulation of the dopaminergic system, and this was limited to those areas of the brain containing large dopaminergic innervation. The number of groups using phMRI techniques continues to grow and meanwhile the neuronal basis of the BOLD response is being elucidated validating this technique as an appropriate tool in neurological and pharmacological research. This is an exciting area of research, as the information obtained from a single study complements that obtained from *in vivo* microdialysis, behavioural and metabolic studies, but additionally may give extra insight into specific brain region involvement in drug or task-induced changes; or show temporal responses that otherwise may not have been detected. As such, phMRI is an ideal tool for characterisation of novel drugs and dose regimes.

REFERENCES

Abekawa T, Ohmori T, Ito K and Koyama T. D1 dopamine receptor activation reduces extracellular glutamate and GABA concentrations in the medial prefrontal cortex. *Brain Res* 867: 250-254, 2000.

Abercrombie ED and Jacobs BL. Systemic naxalone administration potentiates locus coeruleus noradrenergic neuronal activity under stressful but not non-stressful conditions. *Brain Research* 441: 362-366, 1988.

Acquas E, Day JC and Fibiger HC. The potent and selective dopamine D1 receptor agonist A-77636 increases cortical and hippocampal acetylcholine release in the rat. *European journal of Pharmacology* 260: 85-87, 1994.

Adachi K, Watanabe T, Higuchi H, Satoh T and Zsilla G. Halothane potentiates the effect of metamphetamine and nomifensine on extracellular levels in rat striatum: A microdialysis study. B. *British Journal of Anaesthiology* 86: 837-845, 2001.

Adachi YU, Uchihashi Y, Watanabe K and Satoh T. Halothane anesthesia decreases the extracellular level of dopamine in rat striatum: A microdialysis study in vivo. *Journal of Anaesthesia* 14: 82-90, 2000.

Aghajanian GK and Bunney BS. Dopamine"autoreceptors": pharmacological characterization by microiontophoretic single cell recording studies. *Naunyn Schmiedebergs Archives of Pharmacology* 297: 1-7, 1977.

Agid Y, Ruberg M, Javoy-Agid F, Hirsch E, Raisman-Vozari R, Vyas S, Faucheux B, Michel P, Kastner A and Blanchard V. Are dopaminergic neurons selectively vulnerable to Parkinson's disease? *Advances in Neurology* 60: 148-164, 1993.

Ainsworth K, Smith SE and Sharp TE. Repeated administration of fluoxetine, desipramine and tranylcypromine increases dopamine D2-like but not D1-like receptor function in the rat. *Psychopharmacology* 12: 252-257, 1998.

Ainsworth K, Smith SE, Zetterstrom TS, Pei Q, Franklin M and Sharp T. Effect of antidepressant drugs on dopamine D1 and D2 receptor expression and dopamine release in the nucleus accumbens of the rat. *Psychopharmacology (Berl)* 40: 470-477, 1998.

Akaike A, Ohno Y, Sasa M and Takaori S. Excitatory and inhibitory effects of dopamine on neuronal activity of the caudate nucleus neurons in vitro. *Brain Research* 418: 262-272, 1987.

Akgoren N, Dalgaard P and Lauritzen M. Cerebral blood flow increases evoked by electrical stimulation of rat cerebellar cortex: relation to excitatory synaptic activity and nitric oxide synthesis. *Brain Research* 710: 204-214, 1996.

Akgoren N, Fabricius M and Lauritzen M. Importance of nitric oxide for local increases of blood flow in rat cerebellar cortex during electrical stimulation. *Proceedings of the national Academy of Sciences of the U S A* 91: 5903-5907, 1994.

Albin RL, Young AB and Penney JB. The functional anatomy of basal ganglia disorders. *Trends in Neurosciences* 12: 366-375, 1989.

Albrecht D, Quaschling U, Zippel U and Davidowa H. Effects of dopamine on neurons of the lateral geniculate nucleus: an iontophoretic study. *Synapse* 23: 70-78, 1996.

Alfaro V and Palacios L. Differential effects of hypothermia upon blood acid-base state and blood gases in sodium pentobarbital and urethane anaesthetised rats. *Gen Pharmacol* 23: 677-682, 1992.

Altar CA and Hauser K. Topography of substantia nigra innervation by D1 receptor-containing striatal neurons. *Brain Research* 410: 1-11, 1987.

Amalric M and Koob GF. Depletion of dopamine in the caudate nucleus but not in nucleus accumbens impairs reaction-time performance in rats. *Journal of Neuroscience* 7: 2129-2134, 1987.

Amalric M and Koob GH. Functionally selective neurochemical afferents and efferents of the mesocorticolimbic and nigrostriatal dopamine system. *Progress in Brain Research* 99: 209-226, 1993.

Amara SG and Kuhar MJ. Neurotransmitter transporters: recent progress. *Annual Reviews of Neuroscience* 16: 73-93, 1993.

Ances BM, Zarahn E, Greenberg JH and Detre JA. Coupling of neural activation to blood flow in the somatosensory cortex of rats is time-intensity separable, but not linear. *Journal of cerebral blood flow and metabolism* 20: 921-930, 2000.

Anderson PH, Gingrich JA, Bates MD, Dearry A, Falalrdeau P, Senogles SE and Caron MG. Dopamine receptor subtypes: beyond the D1/D2 classification. *Trends in Pharmacological Sciences* 11: 231-236, 1990.

Anderson SMP and Fillenz M. The delayed effect of stress on dopamine synthesis in the rat frontal cortex. *Journal of Physiology* 358: 47P, 1984.

Andrews PL, Davis CJ, Bingham S, .Davidson HIM, Hawthorn J and Maskell L. The abdominal visceral innervation and the emetic reflex: pathways, pharmacology, and plasticity. *Canadian Journal of Physiological Pharmacology* 68: 325-345, 1990.

Angrist BM and Gershon S. The phemomenology of experimentally induced amphetamine psychosis -preliminary observations. *Biological Psychiatry* 2: 95-107, 1970.

Apicella P, Ljungberg T, Scarnati E and Schultz W. Responses to reward in monkey dorsal and ventral striatum. *Experimental Brain Research* 85: 491-500, 1991.

Arbuthnott GW, Fairbrother I.S and Butcher SP. Dopamine release and metabolism in the rat striatum: An analysis by "in vivo" brain microdialysis. *Pharmacology and Therapeutics* 48: 281-293, 1990.

Ariano M A, Kang HC, Haugland RP and Sibley DR. Multiple fluorescent ligands for dopamine receptors. II. Visualization in neural tissues. *Brain Research* 547: 208-222, 1991.

Ariano MA, Wang J, Noblett KL, Larson ER and Sibley DR. Cellular distribution of the rat D4 dopamine receptor protein in the CNS using anti-receptor antisera. *Brain Research* 752: 26-34, 1997.

Armstrong-James JM and Fox K. Spatiotemporal convergence and divergence in the rat S1 barrel cortex. *Journal of comparative neurology* 263: 265-281, 1987.

Arnold HM, Nelson CL, Neigh GN, Sarter M and Bruno JP. Systemic and intra-accumbens administration of amphetamine differentially affects cortical acetylcholine release. *Neuroscience* 96: 675-685, 2000.

Arnt J and Perrigaard J. Synergistic interaction between dopamine D-1 and D2 receptor agonists: Circling behaviour of rats with hemitransaction. *European journal of Pharmacology* 143: 45-53, 1987.

Arthurs OJ and Boniface S. How well do we understand the neural origins of the fMRI BOLD signal? *Trends in Neurosciences* 25: 27-31, 2002.

Asher IM and Aghajanian GK. 6-Hydroxydopamine lesions of olfactory tubercles and caudate nuclei: effect on amphetamine-induced stereotyped behavior in rats. *Brain Research* 82: 1-12, 1974.

Assaf S and Miller JJ. Excitatory action of the mesolimbic dopamine system on septal neurones. *Brain Research* 129: 353-360, 1977.

Attwell D and Laughlin SB. An energy budget for signaling in the grey matter of the brain. *Journal of cerebral blood flow and metabolism* 21: 1133-1145, 2001.

Azzaro AJ, Ziance RJ and Rutledge CO. The importance of neuronal uptake of amines for amphetamine-induced release of 3H-norepinephrine from isolated brain tissue. *Journal of pharmacology and Experimental therapeutics* 189: 110-118, 1974.

Bach AW, Lan NC, Johnson DL, Abell CW, Bembenek ME, Kwan SW, Seeburg PH and Shih JC. cDNA cloning of human liver monoamine oxidase A and B: molecular basis of differences in enzymatic properties. *Proceedings of the National Academy of Sciences of the USA* 85: 4934-4938, 1988.

Baik JH, Picetti R, Saiardi A, Thiriet G, Dierich A, Depaulis A, Le Meur M and Borrelli E. Parkinsonian-like locomotor impairment in mice lacking dopamine D2 receptors. *Nature* 377: 424-428, 1995.

Balis GU and Munroe RR. The pharmacology of chloralose. *Psychopharmacologica* 6: 1-30, 1964.

Bandettini PA, Wong EC, Hinks RS, Tikofsky RS and Hyde JS. Timecoure EPI of human brain function during task activation. *Magnetic Resonance in Medicine* 25: 390-397, 1992.

Bannon MJ, Kelland M and Chiodo LA. Medial forebrain bundle stimulation or D-2 dopamine receptor activation increases preproenkephalin mRNA in rat striatum. *Journal of Neurochemistry* 52: 859-862, 1989.

Bannon MJ and Roth RH. Pharmacology of mesocortical dopamine neurons. *Pharmacological Reviews* 35: 53-68, 1983.

Baraban JM, Wang RY and Aghajanian GK. Reserpine suppression of dorsal raphe neuronal firing: Mediation by adrenergic system. *European journal of Pharmacology* 52: 27-36, 1978.

Basbaum AI and Fields HL. Endogenous pain control mechanisms: Review and hypothesis. *Annals of Neurology* 4: 451-462, 1978.

Behr J, Gloveli T, Schmitz D and Heinemann U. Dopamine depresses excitatory synaptic transmission onto rat subicular neurons via presynaptic D1-like dopamine receptors. *Journal of Neurophysiology* 84: 112-119, 2000.

Belliveau JW, Kennedy DW, McKinstry RC, Buchbinder BR, Weisskoff RM, Cohen BR, Vevea JM, Brady TJ and Rosen BR. Functional mapping of the human visual cortex by magnetic resonance imaging. *Science* 254: 716-719, 1991.

Benkirane S, Arbilla S and Langer SZ. A functional response to D1 dopamine receptor stimulation in the central nervous system: inhibition of the release of [3H]-serotonin from the rat substantia nigra. *Naunyn-Schmeildebergs archives of pharmacology* 355: 505-507, 1987.

Benviste H. Brain Microdialysis. *Journal of Neurochemistry* 52: 1667-1679, 1989.

Berger H. Uber das elektrenkephalogram. *Arch Psychiatr Nervenkr* 87: 527-570, 1929.

Bergman J, Madras BK, Johanson SE and Spealman RD. Effects of cocaine and related drugs in nonhuman primates. III. Self-administration by squirrel monkeys. *Journal of pharmacology and Experimental therapeutics* 251
J Pharmacol Exp Ther 1989 Oct;251(1):150-5: 150-155, 1989.

Bernheimer H and Hornykiewicz ZO. Decreased homovanillic acid concentration in the brain in PArkinsonian subjects as an expression of a disorder of central dopaminergic metabolism. *Kilin Worchenschr* 43: 711-715, 1965.

Berridge KC and Aldridge JW. Super-stereotypy I: enhancement of a complex movement sequence by systemic dopamine D1 agonists. *Synapse* 37: 194-204, 2000.

Besheer J, Jensen HC and Bevins RA. Dopamine antagonism in a novel-object recognition and a novel-object place conditioning preparation with rats. *Behavioural Brain Research* 103: 35-44, 1999.

Bito L, Davson H, Levin E and Snider N. The concentrations of free amino acids and other electrolytes in cerebrospinal fluid, in vivo diasylate of brain, and blood plasma of the dog. *Journal of Neurochemistry* 13: 1057-1067, 1966.

Black KJ, Hershey T, Gado MH and Perlmutter JS. Dopamine D(1) agonist activates temporal lobe structures in primates. *Journal of Neurophysiology* 84: 549-557, 2000.

Blamire AM, Ogowa S, Ugurbil K, Rothman D, McCarthy G, Ellerman JM, Hyder F, RAttner Z and Shulman RG. Dynamic mapping of the human visual-cortex by high speed magnetic resonance imaging. *Proceedings of the National Academy of Science of the USA* 89: 11069-11073, 1992.

Blanchet PJ, Fang J, Gillespie M, Sabounjian L, Locke KW, Gammans R, Mouradian MM and Chase TN. Effects of the full dopamine D1 receptor agonist dihydrexidine in Parkinson's disease. *Clinical Neuropharmacology* 21: 339-343, 1998.

Bleuler E. *Dementia praecox or the group of schizophrenias.* 1950.

Blin J, Ivanoiu A, Coppens A, De Volder A, Labar D, Michel C and Laterre EC. Comparison of cholinergic drug effects on regional brain glucose consumption in rats and humans by means of autoradiography and positron emission tomography. *Brain Research* 635: 196-202, 1997.

Bliss EL, Ailion J and Zwanziger J. Metabolism of norepinephrine, serotonin and dopamine in rat brain with stress. *Journal of pharmacology and Experimental therapeutics* 164: 1968.

Blum K, Noble EP, Sheridan PJ, Montgomery A, Ritchie T, Jagadeeswaran P, Nogami H, Briggs AH and Cohn JB. Allelic association of human dopamine D2 receptor gene in alcoholism. *Journal of the American Medical Association* 263: 2055-2060, 1990.

Blum K, Sheridan PJ, Wood RC, Braverman ER, Chen TJ, Cull JG and Comings D. The D2 dopamine receptor gene as a determinant of reward deficiency syndrome. *Journal of the Royal Society of Medicine* 89: 396-400, 1996.

Bock C, Schmitz B, Kerskins CM, Gyngell ML, Hossman K-A and Hoen-Berlage M. Functional MRI of somatosensory Activation in rat: Effect of hypercapnic up-regulation on perfusion- and BOLD imaging. *Magnetic Resonance in Medicine* 39: 457-461, 1998.

Bodiz R, Kantor S, Szabo G, Szucs A, Eross L and Halasz P. Rythmic ippocampal slow oscillation characteristic REM sleep in humans. *Hippocampus* 11: 747-753, 2001.

Bonuccelli U, Colzi A and Del Dotto P. Pergolide in the treatment of patients with early and advanced Parkinson's disease. *Clinical Neuropharmacolgy* 25: 1-10, 2002.

Bonvento G, Charbonne R, Correze J-L, Burreden J, Selaz J and Lacombe P. Is a chloralose plus halothane induction a suitable regimen for cerebrovascular research? *Brain Research* 665: 213-222, 1994.

Bonvento G, Charbonne R, Correze J-L, Burreden J, Selaz J and Lacombe P. Is a chloralose plus halothane induction a suitable regimen for cerebrovascular research? *Brain Research* 665: 213-222, 1994.

Born AP, Rostrup E, Miranda MJ, Larsson HB and Lou HC. Visual cortex reactivity in sedated children examined with perfusion MRI (FAIR). *Magnetic Resonance Imaging* 20: 199-205, 2002.

Boullin DJ, Adams CB, Mohan J, Green AR, Hunt TM, du Boulay GH and Rogers AT. Effects of intracranial dopamine perfusion: behavioural arousal and reversal of cerebral arterial spasm following surgery for clipping of ruptured cerebral aneurysms. *Proceedings of the Royal Society of Medicine* 70: 55-70, 1977.

Bouron A and Renter H. The D1 dopamine receptor agonist SKF38393 stimulates the release of glutamate in the hippocampus. *Neuroscience* 94: 1063-1070, 1999.

Bouthenet ML, Martres MP, Sales N and Schwartz JC. A detailed mapping of dopamine D-2 receptors in rat central nervous system by autoradiography with [125I]iodosulpride. *Neuroscience* 20: 117-155, 1987.

Boxerman JL, Hamberg LM, Rosen BR and Weisskoff RM. MR contrast due to intravascular magnetic susceptibility perturbations. *Magnetic Resonance in Medicine* 35: 555-566, 1995.

Boyer P. Biochemistry and pharmacology of benzamides. *Sem Hop* 59: 832-835, 1983.

Boyle M. Is schizophrenia what it was? A re-analysis of Kraeplin's and Bleuler's population. *Journal of Historical Behavioual Science* 26: 323-333, 1990.

Boyson SJ, McGonigle P and Molinoff PB. Quantitative autoradiographic localization of the D1 and D2 subtypes of dopamine receptors in rat brain. *Journal of Neuroscience* 11: 3177-3188, 1986.

Bozarth MA and Wise RA. Anatomically distinct opiate receptor fields mediate reward and physical dependence. *Science* 224: 516-617, 1984.

Bracci E, Centonze D, Bernardi G and Calabresi P. Dopamine excites fast-spiking interneurons in the striatum. *Journal of Neurophysiology* 1987: 2190-2194, 2002.

Braff, D. L. and Geyer, M. A. Acute and chronic LSD effects on rat startle: data supporting an LSD-rat model of schizophrenia. 15(6), 909-916. 1980.
Ref Type: Generic

Branco D, Caramona M, Martel F, de Almeida JA and Osswald W. Predominance of oxidative deamination in the metabolism of exogenous noradrenaline by the normal and chemically denervated human uterine artery. *Naunyn-Schmeildebergs archives of pharmacology* 346: 286-293, 1992.

Braun AR and Chase TN. Obligatory D-1/D-2 receptor interaction in the geberation of dopamine agonist related behaviours. *European journal of Pharmacology* 131: 301-306, 1986.

Brazell MP, Mitchell SN, Joseph MH and Gray JA. Acute administration of nicotine increases the in vivo extracellular levels of dopamine, 3,4-dihydroxyphenylacetic acid

and ascorbic acid preferentially in the nucleus accumbens of the rat: comparison with caudate-putamen. *Neuropharmacology* 29: 1177-1185, 1990.

Breier A, Su T-P, Saunders R, Carson RE, Kolachana BS, de Bartolomeis A, Weinberger DR, Weisenfeld N, Malhotra AK, Eckelman WC and Pickar D. Schizophrenia is associated with elevated amphetamine-induced synaptic dopamine concentrations: Evidence from a novel positron emission tomography method. *Proceedings of the National Academy of Sciences of the USA* 94: 2569-2574, 1997.

Breiter HC, Gollub RL, Weisskoff RM, Kennedy DN, Makris N, Berke JD, Goldman JM, Kantor HL, Gastfriend DR, Riorden JP, Mathew RT, Rosen BR and Hymen SE. Acute effects of cocaine on human brain activity and emotion. *Neuron* 19: 591-611, 1997.

Brenner D, Williamson SJ and Kaufman L. Visually evoked magnetic fields of the human brain. *Science* 190: 480-482, 1975.

Brezny I, Buranova D, Kollar B, Varsik P, Kondas M and Cincurova E. Non-convulsive status epilepticus. *Ceska a Slovenska Neurologie a neurochirurgie* 64: 355-360, 2001.

Broca P. Sur le siege de la faculte du langage articule. *Bulletin Society Anatomie du Paris* 2: 355, 1861.

Broekkamp CL and Van Rossum JM. The effect of microinjections of morphine and haloperidol into the neostriatum and the nucleus accumbens on self-stimulation behaviour. *Archives of International Pharmacodynamic Therapeutics* 217: 110-117, 1975.

Brooks DJ. Parkinson`s Disease-a single clinical entity? *Q J Med* 88: 81-91, 1995.

Brucke T, Podreka I, Angerberger P, Wenger S, Topitz A, Kufferle B, Muller C and Deekle L. Dopamine D2 receptor imaging with SPECT -studies in differeft neuropsychiatric disorders. *Journal of cerebral blood flow and metabolism* 11: 220-228, 1991.

Brunello N, Masotto C, Steardo L, Markstein R and Racagni G. New insights into the biology of schizophrenia through the mechanism of action of clozapine. *Neuropsychopharmacology* 13: 177-213, 1995.

Brussel T, Fitch W, Brodner G, Arendt I and Van Aken H. Effects of halothane in low concentrations on cerebral blood flow, cerebral metabolism and cerebrovascular autoregulation in the baboon. *Anaesthesia & Analgesia* 73: 758-764, 1991.

Bull DR, Bakhtiar R and Sheehan MJ. Characterization of dopamine autoreceptors in the amygdala: a fast cyclic voltammetric study in vitro. *Neuroscience Letters* 134: 41-44, 1991.

Bunney BS. Clozapine: A hypothesized mechanism for its unique clinical profile. *British Journal of Psychiatry* 160: 17-21, 1992.

Burdett NG, Menon DK, Carpenter TA, Jones JG and Hall LD. Visualisation of changes in regional cerebral blood flow (rCBF) produced by ketamine using long TE gradient-echo sequences: Preliminary results. *Magnetic Resonance Imaging* 13: 549-553, 1995.

Burgess RC. Functional localisation by neurophysiologic and neuroimaging techniques. *Journal of Clinical Neurophysiology* 12: 405, 1995.

Burns RS, Chiueh CC, Markey SP, Ebert MH, Jacobowitz DM and Kopin IJ. A primate model of parkinsonism: selective destruction of dopaminergic neurons in the pars compacta of the substantia nigra by N-methyl-4-phenyl-1,2,3,6-tetrahydropyridine. *Proceedings of the National Academy of Sciences of the USA* 80: 4546-4570, 1983.

Butcher SP, Fairbrother IS, Kelly JS and Arbuthnott GW. Amphetamine-induced dopamine release in the rat stiatum: an in-vivo microdialysis study. *Journal of Neurochemistry* 55: 981-998, 1988.

Buxton RB and Frank LR. A model for the coupling between cerebral blood-flow and oxygen metabolism during neural stimulation. *Journal of cerebral blood flow and metabolism* 17: 64-72, 1997.

Cain DP, Boon F and Hargreaves EL. Evidence for different neurochemical contributions to long-term potentiation and to kindling and kindling-induced potentiation: role of NMDA and urethane-sensitive mechanisms. *Experimental Neurology* 116: 330-338, 1992.

Calabresi P, Saiardi A, Pisani A, Baik JH, Centonze D, Mercuri NB, Bernardi G and Borrelli E. Abnormal synaptic plasticity in the striatum of mice lacking dopamine D2 receptors. *Journal of Neuroscience* 17: 4536-4544, 1997.

Cameron DL and Williams JJ. D1 receptors facilitate transmitter release. *Nature* 366: 344-347, 1993.

Camps M, Cortes R, Gueye B, Probst A and Palacios JM. Dopamine receptors in human brain: autoradiographic distribution of D2 sites. *Neuroscience* 28: 275-290, 1989.

Carlsson A. The occurance, distribution and physiological role of catecholamines in the nervous system. *Pharmacological Reviews* 11: 1959.

Carlsson, A. Perspectives on the discovery of central monoaminergic transmission. 10, 19-40. 1987.
Ref Type: Generic

Carlsson A. The current status of the dopamine hypothesis of schizophrenia. *Neuropsychopharmacology* 1: 179-186, 1988.

Carlsson A and Lindquist M. Effects of chlorpromazine or haloperidol on formation of 3-methoxytyramine and normetanephrine in mouse brain. *Acta Pharmacalogica et Toxicologica* 20: 140-144, 1963.

Carlsson C, Hagerdal M and Seisjo BK. Influence of amphetamine sulfate on cerebral blood flow and metabolism. *Acta Physiologca Scandinavica* 94: 128-129, 1975.

Caroleo MC, Arbirio M, Di Francesco P, Pulvirenti L, Garaci E and Nistico G. Cocaine induced T cell proliferation in the rat: role of amygdala dopamine D1 receptors. *Neuroscience Letters* 256: 61-64, 1998.

Carr HY and Purcell EM. Effects of diffusion on free precession in nuclear magnetic resonance experiments. *Physics Reviews* 94: 630-638, 1954.

Cash, D., Roberts, T. J., Ireland, M. D., Williams, S. C. R., Hunter, A. J., and Read, S. J. The effect of anaesthetics on regional cerebral metabolism: an fMRI perspective. Journal of cerebral blood flow and metabolism 21(Suppl 1), S109. 2001. Ref Type: Abstract

Cass WA. Decreases in evoked overflow of dopamine in rat striatum after neurotoxic doses of methamphetamine. *Journal of pharmacology and Experimental therapeutics* 280: 105-113, 1997.

Catalano M, Nobile M, Novelli E, Nothen MM and Smeraldi E. Distribution of a novel mutation in the first exon of the human dopamine D4 receptor gene in psychotic patients. *Biological Psychiatry* 34: 459-464, 1993.

Chen AC, LaForge KS, Ho A, McHugh PF, Kellogg S, Bell K, Schluger R, Leal S and Kreek MJ. Potentially functional polymorphism in the promoter region of prodynorphin gene may be associated with protection against cocaine dependence or abuse. *American Journal of Medical Genetics* 114: 429-435, 2002.

Chen J-L, Wei L, Acuff V, Bereczi D, Hans F-J, Otsuka T, Finnegan W, Patlak C and Fenstremacher J. Slightly altered permeability-suface area products imply some cerebral capilllary recruitment during hypercapnia. *Microvascular Research* 48: 190-211, 1994.

Chen W, Kato T, Zhu XH, Strupp J, Ogawa S and Ugurbil K. Mapping of the lateral geniculate nucleus in human brain using fMRI. *Magnetic Resonance in Medicine* 39: 89-96, 1998.

Chen YC, Galpern WR, Browness A-L, MAtthews RT, Bogdanov M, Isacson O, Keltner JR, Rosen BR and Jenkins BG. Detection of Dopaminergic Neurotransmitter Activity using pharmacologic MRI: Correlation with PET, Microdialysis and Behavioural data. *Magnetic Resonance in Medicine* 38: 389-398, 1997.

Cheng SW and North WG. Influence of pentobarbital and urethane on release for magnocellular neurons. *Neuroendocrinology* 54: 482-487, 1991.

Chinen CC and Frusson-Filho R. Conditioning to injection precedures and repeated testing increase SCH23390-induced catalepsy in mice. *Neuropsychopharmacology* 21: 670-678, 1999.

Chou C, Webb AI, Brown MP, Gronwall KK and Vickroy TW. Continious measurement of caffeine and two metabolites in blood and skeletal muscle of

unrestrained adult horses by semi-automated in vivo microdialysis. *Journal of Veterinary Pharmacology and Experimental Therapeutics* 24: 405-414, 2001.

Christensen, A. V., Arnt, J., Hyttel, J., Larsen, J. J., and Svendsen, O. Pharmacological effects of a specific dopamine D-1 antagonist SCH 23390 in comparison with neuroleptics. 34(16), 1529-1540. 1984.
Ref Type: Generic

Chung SJ, Jeong SH, Kang UG, Koo YJ, Ha JH and Kim SY. A retrospective study of cloazapine and electroencephalographic abnormalities in schizophrenic patients. *Progress in Neuro-psychopharmacology & Biological Psychiatry* 26: 139-144, 2002.

Ciccocioppo R, Sanna PP and Weiss F. Cocaine-predictive stimulus induces drug-seeking behavior and neural activation in limbic brain regions after multiple months of abstinence: reversal by D(1) antagonists. *Proceedings of the National Academy of Sciences of the USA* 98: 1976-1981, 2001.

Civelli O, Bunzow JR and Grandy DK. Molecular diversity of the dopamine receptors. *Annual Review of Pharmacology & Toxicoloy* 33: 281-307, 1993.

Clifford JJ, Kinsella A, Tighe O, Rubinstein M, Grandy DK, Low MJ, Croke DT and Waddington JL. Comparative, topographically-based evaluation of behavioural phenotype and specification of D(1)-like:D(2) interactions in a line of incipient congenic mice with D(2) dopamine receptor 'knockout'. *Neuropsychopharmacology* 4: 2001.

Coffin VL, Latranyi MB and Chipkin RE. Acute extrapyramidal syndrome in Cebus monkeys: development mediated by dopamine D2 but not D1 receptors. *Journal of pharmacology and Experimental therapeutics* 249: 769-774, 1989.

Cohen D. Magnetoencephalography: evidence of magnetic fields produced by alpha-rhythm currents. *Science* 161: 784-786, 1968.

Cohen G and Heikikila RE. The generation of hydrogen peroxide superoxide and hydroxyl radical by 6 hydroxydopamine dialuric acid and related cytotoxic compounds. *Journal of Biological Chemistry* 249: 2447-2452, 1974.

Collins JG, Kawahara M, Homma E and Kitahata LM. Alpha-chloralose suppression of neuronal activity. *Life Sciences* 32: 2995-2999, 1983.

Colthorpe KL, Anderson ST, Martin GB and Curlewis JD. Hypothalamic dopamine D1 receptors are involved in the stimulation of prolactin secretion by high environmental temperature in the female sheep. *Journal of Neuroendochrinology* 10: 503-509, 1998.

Comings DE, Rosenthal RJ, Lesieur HR, Rugle LJ, Muhleman D, Chiu C, Dietz G and Gade R. A study of the dopamine D2 receptor gene in pathological gambling. *Pharmacogenetics* 6: 223-234, 1996.

Conley RR, Tamminga CA, Bartko JJ, Richardson C, Peszke M, Lingle J, Hegerty J, Love R, Gounaris C and Zaremba S. Olanzapine compared with chlorpromazine in

treatment-resistant schizophrenia. *American Journal of Psychiatry* 155: 914-920, 1998.

Conti PS, Keppler JS and Halls JM. Positron emission tomography- a financial and operational analysis. *American Journal of Roentgenology* 162: 1279-1286, 1994.

Cools AR and Van Rossum JM. Multiple receptors for brain dopamine in behavior regulation: concept of dopamine-E and dopamine-I receptors. *Life Sciences* 27: 1237-1253, 1980.

Cooper BR, Black WC and Paolino R.M. Decreased septal-forebrain and lateral hypothalamic reward after alpha methyl-p-tyrosine. *Physiological Behaviour* 6: 425-429, 1971.

Craddock D. Anorectic drugs: use in general practice. *Drugs* 11: 378-393, 1976.

Crebelli R and Carere A. Genetic Toxicity of 1,1-2 Trichloethylene. *Mutation Research* 221: 11-37, 1989.

Creese, I., Burt, D. R., and Syder, S. H. Dopamine receptor binding predicts clinical and pharmacological potencies of antischizophrenic drugs. 192(4238), 481-483. 1976.
Ref Type: Generic

Creese I and Iverson SD. The role of the forbrain systems in amphetamine-induced stereotypy in the adult rat following neonatal treatment with 6 hydroxydopamine. *Psychopharmacology* 39: 345-357, 1974.

Crippens D and Robinson TE. Withdrawal from morphine or amphetamine: Different effects on dopamine in the ventral-medial striatum studied with microdialysis. *Brain Research* 650: 56-62, 1994.

Crow TJ. Molecular pathology of schizophrenia: More than one disease process? *British Medical Journal* 280: 1980.

Cudennec A, Fage D, Benavides J and Scatton B. Effects of amisulpride, an atypical antipsychotic which blocks preferentially presynaptic dopamine autoreceptors, on integrated functional cerebral activity in the rat. *Brain Research* 768: 257-265, 1997.

Curran EJ and Watson SJJ. Dopamine receptor mRNA expression patterns by opioid peptide cells in the nucleus accumbens of the rat: a double in situ hybridization study. *Journal of Compuatational Neurology* 361: 57-76, 1995.

Czisch, M., Wetter, T. C., Kaufmann, C., Pollmacher, T., Holsboer, F., and Auer, D. P. Altered Processing of Acoustic Stimuli during Sleep: Reduced Auditory Activation and Visual Deactivation Detected by a Combined fMRI/EEG Study. 16(1), 251-258. 2002.
Ref Type: Generic

Da Prada M, Kettler R, Cesura M and Richards JG. Reversible, enzyme-activated monoamine oxidase inhibitors: new advances. *Pharmacol Res Commun* suppl 4: 1988.

Dalhstrom A and Fuxe K. Evidence for the existance of monoamine-containing neurones in the central nervous system.I. Demonstration of monoamines in the cell bodies of brainstem neurons. *Acta Physiologica Scandinavica* 62: 1-55, 1964.

Damsa G, Westerink BHC, De Vries JB and Horn AS. Measurement of acetylchloine release in freely moving rat by means of anatomical intracerebral dialysis. *Journal of Neurochemistry* 48: 1523-1528, 1987.

Davila R, Manero E, Zumarraga M, Andia I, Schweitzer JW and Friedhoff AJ. Plasma homovanillic acid as a predictor of response to neuroleptics. *Archives of General Psychiatry* 45: 564-567, 1988.

Davis HG, Cox NR and Lindsay JR. Diagnostic excercise: distended abdomen in rats. *Laboratory Animal Science* 35: 392-393, 1985.

Davis MD, Haas HL and Lichtensteiger W. The hypothalamohypophyseal system in vitro: electrophysiology of the pars intermedia and evidence for both excitatory and inhibitory inputs. *Brain Research* 334: 97-104, 1985.

Davis MD, Heffner TG and Cooke LW. Dopamine agonist-induced inhibition of neurotransmitter release from the awake squirrel monkey putamen as measured by microdialysis. *Journal of Neurochemistry* 68: 659-666, 1997.

Dawson TM, Barone P, Sidhu A, Wamsley JK and Chase TN. Quantitative autoradiographic localization of D-1 dopamine receptors in the rat brain: use of the iodinated ligand [125I]SCH 23982. *Neuroscience Letters* 68: 261-266, 1986.

Day J and Fibiger HC. Dopaminergic regulation of cortical acetylcholine release. *Synapse* 12: 281-286, 1992.

De La Garza R2 and Madras BK. [(3)H]PNU-101958, a D(4) dopamine receptor probe, accumulates in prefrontal cortex and hippocampus of non-human primate brain. *Synapse* 37: 232-244, 2000.

De La Torre JC. Impaired brain microcirculation may trigger Alzheimer's disease. *Neuroscience Biobehavioural Review* 18: 397-401, 1994.

De Vries TJ, Cools AR and Shippneberg TS. Infusion of a D1 receptor agonist into nucleus accumbens enhances cocaine-induced behavioural sensitisation. *Neuroreport* 9: 1763-1768, 1998.

Dearry A, Gingrich JA, Falardeau P, Fremeau RTJ, Bates MD and Caron MG. Molecular cloning and expression of the gene for a human D1 dopamine receptor. *Nature* 347: 72-76, 1990.

DeBoer P, Heeringa MJ and Abercrombie ED. Spontaneous release of acetylcholine in striatum is preferentially regulated by inhibitory dopamine D2 receptors. *European journal of Pharmacology* 317: 257-262, 1996.

Delay KL, Deniker P and Harl J. Utilization therapeutique d`une phenothiazine d`action centrale elective. *Annals of Medical Psychology (Paris)* 110: 112-117, 1952.

Delgado JMR, DeFeudis FV, Roth RH, Ryugo DK and Mitruka BK. Dialytrode for long term intracerebral perfusion in awake monkeys. *Archives of International Pharmacodynamics* 198: 9-21, 1972.

Dersch CM, Akunne HC, Partilla JS, Char GU, de Costa BR, Rice KC, Carroll FI and Rothman RB. Studies of the biogenic amine transporters. 1. Dopamine reuptake blockers inhibit [3H]mazindol binding to the dopamine transporter by a competitive mechanism: preliminary evidence for different binding domains. *Neurochemistry Research* 19: 201-208, 1994.

Detre JA, Sirven JI, Alsop DC, O'Connor MJ and French JA. Localization of subclinical ictal activity by functional magnetic resonance imaging: correlation with invasive monitoring. *Annals of Neurology* 38: 618-624, 1995.

Detre JA, Williams DS and Koretsky AP. Nuclear magnetic resonance determination of flow, lactate, and phosphate metabolites during amphetamine stimualtion of the rat brain. *NMR Biomed* 3: 272-278, 1990.

Devous MDS, Trivedi MH and Rush AJ. Regional cerebral blood flow response to oral amphetamine challenge in healthy volunteers. *Journal of nuclear medicine* 42: 535-542, 200.

Dewey RB, Hutton JT, LeWitt PA and Factor SA. A randomized, double-blind, placebo-controlled trial of subcutaneously injected apomorphine for parkinsonian off-state events. *Archives of Neurology* 58: 1385-1392, 2001.

Di Chiara G. The role of dopamine in drug abuse viewed from the perspective of its role in motivation. *Drug Alcohol Depend* 38: 95-137, 1995.

Di Chiara G. Drug addiction as dopamine-dependent associative learning disorder. *European journal of Pharmacology* 375: 13-30, 1999.

Di Chiara G, Acquas E and Carboni E. Drug motivation and abuse: a neurobiological perspective. *Annals of the New York Academy of Sciences* 654: 207-219, 1992.

Di Chiara G and Imperato A. Drugs abused by humans preferentially increase synaptic dopamine concentrations in the mesolimbic system of freely moving rats. *Proceedings of the National Academy of Sciences of the United States of America* 85: 5274-5278, 1988.

Di Monte DA, Wu EY, Irwinm I, Delanney LE and Langston JW. Production and disposition of 1-methyl-4-phenylpyridinium in primary cultures of mouse astrocytes. *Glia* 5: 48-55, 1992.

Di Piero V, Ferracuti S, Sabatine V, Tombari D, De Legge S, Pantano P, Cruccu G and Lenzi GL. Diazepam effects on the cerebral responses to tonic pain: a SPECT study. *Psychopharmacology* 158: 252-258, 2001.

Dickson DW, Feany MB, Yen SH, Mattiace LA and Davies P. Cytoskeletal pathology in non-Alzheimer degenerative dementia: new lesions in diffuse Lewy body disease, Pick's disease, and corticobasal degeneration. *Journal of Neural Transmission* 47: 31-46, 1996.

Digby WM, Dahlbom M and Hoffman EJ. Detector shielding and geometric design factors for a hight-resolution PET system. *IRRR Trans Nucl Sci* NS-37: 644-670, 1990.

Dobrev D, Bergtrasser E, Fischer HD and Andreas K. Restriction and functional changes of dopamine release in rat striatum from young adult and old rats. *Mechanisms in Aging and Development* 80: 107-119, 1995.

Drago J, Padungchaichot P, Accili D and Fuchs S. Dopamine receptors and dopamine transporter in brain function and addictive behaviors: insights from targeted mouse mutants. *Developmental neuroscience* 200(2-3): 188-203, 1998.

Drapeau P and Blaustien MP. Initial release of [3H]dopamine from rat striatal synaptosomes: correlation with calcium entry. *Journal of Neuroscience* 3: 703-713, 1983.

Dubois A, Savasta M, Curet O and Scatton B. Autoradiographic distribution of the D1 agonist [3H]SKF 38393, in the rat brain and spinal cord. Comparison with the distribution of D2 dopamine receptors. *Neuroscience* 19: 125-137, 1986.

Dufresne RL, Valentino DA and Kass DJ. Thioridazine improves affective symptoms in schizophrenic patients. *Psychopharmacology Bulletin* 29: 249-255, 1993.

Dujardin K, Defebvre L, Grunberg C, Becquet E and Destee A. Memory and executive function in sporadic and familial Parkinson's disease. *Brain* (Pt 2): 389-398, 2001.

Earnst KS, Taylor SF, Smet IC, Goldman RS, Tandon R and Berent S. The effects of typical antipsychotics, clozapine, and risperidone on neuropsychological test performance in schizophrenia. *Schizophrenia Research* 40: 255-256, 1999.

Edelman AM, Raese JD, Lazar MA and Barchas JD. In vitro phosphorylation of a purified preparation of bovine corpus striatal tyrosine hydroxylase. *Commun Psychopharmacol* 2: 461-465, 1978.

Edeson RO and Ryall RW. Systematic mapping of descending inhibitory control by the medulla od nociceptive spinal neurons in rats. *Brain Research* 271: 251-262, 1983.

Edvinsson L, Hardebo JE, Harper AM, McCulloch J and Owman C. Effects of dopaminergic agonists and antagonists on isolated cerebral blood vessels. *Acta Neurologica Scandinavica* 60: 350, 1977.

Ehringer E and Hornykiewicz O. Concentrations of norepinephrine and dopamine in brains of patients with diseases of the extrapyramidal motor systems ("Verteilung von noradrenalin und dopamin im gehirn des menschen und ihr verhalten bei erkrankugen des extrapyramidalen systems"). *Kin Wochenschr* 15: 1236-1239, 1960.

Eker C, Hagstadius S, Linden A, Scahlen W and Nordstrom CH. Neurophysiological assessments in reation to CBF after head injuries. *Acta Neurologica Scandinavica* 104: 142-147, 2001.

El-Ghundi M, Fletcher PJ, Drago J, Sibley DR, O'Dowd BF and George SR. Spatial learning deficit in dopamine D(1) receptor knockout mice. *European journal of Pharmacology* 383: 95-106, 1999.

El-Maghrabi EA and Eckenhoff RG. Inhibition of dopamine transport in rat brain synaptosomes by volatile anesthetics. *Anesthesiology* 78: 50-56, 1993.

Elizan T, Moros DA and Yahr MD. Early combination of selegiline and low-dose levodopa as initial symptomatic therapy in Parkinson's disease. Experience in 26 patients receiving combined therapy for 26 months. *Archives of Neurology* 48: 31-34, 1991.

Engber TM, Anderson JJ, Boldry RC, Kuo S and Chase TN. N-methyl-D-aspartate receptor blockade differentially modifies regional cerebral metabolic responses to D1 and D2 dopamine agonists in rats with a unilateral 6-hydroxydopamine lesion. *Neuroscience* 54: 1051-1061, 1993.

Engber TM, Susel Z, Kuo S and Chase TN. Chronic levodopa treatment alters basal and dopamine agonist-stimulated cerebral glucose utilization. *Journal of Neuroscience* 10: 3889-3895, 1990.

Ernst RR and Anderson WA. Applications of Fourier transform spectroscopy to magnetic resonance. *Reveiws of Scientific Instruments* 37: 93-102, 1966.

Fabbrini G, Juncos J, Mouradian M, Serrati C and Chase TN. Levodopa pharmacokinetic mechanisms and motor fluctuations in Parkinson's disease. *Annals of Neurology* 21: 370-379, 1987.

Farde L, Hall H, Ehrin E and Sedvall G. Quantitative analysis of D2 dopamine receptor binding in the living human brain by PET. *Science* 231: 258-621, 1986.

Farde L, Von bahr C, Wahlen A, Nilsson L and Widman M. The new selective D2-dopamine receptor antagonist raclopride--pharmacokinetics, safety and tolerability in healthy males. *International Clinical Psychopharmacology* 4: 115-126, 1989.

Feenstra MG, Kalsbeek A and van Galen H. Neonatal lesions of the ventral tegmental area affect monoaminergic responses to stress in the medial prefrontal cortex and other dopamine projection areas in adulthood. *Brain Research* 596: 169-182, 1992.

Feldman RG, Kaye JA and Lannon MC. Parkinson`s Disease: Follow-up after "drug holiday". *Journal of Clinical Pharmacology* 26: 662-667, 1986.

Feldman RS, Meyer JS and Quenzer LF. *Principles of Neuropsychopharmacology*. Sunderland, Massachausetts: Sinauer Associates inc., 1997.

Ferger B, Kropf W and Kuschinsky K. Studies on electroencephalogram (EEG) in rats suggest that moderate doses of cocaine or d-amphetamine activate D1 rather than D2 receptors. *Psychopharmacology (Berl)* 114: 297-308, 1994.

Fergus A and Lee KS. Regulation of cerebral microvessels by glutamatergic mechanisms. *Brain Research* 754: 35-45, 1997.

Field KJ, White WJ and Lang CM. Anaesthetic effects of chloral hydrate, pentobarbitone and urethane in the adult male rat. *Laboratory Animal Science* 27: 258-269, 1993.

Fields HL. *Pain*. New York: McGraw-Hill, 1987.

Filloux F, Dawson TM and Wamsley JK. Localization of nigrostriatal dopamine receptor subtypes and adenylate cyclase. *Brain Research Bulletin* 20: 447-459, 1988.

Fink-Jensen A, Ingwersen SH, Nielsen PG, Hansen L, Nielsen EB and Hansen AJ. Halothane anesthesia enhances the effect of dopamine uptake inhibition on interstitial levels of striatal dopamine. *Naunyn Schmiedebergs Archives of Pharmacology* 350: 239-244, 1994.

Fisher JL, Pidoplichko VI and Dani JA. Nicotine modifies the activity of ventral tegmental area dopaminergic neurons and hippocampal GABAergic neurons. *Journal of Physiology* 92: 209-213, 1998.

Flourins P. *Recherches experimentales sur les proprietes et les fonctions du systeme nerveux dans les animaux vertebres*. pARIS: Chez Crevot, 1824.

Folle LE and Levesque RI. Circulatory, respiratory and acid-base balance changes produced by anesthetics in the rat. *Acta Biol Med Ger* 35: 605-612, 1976.

Ford AP and Marsden CA. Influence of anaesthetics on rat striatal dopamine metabolism in vivo. *Brain Research* 379: 162-166, 1986.

Forman SD, Silva AC, Dedousis N, Barbier EL, Fernstrom JD and Koretsky AP. Simultaneous glutamate and perfusion fMRI responses to regional brain stimulation. *Journal of cerebral blood flow and metabolism* 18: 1064-1070, 1998.

Fox PT and Raichle ME. Focal physiological uncoupling of cerebral blood flow and oxidative metabolism during somatosensory stimulation in human subjects. *Proceedings of the National Academy of Science of the United States of America* 83: 1140-1144, 1986.

Frahm J, Kruger K, Merbolt KD and Kleinschmidt A. Dynamic uncoupling and recoupling of perfusion and oxidative metabolism during focal brain activation in man. *Magnetic Resonance in Medicine* 35: 143-148, 1996.

Frantz KJ and Van Hartesveldt C. Sulpiride antagonizes the biphasic locomotor effects of quinpirole in weanling rats. *Psychopharmacology (Berl)* 119: 299-304, 1995.

Freed, W. J. The therapeutic latency of neuroleptic drugs and nonspecific postjunctional supersensitivity. 14(2), 269-277. 1988.
Ref Type: Generic

Freedman NL. A sliding gas delivery system and ventilating chamber for small animals fixed in standard stereotaxic instuments. *Behavioural research methods, intruments and computers* 119: 299-304, 1992.

Freedman SB, Patel S, Marwood R, Emms F, Seabrook GR, Knowles MR and McAllister G. Expression and pharmacological characterization of the human D3 dopamine receptor. *Journal of pharmacology and Experimental therapeutics* 268: 417-426, 1994.

Freeman AS, Meltzer LT and Bunney BS. Firing properties of substantia nigra doaminergic neurons in freely moving rats. *Life Sciences* 36: 1983-1994, 1985.

Friedemann MN and Gerhardt GA. Regional effects of aging on dopaminergic function in the Fischer-344 rat. *Neurobiology of Aging* 13: 325-332, 1992.

Friston KJ, Ashburner J, Poline JB, Frith CD, Heather JD and Frackowiak RSJ. Spatial Registration and Normalization of Images. *Human Brain Mapping* 2: 165-189, 1995.

Friston KJ, Holmes AP, Price CJ, Buchel C and Worsley KJ. Multisubject fMRI studies and conjunction analyses. *Neuroimage* 10: 385-396, 1999.

Friston KJ, Holmes AP, Worsley KJ, Poline JP, Frith CD and Frackowiak RSJ. Statistical Parametric Maps in Functional Imaging: A General Linear Approach. *Human Brain Mapping* 2: 189-210, 1995.

Fritz G and Hitzig E. *In: Some papers on the cerebral cortex (translated from "Uber die elektrische Erregbarkeit des Grosshirns").* 1870.

Fuller RW and Hemrik-Lueke SK. Long lasting depletion of striatal dopamine by a single injection of amphetamine in imprindole treated rats. *Science* 209: 305-307, 1980.

Fuxe K, Harfstrand A, Agnati LF, Kalia M, Fredholm B, Svensson T, Gustafsson JA, Lang R and Ganten D. Central catecholamine-neuropeptide Y interactions at the pre- and postsynaptic level in cardiovascular centers. *Journal of Cardiovascular Pharmacology* 10: S1-S13, 1987.

Gage PW and Robertson B. Prolongation of inhibitory postsynaptic currents by pentobarbitone, halothane and ketamine in CA1 pyramidal cells in rat hippocampus. *British Journal of Pharmacology* 85: 675-681, 1985.

Gall FJ and Spurzheim JC. *Anatomie und physiologie des Nervensystems im Allgemeine und des Gerhirns Usbesondere?* R. Scholl Paris, 1810.

Gambarana C, Ghiglieri O and Graziella de Montis M. Desensitization of the D1 dopamine receptors in rats reproduces a model of escape deficit reverted by imipramine, fluoxetine and clomipramine. *Progress in Neuro-psychopharmacology & Biological Psychiatry* 19: 741-755, 1995.

Gambill JD and Kornetsky C. Effects of chronic d-amphetamine on social behavior of the rat: implications for an animal model of paranoid schizophrenia. *Psychopharmacology (Berl)* 50: 215-223, 1976.

Gao WJ, Krimer LS and Goldman-Rakic PS. Presynaptic regulation of recurrent excitation by D1 receptors in prefrontal circuits. *Proceedings of the National Academy of Sciences of the USA* 98: 295-300, 2001.

Garau L, Govoni S, Stefanini.E, Trabucchi M and Spano PF. Dopamine receptors : pharmacological and anatomical eveidences indicate that two distinct dopamine receptors populations are present in rat striatum. *Life Sciences* 23: 1745-1750, 1978.

Garey LJ. *Brodmann's "Localisation in the Cerebral Cortex"*. Imperial College Press, 1999.

Garrett BE and Holtzman SG. D1 and D2 dopamine receptor antagonists block caffeine-induced stimulation of locomotor activity in rats. *Pharmacology Biochemistry Behaviour* 47: 89-94, 1994.

Garris PA and Wightman RM. Different kinetics govern dopaminergic transmission in the amygdala, prefrontal cortex, and striatum: an in vivo voltammetric study. *Journal of Neuroscience* 14: 442-250, 1994.

Gaspar P, Berger B, Alvarez C, Vigny A and Henry JP. Catecholaminergic innervation of the septal area in man: immunocytochemical study using TH and DBH antibodies. *The Journal of Comparative Neurology* 241: 12-33, 1985.

Gatley J and Volkow ND. Addiction and imaging of the living human brain. *Drug and alcohol dependance* 51: 97-108, 1998.

Gawin FH. Cocaine Addiction: Psychology and Neurophysiology. *Science* 251: 1580-1586, 1991.

Gawin FH and Ellinwood EHJ. Cocaine and other stimulants. Actions, abuse, and treatment. *New England Medical Journal* 318: 1172-1182, 1988.

Gehlert DR. Quantitative autoradiography of Gpp(NH)p sensitive and insensitive [3H]quinpirole binding sites in the rat brain. *Synapse* 14: 113-120, 1993.

Gehlert DR, Gackenheimer SL, Seeman P and Schaus J. Autoradiographic localization of [3H]quinpirole binding to dopamine D2 and D3 receptors in rat brain. *European journal of Pharmacology* 211: 189-194, 1992.

Gehlert DR and Wamsley JK. Autoradiographic localization of [3H]sulpiride binding sites in the rat brain. *European journal of Pharmacology* 98: 311-312, 1984.

Geller E, Halpern P, Chernilas J, Niv D and Miller HB. Cardiorespiratory effects of antagonism of diazepam sedation with flumazenil in patients with cardiac disease. *Anesthesiology and Analgesia* 72: 207-211, 1991.

George JS, Aine CJ, Mosher JC, Schmidt DM, Ranken DM, Schlitt HA, Wood CC, Lewine JD, Sanders JA and Belliveau JW. Mapping function in the human brain with magnetoencephalography, anatomical magnetic resonance imaging, and functional magnetic resonance imaging. *Journal of Clinical Neurophysiology* 12: 406-413, 1995.

Gerfen CR. The neostriatal mosaic: Multiple levels of compartmental organisation in the basal ganglia. *Annual Reviews of Neuroscience* 15: 285-320, 1992.

Gerfen CR, Engber TM, Mahan LC, Susel Z, Chase TN, Monsma FJJ and Sibley DR. D1 and D2 dopamine receptor-regulated gene expression of striatonigral and striatopallidal neurons. *Science* 250: 1429-1432, 1990.

Gerlach J, Behnke K, Heltberg J, Munk-Anderson E and Nielsen H. Sulpiride and haloperidol in schizophrenia: a double-blind cross-over study of therapeutic effect, side effects and plasma concentrations. *British Journal of Psychiatry* 147: 283-288, 1985.

German DC and Bowden DM. Catecholamine systems as the neural substrate for intracranial self-stimulation: a hypothesis. *Brain Research* 73: 381-419, 1974.

Geyer MA, Dawsey WJ and Mandall AJ. Differential effects of caffeine, D-amphetamine and methylphenidatw on individual raphe call flourescence: A micro-spectroflourometric demonstration. *Brain Research* 106: 241-256, 1975.

Geyer MA, Russo PV, Segal DS and Kuczenski R. Effects of apomorphine and amphetamine on patterns of locomotor and investigatory behavior in rats. *Pharmacology, Biochemistry and Behaviour* 28: 393-399, 1987.

Gilbert DB and Cooper SJ. Analysis of dopamine D1 and D2 receptor involvement in d- and l-amphetamine-induced anorexia in rats. *Brain Research Bulletin* 4: 385-389, 1985.

Giros B and Caron MG. Molecular characterization of the dopamine transporter. *Trends in Pharmacological Sciences* 14: 3-9, 1993.

Giros B, Jaber M, Jones SR, Wrightman RM and Caron MG. Hyperlocomotion and indifference to cocaine and amphetamine in mice lacking the dopamine transporter. *Nature* 379: 606-612, 1996.

Glass HI and Harper AM. Measurements of regional blood flow in cerebral cortex of man through intact skull. *British Medical Journal* 1: 593, 1963.

Goldstein A, Tachibana S, Lowney LI, Hunkapiller M and Hood L. Dynorphin- (1-13), an extraordinarily potent opiod. *Proceedings of the National Academy of Science of the USA* 76: ??, 1979.

Goldstein JM, Litwin LC, Sutton EB and Malick JB. D-2 dopamine antagonist-like effects of SCH 23390 on A9 and A10 dopamine neurons. *Life Sciences* 40: 1039-1044, 1987.

Gollub RL, Breiter H.C, Kantor H, Kennedy D, Gastfriend D, Mathew RT, Makris N, Guimaraes A, Riorden J, Campbell T, Foley M, Hymen SE, Rosen B and Weisskoff R. Cocaine decreases cortical cerebral blood flow but does not obscure regional activation in functional magnetic resonance imaging in human subjects. *Journal of cerebral blood flow and metabolism* 18: 724-734, 1998.

Gomez-Tortosa E, Ingraham AO, Irizarry MC and Hyman BT. Dementia with Lewy bodies. *Journal of American Geriatric Society* 46: 1449-1458, 1998.

Gonenc S, Acikgoz O, Kayatekin BM, Uysal N and Akhisaroglu M. Effects of footshock stress on superoxide dismutase and glutathione peroxidase enzyme activities and thiobarbituric acid reactive substances levels in the rat prefrontal cortex and striatum. *Neuroscience Letters* 289: 107-110, 2000.

Gonzalez-Nicolini V and McGinty JF. NK-1 receptor blockade decreases amphetamine-induced behavior and neuropeptide mRNA expression in the striatum. *Brain Research* 931: 41-49, 2002.

Gordon FJ, Brody MJ and Johnson AK. Regional depletion of central nervous system catecholamines: effects on blood pressure and drinking behavior. *Brain Research* 345: 285-97, 1985.

Gordon JH, Clopton JK, Curtin JC and Koller WC. Chronic autoreceptor blockade and neuroleptic-induced dopamine receptor hypersensitivity. *Pharmacology, Biochemistry and Behaviour* 26: 223-228, 1987.

Grandy DK and Civelli O. Molecular biology of dopamine receptors. *Trends in Pharmacological Sciences* 13: 61-69, 1992.

Grandy DK, Marchionni MA, Makam H, Stofko RE, Alfano M, Frothingham L, Fischer JB, Burke-Howie KJ, Bunzow JR and Server AC. Cloning of the cDNA and gene for a human D2 dopamine receptor. *Proceedings of the National Academy of Sciences U S A* 24: 9762-9766, 1989.

Greenwald MK, Schuster CR, Johanson CE and Jewell L. Automated measurement of motor activity in human subjects: effects of repeated testing and d-amphetamine. *Pharmacology, Biochemistry and Behaviour* 59: 59-65, 1998.

Grinspoon L and Hebdblom P. *The speed culture: amphetamine use and abuse in America*. Cambride MA: Harvard University Press, 1975.

Gsell W, De Sadeleer C, Marchalant Y, MacKenzie ET, Schumann P and Dauphin F. The use of cerebral blood flow as an index of neuronal activity in functional neuroimaging: experimental and pathophysiological considerations. *Journal of Chemical Neuroanatomy* 20: 215-224, 2000.

Guarraci FA, Frohardt RJ and Kapp BS. Amygdaloid D1 dopamine receptor involvement in Pavlovian fear conditioning. *Brain Research* 827: 28-40, 1999.

Guidotti A and Costa E. Commentary: Trans-synaptic regulation of typrosine 3-mono-oxygenase biosynthesis in rat adrenal medulla. *Biochemical Pharmacology* 26: 817-823, 1977.

Guix T, Hurd YL and Ungerstedt U. Amphetamine enhances extracellular concentrations of dopamine and acetylcholine in dorsolateral striatum and nucleus accumbens of freely moving rats. *Neuroscience Letters* 138: 137-140, 1992.

Guyen TV, Brownell A-L, Chen YI, Livni E, Coyle JT, Rosen BR, Cavagna F and Jenkins BG. Detection of the effect of dopamine receptor supersensitivity using pharmacological MRI and correlation with PET. *Synapse* 36: 57-65, 2000.

Gybels GM. Defining idiopathic Parkinson`s Disease. *Noradrenergic mechanisms in Parkinson`s Disease* CRC Press. Boco Raton: 1-9, 1994.

Gyngell ML, Bock C, Schmutz B, Hoehn-Berlage M and Hossman K-A. Variation of functional magnetic resonance signal in response to somatosensory stimulation in alpha-chloralose anaesthetised rats. *Magnetic Resonance in Medicine* 36: 13-15, 1996.

Hadfield MG and Nugent EA. Cocaine: comparative effect on dopamine uptake in extrapyramidal and limbic systems. *Biochemical Pharmacology* 32: 1983.

Hagino H, Tabuchi E, Kurachi M, Saitoh O, Sun Y, Kondoh T, Ono T and Torii K. Effects of D2 dopamine receptor agonist and antagonist on brain activity in the rat assessed by functional magnetic resonance imaging. *Brain Research* 813: 367-373, 1998.

Hahn EL. *Physics Reviews* 94: 580-594, 1950.

Hall H, Farde L, Halldin C, Hurd YL, Pauli S and Sedvall G. Autoradiographic localization of extrastriatal D2-dopamine receptors in the human brain using [125I]epidepride. *Synapse* 23: 115-123, 1996.

Hall H, Halldin C, Dijkstra D, Wikstrom H, Wise LD, Pugsley TA, Sokoloff P, Pauli S, Farde L and Sedvall G. Autoradiographic localisation of D3-dopamine receptors in the human brain using the selective D3-dopamine receptor agonist (+)-[3H]PD 128907. *Psychopharmacology (Berl)* 128: 240-247, 1996.

Hall H, Kohler C, Gawell L, Farde L and Sedvall G. Raclopride, a new selective ligand for the dopamine-D2 receptors. *Progress in Neuro-Psychopharmacology and Biological Psychiatry* 12: 559-568, 1988.

Hamamura T and Fibiger HC. Enhanced stress-induced dopamine release in the prefrontal cortex of amphetamine-sensitized rats. *European journal of Pharmacology* 237: 65-71, 1993.

Hamburger A and Nystrom B. Extra- and intracellular amino acids in the hippocampus during development of hepatic encephalopathy. *Neurochemistry Research* 9: 1181-1192, 1984.

Hamilton ME, Mele A and Pert A. Striatal extracellular dopamine in concious vs. anaesthetised rats: effects of chloral hydrate anaesthetic on responses to drugs of different classes. *Brain Research* 597: 1992.

Hanriot M and Richet C. *D`une substance derivee du chloral ou chloralose , et de ses effets physiologiques et therapeutiques*. Paris: C.R. Acad. Sci, 1893.

Hansen TD, Warner DS, Todd MM and Vust LJ. The role of cerebral metabolism in determining the local cerebral blood flow effects of volatile anesthetics: evidence for

persistent flow-metabolism coupling. *Journal of cerebral blood flow and metabolism* 9: 323-328, 1989.

Hardie RJ, Lees AJ and Stern GM. On-off fluctuations in arlinson`s disease: a clinical and neuropharmacological study. *Brain* 107: 487-509, 1984.

Harding RK, Hugenholtz H, Kucharczyk J and Lem. Central mechanisms for apomorphine-induced emesis in the dog. *European journal of Pharmacology* 144: 61-65, 1987.

Harel NA, Shmuel A, Lee S and Duong TQ. Observations of positive and negative BOLD signals in the visual cortex. *Proceedings of the 8th Scientific meeting and exhibition of the International Society for Magnetic Resonance in Medicine* 650: 2001.

Harris GT, Lewis RF, Satlin A, English CD, Scott TM, Yurgelun-Todd DA and Renshaw PF. Dynamic suscpetability contrast MRI of regional cerebral blood flow in Alzheimer`s Disease. *American Journal of Psychiatry* 153: 721-724, 1996.

Hashemi RH and Bradley Jr WG. *MRI the basics*. Lipponcott Williams & Wilkins, 1997.

Heath RG. Correlation of brain function with emotional behavior. *Biological Psychiatry* 11: 463-480, 1976.

Heeger D, Boynton GM, Demb JB, Seideman E and Newsome WT. Motion occupancy in visual cortex. *Journal of Neuroscience* 19: 7162-7174, 1999.

Heeger DJ, Huk AC, Gieslen WS and Albrecht DG. Spike versus BOLD: What does neuroimaging tell us about neuronal activity? *Nature Neuroscience* 3: 631-633, 2000.

Heffernan MS. Comparative effects of microcurrent stimulation on EEG spectrum and correlation dimension. *Integrative Physiological & Behavioral Science* 31: 202-209, 1996.

Heikkila RE, Sonsalla PK and Duvoisin RC. Biochemical models of Parkinson`s Disease. edited by A.B Boulton GBBAVJ. 1989, p. 351-384.

Hennig J, Nauerth A and Friedburg H. RARE imaging: a fast imaging method for clinical MR. *Magnetic Resonance in Medicine* 3: 823-833, 1986.

Hernandez L, Lee F and Hoebel BG. Microdialysis in the nucleus accumbens during feeding or drugs of abuse: amphetamine, cocaine, and phencyclidine. *Annals of the New York Academy of Sciences* 537: 508-511, 1988.

Hinke RM, Hu XP, Stillman AE, Kin SG, Merkle H, Salmi R and Ugurbil K. Functional magmnetic resonance imaging of brocas area during internal speech. *Neuroreport* 4: 675-678, 1993.

Hock C, Muller-Spahn F, Schuh-Hofer S, Hofmann M, Dirnagl U and Villringer A. Age dependency of changes in cerebral hemoglobin oxygenation during brain

activation: a near-infrared spectroscopy study. *Journal of cerebral blood flow and metabolism* 15: 1103-1108, 1995.

Hoggard N, Wilkinson ID and Griffiths PD. The imaging of ischaemic stroke. *Clinical Radiology* 56: 171-183, 2001.

Holzegrefe H, Everit J and Wright E. Alpha chloralose as a canine anaesthetic. *Laboratory Animal Science* 37: 587-595, 1987.

Horn A.S. Dopamine uptake: a review of progress in the last decade. *Progress in Neurobiology* 34: 387-400, 1990.

Hornykiewicz O. Dopamine and brain fuction. *Pharmacological Reviews* 18: 925-964, 1966.

Hounsfield GN. Computerized transverse axial scanning (tomography). 1. Description of system. *British Journal of Radiology* 46: 1016-1022, 1973.

Houston GC, Papadakis NG, Carpenter TA, Hall LD, Mukherjee B, James MF and Huang CL-H. Mapping of brain activation in response to pharmacological agents using fMRI in the rat. *Magnetic Resonance Imaging* 19: 905-919, 2001.

Huang W, Plyka I, Li H, Eisenstein EM, Volkow ND and Springer CS, Jr. Magnetic resonance imaging (MRI) detection of the murine brain response to light: temporal differentiation and negative functional MRI changes. *Proc Natl Acad Sci U S A* 93: 6037-6042, 1996.

Huff RM and Molinoff PB. Assay of dopamine receptors with [alpha-3H]flupenthixol. *Journal of pharmacology and Experimental therapeutics* 232: 57-61, 1985.

Hughes J. Search for the endogenous ligand of the opiate receptor. *Neuroscience* 13: 55-58, 1975.

Hurd YL, McGregor A and Ponten M. In vivo amygdala dopamine levels modulate cocaine self-administration behaviour in the rat: D1 dopamine receptor involvement. *European Journal of Neuroscience* 12: 2541-2548, 1997.

Hurd YL and Ungerstedt U. Cocaine: An in vivo microdialysis evaluation of of its acute action on dopamine transmission in rat striatum. *Synapse* 3: 48, 1989.

Hurd YL and Ungerstedt V. In vivo neurochemical profile of dopamine uptake inhibitiors and releasers in cat caudate-putamen. *European journal of Pharmacology* 166: 251-260, 1989.

Huttenlocher PR, de Courten C, Garey LJ and Van der Loos H. Synaptogenesis in human visual cortex--evidence for synapse elimination during normal development. *Neuroscience Letters* 33: 247-252, 1982.

Hyder F, Behar KL, Martin MA, Blamire AM and Shulman RG. Dynamic magnetic resonance imaging of the rat brain during forepaw stimulation. *Journal of cerebral blood flow and metabolism* 14: 649-655, 1994.

Hyder F, Rothman DL, Mason GF, Rangarajan A, Behar KL and Shulman RG. Oxidative Glucose Metabolism in the rat brain during single forepaw stimulation: A spatially localised 1H[13C] Nuclear Magnetic Resonance Study. *Journal of cerebral blood flow and metabolism* 17: 1040-1047, 1997.

Hyder F, Rothman DL and Shulman RG. Total neuroenergetics support localized brain activity: Implications for the interpretation of fMRI. *Proceedings of the national Academy of Sciences of the U S A* 99: 10771-10776, 2002.

Hyman SE. Addiction to cocaine and amphetamine. *Neuron* 16: 901-904, 1996.

Imperato A, Puglisi-Allegra S, Casolini P and Angelucci L. Changes in brain dopamine and acetylcholine release during and following stress are independant of the pituitary adrenocortical axis. *Brain Research* 538: 111-117, 1991.

Ingvar DH and Lassen NA. Quantitative determination of regional cerebral blood-flow. *Lancet* 2: 806-807, 1961.

Ingvar M, Lindvall O and Stenevi U. Apomorphine-induced changes in local cerebral blood flow in normal rats and after lesions of the dopaminergic nigrostriatal bundle. *Brain Research* 262: 259-265, 1983.

Inoue K, Kiriike N, Fujisaki Y, Okuno M, Ito H and Yamagami S. D2 receptors in the ventrolateral striatum are involved in feeding behavior in rats. *Pharmacology, Biochemistry and Behaviour* 50: 153-161, 1995.

Iorio LC, Barnett A, Leitz FH, Houser VP and Korduba CA. SCH 23390, a potential benzazepine antipsychotic with unique interactions on dopaminergic systems. *Pharmacology and Experimental Therapeutics* 226: 462-468, 1983.

Iverson LL. Uptake mechanisms for neurotransmitter amines. *Biochemical Pharmacology* 23: 1927-1935, 1974.

Ives JR, Warach S, Schmitt F, Edelman RR and Schomer DL. Monitoring the patient's EEG during echo planar MRI. *Electroencephalography and Clinical Neurophysiology* 87: 417-420, 1993.

Izzo, E., Orsini, C., Koob, G. F., and Pulvirenti, L. A dopamine partial agonist and antagonist block amphetamine self-administration in a progressive ratio schedule. 68(4), 701-708. 2001.
Ref Type: Generic

Jaber M, Robinson SW, Missale C and Caron MG. Dopamine receptors and brain function. *Neuropharmacology* 35: 1503-1519, 1996.

Jackson JH. *Selected writings of John Hughlings Jackson.* London: Hodder & Stoughton, 1931.

Jarvie KR and Caron MG. Heterogeneity of dopamine receptors. *Advances in Neurology* 60: 325-333, 1993.

Jaworski JN, Gonzales RA and Randall PK. Effect of dopamine D2/D3 receptor antagonist sulpiride on amphetamine-induced changes in striatal extracellular dopamine. *European journal of Pharmacology* 418: 201-206, 2001.

Jellinger K. Neuropathological substrates of Alzheimer's disease and Parkinson's disease. *Journal of Neural Transmission* 24: 109-129, 1987.

Johnson B. *Intravenous Anaesthesia: Modern Practice in Anaesthesia*. 1949.

Johnson RG, Jr. Proton pumps and chemiosmotic coupling as a generalized mechanism for neurotransmitter and hormone transport. *Ann N Y Acad Sci* 493: 162-177, 1987.

Johnston RR, Way WL and Miller RD. Alteration of anaesthetic requirement by amphetamine. *Anaestheology* 36: 1972.

Johnstone EC, Crow TJ, Frith CD, Husband J and Kreel L. Cerebral venticular size and cognitive impairment in chronis scchizophrenia. *Lancet* 2: 924-926, 1976.

Jones AP, Hughes DG, Brettle DS, Robinson L, Dykes JR, Aziz Q, Hamdy S, Thompson DG, Derbyshire SWG, Chen ACN and Jones AKP. Experiences with functional magnetic resonance imaging at 1 tesla. *British Journal of Radiology* 7: 160-166, 1998.

Jouvet M. Biogenic amines and the states of sleep. *Science* 163: 1969.

Jueptner M and Weiller C. Review: Does measurement of regional cerebral blood flow reflect synaptic activity?-implications for PET and fMRI. *Neuroimage* 2: 1995.

Jung MY, Skryabin BV, Arai MAS, Fu D, Brosius J, Robakis NK, Polites HG, Pintar JE and Schmauss C. Potentiation of the D2 mutant motor phenotype in mice lacking dopamine D2 and D3 receptors. *Neuroscience* 91: 911-924, 1999.

Kalivas PW and Duffy P. Effect of acute and daily cocaine treatment on extracellular dopamine in the nucleus accumbens. *Synapse* 5: 48-58, 1990.

Kalivas PW and Duffy P. D1 receptors modulate glutamate transmission in the ventral tegmental area. *Journal of Neuroscience* 7: 5379-5388, 1995.

Kalivas PW and Duffy P. Dopamine regulation of extracellular glutamate in the nucleus accumbensBrain Research. *Brain Research* 761: 173-177, 1997.

Kandel E, Schwartz JH and Jessel TM. *Principles of Neural Science*. Norwalk C.T: Appleton -Lange, 1991.

Karoum F, Chrapusta SJ, Brinjak R, Hitri A and Wyatt RJ. Regional effects of amphetamine, cocaine, nomifensine and GBR12909 on the dynamics of dopamine release and metabolism in the rat brain. *British Journal of Pharmacology* 113: 1391-1399, 1994.

Kebabian JW and Calne DB. Multiple receptors for dopamine. *Nature* 5692: 1979.

Kebabian JW, Petzold GL and Greengard P. Dopamine-sensitive adenylate cyclase in caudate nucleus of rat brain, and its similarity to the "dopamine receptor". *Proceedings of the National Academy of Sciences of the USA* 69: 2145-2149, 1972.

Kelland MD, Chiodo LA and Freeman AS. Anaesthetic influences on the basal activity and pharmacological responsiveness of nigrostriatal dopamine neurons. *Synapse* 6: 207-209, 1990.

Kelly MA, Rubinstein M, Asa SL, Zhang G, Saez C, Bunzow JR, Allen RG, Hnasko R, Ben-Jonathan N, Grandy DK and Low MJ. Pituitary lactotroph hyperplasia and chronic hyperprolactinemia in dopamine D2 receptor-deficient mice. *Neuron* 19: 103-113, 1997.

Kelly MA, Rubinstein M, Phillips TJ, Lessov CN, Burkhart-Kasch S, Zhang G, Bunzow JR, Fang Y, Gerhardt GA, Grandy DK and Low MJ. Locomotor activity in D2 dopamine receptor-deficient mice is determined by gene dosage, genetic background, and developmental adaptations. *Journal of Neuroscience* 18: 3470-3479, 1998.

Kelly P and Iverson SD. Selective 6 OHDA-induced destruction of mesolimbic dopamine neurons: Abolition of psychomotorstimulant-induced locomotor activities in rats. *European journal of Pharmacology* 40: 45-56, 1976.

Kelly PH, Seviour PW and Iversen SD. Amphetamine and apomorphine responses in the rat following 6-OHDA lesions of the nucleus accumbens septi and corpus striatum. *Brain Research* 94: 507-522, 1975.

Kessler RC, Nelson CB, McGonagle KA, Edlund MJ, Frank RG and Leaf PJ. The epidemiology of co-occurring addictive and mental disorders: implications for prevention and service utilization. *American Journal of Orthopsychiatry* 66: 17-31, 1996.

Khan AM, Stanley BG, Bozzetti L, Chin C, Stivers C and Curras-Collazo MC. N-methyl-D-aspartate receptor subunit NR2B is widely expressed throughout the rat diencephalon: an immunohistochemical study. *Journal of comparative neurology* 428: 428-449, 2000.

Kida I, Hyder F and Behar KL. Inhibition of voltage-dependent sodium channels suppresses the functional magnetic resonance imaging response to forepaw somatosensory activation in the rodent. *Journal of cerebral blood flow and metabolism* 21: 585-591, 2001.

Kida IKRP, Rothman DL, Behar KL and Hyder F. High resolution CMRO2 mapping in rat cortex: A multiparametric approach to calibration of BOLD image contrast at 7 Tesla. *Journal of cerebral blood flow and metabolism* 20: 847-860, 2000.

Kim DS, Szczypka M and Palmiter RD. Dopamine-deficient mice are hypersensitive to dopmamine receptor agonists. *Journal of pharmacology and Experimental therapeutics* 20: 4405-4413, 2000.

Kim SG, Asche J and Georgopolous AP. Functional imaging of human motor cortex at high magnetic field. *Journal of Physiology* 69: 297-302, 1993.

Klaus S, Bahlmann L, Gliemroth J and Schmucker P. Metabolic monitoring in acute cardiac failure using microdialysis: A case report. *Intensive care medicine* 27: 532, 2001.

Knepper SM, Grunwald GL and Rutledge CO. Inhibition of norepinephrine transport into synaptic vesicles by amphetamine analogs. *Journal of Pharmaclogy and Experimental Therapeutics* 247: 487-494, 1988.

Koepp MJ, Gunn RN, Lawrence AD, Cunningham VJ, Dagher A, Jones T, Brooks DJ, Bench CJ and Grasby PM. Evidence for striatal dopamine release during a video game. *Nature* 393: 266-268, 1998.

Kokkinidis L and Zacharko RM. Response sensitization and depression following long-term amphetamine treatment in a self-stimulation paradigm. *Psychopharmacology (Berl)* 68: 73-76, 1980.

Kolb B. Functions of the frontal cortex of the rat. *Brain Research Reviews* 8: 65-98, 1984.

Kolb B and Wishaw IQ. *Fundamentals of Neuropsychology*. New York: Freeman, 1985.

Konuma K. Use and abuse of amphetamines in Japan. In: Amphetamine and Its Analogs, edited by San Diego. San Diego: Academic Press Inc, 1994, p. 415-435.

Koob G.F. Drug addiction: the Yin and Yang of hedonic homeostasis. *Neuron* 16: 893-896, 1996.

Koob GF. Drugs of abuse: anatomy, pharmacology and function of reward pathways. *Trends in Pharmacological Sciences* 13: 177-184, 1992.

Koob GF, Fray PJ and Iverson SD. Self-stimulation at the lateral hypothalamus and locus coeruleus after specific unilateral lesions of the dopamine system. *Brain Research* 148: 123-140, 1978.

Koob GF and Le Moal M. Drug abuse: hedonic homeostatic dysregulation. *Science* 278: 52-58, 1997.

Koos T and Tepper JM. Inhibitory control of the neostriatal projection neurons by GABAergic interneurons. *Nature Neuroscience* 2: 476-472, 1999.

Kopin IJ. Catecholamine metabolism: Basic aspects and clinical significance. *Pharmacological Reviews* 37: 333-364, 1985.

Koshikawa N, Tomiyama K, Omiya K and Kobayashi M. Ketamine anaesthesia has no effect on striatal dopamine metabolism in rats. *Brain Research* 444: 394-396, 1988.

Kraeplin E. *Textbook of Psychiatry*. Edinburgh: Livingston, 1913.

Krause CM, Salimen PA, Sillanamaki L and Hulopainem IE. Even related desynchronization and synchronization during a memory task in children. *Clinical Neurophysiology* 112: 2233-2240, 2001.

Krimer LS, Muly ECI, Williams GV and Goldman-Rakic PS. Dopaminergic regulation of cerebral microcirculation. *Nature Neuroscience* 1: 286-289, 1998.

Kruger, L. and Albe-Fessard, D. Distribution of responses to somatic afferent stimuli in the diencephalon of the cat under chloralose anaesthesia. 2, 442-467. 1960. Ref Type: Generic

Kuczenski R and Segal D. Concomitant characterisation of behavioral and striatal neurotransmitter response to amphetamine using in vivo microdialysis. *Journal of Neuroscience* 9: 2051-2065, 1989.

Kuczenski R and Segal DS. Differential effects of amphetamine and dopamine uptake blockers (cocaine, nomifensine) on caudate and accumbens dialysate dopamine and 3-methoxytyramine. *Journal of pharmacology and Experimental therapeutics* 292: 1085-1094, 1992.

Kuhl DE and Edwards RQ. Image separation isotope scanning. *Radiology* 80: 1963.

Kwong KK, Belliveau JW, Chesler DA, Goldberg IE, Weisskoff RM, Poncelet BP, Kennedy DN, Hoppel BE, Cohen MS, Turner R, Cheng HM, Brady TJ and Rosen BR. Dynamic magnetic resonance imaging of human brain activation during primary sensory stimulation. *Proceedings of the National Academy of Sciences of the USA* 89: 5675-5679, 1992.

LaBerge D. Attention, consciousness, and electrical wave activity within the cortical column. *International Journal of psychophysiology* 43: 5-24, 2001.

Lacey MG, Mercuri NB and North RA. Dopamine acts on D2 receptors to increase potassium conductance in neurones of the rat substantia nigra zona compacta. *Journal of Physiology* 397-416, 1987.

Laduron P. Brain dopamine receptor: Multiple binding sites or physiological receptor site. *Advances in Dopamine Research (M Kohsaka, ed) Pergamon, Oxford, UK* 71-76, 1982.

Lahoste GJ, Yu J and Marshall JF. Striatal Fos expression is indicative of dopamine D1/D2 synergism and receptor supersensitivity. *Proceedings of the National Academy of Sciences of the USA* 90: 7451-7455, 1993.

Lahti KM, Ferris CF, Li.F, Sotak CH and King JA. Imaging brain activity in concious animals using functional MRI. *Journal of Neuroscience Methods* 82: 75-83, 1998.

Lannes B, Micheletti G, Warter JM, Kempf E and Di Scala G. Behavioural, pharmacological and biochemical effects of acute and chronic administration of ketamine in the rat. *Neuroscience Letters* 128: 177-181, 1991.

Larsen M and Langmoen IA. The effect of volatile anaesthetics on synaptic release and uptake of glutamate. *Toxicology Letters* 100-101: 59-64, 1998.

Lauritzen M. Relationship of spikes, synaptic activity, and local changes of cerebral blood flow. *Journal of cerebral blood flow and metabolism* 21: 1367-1383, 2001.

Lawrence KSS, Ye FQ, Lewis BK, Frank JA and McLaughlin AC. Drug effects on oxidative metabolism and cerebral blood flow changes in sensorimotor activation. *Proceedings of the 10th Scientific meeting and exhibition of the International Society form Magnetic Resonance in Medicine, Hawaii* 2002.

Le Moine C and Bloch B. Expression of the D3 dopamine receptor in peptidergic neurons of the nucleus accumbens: comparison with the D1 and D2 dopamine receptors. *Neuroscience* 73: 131-143, 1996.

Lees AJ, Katzenschlager R, Head J and Ben-Shlomo Y. Ten-year follow-up of three different initial treatments in de-novo PD: a randomized trial. *Neurology* 57: 1687-1694, 2001.

Leite-Morris KA, Fukudome EY and Kaplan GB. Opiate-induced motor stimulation is regulated by gamma-aminobutyric acid type B receptors found in the ventral tegmental area in mice. *Neuroscience Letters* 317: 119-122, 2002.

Lester J, Fink S, Aronin N and DiFiglia M. Colocalization of D1 and D2 dopamine receptor mRNAs in striatal neurons. *Brain Research* 621: 106-110, 1993.

Lewis DM, Bond HR and Curry SH. Sulpiride trial in chronic schizophrenia with comparison of two dosage regimens. *Psychopharmacology (Berl)* 80: 259-262, 1983.

Lieberman AN and Goldstein M. Bromocriptine in Parkinson disease. *Pharmacol Rev* 37: 217-227, 1985.

Lindauer U, Villringer A and Dirnagl U. Characterization of CBF response to somatosensory stimulation: model and influence of anesthetics. *American Journal of Physiology* 264: 1223-8, 1993.

Lindvall O and Bjorklund A. The organization of the ascending catecholamine neuron systems in the rat brain as revealed by the glyoxylic acid fluorescence method. *Acta Physiol Scand Suppl* 412: 1-48, 1974.

Lindvall O, Bjorklund A and Skagerberg G. Selective histochemical demonstration of dopamine terminal systems in rat di- and telencephalon: new evidence for dopaminergic innervation of hypothalamic neurosecretory nuclei. *Brain Research* 306: 19-30, 1984.

Lindvall O, Ingvar M and Stenevi U. Effects of methamphetamine on blood flow in the caudate-putamen after lesions of the nigrostriatal bundle in the rat. *Brain Research* 211: 211-216, 1981.

Lindvall O and Stenevi U. Dopamine and noradrenaline neurons projecting to the septal area in the rat. *Cell Tissue Research* 190: 383-407, 1978.

Lippa AS, Antelman SM, FIsher AE and Canfield DR. Neurochemical mediation of reward: a significant role for dopamine? *Pharmacology, Biochemistry and Behaviour* 1: 23-28, 1973.

Llorens-Cortes C, Zini S, Gros C and Schwartz J. Dopaminergic regulation of enkephalin release. *Neurochemistry* 4: 1956.

Lnenicka GA and Hong SJ. Activity-dependent changes in voltage-dependent calcium currents and transmitter release. *Molecular Neurobiology* 14: 37-66, 1997.

Logothetis NK, Pauls J, Augath M, Trinath T and Oeltermann A. Neurophysiological investigation of the basis of the fMRI signal. *Nature* 412: 150-157, 2001.

London.E.D, Cascella NG, Wong DF, Phillips RL, Daniels RF, Links JM and Wagner HN. Cocaine induced reduction of glucose utilisation in the human brain. *Archives of General Psychiatry* 47: 567-574, 1990.

Louilot A, Simon H, Taghzouti K and Le Moal M. Modulation of dopaminergic activity in the nucleus accumbens following facilitation or blockade of the dopaminergic transmission in the amygdala: a study by in vivo differential pulse voltammetry. *Brain Research* 346: 141-145, 1985.

Lowe A, Symms M, Shoaib M and Williams S. Group statistical parametic mapping in rat pharmalogical MRI. *ISMRM-ESMRMB Joint Annual Meeting Proceedings* 1735, 2001.

Lowe MJ, Lurito JT, Mathews VP, Phillips MD and Hutchins GD. An investigation of the value of spin-echo-based fMRI using a Stroop color-word matching task and EPI at 3 T. *Neuroimage* 15: 719-726, 2000.

Lucki I and Harvey JA. Increased sensitivity to d- and l-amphetamine action after midbrain raphe lesions as measured by locomotor activity. *Neuropharmacology* 18: 243-249, 1979.

Lui F, Wan Q, Pristupa ZB, Yu X-M, Wang YT and Nizik HB. Direct protein-protein coupling enables cross talk between dopamine and [gamma-] aminobutyricacid A receptors. *Nature* 403: 274-280, 2000.

Lumb W and Jones E.In: Veterinary Anaesthesia, Philadelphea, PA: Lea & Febiger, 1984, p. 315-317.

Lupien SJ and McEwan BS. The acute effects of corticosteroids on cognition: integration of animal and human model studies. *Brain Research Reviews* 24: 1-27, 1997.

Mabry PD and Campbell BA. Serotinergic inhibition of catecholamine-induced behavioural arousal. *Brain Research* 49: 381-391, 1973.

Maggi CA and Meli A. Suitability of urethane anesthesia for physiopharmacological investigations in various systems. Part 1: General considerations. *Experientia* 42: 109-114, 1986.

Makeig S, Westerfield M, Juag TP, Enghoff S, Townsend J, Courchesch E and Sejhowski TJ. Dynamic brain sources of visual evoked responses. *Science* 295: 690-694, 2002.

Maldonado R, Saiardi A, Valverde O, Samad TA, Roques BP and Borrelli E. Absence of opiate rewarding effects in mice lacking dopamine D2 receptors. *Nature* 388: 586-589, 1997.

Malonek D and Grinvald.A. Interactions between electrical activity and cortical microcirculations revealed by imaging spectroscopy. *Science* 272: 551-554, 1996.

Mann PJG and Quastel JH. Benzedrine and brain metabolism. *Biochemical Journal* 34: 414-431, 1940.

Mansour A, Meador-Woodruff JH, Civelli O, Akil H and Watson SJ. Localisation of dopamine D2 receptor mRNA and D1 and D2 receptor bindig in the rat brain and pituitary: an in situ hybridisation-receptor autoradiographic analysis. *The journal of neuroscience* 10: 2587-2600, 1990.

Mantz J, Varlet C, Lecharny JB, Henzel D, Lenot P and Desmonts JM. Effects of volatile anesthetics, thiopental, and ketamine on spontaneous and depolarization-evoked dopamine release from striatal synaptosomes in the rat. *Anesthesiology* 80: 352-363, 1994.

Marota JJ, Mandeville JB, Weisskoff RM, Moskowitz MA, Rosen BR and Kosofsky BE. Cocaine activation discriminates projections by temporal response: An fMRI study. *Neuroimage* 11: 13-23, 2000.

Marota JJA, Moskowitz CMA, Weisskoff RM, Rosen BR and Mandeville JB. Investigation of the early response to rat forepaw stimulation. *Magnetic Resonance in Medicine* 41: 247-252, 1999.

Marsden CD and Parkes JD. Success and problems of long-termlevodopa therapy in Parkinson`s disease. *Lancet* i: 1977.

Marshall WH, Woolsey CN and Bard P. Observations on cortical somatosensory mechanisms of the cat and monkey. *Journal of Neurophysiology* 4: 1-25, 1941.

Martin E, Thiel T, Joeri P, Loenneker T, Ekatodramis D, Huisman T, Hennig J and Marcar VL. Effect of pentobarbital on visual processing in man. *Human Brain Mapping* 10: 132-139, 2000.

Martin WR and Sloan JW. Neurophamacology and neurochemistry of subjective effects of analgesia and dependance produced by narcotic substances. In: Journal Title: Handbook of Experimental Pharmacology. Drug Addiction 1: Morphine, Sedative/|Hypnotic and Alcohol dependance, Berlin: Springer, 1977, p. 43-158.

Martin-Soelch C, Leenders KL, Chevalley AF, Missimer J, Kunig G, Magyar S, Mino A and Schultz W. Reward mechanisms in the brain and their role in dependence: evidence from neurophysiological and neuroimaging studies. *Brain Research Reviews* 36: 139-149, 2001.

Martres MP, Bouthenet ML, Sales N, Sokoloff P and Schwartz JC. Widespread distribution of brain dopamine receptors evidenced with [125I]iodosulpride, a highly selective ligand. *Science* 228: 752-755, 1985.

Masserano JM, Viullet PR, Tank A and Weiner N. The role of tyrosine hydroxylase in the regulation of catecholaime synthesis. In: The handbook of catecholamine synthesis, edited by Trendelenburg U and Weiner N. Berlin: Springer-Verlag, 1989, p. 427-469.

Massott M and Longo VG. Alpha chloralose and the central dopaminergic system. *Journal of pharmacy and Pharmacology* 30: 667, 1978.

Mata M, Fink DJ, Gainer H, Smith CB, Dadidsen L, Savaki H, Schwartz WJ and Sokoloff L. Activity-dependant energy metabolism in rat posterior pituitary primarily reflects sodiumm pump activity. *Journal of Neurochemistry* 34: 213-215, 1980.

Mathiesen C, Caesar K, Akgoren N and Lauritzen M. Modification of activity-dependent increases of cerebral blood flow by excitatory synaptic activity and spikes in rat cerebellar cortex. *Journal of Physiology* 512: 555-566, 1998.

Matthew RJ and Wilson WH. Substance abuse and cerebral blood flow. *American Journal of Psychiatry* 148: 292-305, 1991.

Mattson MP. Calcium as sculptor and destroyer of neural circuitry. *Experimental Gerontology* 27: 29-49, 1992.

McCabe RT, Hanson GR, Dawson TM, Wamskey JK and Gibb JW. Methamphetamine-induced reduction in D1 and D2 dopamine receptors as evidenced by autoradiography: comparison with tyrosine hydroxylase activity. *Neuroscience* 23: 253-261, 1987.

McCulloch J, Savaki HE and Sokoloff L. Distribution of effects of haloperidol on energy metabolism in the rat brain. *Brain Research* 243: 81-90, 1982.

McCulloch J and Teasdale G. Effects of apomorphine upon local cerebral blood flow. *European journal of Pharmacology* 55: 99-102, 1979.

McGregor A and Roberts DC. Effect of medial prefrontal cortex injections of SCH 23390 on intravenous cocaine self-administration under both a fixed and progressive ratio schedule of reinforcement. *Behavioural Brain Research* 67: 75-80, 1995.

McKinney WT and Moran EC. Animal models of schizophrenia. *American Journal of Psychiatry* 138: 478-483, 1981.

McQuade RD, Chipkin R, Amlaiky N, Caron M, Iorio L and Barnett A. Characterization of the radioiodinated analogue of SCH 23390: in vitro and in vivo D-1 dopamine receptor binding studies. *Life Sciences* 43: 1151-1160, 1988.

Meador-Woodruff JH, Mansour A, Grandy DK, Civelli O and Watson SJ. Distribution of the D5 receptors mRNA in the rat brain. *Neuroscience Letters* 145: 209-212, 1992.

Meador-Woodruff JH, Mansour A, Healty DJ, Kuehn R, Zhou AQ, Bunzou JR, Akil H, Civelli O and Watson SJJ. Comparison of the distribution of D1 and D2 receptor mRNAs in the rat brain. *Neuropsychopharmacology* 15: 231-242, 1991.

Meek JH, Firbank M, Elwell CE, Atkinson J, Braddick O and Wyatt JS. Regional hemodynamic responses to visual stimulation in awake infants. *Pedriatic Research* 43: 840-843, 1998.

Meek JH, Elwell CE, Khan MJ, Romaya J, Wyatt JS, Delpy DT and Zeki S. Regional changes in cerebral haemodynamics as a result of a visual stimulus measured by near infrared spectroscopy. *Proceedings of the Royal Society London Biological Sciences* 261: 351-356, 1995.

Meixenberger J, Kunze E, Barcsay E, Vaeth A and Roosen K. Clinical cerbral microdialysis: Brain metabolism and brain tissue oxygenatiom after acute brain injury. *Neurological Research* 23: 801-806, 2001.

Meltzer H. Do loxapine plus cyproheptadine make an atypical antipsychotic? PET analysis of their Dopamine D2 and Seratonin 2 receptor occupancy. *Archives of General Psychiatry* 55: 666-668, 1996.

Mendez JS and Finn BW. Use of 6-hydroxydopamine to create lesions in catecholamine neurons in rats. *Journal of Neurosurgery* 42: 166-173, 1975.

Millan MJ, Audinot V, Rivet JM, Gobert A, Vian J, Prost JF, Spedding M and Peglion JL. S 14297, a novel selective ligand at cloned human dopamine D3 receptors, blocks 7-OH-DPAT-induced hypothermia in rats. *European journal of Pharmacology* 260: 3-5, 1994.

Milusheva EA, Doda M, PE, Lajtha A, Sershen H and Vizi ES. Regulatory interactions among axon terminals affecting the release of different transmitters from rat striatal slices under hypoxic and hypoglycemic conditions. *Journal of Neurochemistry* 59: 946-952, 1992.

Milusheva EA, Doda M, Baranyi M and Vizi ES. Effect of hypoxia and glucose deprivation on ATP level, adenylate energy change and (Ca2+)o-dependent and independent release of [3H]dopamine in rat striatal slice. *Neurochemistry International* 28: 501-507, 1996.

Mintun MA, Lundstrom BN, Snyder AZ, Vlassenko AG, Shulman GL and Raichle ME. Blood flow and oxygen delivery to human brain during functional activity: theoretical modeling and experimental data. *Proceedings of the national Academy of Sciences of the U S A* 98: 6859-6869, 2001.

Miyano K, Tanifuji Y and Eger II I. The effect of halothane on striatal dopamine: an in vivo microdialysis study. *Brain Research* 605: 342-344, 1993.

Mogenson GJ, Robertson A and Wu M. Self-stimulation of the nucleus accumbens and ventral tegmented area of Tsai attenuated by microinjections of spiroperidol into the nucleus accumbens. *Brain Research* 171: 247-259, 1979.

Moghaddam B, Berridge CW, Goldman-Rakic PS, Bunney BS and Roth RH. In vivo assessment of basal and drug-induced dopamine release in cortical and subcortical regions of the anesthetized primate. *Synapse* 13: 215-222, 1993.

Moghaddam B and Bunney BS. Acute effects of typical and atypical antipsychotic drugs on the release of dopamine from prefrontal cortex, nucleus accumbens, and striatum of the rat: an in vivo microdialysis study. *Journal of Neurochemistry* 54: 1755-1760, 1990.

Moghaddam B and Bunney BS. Utilization of microdialysis for assessing the release of mesotelencephalic dopamine following clozapine and other antipsychotic drugs. *Progress in Neuro-Psychopharmacology and Biological Psychiatry* 14 Suppl: 51-7, 1990.

Molloy AG and Waddington JL. Dopaminergic behaviour stereospecific promoted by the D1 agonist R-SK & F 38393 and selectively blocked by the D1 antagonist SCH 23390. *Psychopharmacology* 82: 409-410, 1984.

Monks TJ, Hanzlik RP, Cohen GM, Ross D and Graham CDG. Quninone chemistry and toxicity. *Toxicology and applied pharmacology* 112: 2-16, 1992.

Monroe RR, Balis GU and Ebersberger E. Anticonvulsant activity of alpha and beta chloralose in rats. *Current therapeutic research* 5: 154-165, 1963.

Monroe RR, Balis GU and Ebersberger E. The hypnotic effects of alpha and beta chloralose in rats. *Current therapeutic research* 5: 141-153, 1963.

Moore AH, Hovda DA, Cherry SR, Villablanca JP, Pollack DB and Phelps ME. Dynamic changes in cerebral glucose metabolism in conscious infant monkeys during the first year of life as measured by positron emission tomography. *Developmental Brain Research,* 120: 141-150, 2000.

Moore JA and Appenteng K. Contasting effects of urethane and pentobarbitone anaesthesia on the electrical properties of rat jaw-elevator motoneurones. *Brain Research* 139-142, 1990.

Moore RY and Bloom FE. Central catecholamine neuron systems: anatomy and physiology of the dopamine systems. *Annual Reviews of Neuroscience* 1: 1978.

Morelli M, Mennini T and Di Chiara G. Nigral dopamine autoreceptors are exclusively of the D2 type: quantitative autoradiography of [125I]iodosulpride and [125I]SCH 23982 in adjacent brain sections. *Neuroscience* 3: 865-870, 1988.

Moro V, Badaut J, Springhetti V, Edvinsson L, Seylaz J and Lasbennes F. Regional study of the co-localisation of neuronal nitric oxide synthase with muscarinic receptors in the rat cerebral cortex. *Neuroscience* 69: 797-805, 1995.

Mottola DM, Kilts JD, Lewis MM, Connery HS, Walker QD, Jones SR, Booth RG, Hyslop DK, Piercey M, Wightman RM, Lawler CP, Nichols DE and Mailman RB. Functional selectivity of dopamine receptor agonists. I. Selective activation of postsynaptic dopamine D2 receptors linked to adenylate cyclase. *Journal of pharmacology and Experimental therapeutics* 301: 1166-1178, 2002.

Muly EC3, Szigeti K and Goldman-Rakic PS. D1 receptor in interneurons of macaque prefrontal cortex: distribution and subcellular localization. *Journal of Neuroscience* 18: 10553-10565, 1998.

Murphy JM, McBride WJ, Lumeng L and Li TK. Contents of monoamines in forebrain regions of alcohol-preferring (P) and -nonpreferring (NP) lines of rats. *Pharmacology, Biochemistry and Behaviour* 26: 389-392, 1987.

Nahas Z, Speer A, Lorberbaum J, Molloy M, Leberatos C, Risch SC and George MS. Safety of rTMS: MRI scans before and after 2 weeks of dialy left prefrontal rTMS for depression. *Biological Psychiatry* 43: Suppl, 1998.

Nash JF and Yamamoto BK. Effect of D-amphetamine on the extracellular concentrations of glutamate and dopamine in iprindole-treated rats. *Brain Research* 627: 1-8, 1993.

Nehls D, Park C, MacCormack A and McCulloch J. The effect of n-methyl-d-aspartate receptor blockade with MK801 upon the relationship between cerebral blood flow and local cerebral glucose utilisation in the rat. *Brain Research* 511: 1990.

Neisewander JL, Fuchs RA, O'Dell LE and Khroyan TV. Effects of SCH-23390 on dopamine D1 receptor occupancy and locomotion produced by intraaccumbens cocaine infusion. *Synapse* 30: 194-204, 1998.

Ng Cheong Ton JM, Gerhardt GA, Friedemann M, Etgen AM, Rose GM, Sharpless NS and Gardner EL. The effects of delta 9-tetrahydrocannabinol on potassium-evoked release of dopamine in the rat caudate nucleus: an in vivo electrochemical and in vivo microdialysis study. *Brain Research* 451: 59-68, 1988.

Nielsen, E. B. and Scheel-Kruger, J. Cueing effects of amphetamine and LSD: Elicitation by direct microinjection of the drugs inot the nucleus accumbens. 125, 85-92. 1986.
Ref Type: Generic

Nieoullon A and Dusticier N. Effects of alpha-chloralose on the nigrostriatal dopaimnergic system in the cat. *European journal of Pharmacology* 65: 403-410, 1980.

Noble EP. The D2 dopamine receptor gene: a review of association studies in alcoholism and phenotypes. *Alcohol* VOLUME!!!: 33-45, 1998.

Norris DG, Zysset S, Mildner T and Wiggins CJ. An investigation of the value of spin-echo-based fMRI using a Stroop color-word matching task and EPI at 3 T. *Neuroimage* 15: 719-726, 2002.

Nudo RJ and Masterton RB. Stimulation-induced [14C]2-deoxyglucose labeling of synaptic activity in the central auditory system. *The Journal of Comparative Neurology* 245: 553-565, 1986.

O'Boyle KM and Waddington JL. Selective and stereospecific interactions of R-SK & F 38393 with [3H]piflutixol but not [3H]spiperone binding to striatal D1 and D2 dopamine receptors: comparisons with SCH 23390. *European journal of Pharmacology* 98: 433-436, 1984.

O'Connor WT. Functional neuroanatomy of the ventral striopallidal GABA pathway. New sites of intervention in the treatment of schizophrenia. *Journal of Neuroscience Methods* 109: 31-39, 2001.

Ogawa S, Lee T-M, Nayak AS and Glynn P. Oxygenation-sensitive contrast in magnetic resonance image of rodent brain at high magnetic fields. *Magnetic Resonance in Medicine* 14: 68-78, 1990.

Ogawa S, Menon RS, Tank DW, Kim S-G, Merkle H, Ellermann JM and Ugurbil K. Functional brain mapping by blood oxygenation level-dependant contrast magnetic resonance imaging. A comparison of signal changes with a biophysical model. *Biophysical Journal* 63: 803-812, 1993.

Ogawa S, Tank DW, Menon R, Ellerman JM, Kim S-G, Merkle H and Ugurbil K. Intrinsic signal changes accompanying sensory stimulations: functional brain mapping with magnetic resonance imaging. *Proceedings of the National Academy of Science of the USA* 89: 1951-5955, 1992.

Ogino K, Hobara T and Kobayashi Hea. Gastric mucosal injury induced by chloral hydrate. *Toxicology Letters* 52: 129-133, 1990.

Okubo Y, Suhara T, Suzuki K, Kobayashi K, Inoue O, Terasaki O, Someya Y, Sassa T, Sudo Y, Matsushima E, Iyo M, Tateno Y and Toru M. Decreased prefrontal dopamine D1 receptors in schizophrenia revealed by PET. *Nature* 385: 634-636, 1997.

Olds J and Milner P. Positive reinforcement produced by electrical stimulation of septal area and other regions of rat brain. *Journal of comparative and physiological psychology* 47: 419-427, 1954.

Olsen CM and Duvauchelle CL. Intra-prefrontal cortex injections of SCH 23390 influence nucleus accumbens dopamine levels 24 h post-infusion. *Brain Research* 922: 80-86, 2001.

Onali P, Olianas MC and Gessa GL. Characterization of dopamine receptors mediating inhibition of adenylate cyclase activity in rat striatum. *Molecular Pharmacology* 28: 138-145, 1985.

Onozawa H, Miyano K and Tanifuji Y. Effect of dopamine content in rat brain striatum on anesthetic requirement: An in vivo microdialysis study. *Brain Research* 817: 192-195, 1999.

Opacka-Juffry J, Ahier RG and Cremer JE. Nomifensine-induced increase in extracellular striatal dopamine is enhanced by isoflurane anaesthesia. *Synapse* 7: 169-171, 1991.

Orzi F, Morelli M, Fieschi C and Pontieri FE. Metabolic mapping of the pharmacological and toxicological effects of dopaminergic drugs in experimental animals. *Cerebrovascular and Brain Metabolism Reviews* 5: 95-121, 1993.

Ossenkopp, K. P., Macrae, L. K., and Teskey, G. C. Automated multivariate measurement of spontaneous motor activity in mice: time course and reliabilities of the behavioral measures. 27(3), 565-568. 1987.
Ref Type: Generic

Pahwa R, Lyons K, McGuire D, Silverstein P, Zwiebel F, Robischon M and Koller WC. Comparison of standard carbidopa-levodopa and sustained-release carbidopa-levodopa in Parkinson's disease: pharmacokinetic and quality-of-life measures. *Movement Disorders* 12: 677-681, 1997.

Palacios JM and Wiederhold KH. Dopamine D2 receptor agents, but not dopamine D1, modify brain glucose metabolism. *Brain Research* 327: 390-394, 1985.

Palmer JT, de Crespigny AJ, Williams S-P, Busch E and van Bruggen N. High-Resolution mapping of discrete representational areas in rat somatosensory cortex using blood volume dependant functional MRI. *Neuroimage* 9: 383-392, 1999.

Parada MA, Puig de Parada M and Hoebel BG. Rats self-inject a dopamine antagonist in the lateral hypothalamus where it acts to increase extracellular dopamine in the nucleus accumbens. *Pharmacology, Biochemistry and Behaviour* 52: 179-187, 1995.

Parkinson J. *An essay on the shaking palsy*. London: Whittingham & Rowland, 1817.

Parsons LH and Justice JBJ. Serotonin and dopamine sensitization in the nucleus accumbens, ventral tegmental area, and dorsal raphe nucleus following repeated cocaine administration. *Journal of Neurochemistry* 61: 1993.

Parsons LH, MKerr T and Weiss F. Simple microbore high performance chromatography for the determination of dopamine and cocaine form a single in vivo microdialysis sample. *Journal of Chromatography B* Journal of Chromatography B709: 35-45, 1998.

Pasternak GW. Pharmacological mechanisms of opiod analgesics. *Clinical Neuropharmacolgy* 16: 1-18, 1993.

Paxinos G and Watson C. *The Rat Brain in Stereotaxic Coordinates*. Academic Press, Hacourt Brace & Company, 1998.

Pearlson GD, Jeffrey PJ, Harris G.J, Ross CA, Fischman MW and Camargo EE. Correlation of acute cocaine-induced changes in local cerebral blood flow with subjective effects. *American Journal of Psychiatry* 150: 495-497, 1993.

Peeters R, Tindemans I, Verhoye M and an Der Linden A. Simultaneous fMRI and EEG recordings of awake and anaesthetised conditioning of rats during forepaw stimulation. *Proceedings of the 8th Scientific meeting and exhibition of the International Society form Magnetic Resonance in Medicine Denver, U SA* 860, 2000.

Penfield W and Rasmussen T. *The cerebral cortex of man: A clinical study of localisation of function*. New York: MacMillian, 1950.

Phillips AG. Brain reward circuitry: a case for separate systems. *Brain Research Bulletin* 12: 195-201, 1984.

Phillips AG and Fibiger HC. Decreased resistance to extinction after haloperidol: implications for the role of dopamine in reinforcement. *Pharmacology, Biochemistry and Behaviour* 10: 751-760, 1979.

Phillips TJ, Brown KJ, Burkhart-Kasch S, Wenger CD, Kelly MA, Rubinstein M, Grandy DK and Low MJ. Alcohol preference and sensitivity are markedly reduced in mice lacking dopamine D2 receptors. *Nature Neuroscience* 1: 610-615, 1998.

Piano JZ and Pogacnik A. Dopamine D2 receptor mRNA measured in serial sections of the rat anterior pituitary. *Pflugers Archives* 442: 209-10, 2001.

Piccini P, Brooks DJ, Korpela K, Puvese N, Karlsson M and Gordin A. The catechol-O-methyl transferase inhibitor entacapone enhances the pharmacokinetic and clinical response to Siminet CR in Parkinson`s Disease. *Journal of Neurology, Neurosurgery and Psychiatry* 68: 589-594, 2000.

Picetti R, Saiardi A, Abdel ST, Bozzi Y, Baik JH and Borrelli E. Dopamine D2 receptors in signal transduction and behavior. *Crit Rev Neurobiol* 11: 121-142, 1997.

Pierre PJ and Vezina P. D1dopamine receptor blockade prevents the facilitation of amphetamine self-stimulation induced by prior exposure to the drug. *Journal of Neurology, Neurosurgery and Psychiatry* 138: 159-166, 1998.

Pifl C, Giros B and Caron MG. The dopamine transporter-The cloned target site of Parkinsonism-inducing toxins and drugs of abuse. *Advances in Neurology* 69: 235-238, 1996.

Pizzolato G, Soncrant TT, Larson DM and Rapoport SI. Stimulatory effect of the D2 antagonist sulpiride on glucose utilization in dopaminergic regions of rat brain. *Journal of Neurochemistry* 49: 631-638, 1987.

Pizzolato G, Soncrant TT and Rapoport SI. Haloperidol and cerebralmetabolism in the concious rat: relation to pharmacokinetics. *Acta aneasthiologica ScandinavicaJournal of Neurochemistry* 43: 724-732, 1984.

Plaznik A, Stefanski R, Paleijko W and Kostowski W. Accumbens GABA-ergic innervation contributes to the stressor-induced locomotor depression in rats. *Polish Journal of pharamcological pharmacy* 44: 5-14, 1992.

Pocock G and Richards CD. Excitatory and inhibitory synaptic mechanisms in anaesthesia. *British Journal of Anaesthesia* 71: 134-147, 1993.

Porceddu ML, Giorgi O, Ongini E, Mele S and Biggio G. 3H-SCH 23390 binding sites in the rat substantia nigra: evidence for a presynaptic localization and innervation by dopamine. *Life Sciences* 39: 321-328, 1986.

Posse S, Muller-Gartner HW and Dager SR. Functional magnetic resonance studies of brain activation. *Seminars in Clinical Neuropsychiatry* 1: 76-88, 1996.

Powers WJ, Fox PT and Raichle ME. The effect of carotid artery disease on the cerebrovascular response to physiologic stimulation. *Neurology* 38: 1475-1478, 1988.

Powers WJ, Hirsch IB and Cryer PE. Effect of stepped hypoglycemia on regional cerebral blood flow response to physiological brain activation. *American Journal of Physiology* 270: 554-9, 1996.

Preece M, Mukherjee B, Huang CL, Hall LD, Leslie RA and James MF. Detection of pharmacologically mediated changes in cerebral activity by functional magnetic resonance imaging: the effects of sulpiride in the brain of the anaesthetised rat. *Brain Research* 916: 107-114, 2001.

Puce A. Comparative asssessment of sensorimotor function using funcional magnetic resonance imaging and electrophysiological methods. *Journal of Clinical Neurophysiology* 12: 450-459, 1995.

Pugsley T and Lippman W. Effects of tandamine and pirandamine, new potential antidepressants, on the brain uptake of norepinephrine and 5-hydroxytryptamine and related activities. *Psychopharmacology (Berl)* 47: 33-41, 1976.

Pulvirenti L and Koob GF. Lisuride reduces psychomotor retardation during withdrawal from chronic intravenous amphetamine self-administration in rats. *Neuropsychopharmacology* 8: 213-218, 1993.

Rabinowitz J and Davidson M. Risperidone versus haloperidol in long-term hospitalized chronic patients in a double blind randomized trial: A post hoc analysis. *Schizophrenia Research* 50: 89-93, 2001.

Raichle ME, Grubb RLJ, Gado MH, Eichling JO and Ter-Pogossian MM. Correlation between regional cerebral blood flow and oxidative metabolism. In vivo studies in man. *Archives of Neurology* 33: 523-536, 1976.

Raiteri M, Cerruto F, Cervoni AM and Levi G. Dopamine can be released by two mechanisms differentially affected by the dopamine transporter inhibitor nomifensine. *Journal of pharmacology and Experimental therapeutics* 208: 195-202, 1979.

Rascol O, Bin O, Thalamas SC, Descombes S, Soubrouillard C, Azulay P, Fabre N, Viallet F, Latnitzegger K, Wright S, CArter JH and Nutt JG. Opposing roles of dopamine D1 and D2 receptorsin modulatio of rat nucleus accumbens. *Annals of Neurology* 45: 736-741, 1999.

Rasmussen JGC. Drug treatments for schizophrenia--past, present, and future. *International Journal of Psychiatry in Clinical Practice* 1: 1997.

Rees G and Friston K. A direct quantitative relationship between the functional properties of human and macaque V5. *Nature Neuroscience* 3: 716-723, 2000.

Richardson.N.R and Roberts DC. Progressive ratio schedules in drug self-administration studies in rats: a method to evaluate reinforcing efficacy. *Journal of Neuroscience Methods* 66: 1-11, 1996.

Rinne JO, Laihinen A, Nagren K, Bergman J, HM, Solin O, Ruotsalainen U and Rinne UK. Positron emission tomography of brain dopamine D-1 receptors with 11C-SCH 23390 in Parkinson's disease. *Acta Radiol Supplemen* 376: 152, 1991.

Rinne JO, Laihinen A, Nagren K, Bergman J, SO, Haaparanta M, Ruotsalainen U and Rinne UK. PET demonstrates different behaviour of striatal dopamine D-1 and D-2 receptors in early Parkinson's disease. *Journal of Neuroscience Research* 4: 494-499, 1990.

Robbin TW and Everitt BJ. Neurobehavioural mechanisms of reward and motivation. *Current opinion in Neurobiology* 6: 228-236, 1996.

Roberts DA, Detre JA, Bolinger L, Insko EK and Leigh JS. Quantitative magnetic resonance imaging of human brain perfusion at 1.5T using steady state inversion of arterial water. *Proceedings of the National Academy of Science of the USA* 91: 33-37, 1994.

Robertson GS, Damsa G and Fibiger HC. Characterisation of dopamine release in the substantia nigra by in-vivo microdialysis in the freely moving rat. *Journal of Neuroscience* 11: 229-2216, 1991.

Robinson TE and Becker JB. Enduring changes in brain and behavior produced by chronic amphetamine administration: a review and evaluation of animal models of amphetamine psychosis. *Brain Research* 396: 157-198, 1986.

Robinson TE and Justice JBJ. Microdialysis in the neurosciences. *Techniques in the behaviorial and neurosciences* 7: 1991.

Rockhold RW, Byrne M, Sprabery S and Bennet JG. Urethane anaesthesia reverses the protective effect of noncompetitive NMDA receptor antagonists against cocaine intoxification. *Life Sciences* 54: 321-330, 1994.

Roland PE, Erikson L, Stone-Elander S and Widen L. Does mental activity change the oxidative metabolism of the brain? *Journal of Neuroscience* 7: 2372-2389, 1987.

Rosen BR, Belliveau JW, Aronen HJ, Kennedy D, Buchbinder BR, Fischman A, Gruber M, Glas J, Weiskoff RM, Cohen MS, Hochberg FH and Brady JJ. Susceptability contrast imaging of cerebral blood volume: human experience. *Magnetic Resonance in Medicine* 22: 293-299, 1991.

Rossetti ZL, Hmaidan Y and Gessa GL. Marked inhibition of mesolimbic dopamine release: a common feature of ethanol, morphine, cocaine and amphetamine abstinence in rats. *European journal of Pharmacology* 221: 227-234, 1992.

Rossi G, Pasternak GW and Bodnar RJ. Synergistic brainstem interactions for morphine analgesia. *Brain Research* 624: 171-180, 1993.

Roth BL, Meltzer HY and Khan N. Binding of typical and atypical antipsychotic drugs to multiple neurotransmitter receptors. *Advances in Pharmacology* 42: 482-485, 1998.

Rother J, Knab R, Hamzei F, Fiehler J, Reichenbach JR, Buchel C and Weiller C. Negative dip in BOLD fMRI is caused by blood flow--oxygen consumption uncoupling in humans. *Neuroimage* 15: 98-102, 2002.

Roy C and Sherrington C. On the regulation of the blood supply of the brain. *Journal of Physiology* 11: 85-108, 1890.

Rubinstein M, Phillips TJ, Bunzow JR, Falzone TL, Dziewczapolski G, Zhang G, Fang Y, Larson JL, McDougall JA, Chester JA, Saez C, Pugsley TA, Gershanik O, Low MJ and Grandy DK. Mice lacking dopamine D4 receptors are supersensitive to ethanol, cocaine, and methamphetamine. *Cell* 90: 991-1001, 1997.

Ruskin DN, Debra AB and Walters JR. Multisecond oscillations in firing rate in the globus pallidus: synergistic modulation by D1 and D2 dopamine receptors. *Journal of Pharmacology and Experiemntal Therapeutics* 290: 1493-1501, 1999.

Ryan LJ, Martone ME, Linder JC and Groves PM. Cocaine, in contrast to D-amphetamine, does not cause axonal terminal degeneration in neostriatum and agranular frontal cortex of Long-Evans rats. *Life Sci* 43: 1403-1409, 1988.

Saiardi A, Bozzi Y, Baik JH and Borelli E. Antiproliferative role of dopamine: loss of D2 receptors causes hormonal dysfunction and pituitary hyperplasia. *Neuron* 16: 299-321, 1997.

Salamone JD. Complex motor and sensorimotor functions of striatal and accumbens dopamine: involvement in instrumental behavior processes. *Psychopharmacology (Berl)* 107: 160-174, 1992.

Sams-Dodd F. A test of the predictave validity of animal models of schizophrenia based on phencyclidine and d-amphetamine. *Neuropsychopharmacology* 18: 293-304, 1998.

Sandkuler J and Gebhart GF. Characterisation of inhibition of a spinal nociceptive reflex by stimulation medially and laterally in the midbrain and medulla in the pentobarbital anaesthetised rat. *Brain Research* 305: 67-76, 1984.

Sappey-Marnier D, Calabrese G, Fein G, Hugg JW, Biggins C and Weiner MW. Effect of photic stimulation on human visual cortex lactate and phosphates using 1H and 31P magnetic resonance spectroscopy. *Journal of cerebral blood flow and metabolism* 35: 143-148, 1996.

Sarapura V and Schlaff WD. Recent advances in the understanding of the pathophysiology and treatment of hyperprolactinemia. *Current Opinion of Obstetics and Gynecology* 5: 360-367, 1993.

Sato S, Balish M and Muratore R. Principles of magnetoencephalography. *Journal of Clinical Neurophysiology* 8: 144-156, 1991.

Saulskaya NB, Mikhailova MO, Pudovkina OL and Gorbachevskaia AI. Changes in glutamate release in the rat nucleus accumbens during food and pain reinforcement. *Zh Vyssh Nerv Deiat Im I P Pavlova* 50: 124-132, 2000.

Saunders RC, Kolachana BS and Weinberger DR. Local pharmacological manipulation of extracellular dopamine levels in the dorsolateral prefrontal cortex and caudate nucleus in the rhesus monkey: an in vivo microdialysis study. *Experimental Brain Research* 98: 44-52, 1994.

Sawaguchi T and Goldman-Rakic PS. D1 dopamine receptors in prefrontal cortex: involvement in working memory. *Science* 251: 947-50, 1991.

Sax DS and Tarsy D. Side-effects of L-Dopa. *New England Medical Journal* 285: 1033, 1971.

Schiorring E. Psychopathology induced by "speed drugs". *Pharmacology, Biochemistry and Behaviour* 14: 109-122, 1981.

Schmauss C, Haroutunian V, Davis KL and Davidson M. Selective loss of dopamine D3-type receptor mRNA expression in parietal and motor cortices of patients with chronic schizophrenia. *Proceedings of the national Academy of Sciences of the U S A* 90: 8942-8946, 1993.

Schneck JF. The role of magnetic susceptability. *Medical Physics* 23: 815-850, 1996.

Schneider WNDC and Cohen JD. Functional topographic mapping of the cortical ribbon in human vision with conventional MRI scanners. *Nature* 365: 150-152, 1993.

Schultz W. Depletion of dopamine in the striatum as an experiemtal model of Parkinsonism: Direct effects and adaptive mechanisms. *Progress in Neurobiology* 18: 121-166, 1982.

Sedvall G, Farde L, Nyback H, Pauli S, Persson A, Savic I and Wiesel FA. Recent advances in psychiatric brain imaging. *Acta Radiol Supplement* 374: 1990.

Seeman MV. Schizophrenia: D4 receptor elevation. What does it mean? *Journal of Psychiatry and Neuroscience* 19: 171-176, 1994.

Seeman P and Grigoriadis D. Dopamine D2 receptor dissociation constant for spiperone: identical values using 3H-labeled agonist or 3H-labeled antagonist. *Biochemical Pharmacology* 34: 4065-4066, 1985.

Seeman P, Guan HC and Van Tol HH. Schizophrenia: elevation of dopamine D4-like sites, using [3H]nemonapride and [125I]epidepride. *European journal of Pharmacology* 286: 3-5, 1995.

Seeman P, Lee T, Chan-Wong M and Wong K. Antipsychotic drug doses and neuroleptic dopamine receptors. *Nature* 261: 717-719, 1976.

Seeman P, Tedesco JL, Lee T, Chau-Wong M, Muller P, Bowles J, Whitaker PM, McManus C, Tittler M, Weinreich P, Friend WC and Brown GM. Dopamine receptors in the central nervous system. *Fed Proc* 37: 131-136, 1978.

Segal DS. Behavioral characterization of d- and l-amphetamine: neurochemical implications. *Science* 190: 475-477, 1975.

Seiden LS and Ricarte GA. Neurotoxicity of methamphetamine and related drugs. *Psychopharmacology: Third generation of progress Raven, New York* 359-366, 1987.

Seiden LS, Sabol KE and Ricaurte GA. Amphetamine: effects on catecholamine systems and behaviour. *Annu Rev Pharmacol Toxicol* 32: 639-677, 1993.

Seiden LS and Vosmer G. Formation of 6 hydroxy-dopamine in caudate nucleus of the rat brain after a single large dose of methylamphetamine. *Pharmacology, Biochemistry and Behaviour* 21: 29-31, 1984.

Seitz RJ and Roland PE. Vibratory stimulation increases and decreases the regional cerebreal blood flow and oxygen metabolism: A PET study. *Acta Neurologica Scandinavica* 86: 60-67, 1992.

Self DW, Barnhart WJ, Lehman DA and Nestler EJ. Opposite modulation of cocaine-seeking behavior by D1- and D2-like dopamine receptor agonists. *Science* 271: 1586-1589, 1996.

Self DW, Karanian DA and Spencer JJ. Effects of the novel D1 dopamine receptor agonist ABT-431 on cocaine self-administration and reinstatement. *Annals of the New York Academy of Sciences* 909: 133-144, 2000.

Severina IS, Klimova GI and Nersisian AA. Effect of solubilization by methylethylketone of rat liver mitochondrial monoamine oxidase on inhibition by clorgyline and deprenyl of the enzyme activity. *Biokhimiia* 46: 2043-2055, 1981.

Shah YB, Prior M, Dixon AL, Marsden CA and Morris PMG. Effect of the canabinoid agonist HU210 on BOLD response in rat brain as determined by fMRI. *Proceedings of the 9th Scientific meeting and exhibition of the International Society form Magnetic Resonance in Medicine Glasgow, Scotland, U K* 1345, 2001.

Sharp T, Zetterstrom T, Ljunberg T and Ungerstedt U. A Direct comparison of amphetamine-induced behaviours and regional dopamine release in the rat using intracerebral dialysis. *Brain Research* 401: 322-330, 1987.

Shenton ME, Dickey CC, Frumin M and McCarley RW. A review of MRI findings in schizophrenia. *Schizophrenia Research* 49: 1-52, 2001.

Shih JC, Chen K and Ridd MJ. Monoamineoxidase: from genes to behaviour. *Annual Reviews of Neuroscience* 22: 197-217, 1999.

Shimamura M and Yamauchi T. Neural mechanisms of the chloralose jerk with special reference to its relationship with the spino-bulbo-spinal reflex. *Japanese Journal of Physiology* 17: 1967.

Shimukawa A, Jin QH, Ishizuka Y, Kunitake T, Takasaki M and Kannan H. Effects of anaesthetics on norepinephrine release in the hypothalamic paraventricular nucleus region of awake rats. *Neuroscience Letters* 244: 21-24, 1998.

Shippenberg TS, Bals-Kubik R and Herz A. Examination of the neurochemical substrates mediating the motivational effects of opioids: role of the mesolimbic dopamine system and D-1 vs. D-2 dopamine receptors. *Journal of pharmacology and Experimental therapeutics* 265: 53-59, 1993.

Shiraishi M, Kamiyama Y, Huttemeier PC and Benveniste H. Extracellular glutamate and dopamine measured by microdialysis in the rat striatum during blockade of synaptic transmission in anesthetized and awake rats. *Brain Research* 759: 221-227, 1997.

Shmuel A, Yacoub E, Pfeuffer J, Van de Moortele P-F, Adriany G, Ugurbil K and Hu X. Sustained Negative BOLD and Blood Flow Response and its Coupling to the Positive Response in the Human Brain. *Proceedings of the 10th Scientific meeting and exhibition of the International Society form Magnetic Resonance in Medicine, Hawaii* 642, 2002.

Shui HA, Peng YI and Tsai YF. Recovery of high potassium-evoked dopamine release after depolarization challenge in the striatum of young and old male rats. *Neuroscience Letters* 257: 1-4, 1998.

Shulman R, Rothman DL and Hyder F. Stimulated changes in localised cerebral energy consumption under anaesthesia. *Proceedings of the National Academy of Sciences of the USA* 96: 3245-3250, 1999.

Shulman RG and Rothman.D.L. Interpreting functional imaging studies in terms of neurotransmitter cycling. *Proceedings of the national Academy of Sciences of the U S A* 95: 11993-11998, 1998.

Sibson NR, Dhankhar A, Mason GF, Rothman DL, Behar KL and Shulman RG. Stoichiometric coupling of brain glucose metabolism and glutamatergic neuronal activity. *Proceedings of the national Academy of Sciences of the U S A* 95: 316-321, 1998.

Siegfried, B., Hefti, F., Lichtensteiger, W., and Huston, J. P. Lateralized hunger: ipsilateral attenuation of cortical spreading depression-induced feeding after unilateral 6-OHDA injection into the substantia nigra. Brain Research 160 327-40(2), 327-340. 1979.
Ref Type: Journal (Full)

Siever LJ, Amin F, Coccaro EF, Trestmanm R, Silverman J, Horvath TB, Mahon TR, Knott P, Altstiel L and Davidson M. CSF homovanillic acid in schizotypal personality disorder. *American Journal of Psychiatry* 150: 149-151, 1993.

Silva AC, Zhang W, Williams DS and Koretsky AP. Multi-slice MRI of rat brain perfusion during amphetamine stimulation using arterial spin labelling. *Magnetic Resonance in Medicine* 33: 209-214, 1995.

Silverman J and Muir WW. Special Topic overview: A review of laboratory animal anesthesia with chloral hydrate and chloralose. *Laboratory Animal Science* 210-216, 1993.

Simon H, Scatton B and Le Moal M. Dopaminergic A10 neurons are involved in cognitive functions. *Nature* 286: 150-151, 1980.

Simonsen CZ, Ostergaard L, Smith DF, Vestergaard-Poulsen P and Gyldensted C. Comparison of gradient-echo and spin echo imaging: CBF, CBV, and MTT Measurements by bolus tracking. *Journal of Magnetic Resonance Imaging* 12: 411-416, 2000.

Singewald N, Schneider C and Philippu A. Effects of neuroactive compounds, noxious and cardiovascular stimuli on the release of amino acids in the rat locus coeruleus. *Neuroscience Letters* 180: 55-58, 1994.

Slawek J, Bojok E and Szady J. Incidence of dementia in Parkinsosn`s Disease. *Neurol Neurochir Pol* 35: 569-581, 2001.

Smith AJ, Blumenfeld H, Behar KL, Rothman DL, Shulman RG and Hyder F. Cerebral energetics and spiking frequency: The neurophysiological basis of fMRI. *Proceedings of the national Academy of Sciences of the U S A* 99: 10765-10770, 2002.

Smith RC, Calderon M, Racichandran GK, Largen J, Vroulis G, Shvartsburd A, Gordon J and Schoolar JC. Nuclear magnetic resonance in schizophrenia: a preliminary study. *Psychiatry Research* 12: 137-147, 1984.

Sokoloff L. Relationships among local functional activity, energy metabolism, and blood flow in the central nervous system. *Fed Proc* 40: 2311-2316, 1981.

Sokoloff P, Andrieux M, Besancon R, Pilon C, Martres MP, Giros B and Schwartz JC. Pharmacology of human dopamine D3 receptor expressed in a mammalian cell line: comparison with D2 receptor. *European journal of Pharmacology* 225: 331-337, 1992.

Sokoloff P, Giros B, Martres M, Bouthnet ML and Schwartz JC. Molecular cloning and characterisation of a novel dopamine receptor. *Nature* 347: 146-151, 1990.

Sokoloff P, Martres MP and Schwartz JC. 3H-apomorphine labels both dopamine postsynaptic receptors and autoreceptors. *Nature* 288: 283-286, 1980.

Sonsalla PK, Nicklas WJ and Heikkila RE. Role for excitatory amino acids in methamphetamine-induced nigrostriatal dopaminergic toxicity. *Science* 243: 398-400, 1989.

Sorg BA, Li N and Wu W-R. Dopamine D1 receptor activation in the medial prefrontal cortex prevents the expression of cocaine sensitzation. *Journal of pharmacology and Experimental therapeutics* 297: 501-508, 2001.

Sotnikova TD, Gainetdinov RR, Grekhova TV and Rayevski KS. Effects of intrastriatal infusion of D2 and D3 dopamine receptor preferring antagonists in rat dorsal striatum (in vivo microdialysis study). *Pharmacol Res* 43: 283-290, 2001.

Spano PF, Govoni S and Trabucci M. Studies on the pharmacological properties of dopamine receptors in various areas of the central nervous system. *Advances in Biochemistry and Psychopharmacology* 19: 155-165, 1978.

Spano PF, Trabucci M and Di Chiara G. Localisation of dopamine-sensitive adelylate sensitive on neurons originating from corpus striatum. *Science* 196: 1977.

Spealman RD, Barrett-Larimore RL, Rowlett JK, Platt DM and Khroyan TV. Pharmacological and environmental determinants of relapse to cocaine-seeking behavior. *Pharmacology Biochemistry Behaviour* 64: 327-336, 1999.

Speer AM, Upadhyaya VH, Bohning DE, Risch SC, Vincent DJ and George MS. New windows into bipolar illness: serial perfusion MRI scanning in rapid-cycling bipolar patients. *APA New Research* 111: Abstract, 1997.

Sperry RW. Hemispheric disconnection and unity in concious-awareness. *American Psychologist* 23: 476-483, 1968.

Springer CS. Bulk magnetic suseptability frequency shifts in cell suspensions. *NMR Biomedicine* 7: 75-99, 1994.

Stafanini E and Clement-Cormier Y. Detection of dopamine receptors in the area postrema. *European journal of Pharmacology* 74: 257-260, 1981.

Stahle A, Collin AK and Ungerstedt U. Effects of halothane anaesthesia on extracellular levels of dopmaine, dihydroxy-phenylacetic acid and 5-hydroxyindoleacetic acid in rat striatum: a microdialysis study. *Naunyn-Schmeildebergs archives of pharmacology* 342: 136-140, 1990.

Stanton DM and Solomon PR. Microinjections of D-amphetamine into the nucleus accumbens and caudate-putamen differentially affect stereotypy and locomotion in the rat. *Journal of Neurochemistry* 12: 159-162, 1984.

Stein EA, Pankiewicz J, Harsch HH, Cho JK, Fuller SA, Hoffmann RG, Hawkins M, Rao SM, Bandettini PA and Bloom AS. Nicotine-induced limbic cortical activation in the human brain: a functional MRI study. *American Journal of Psychiatry* 155: 1009-1015, 1998.

Steiner H and Gerfen CR. Dynorphin opioid inhibition of cocaine-induced, D1 dopamine receptor-mediated immediate-early gene expression in the striatum. *The Journal of Comparative Neurology* 353: 200-212, 1995.

Steiner H and Gerfen CR. Dynorphin regulates D1 dopamine receptor-mediated responses in the striatum: relative contributions of pre- and postsynaptic mechanisms in dorsal and ventral striatum demonstrated by altered immediate-early gene induction. *Comparative Neurology* 376: 530-541, 1996.

Steiner H and Gerfen CR. Role of dynorphin and enkephalin in the regulation of striatal output pathways and behaviour. *Experimental Brain Research* 123: 60-76, 1998.

Stellar JR and Corbett D. Regional neuroleptic microinjections indicate a role for nucleus accumbens in lateral hypothalamic self-stimulation reward. *Brain Research* 477: 126-143, 1989.

Steranka LR and Sanders-Bush E. Long-term exposure of continious exposure to amphetamine on brain dopamine concentration and synaptosomal uptake in mice. *European journal of Pharmacology* 65: 439-443, 1980.

Stern G. MPTP: clinical implications. *Journal of Neural Transmission* 20: 77-81, 1986.

Stinus L and Thierry AM. Self-stimulation and catecholamines. II. Blockade of self-stimulation by treatment with alpha-methylparatyrosine and the reinstatement by catecholamine precursor administration. *Brain Research* 64: 189-198, 1973.

Stoelting RK, Creasser CW and Martz RC. Effect of cocaine administration on halothane MAC in dogs. *Anaesthesia Analgesia* 54: 422-424, 1975.

Stoff DM, Jeste DV, Gillin JC, Moja EA, Cohen L, Stauderman KA and Wyatt RJ. Behavioral supersensitivity to beta-phenylethylamine after chronic administration of haloperidol. *Biological Psychiatry* 19: 101-106, 1984.

Storer RJ, Butler P, Hoskin KL and Goadsby PJ. A simple method, using 2-hydroxypropyl-beta-cyclodextrin, of administering alpha cloralose at room temperture. *Journal of Neuroscience Methods* 77: 49-53, 1997.

Storey VJ, Middlemiss DN and Reavill C. Effect of haloperidol and (-)-sulpiride on dopamine agonist-induced hypoactivity. *Neuropharmacology* 34: 449-455, 1995.

Subramaniam S, Lucki I and McGonigle P. Effects of chronic treatment with selective agonists on the subtypes of dopamine receptors. *Brain Research* 571: 312-322, 1992.

Sunahara RK, Guan HC, O`Dowd BF, Seeman P and Laurier LG. Cloning of the gene for a human dopamine D5 receptor with a higher affinity for dopamine than D1. *Nature* 350: 614-619, 1991.

Sunahara RK, Niznik HB, Weiner DM, Stormann TM, Brann MR, Kennedy JL, Gelernter JE, Rozmahel R, Yang YL, Israel Y, SP and O`Dowd BF. Human dopamine D1 receptor encoded by an intronless gene on chromosome 5. *Nature* 347: 80-83, 1990.

Surmeier DJ, Eberwine J, Wilson CJ, Cao Y, Stefani A and Kitai ST. Dopamine receptor subtypes colocalize in rat striatonigral neurons. *Proceedings of the national Academy of Sciences of the U S A* 89: 10178-10182, 1992.

Suzuki A, Kondo T, Otani K, Mihara K, Yasui-Furukori N, Sano A, Koshiro K and Kaneko S. Association of the TaqI A polymorphism of the dopamine D(2) receptor gene with predisposition to neuroleptic malignant syndrome. *American Journal of Psychiatry* 158: 1714-1716, 2001.

Szechtman H, Eckert MJ, Tse WS, Boersma JT, Bonura CA, McClelland JZ, Culver KE, Eilam D and (2001) 2:4. Compulsive checking behavior of quinpirole-sensitized rats as an animal model of Obsessive-Compulsive Disorder (OCD): form and control. *BMC Neuroscience* 2: 2001.

Szumlinski KK and Szechtman H. D2 receptor blockade in the dorsal raphe increases quinpirole-induced locomotor excitation. *Neuroreport* 13: 563-566, 2002.

Tabuchi E, Yokawa T, Ono T, Niijma A and Torii K. Brain areas activated by ingestion using fMRI of awake rats. *Society for Neuroscience* 21: 967, 1995.

Tajuddin NF and Druse MJ. Effects of chronic alcohol consumption and aging on dopamine D2 receptors in Fischer 344 rats. *Alcoholism, Clinical and Experimental Research* 20: 144-151, 1996.

Talairach J and Tournoux P. *Co-planar Stereotaxic Atlas of the Human Brain: 3-Dimensional Proportional System - an approach to Cerebral Imaging*. New York, NY: Thieme Medical Publishers, 1988.

Tatsumi, M., Groshan, K., Blakely, R. D., and Richelson, E. Pharmacological profile of antidepressants and related compounds at human monoamine transporters. 340(2-3), 249-258. 1997.
Ref Type: Generic

Tepper J, Creese I and Schwartz DH. Stimulus evoked changes in neostriatal dopamine levels in awake and anaesthetised rats as measured by microdialysis. *Brain Research* 559: 283-292, 1991.

Thanos PK, Volkow ND, Freimuth P, Umegaki H, Ikari H, Roth G, Ingram DK and Hitzemann R. Overexpression of dopamine D2 receptors reduces alcohol self-administration. *Journal of Neurochemistry* 78: 1094-1103, 2001.

Tolwani RJ, Jakowec MW, Petzinger GM, Green S and Waggie K. Experimental models of Parkinson's disease: insights from many models. *Laboratory Animal Science* 49: 363-371, 1999.

Towle AC, Criswell HE, Maynard EH, Lauder JM, Joh TH, Mueller RA and Breese GR. Serotonergic innervation of the rat caudate following a neonatal 6-hydroxydopamine lesion: an anatomical, biochemical and pharmacological study. *Pharmacology Biochemistry Behaviour* 34: 367-374, 1989.

Trugmam JM. D1/D2 actions of dopmainegic drugs studies with [14C]-2-deoxyglucose autoradiography. *Progress in Neuro-psychopharmacology & Biological Psychiatry* 19: 1995.

Trugman JM and James CL. Rapid development of dopaminergic supersensitivity in reserpine-treated rats demonstrated with 14C-2-deoxyglucose autoradiography. *Journal of Neuroscience* 12: 2875-2879, 1992.

Trugman JM and James CL. D1 dopamine agonist and antagonist effects on regional cerebral glucose utilization in rats with intact dopaminergic innervation. *Brain Research* 607: 270-274, 1993.

Tsukada H, Nishiyama S, Kakiuchi T, Ohba H, Sato K and Harada N. Is synaptic dopamine concentration the exclusive factor which alters the in vivo binding of [11C]raclopride: PET studies combined with microdialysis in conscious monkeys. *Brain Research* 841: 160-169, 1999.

Tzschenke TM. Pharmacology and behavioural pharmacology of the mesocrotical dopamine system. *Progress in Neurobiology* 63: 241-320, 2001.

Tzschenke, T. M. Pharmacology and behavioural pharmacology of the mesocrotical dopamine system. 63, 241-320. 2001.
Ref Type: Generic

Uchihashi Y, Bencsics A, Umeda E, Nkai T, Sato T and Vizi ES. Na+ channel block prevents the ischemia-induced release of norepinephrine from spinal cord slices. *European journal of Pharmacology* 346: 145-150, 1998.

Ueki M, Mies G and Hossman K-A. Effect of alpha chloralose, halothane, pentobarbital and nitrous oxide on metabolic coupling in the somatosensory cortex. *Acta aneasthiologica Scandinavica* 36: 318-322, 1992.

Uftring SJ, Wachtel SR, Chu D, McCandless C, Levin DN and de Wit H. An fMRI study of the effect of amphetamine on brain activity. *Neuropsychopharmacology* 25: 925-935, 2001.

Ugurbil K, Adriany G, Anderson P, Chen W, Gruetter R, Hu XP, Merkle H, Kim DS, Kim SG, Strupp J, Zhu XH and Ogowa S. Magnetic resonance studies of brain function and neurochemistry. *Annual Review of Biomedical Engineering* 2: 633-660, 2000.

Ugurbil K, Ogawa S, Menon R, Kim S-GH, X and Hinke R. *Mapping brain function non-invasively by nuclear magnetic resonance. New Horizons in Neuropsychology.* Amsterdam: Elsvier Science, 1994.

Ungerstedt U. Stereotaxic mapping of the monoamine pathways in the rat brain. *Acta Physiologca Scandinavica* 367: 1-48, 1971.

Ungerstedt U and Hallstrom A. In vivo microdialysis--a new approach to the analysis of neurotransmitters in the brain. *Life Sciences* 41: 861-4, 1987.

Usiello A, Baik JH, Rouge-Pont F, Picetti R, Dierich A, LeMeur M, Piazza PV and Borrelli E. Distinct functions of the two isoforms of dopamine D2 receptors. *Nature* 408: 199-203, 2000.

Vaccheri A, Dall'Olio R, Gandolfi O and Montanaro N. Involvement of different dopamine receptors in rat diphasic motility response to apomorphine. *Psychopharmacology (Berl)* 89: 265-268, 1986.

Valenstein E. A note on anaesthetising rats and ginuea pigs. *Journal of Experimental Animal Behavour* 4: 6, 1961.

Van Tol, H. H. M., Bunzow, J. R., Guan, H. C., Sunahara, R. K., Seeman, P., Niznik, H. B., and Civelli, O. Cloning of a human dopamine D4 receptor gene with high affinity for the antipsychotic clozapine. 350(6391), 610-614. 1991.
Ref Type: Generic

Vanderschuren LJ, Warden G, De Vries TJ, Mulder AH and Schoffelmeer AN. Opposing roels of D1 and D2 receptors in modulation of rat nucleus accumbens noradrenaline release. *Journal of Neuroscience* 19: 4123-4131, 1999.

Vezina P. D1 dopamine receptor activation is necessary for the induction of sensitization by amphetamine in the ventral tegmental area. *Journal of Neuroscience* 16: 2411-2420, 1996.

Volkow ND, Mullani N, Gould L, Adler SS, Guyen RW, Overall JE and Dewey S. Effects of acute alcohol intoxification on cerebral blood flow measure with PET. *Psychiatry Research* 24: 1988.

Volkow ND, Wang GJ, Fowler JS, Gatley SJ, Logan J, Ding YS, Hitzemann R and Pappas N. Dopamine transporter occupancies in the human brain induced by therapeutic doses of oral methylphenidate. *American Journal of Psychiatry* 155: 1325-1331, 1998.

Vollenweider FX, Maguire RP, Leenders KL, Mathys K and Angst J. Effects of high amphetamine dose on (mood and) cerebral glucose metabolism in normal volunteers using positron emission tomography (PET). *Psychiatry Research* 83: 149-162, 1998.

Waldvogel DP, Van Gelderen, Muellbacher W, Ziemann U, Immisch I and Hallett M. The relative metabolic demand of inhibition and excitation. *Nature* 406: 995-998, 2000.

Walters DE and Howard SG. The D1 agonist SKF 38393 increases dopamine release in the developing rat striatum. *European Journal Pharmacology* 184: 257-264, 1990.

Wamsley JK, Alburges ME, McQuade RD and Hunt M. CNS distribution of D1 receptors: use of a new specific D1 receptor antagonist, [3H]SCH39166. *Neurochemistry International* 20: 123S-128S, 1992.

Wang Y, Chan GL, Holden JE, Dobko T, Mak E, Schulzer M, Huser JM, Snow BJ, Ruth TJ, Calne DB and Stoessl AJ. Age-dependent decline of dopamine D1 receptors in human brain: a PET study. *Synapse* 30: 56-61, 1998.

Warburton EC, Mitchell SN and Joseph MH. Calcium dependance of sensitised dopamine release in rat nucleus accumbens following amphetamine challenge: implications for the disruption of latent inhibition. *Behavioral Pharmacology* 7: 119-129, 1996.

Watts VJ, Lawler CP, Gilmore JH, Southerland SB, Nichols DE and Mailman RB. Dopamine D1 receptors: efficacy of full (dihydrexidine) vs. partial (SKF38393) agonists in primates vs. rodents. *European journal of Pharmacology* 242: 165-72, 1993.

Wechsler LR, Saraki HE and Sokoloff L. Effects of D and L amphetamine on local cerebral glucose utilisation in the concious rat. *Journal of Neurochemistry* 32: 15-22, 1979.

Weiner, I., Lubow, R. E., and Feldon, J. Disruption of latent inhibition by acute administration of low doses of amphetamine. 30(4), 871-878. 1988.
Ref Type: Generic

Weisskoff RM, Zuo CS, Boxerman JL and Rosen BR. Microscopic susceptibility variation and transverse relaxation: theory and experiment. *Magnetic Resonance in Medicine* 31: 601-610, 1994.

Wernicke C. *The symptom complex of aphasia: a physiological study on the anatomical basis*. 1876.

Westerink BH, Teisman A and De Vries JB. Increase in dopamine release from the nucleus accumbens in response to feeding: a model to study interactions between drugs and naturally activated dopaminergic neurons in the rat brain. *Naunyn-Schmeildebergs archives of pharmacology* 349: 230-235, 1994.

Westerink BHC and Tuinte MHJ. Chronic use of intracerebral dialysis for the in vivo measurement of 3,4 hydroxyphenylethylamine and its metabolite 3,4 hydroxyphenylacetic acid. *Journal of Neurochemistry* 46: 181-185, 1986.

Wiesel FA, Farde L, Nordstrom AL and Sedvall G. Central D1- and D2-receptor occupancy during antipsychotic drug treatment. *Progress in Neuropsychopharmacology and Biological Psychiatry* 14: 759-767, 1990.

Williams DS, Detre JA, Leigh JS and Koretsky AP. Magnetic resonance imaging of perfusion using spin inversion of arterial water. *Proceedings of the National Academy of Science of the USA* 89: 212-216, 1992.

Williams GV and Goldman-Rakic PS. Modulation of memory fields by dopamine D1 receptors in prefrontal cortex. *Nature* 376: 572-575, 1995.

Winters W and Spooner C. A neurophysiological comparison of alpha chloralose with gamma-hydroxybutyrate in cats. *Electoenceph Clin Neurophysiol* 20: 83-90, 1966.

Wirtshafter D and Krebs JC. Interactive effects of stimulation of D1 and D2 dopamine receptors on Fos expression in the lateral habenula. *Brain Research* 750: 245-250, 1997.

Wise RA. Action of drugs of abuse on brain reward systems. *Pharmacol Biochem Behav* 13: 213-223, 1980.

Wise RA. Neurobiology of Addiction. *Current opinion in Neurobiology* 6: 243-251, 1996.

Wise RA and Bozarth MA. Brain mechanisms of drug reward and euphoria. *Psychiatric Medicine* 3: 445-460, 1985.

Wise RA and Bozarth MA. A psychomotor stimulant theory of addiction. *Psychology Reviews* 94: 469-492, 1987.

Withers NW, Pulvirentini L, Koob GF and Gillin JC. Cocaine abuse and dependence. *Journal of Clinical Psychopharmacology* 15: 63-78, 1995.

Wolf ME and Xue CJ. Amphetamine-induced glutamate efflux in the rat ventral tegmental area is prevented by MK-801, SCH 23390, and ibotenic acid lesions of the prefrontal cortex. *Journal of Neurochemistry* 73: 1529-1538, 1999.

Wolterink G, Phillips G, Cador M, Donselaar-Wolterink I, Robbins TW and Everitt BJ. Relative roles of ventral striatal D1 and D2 dopamine receptors in responding with conditioned reinforcement. *Psychopharmacology (Berl)* 110: 355-364, 1993.

Wong DT, Bymaster FP, Reid LR, Fuller RW, Perry KW and Kornfeld EC. Effect of a stereospecific D2-dopamine agonist on acetylcholine concentration in corpus striatum of rat brain. *Journal of Neural Transmission* 58: 55-67, 1983.

Woods RP, Cherry SR and Mazziota JC. Rapid automated algorithm for aligning and reslicing PET images. *Journal of Computer Assisted Tomography* 16: 620-633, 1992.

Woolverton WL and Cervo L. Effects of central dopamine depletion on the d-amphetamine discriminative stimulus in rats. *Psychopharmacology* 88: 196-200, 1986.

Wooten GF and Trugman JM. The dopamine motor system. *Movement Disorders* 4: S38-S47, 1989.

Worsley JN, Moszczynska A, Falardeau P, Kalasinsky KS, Schmunk G, Guttman M, Furukawa Y, Ang L, Adams V, Reiber G, Anthony RA, Wickham D and Kish SJ. Dopamine D1 receptor protein is elevated in nucleus accumbens of human, chronic methamphetamine users. *Mol Psychiatry* 5: 664-672, 2000.

Worsley KJ, Evans AC, Marrett S and Neelin P. A three-dimensional statistical analysis for CBF activation studies in human brain. *Journal of cerebral blood flow and metabolism* 12: 900-918, 1992.

Wozniak KM, Pert A, Mele A and Linnoila M. Focal application of alcohols elevates extracellular dopamine in rat brain: a microdialysis study. *Brain Research* 540: 31-40, 1991.

Wu MT, Hsiejh JC, Xiong J, Yandg CF, Pan HB, Chen YC, Tsai G, Rosen BR and Kwong KK. Central nervous pathway for acupuncture stimulation: localization of processing with functional MR imaging of the brain--preliminary experience. *Radiology* 212: 133-141, 1999.

Wurtman RJ, Larin F, Mostafapour S and Fernstrom JD. Brain catechol synthesis: control by train tyrosine concentration. *Science* 185: 183-184, 1974.

Xu R, Parlow AF and Wang Y. The effects of dopamine and D2 receptor antagonists on pituitary hormone secretion are intact in mice lacking dopamine D2L receptor. *Brain Research* 939: 95-99, 2002.

Yaksh TL and Yamamura HI. Factors affecting performance of the push-pull cannula in brain. *Journal of Applied Physiology* 37: 428-433, 1974.

Yamada H, Sadato N, Konishi Y, Kimura K, Tanaka M, Yonekura Y and Ishii Y. A rapid brain metabolic change in infants detected by fMRI. *Neuroreport* 8: 3775-3778, 1997.

Yang X, Hyder F and Shulman R. Activation of Single Whisker Barrel in rat brain localised by functional magnetic resonance. *Proceedings of the National Academy of Sciences of the United States of America* 93: 475-478, 1996.

Yang X, Hyder F and Shulman RG. Functional magnetic resonance imaging BOLD signal coincides with electrical activity in the rat whisker barrels. *Magnetic Resonance in |Medicine* 38: 874-877, 1997.

Yang X, Renkens R, Hyder F, Siddeek M, Greer CA, Shepard GM and Shulman RG. Dynamic mapping at the laminar level of odor-elicited responses in rat olfactory bulb by functional MRI. *Proceedings of the National Academy of Science of the USA* 95: 7713-7720, 1998.

Yarowsky, P. J. and Ingvar, D. H. Symposium summary. Neuronal activity and energy metabolism. 40(9), 2352-2362. 1981.
Ref Type: Generic

Yim HJ, Schallert T, Randall PK, Bungay PM and Gonzales RA. Effect of ethanol on extracellular dopamine in rat striatum by direct perfusion with microdialysis. *Journal of Neurochemistry* 68: 1527-1533, 1997.

Ylitalo P, Saarnivaara L and Ahtee L. Effect of ketamine anaesthesia on the content of monoamines and their metabolites in the rat brain. *Acta Anaesthiologica Scandinavica* 20: 216-220, 1976.

Yoshimoto K, McBride WJ, Lumeng L and Li TK. Ethanol enhances the release of dopamine and serotonin in the nucleus accumbens of HAD and LAD lines of rats. *Alcohol Clinical Experiemntal Therapeutics* 16: 781-785, 1992.

Young AM, Crowder JM and Bradform HF. Potentiation of excitatory amino acids release in the striatum: complementary in vivo and in vitro experiments. *Journal of Neurochemistry* 50: 337-345, 1988.

Young AMJ, Aheir RG, Upton RL, Joseph MH and Gray JA. Increased extracellular dopamine in the nucleus accumbens of the rat during associative learning of neutral stimuli. *Neuroscience* 83: 1175-1183, 1998.

Young AMJ, Joseph MH and Gray JA. Increased dopamine release in vivo in nucleus accumbens and caudate nucleus of the rat during drinking: A microdialysis study. *Neuroscience* 83: 1175-1183, 1992.

Yung KKL, Smith AD, Levey AI and Bolam JP. Synaptic connections between spiny neurons of the direct and indirect pathwaysof the neistriatum of the rat: Evidence from dopamine receptor and neuropeptide immunostaining. *European Journal of Neuroscience* 8: 861-869, 1996.

Zetterstrom T, Sharp T, Marsden CA and Ungerstedt U. In vivo measurement of dopamine metabolites by intracerebral dialysis: Changes after d-amphetamine. *Journal of Neurochemistry* 41: 1769-1745, 1983.

Zhao Y, Kerscher N, Eysel U and Funke K. D1 and D2 receptor-mediated dopaminergic modulation of visual responses in cat dorsal lateral geniculate nucleus. *Journal of Physiology* 539: 223-238, 2002.

Zhou QY, Grandy DK, Thambi L, Kushner JA, Van Tol HH, Cone R, Pribnow D, Salon J, Bunzow JR and Civelli O. Cloning and expression of human and rat D1 dopamine receptors. *Nature* 347: 76-80, 1990.

Zhu B.T. Catechol-O-Methyltransferase (COMT)-mediated methylation metabolism of endogenous bioactive catechols and modulation by endobiotics and xenobiotics: importance in pathophysiology and pathogenesis. *Curr Drug Metab* 3: 321-349, 2002.

Zhu XH, Kim SG, Andersen P, Ogawa S, Ugurbil K and Chen W. Simultaneous oxygenation and perfusion imaging study of functional activity in primary visual cortex at different visual stimulation frequency: quantitative correlation between BOLD and CBF changes. *Magnetic Resonance in Medicine* 40: 703-711, 1998.

Zigmond RE, Swarzschild MA and Ritenhouse AR. Acute regulation of tyrosine hydroxylase by nerve activity and by neurotransmitters via phosphorylation. *Annual Reviews of Neuroscience* 12: 415-461, 1989.

Zimmer A, Valjent E, Konig M, Zimmer AM, Robledo P, Hahn H, Valverde O and Maldonado R. Absence of delta -9-tetrahydrocannabinol dysphoric effects in dynorphin-deficient mice. *Journal of Neuroscience* 21: 9499-9505, 2001.